End Theory: Evans Node Dialect

Complete Working Treatise

Ontology, benchmark proofs, compact equations, expanded derivations, 275-constant audit, and author revision workbench

Ryan

Independent research programme

Working manuscript v3.0 | 6 August 2026

Scientific status. This document is a theory specification and a reproducible metrological audit. It is not a report of 275 new predictions, completed empirical validation, or a completed theory of everything. It identifies a coherent ontology, supplies one explicit benchmark dynamics, proves several properties of that benchmark, and states the missing results that must be obtained before claims about quantum mechanics, the Standard Model, gravity, cosmology, or new particles are warranted. Here, "proof" always means a consequence of the stated benchmark assumptions; it never means that nature realizes those assumptions.

Abstract

This working treatise consolidates the two controlling reconstructions of the End Theory: Evans Node Dialect/Matrix Node Theory (END/MNT) with the complete 275-quantity CODATA audit and a paired equation workbench. The ontology proposes that ordered, locally capacity-limited relational changes precede metric space and operational time; persistent coarse-grained patterns may then define nodes, fields, clocks, and geometry. One explicit scalar graph benchmark is developed from a discrete action. Deterministic recursion, the weighted-Laplacian spectrum, exact lattice dispersion, a linear stability domain, a mass-gap definition, and an exact link-gauge invariance are derived within that benchmark. These internal proofs are separated from uncompleted physical bridges to chiral matter, quantum probabilities, gravity, torsion, cosmology, and measured constants. The CODATA register preserves 275 individual profiles and distinguishes exact definitions, conventional references, adjusted empirical inputs, dependent identities, and legitimate predictions; the present END/MNT microscopic equations yield no independently predicted numerical CODATA constant. Fifty-five paired workbench modules then state a compact equation chain on one page and expand its assumptions, algebra, dimensions, interpretation, author-edit point, and falsifier on the next. Blue bold indices and a revision ledger make every premise and proposed identification traceable. The result is deliberately a working scientific specification: it preserves Ryan's relational and progression-limited vision while exposing inherited AI-generated ambiguities, circular fits, dimensional errors, and every remaining completion gate.

Plain-language summary. The central idea survives: reality may be a sequence of constrained relational updates, and stable repeating structures in that sequence may appear to us as space, particles, fields, and gravity. What does not survive is the claim that naming those correspondences is already a derivation. This reconstruction supplies the cleanest mathematics currently justified and draws a bright line between a definition, a calibration, a consequence, and a prediction.

Contents

Part I — A feature for curious general readers

1 What if space is what survives?

Physics became simple once before. The great equations of the twentieth century compressed motion, gravity, and quantum behaviour into astonishingly economical forms. End Theory: Evans Node Dialect asks whether that simplicity may be the visible surface of a deeper process: a universe assembled from relations that repeatedly survive their own change.

1.1 Begin by taking away the stage

Nearly every picture of the cosmos starts with a stage. Galaxies drift through space. Clocks tick in time. Fields spread across positions that already exist. Even when the stage curves, as it does in general relativity, the mathematical story begins with a spacetime geometry on which matter and radiation live.

Now try a harder thought experiment. Remove the actors, then remove the stage. There are no coordinates, metres, seconds, or background grid waiting to be occupied. What could still be real?

One possible answer is *relation*: this potential state can influence that one; this joint change is allowed; another is forbidden. Relation is not yet distance. Order is not yet duration. Yet a network of allowed transitions can possess structure before it possesses geometry.

That is the beginning of END/MNT. Its central proposal is that observed physics may be the durable, large-scale description of a deterministic relational process with finite local transition capacity. The familiar world would not be made of little beads sitting in a pre-existing void. Instead, bead, void, and motion would all be effective ideas that become useful after patterns persist.

This places the project near several serious traditions without making it identical to them. Regge calculus replaces smooth geometry with discrete simplicial pieces; lattice gauge theory places gauge variables on links and keeps local symmetry exact at finite spacing; causal-set research asks whether order and discreteness can precede continuum geometry. END/MNT adds its own emphasis: stabilized frames, persistent relational patterns, and a locally bounded capacity for change.

The proposal is ambitious. Its repaired form is deliberately modest about what has been achieved. The ontology is a map of what should be derived. The scalar graph equation is a benchmark showing that part of the map can be made explicit. The bridges to quantum probability, the Standard Model, and gravity remain incomplete. That distinction is not a weakness to hide. It is the line separating an imaginative framework from a scientific theory that can survive contact with nature.

1.2 The flipbook is not the clock

Picture an endless flipbook. Each page contains a complete configuration, and each page follows the previous one according to a rule. A character inside the book may build a clock from a recurring pattern: a pendulum, an atomic transition, or a repeating pulse. The clock counts its own cycles as the pages turn. The page number and the clock reading are not the same thing.

This matters because END/MNT wants physical time to emerge. The fundamental label n merely orders updates. Operational time appears only when a stable subsystem supplies a repeatable observable. In a homogeneous regime, clock time might be proportional to update count. In a loaded or geometrically distorted regime, the local tick duration may differ.

The thought experiment immediately creates a burden. If progression imbalance is meant to reproduce gravitational time dilation, a clock pattern in one region must accumulate fewer operational cycles than a comparable clock elsewhere, even when both histories can be compared within the micro-description. Declaring each frame to be one universal instant will not do; the tick rate must come out of the dynamics.

The same discipline repairs the word "energy." Earlier versions spoke of energy as frame-to-frame change. Change may be a microscopic correlate of energy, but it is not yet energy in the physicist's quantitative sense. In an effective time-translation-invariant regime, energy should be a conserved Hamiltonian or Noether charge with measurable units. The theory must derive that bridge rather than define it by metaphor.

1.3 How persistence can become space

The next step is selection by survival. Suppose the microscopic process explores an immense variety of local arrangements. Most appear and disappear. Some recur. Others remain recognizable while moving, rotating, or changing phase. Recognizability can be formalized by coarse-graining the microstate at resolution R and asking whether the result stays within a declared tolerance of an allowed transformed copy over many updates.

The survivors are candidates for nodes. Connect persistent clusters that directly exchange influence and give each link a positive weight representing interaction strength or transfer capacity. The resulting graph has paths. If stronger relations correspond to shorter effective links, the cheapest path between two clusters defines a graph distance. Geometry has begun to appear.

But a graph is not automatically three-dimensional space. A successful model must show that neighborhoods possess a stable effective dimension, that long-distance behaviour becomes sufficiently isotropic, and that the same metric organizes the propagation of every relevant low-energy mode. It must explain why the continuum is Lorentzian and why there is one invariant speed to extraordinary precision. Drawing nodes is easy; deriving a 3+1-dimensional spacetime is a calculation.

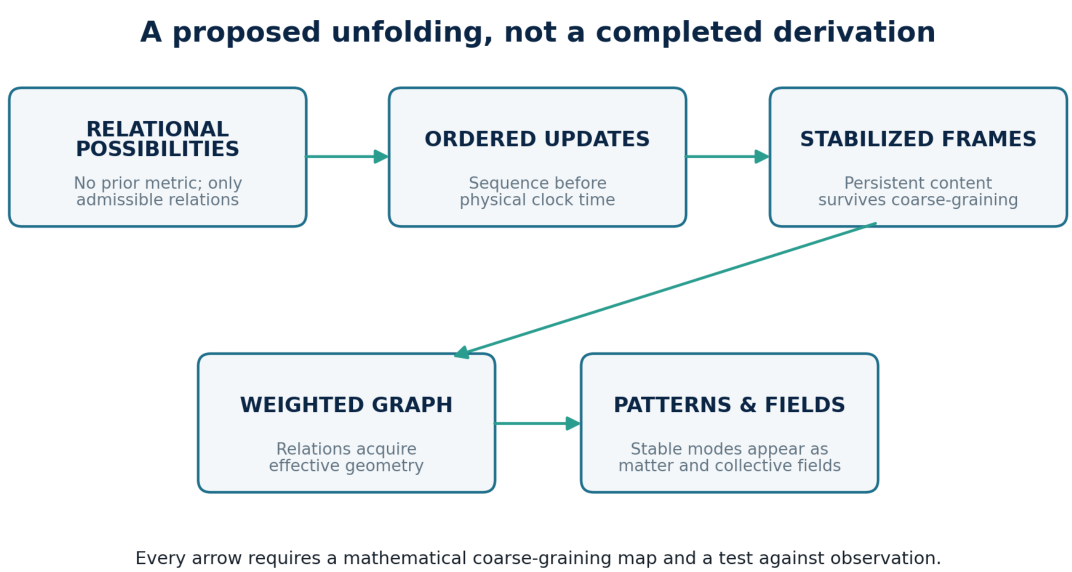

Figure 1: The proposed unfolding. Every arrow is a calculation still required: persistence, graph formation, continuum geometry, stable patterns, and effective observables.

1.4 A universe with a local speed limit on change

END/MNT's most distinctive structural idea is not simply discreteness. It is a finite *local transition capacity*. Imagine a road network in which every intersection can process at most one normalized unit of traffic during a tick. Congestion at one intersection changes nearby routes and its effects propagate, but a driver does not need the total traffic count for every road in the universe before moving through the next light.

The original ontology used a global capacity sum. On a large or infinite lattice that can diverge and can make distant regions instantaneously interdependent. The repaired law is local: every node i carries a demand $\mathcal{C}_i$, computed from changes at that node and its finite neighbourhood, and admissible evolution requires $0 \leq \mathcal{C}_i \leq 1$.

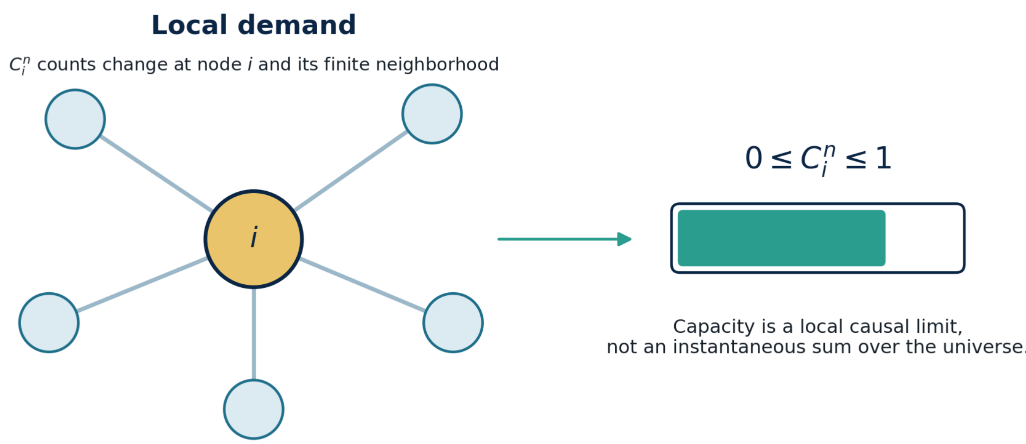

Figure 2: A local capacity bound avoids an instantaneous global accountant. Disturbances influence distant regions only through successive neighbourhood updates.

A bound like this could limit propagation, constrain local acceleration, create nonlinear thresholds, and force highly loaded regions to redistribute change. It could also do none of the hoped-for physical jobs if its detailed update rule produces instability or contradicts precision experiments. The value lies in making the idea concrete enough to find out.

The benchmark action below converts one version of the intuition into mathematics. Neighbouring coordinates resist disagreement like coupled springs; an onsite term sets a gap; a nonlinear potential permits richer patterns. The resulting update is explicit and deterministic. Its plane waves have an exact lattice dispersion relation, and its high-frequency stability condition can be checked before any comparison with particle data. A model that cannot preserve its own admissible set or converge under refinement should not be asked to explain the Higgs boson.

1.5 Why a particle might be a verb

In ordinary speech a particle sounds like a tiny noun: a thing occupying a location. In a relational theory a particle may be closer to a verb, a localized activity that keeps recreating its identity while moving through the network.

Think of a stadium wave. No spectator travels around the arena, yet a coherent pattern does. Now make the pattern nonlinear, self-stabilizing, and capable of carrying invariant labels. Such a structure could, in principle, possess a rest-energy gap, scatter from other structures, and survive transport.

The analogy is useful only if the mathematics goes further. A particle candidate needs a solution or invariant manifold. Perturbations around it must have a stable spectrum. Motion must obey a dispersion relation. Conserved labels must come from exact symmetries or topology. Interactions must produce calculable amplitudes and decay channels. Finally, the coarse observables must connect to what a detector records.

Mass then becomes a rest-energy gap or an eigenvalue of a stability operator. Charge becomes a representation label of a gauge symmetry or a topological invariant. Spin requires the correct transformation behaviour. None of these can be obtained by naming a frequency after a known particle and substituting $\omega = mc^2/\hbar$; that merely rewrites the measured mass.

1.6 Phase, loops, and the route to gauge fields

Phase is one of the theory's strongest surviving ideas because it has a natural exact language on a graph. Assign a complex value $\psi_i = \rho_i \mathrm{e}^{\mathrm{i}\theta_i}$ to node i. A direct phase difference depends on the local phase convention. To compare phases consistently, place a link variable $U_{ij} = \mathrm{e}^{\mathrm{i}qA_{ij}}$ between neighbouring nodes. The magnitude of the covariant difference $U_{ij}\psi_j - \psi_i$ stays unchanged when node phases and link phases transform together.

Take the ordered product of link variables around a closed elementary loop. The plaquette holonomy is gauge invariant and can become gauge curvature at long distance. For END/MNT the lesson is precise: phase alignment can be retained, but electromagnetism does not emerge from a suggestive line integral alone. The theory must specify node representations, link transformations, loop observables, dynamics, and the continuum limit. Chiral fermions create an additional obstacle because naive lattice formulations tend to produce unwanted doubled species.

1.7 EQEF, deferred change, and geometric imbalance

The Evans Quantum Energy Field has carried several meanings across the project's history. The canonical reconstruction narrows them. At the first level, EQEF is a ledger. If local demand is $\mathcal{C}_i$, residual capacity is $r_i = 1 - \mathcal{C}_i$. A causal balance equation may track how residual capacity is transported, stored, or released among neighbouring regions. The quantity is dimensionless until a physical normalization is supplied; it is not automatically a new form of energy.

At the second level, coarse-graining may produce a field $\chi(x)$ representing fluctuations of residual capacity around a background. One can write a conservative effective action with a kinetic term, potential, and couplings to curvature. Depending on the potential, such a field might influence cosmology. Many scalar fields can do that. END/MNT becomes distinctive only if its discrete update fixes the coefficients or produces a relation that survives held-out observations.

The same restraint applies to torsion. In Riemann–Cartan geometry, torsion measures the infinitesimal failure of a transported parallelogram to close. Imagine taking one tiny step east, one north, then reversing both moves. If local translation rules are imbalanced, the endpoint may miss the start. The mismatch per enclosed area is a geometrically meaningful candidate for "progression imbalance." The theory must still derive the tetrad, spin connection, torsion source, and effective coefficients.

1.8 The quantum challenge cannot be skipped

A deterministic micro-history does not by itself reproduce quantum mechanics. Quantum theory predicts probabilities, interference, and entanglement with astonishing accuracy. Bell experiments rule out a broad class of local, measurement-independent hidden-variable theories. A deterministic completion must state the complete ontic state λ, how preparations generate an ensemble, how settings enter, how outcomes are read, and which assumption behind the Bell bound is altered.

Logical options include operational nonlocality, measurement dependence, retrocausal structure, contextual outcomes, or another explicitly defined departure from the usual assumptions. "The two particles shared an earlier frame" is not enough. A common past produces ordinary correlations, but not the full Bell-violating pattern under local, measurement-independent conditions.

The Born rule is a separate demand. If stable amplification or a capacity threshold creates localization, the model must calculate outcome frequencies and recover the squared-amplitude rule in the appropriate regime. It must preserve operational no-signalling and state what happens to conservation laws during localization. END/MNT retains a deterministic intent and a useful language of frame histories, phase dispersal, and stable amplification. Its quantum completion remains open.

1.9 How the universe could unfold

With those cautions in place, the proposed cosmic story can be told as a sequence. First comes a pre-geometric relational regime: possible states and admissible joint changes, but no established physical distance. Ordered updates create histories. Recurrent structures begin to store information about their own past. Persistence separates durable patterns from transient noise.

As persistent clusters interact, a weighted graph stabilizes. Its large-scale neighbourhoods acquire regular dimension and approximately isotropic distance. Collective disturbances develop long-wavelength dispersion. Operational clocks emerge from repeating patterns. A shared conversion between graph propagation and clock readings produces an effective causal speed.

Nonlinear stable modes become particle candidates. Link phases and loop holonomies organize gauge-like interactions. Symmetry breaking in an effective scalar sector may generate mass matrices, but those matrices must ultimately be computed from the node operator rather than tuned to the observed spectrum. Regions approaching local capacity respond nonlinearly. If coarse-grained progression imbalance universally affects clock rates and trajectories, an effective geometry may emerge. If residual capacity develops a slowly evolving collective mode, an EQEF-like field may contribute to cosmic dynamics.

This is a proposed unfolding, not an established chronology of the observed early universe. A real cosmology requires background and perturbation equations, initial conditions, light-element abundances, microwave-background spectra, structure formation, and late-time expansion, all derived from the same frozen model. Substituting standard ΛCDM parameters into standard equations would test ΛCDM, not END/MNT.

1.10 What was removed, and why the project is stronger

The theory's history contains many numerical targets: particle masses, resonances, coupling values, dark-sector signals, gravitational-wave echoes, and aggregate alignment percentages. Some were suggestive. Several used measured constants as inputs and then counted their reappearance as predictions. Others mixed dimensions, changed parameter meanings, or proposed experimental windows without an interaction model. Those claims are retired from the canonical scientific record.

The removal includes unfrozen resonances at incompatible energies; a Higgs expression with inserted measured constants and incorrect dimensions; a dimensionally wrong gravitational formula; a cosmological-constant value with Planck-unit and SI units confused; masses generated by substituting measured frequencies; and "validation" scores without a common likelihood, covariance, parameter count, or held-out dataset.

What remains is less spectacular on a poster and more valuable in a calculation: an ordered ontology, local capacity law, concrete graph-field action, explicit update, exact dispersion relation, stability bound, gauge-invariant phase extension, disciplined meaning for EQEF and torsion, and staged falsification programme. Science does not become smaller when a weak claim is removed. The search space becomes clearer.

1.11 The experiment before the experiments

The first serious test should happen on a computer before another global data fit. Implement the scalar benchmark on square, cubic, and approximately isotropic irregular graphs. Verify the exact dispersion relation numerically. Map the stability boundary. Add compact phases and link variables, then unit-test gauge invariance. Construct one local capacity-preserving completion and measure its conservation residuals under refinement.

Only then search for stable localized nonlinear patterns. Freeze all parameters before comparing any pattern with a particle mass. Report dimensionless gaps, scattering behaviour, and failure regions. If patterns disappear under perturbation or continuum anisotropy does not shrink as predicted, say so.

Later gates are harder. A gauge and chiral sector must avoid doubling and anomalies. A quantum module must reproduce preparation-dependent probabilities and Bell correlations. A gravitational coarse-graining must yield universal free fall, the Newtonian limit, relativistic propagation, and allowed corrections. External tests require preregistration, versioned code, declared calibration data, held-out data, and comparison with simpler baselines. This programme can fail early and cheaply. That is an advantage: a theory that risks nothing teaches nothing.

1.12 Complexity returns with a purpose

The twentieth century gave physics equations of breathtaking compression. General relativity turned gravity into geometry. Quantum field theory organized particles as excitations of fields and interactions as symmetries. The Standard Model became extraordinarily successful even as its list of fields, parameters, and unexplained patterns grew.

END/MNT asks whether the next layer may be conceptually simple but dynamically complex: local relations updating under one rule, producing multiple effective descriptions at different scales. Complexity is not an excuse to fit anything. It is the complexity of emergence, the way a local rule can create phases, defects, collective modes, effective geometry, and information-processing structures.

The question is not whether a sufficiently elaborate network can imitate known physics. It can. The question is whether one constrained micro-model predicts several independent structures that were not inserted: a common invariant speed, stable dimension, gauge group, chiral content, mass ratios, quantum statistics, and gravitational response. If it can, physics will have become complex again beneath the equations we know while becoming more unified in its foundations. If it cannot, the failed attempt will still clarify what a relational theory must do.

That is the invitation of End Theory: Evans Node Dialect. Do not believe it because the picture feels complete. Follow the equations until the picture either becomes unavoidable or breaks.

Editorial note. Scientific American describes 2,000–4,000-word features but does not accept AI-generated pitches or drafts. Part I is a public research base, not a file to submit unchanged. Ryan would need to rewrite it independently and add reporting plus critical outside voices.

Part II — Canonical scientific specification

2 Outcome of the reconstruction

The source set contains three different generations of the theory. The earliest UMNT and END drafts contain valuable intuitions but also dimensional errors, inserted experimental values, incompatible particle forecasts, and prose that treats analogies as proofs. The November 2025 ontology, lexicon, structural, and validation documents impose a better conceptual hierarchy and explicitly reject circular fitting, but their mathematics remains partly schematic. The August 2026 technical audit correctly identifies the submission blockers, although it did not have the full later ontology available when it selected a fixed node lattice as the working starting point.

This reconstruction resolves that conflict with the following priority rule:

1. The ontology controls the meaning of the objects.
2. Mathematical consistency controls the equations.
3. Later explicit redefinitions supersede older prose.
4. An older formula is retained only if it has defined variables, compatible dimensions, a stable dynamical interpretation, and a map to the ontology.
5. A numerical claim is retained only if it has a frozen prediction function, parameter policy, data provenance, uncertainty model, and reproducible code.

Canonical scientific claim. The present END/MNT is a deterministic relational-frame hypothesis with an emergent graph-field phase and a finite local transition capacity. A scalar/phase lattice is one benchmark realization, not the uniquely derived microphysics. The programme becomes a physical theory only when one complete update law and coarse-graining map generate parameter-fixed, held-out observables.

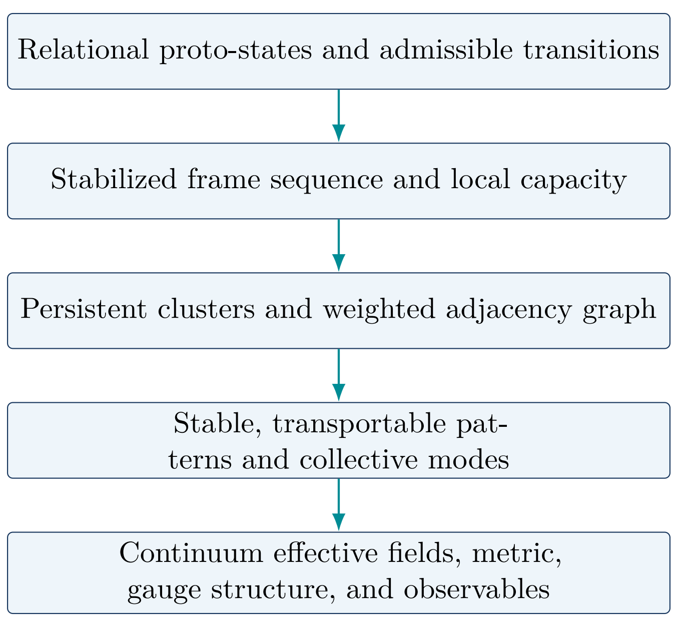

Figure 3: The repaired hierarchy. Arrows are required coarse-graining or emergence maps; they are not rhetorical equivalences. Every arrow must eventually be supplied as an explicit mathematical construction.

3 Canonical ontology

3.1 Axiom O1: relational proto-state, not a prior spacetime

Let $\mathcal{P}$ be a configuration space of proto-degrees of freedom. An element $p \in \mathcal{P}$ may carry internal coordinates such as an amplitude-like value, a compact phase label, and discrete type labels. These coordinates are not yet physical position, time, energy, spin, or charge. In particular, the earlier phrase "pre-geometric frequency" is replaced by *phase propensity*: physical frequency is cycles per physical time and therefore cannot be primitive if physical time is meant to emerge.

The primitive relational structure is an admissibility relation $R \subset \mathcal{P} \times \mathcal{P}$ or, more generally, a hypergraph of allowed joint transitions. Calling two proto-degrees "local" at this level means that the update rule couples them directly; it does not mean that they are close in a pre-existing metric.

3.2 Axiom O2: ordered updates precede metric time

The fundamental history is an ordered sequence of micro-configurations

$$X_0 \prec X_1 \prec X_2 \prec \cdots, \qquad X_n \in \mathcal{X}. \tag{1}$$

The index n is an update order, not automatically a clock reading. A physical clock is a persistent subsystem K with a monotonic observable $Q_K[X_n]$. The elapsed time assigned by that clock is

$$t_K(n_2) - t_K(n_1) = \sum_{n=n_1}^{n_2-1} \delta\tau_K(X_n), \tag{2}$$

where the local tick duration must be derived from the clock dynamics. A universal relation $t = n\delta\tau$ is therefore a homogeneous-limit approximation, not a foundational identity.

Thought experiment 1: the flipbook and the clock

A flipbook has an ordered page number, but the page number alone does not tell a character how long one second lasts. Put two oscillating patterns in the book, one in a quiet region and one in a highly loaded region. If END is to reproduce gravitational time dilation, the second pattern must complete fewer operational ticks between comparable frame records. Merely declaring each page to be one universal instant cannot produce that result. Equation (2) states what must be calculated.

3.3 Axiom O3: a frame is a stabilized coarse-grained equivalence class

Choose a coarse-graining map $C_R : \mathcal{X} \to \mathcal{X}_R$ at resolution R, a norm $\|\cdot\|_R$, and a tolerance ϵ_R. A macrostructure is persistent over N updates if

$$\|C_R X_{n+m} - \mathcal{T}_m C_R X_n\|_R \le \epsilon_R, \quad 0 \le m \le N, \tag{3}$$

for an allowed transport, phase, or symmetry operation $\mathcal{T}_m$. A *frame* $\mathcal{F}_n$ is the equivalence class of micro-configurations with the same resolved persistent content at update n. This replaces the earlier set notation $\mathcal{F}_n \subset \mathcal{P}^{N_n}$, which did not state the equivalence relation or stabilization test.

3.4 Axiom O4: space is the geometry of persistent relations

Persistent clusters become candidate nodes. Let V_n be the set of clusters satisfying (3); define a symmetric weight $w_{ij}^{(n)} \geq 0$ from direct interaction strength, transfer capacity, or a specified correlation functional. The effective graph is

$$G_n = (V_n, E_n, w^{(n)}), \qquad (i,j) \in E_n \iff w_{ij}^{(n)} > w_{\min}. \tag{4}$$

A graph distance can then be defined by

$$d_G(i,j) = \inf_{\gamma: i \to j} \sum_{e \in \gamma} \ell_e, \qquad \ell_e = \ell_0 f(w_e), \tag{5}$$

with a declared positive decreasing function f. An approximately smooth spatial metric is justified only if graph neighborhoods have stable dimension, isotropy, and scaling over a range of resolutions. Co-occurrence in one frame is insufficient by itself.

3.5 Axiom O5: the fundamental capacity is local and causal

The older ontology imposed a single sum $\sum_i \mathcal{C}_i(n) \leq \Lambda_{\text{lim}}$ over the whole lattice. On an infinite lattice that sum may diverge; on any large lattice it makes distant updates instantaneously interdependent. The canonical constraint is instead local:

$$0 \leq \mathcal{C}_i^n \leq 1 \quad \text{for every node and update,} \tag{6}$$

where $\mathcal{C}_i^n$ is a dimensionless demand constructed from changes in node i and its finite neighborhood. A regional budget is derived by summing (6) over a finite domain; it is not a separate instantaneous law.

For a generalized scalar benchmark introduced below, one admissible demand is

$$\mathcal{C}_i^n = \frac{1}{E_*}\left[\frac{\mu}{2}\left(\frac{q_i^{n+1} - q_i^n}{\delta\tau}\right)^2 + \frac{\kappa}{4}\sum_j w_{ij}(q_i^n - q_j^n)^2 + V_+(q_i^n)\right], \tag{7}$$

where $E_* > 0$ is a local energy-capacity scale and $V_+ \geq 0$. Equation (7) is a model choice, not yet a derivation from the proto-state layer.

Thought experiment 2: a road network with a local load limit

Imagine every intersection can process at most one normalized unit of traffic per tick. Congestion in one neighborhood changes later routes and can propagate outward, but a driver on the other side of the universe does not have to know the total traffic everywhere before moving. This is the difference between the local condition $\mathcal{C}_i \leq 1$ and an instantaneous global sum. Progression imbalance is the persistent pattern of delayed or redirected updates caused by the local limits.

3.6 Axiom O6: a complete theory requires a capacity-preserving update map

Define the admissible state set $\mathcal{A} = \{X : \mathcal{C}_i[X] \leq 1 \ \forall i\}$. Determinism requires a single-valued map

$$X_{n+1} = U_{\boldsymbol{p}}(X_n, X_{n-1}), \qquad U_{\boldsymbol{p}} : \mathcal{A} \times \mathcal{A} \to \mathcal{A}, \tag{8}$$

with parameter vector $\boldsymbol{p}$, boundary conditions, and a declared treatment of graph changes. Neither the phrase “the system reorganizes” nor a post hoc node-merging rule specifies $U_{\boldsymbol{p}}$. The uncapped benchmark in section 4 supplies an explicit update in one sector. A unique, conservation-compatible completion when $\mathcal{C}_i = 1$ remains open.

3.7 Axiom O7: patterns, particles, and fields

A pattern type P is an equivalence class of configurations that is localized or controlled in support, stable under $U_{\boldsymbol{p}}$, and transportable under graph symmetries. A particle claim requires at least:

1. a solution or invariant manifold representing the pattern;
2. a stability spectrum under perturbations;
3. a dispersion relation and conserved quantum numbers;
4. an interaction rule yielding scattering or decay amplitudes; and
5. a continuum map connecting the pattern to detector observables.

Fields are coarse-grained collective coordinates for ensembles of patterns. This definition preserves the ontology's core insight while preventing a name such as "electron pattern" from being treated as a calculated electron.

3.8 Axiom O8: deterministic intent is not yet a quantum completion

The micro-history may be deterministic, but agreement with quantum experiments does not follow from determinism or chaos alone. The model must specify an ensemble measure, preparation map, measurement setting, outcome map, and the assumption in Bell's theorem that is modified. This constraint is developed in section 8.

4 A minimal deterministic graph-field benchmark

This section gives one mathematically closed low-level sector. It is deliberately modest: it proves that the ontology can support explicit dynamics and testable continuum behavior. It does not derive the ontology uniquely, the Standard Model, or gravity.

4.1 State, graph, and discrete action

Take a fixed weighted graph $G = (V, E, w)$ during one stabilized phase. Each node carries a real coordinate q_i^n. Let $\mu > 0$ be a generalized node inertia, $\kappa > 0$ a link stiffness, $\Omega_0 \geq 0$ an onsite frequency, and $W(q)$ a nonlinear potential. The discrete action is

$$S_0 = \sum_n \delta\tau \left[\frac{\mu}{2} \sum_i \left(\frac{q_i^{n+1} - q_i^n}{\delta\tau} \right)^2 - \frac{\kappa}{2} \sum_{(ij)\in E} w_{ij} (q_i^n - q_j^n)^2 - \frac{\mu\Omega_0^2}{2} \sum_i (q_i^n)^2 - \sum_i W(q_i^n) \right]. \tag{9}$$

All terms in the bracket have units of energy. The graph Laplacian is

$$(L_G q)_i = \sum_j w_{ij} (q_i - q_j). \tag{10}$$

Varying (9) with fixed endpoint configurations gives the explicit leapfrog update

$$q_i^{n+1} = 2q_i^n - q_i^{n-1} - \delta\tau^2 \left[\Omega_0^2 q_i^n + \frac{\kappa}{\mu} (L_G q^n)_i + \frac{1}{\mu} W'(q_i^n) \right]. \tag{11}$$

Given q^{n-1}, q^n, the graph, and the parameters, (11) determines q^{n+1} without a random draw.

Proposition 1 (Deterministic benchmark evolution)**.** *For a finite graph, fixed parameters $\mu > 0$, $\kappa > 0$, $\Omega_0 \geq 0$, and differentiable W, the map in (11) is single-valued for every pair $(q^{n-1}, q^n) \in \mathbb{R}^{2|V|}$.*

Proof. The weighted graph Laplacian is a finite linear operator, and $W'(q_i^n)$ is a single real number at each node. Every term on the right of (11) is therefore determined by the supplied pair of states. This proves algebraic determinism of the benchmark. It does not prove boundedness, admissibility, or physical completeness. □

Equation (11) is the explicit *uncapped* benchmark. A fundamental END update must additionally map admissible data back into the capacity set $\mathcal{A}$ whenever the tentative update would violate (6). Arbitrary clipping or merging is not acceptable because it can violate energy, momentum, reversibility, or locality.

4.2 A local transition limiter, and why it is not yet the final rule

One can make a narrow part of the capacity idea fully explicit. Let the static demand at the departure state be

$$S_i^n = \frac{\kappa}{4}\sum_j w_{ij}(q_i^n - q_j^n)^2 + V_+(q_i^n), \qquad 0 \leq S_i^n \leq E_*, \tag{12}$$

and let $v_i^* = (q_i^{*,n+1} - q_i^n)/\delta\tau$ be the velocity proposed by the uncapped update. Define

$$s_i^n = \begin{cases} 1, & v_i^* = 0, \\ \min\left\{1, \sqrt{\dfrac{2(E_* - S_i^n)}{\mu(v_i^*)^2}}\right\}, & v_i^* \neq 0, \end{cases} \qquad q_i^{n+1} = q_i^n + \delta\tau\, s_i^n v_i^*. \tag{13}$$

For the transition demand

$$\widetilde{\mathcal{C}}_i^n = \frac{\mu(s_i^n v_i^*)^2/2 + S_i^n}{E_*}, \tag{14}$$

(13) guarantees $0 \leq \widetilde{\mathcal{C}}_i^n \leq 1$ node by node.

Proof. If the tentative kinetic demand is no larger than $E_* - S_i^n$, then $s_i^n = 1$ and the inequality already holds. Otherwise the second branch gives $\mu(s_i^n v_i^*)^2/2 = E_* - S_i^n$, so $\widetilde{\mathcal{C}}_i^n = 1$. Every quantity uses only node i, its finite neighbourhood through S_i^n, and the tentative local update. □

This construction proves that a deterministic local limiter is possible, but it is not promoted to the canonical law. It may dissipate the benchmark energy, it need not preserve momentum or time reversal, and it does not by itself guarantee that the next static load S_i^{n+1} remains below E_*. A final completion must solve those three problems or identify a principled reason to relax the corresponding conservation law.

4.3 Exact dispersion relation

For $W = 0$ on a d-dimensional hypercubic graph with spacing a and unit nearest-neighbor weights, insert

$$q_i^n = A\exp[\mathrm{i}(\boldsymbol{k}\cdot\boldsymbol{x}_i - \omega n\delta\tau)] \tag{15}$$

into **(11)**. Since the graph-Laplacian eigenvalue is

$$\lambda_G(\boldsymbol{k}) = 4\sum_{r=1}^{d} \sin^2\left(\frac{k_r a}{2}\right), \tag{16}$$

one obtains the exact relation

$$\frac{4}{\delta\tau^2}\sin^2\left(\frac{\omega\delta\tau}{2}\right) = \Omega_0^2 + \frac{4c_0^2}{a^2}\sum_{r=1}^{d}\sin^2\left(\frac{k_r a}{2}\right), \qquad c_0^2 \equiv \frac{a^2\kappa}{\mu}. \tag{17}$$

Theorem 1 (Exact free-field lattice spectrum)**.** *On a d-dimensional periodic hypercubic graph with $W = 0$, every plane-wave eigenmode of* **(11)** *satisfies* **(17)***; conversely every real solution of* **(17)** *generates a free normal mode.*

Proof. For a plane wave, the second time difference is

$$q_i^{n+1} - 2q_i^n + q_i^{n-1} = -4\sin^2(\omega\delta\tau/2)q_i^n.$$

The nearest-neighbour graph Laplacian gives

$$(L_G q^n)_i = 4\sum_{r=1}^{d}\sin^2(k_r a/2)q_i^n.$$

Substitution into **(11)**, followed by division by the nonzero mode amplitude, yields **(17)**. Reversing the substitution proves the converse. □

At $|\boldsymbol{k}|a \ll 1$, $|\omega|\delta\tau \ll 1$,

$$\omega^2 = \Omega_0^2 + c_0^2|\boldsymbol{k}|^2 - \frac{c_0^2 a^2}{12}\sum_r k_r^4 + \frac{\omega^4\delta\tau^2}{12} + O(a^4k^6, \delta\tau^4\omega^6). \tag{18}$$

The leading continuum speed is therefore $c_0 = a\sqrt{\kappa/\mu}$, not automatically $a/\delta\tau$. The latter is a one-link-per-update kinematic scale. Equating it with the measured invariant speed requires an additional dynamical condition.

For $\Omega_0 = 0$, the group velocity in one dimension follows directly from implicit differentiation:

$$v_g(k) = \frac{\mathrm{d}\omega}{\mathrm{d}k} = c_0\frac{\cos(ka/2)}{\sqrt{1-(c_0\delta\tau/a)^2\sin^2(ka/2)}}. \tag{19}$$

At small ka, $v_g = c_0 + O(k^2a^2)$; near the Brillouin-zone edge it bends away from the continuum value. In more than one dimension the quartic term $\sum_r k_r^4$ in **(18)** distinguishes axes from diagonals. Thus a regular microscopic lattice generically predicts high-frequency dispersion and anisotropy. The scale a is not predicted until fixed by an independent part of the model, so no observational amplitude is claimed here.

4.4 Stability and the meaning of a mass gap

For the explicit update to have real ω for every lattice mode, the right side of **(17)** must not exceed $4/\delta\tau^2$. A sufficient free-field condition is

$$\frac{\delta\tau^2\Omega_0^2}{4} + d\left(\frac{c_0\delta\tau}{a}\right)^2 \le 1. \tag{20}$$

This is a concrete failure test: violating **(20)** produces unstable high-frequency modes in this benchmark.

Proposition 2 (Linear stability domain)**.** *For the free periodic hypercubic benchmark, all normal-mode frequencies are real if and only if*

$$0 \le \delta\tau^2 \left[\Omega_0^2 + \frac{4c_0^2}{a^2} \sum_r \sin^2(k_r a/2) \right] \le 4$$

for every lattice wave vector. Condition (20) *is the resulting worst-case criterion.*

Proof. The left side of (17) is $4\sin^2(\omega\delta\tau/2)/\delta\tau^2$. A real ω exists precisely when the dimensionless right side lies in $[0, 4]$. The maximum spatial eigenvalue is $4d$, attained at a Brillouin-zone corner, which gives (20). □

If a relativistic quantum field description is justified and an action-phase scale $\hbar_*$ has been independently fixed, the gap maps to an effective rest mass through

$$E^2 = \hbar_*^2\omega^2 \simeq c_0^2\hbar_*^2 k^2 + m_{\text{eff}}^2 c_0^4, \qquad m_{\text{eff}} = \frac{\hbar_*\Omega_0}{c_0^2}. \tag{21}$$

Equation (21) is a dictionary. It predicts no particle mass until Ω_0 is obtained from a fixed node model without using that mass.

Worked example: a result that is not fitted to nature

Choose lattice units $a = 1$, $\mu = 1$, $\kappa = 1$, $\Omega_0 = 0.4$, and $\delta\tau = 0.5$ in $d = 3$. Then $c_0 = 1$ and the stability number is

$$\frac{\delta\tau^2\Omega_0^2}{4} + 3\left(\frac{c_0\delta\tau}{a}\right)^2 = 0.01 + 0.75 = 0.76 < 1.$$

The entire free spectrum is therefore linearly stable. For a mode $\boldsymbol{k} = (\pi/3, 0, 0)$, (17) gives

$$\omega = \frac{2}{\delta\tau} \arcsin\left[\frac{\delta\tau}{2}\sqrt{\Omega_0^2 + 4\sin^2(\pi/6)}\right] \simeq 1.091,$$

whereas the leading continuum approximation gives $\sqrt{0.4^2 + (\pi/3)^2} \simeq 1.121$. The 2.7% difference is an internally predicted discretization effect for these chosen dimensionless parameters. It is not evidence about the physical universe because the parameters were not derived or calibrated to a real system.

Thought experiment 3: a wave crossing tiled space

Tap one tile and watch a long-wavelength ripple. Its speed depends on tile spacing, coupling stiffness, and tile inertia. Knowing only that updates happen every $\delta\tau$ does not tell you the ripple speed. The exact sine functions in (17) also show how a microscopic grid reveals itself: short waves bend away from the smooth relativistic relation and become direction-dependent. That deviation is a real prediction only after a, μ, κ are fixed elsewhere.

4.5 A gauge-invariant phase extension

The legacy theory emphasizes phase alignment. Let $\psi_i = \rho_i e^{i\theta_i}$ be a complex node coordinate and assign an oriented link variable $U_{ij} = e^{iqA_{ij}}$, with $U_{ji} = U_{ij}^{-1}$. The link difference

$$|D_{ij}\psi|^2 \equiv |U_{ij}\psi_j - \psi_i|^2 \tag{22}$$

is invariant under

$$\psi_i \to e^{iq\alpha_i}\psi_i, \qquad U_{ij} \to e^{iq\alpha_i} U_{ij} e^{-iq\alpha_j}. \tag{23}$$

For a closed plaquette $\Box$, $U_\Box = \prod_{(ij)\in\Box} U_{ij}$ is also invariant. A gauge sector may therefore contain

$$S_{\text{gauge}} = \beta \sum_{\Box} (1 - \operatorname{Re} U_\Box), \tag{24}$$

which has the Maxwell/Yang-Mills form in an appropriate continuum limit. A line integral of a phase alone does not establish gauge emergence; (22)–(24) state the missing structure.

Proposition 3 (Exact link-gauge invariance)**.** *The quantities $|D_{ij}\psi|^2$ and $\operatorname{Re} U_\Box$ are invariant under (23) at finite lattice spacing.*

Proof. The transformed link difference is

$$U'_{ij}\psi'_j - \psi'_i = e^{iq\alpha_i}(U_{ij}\psi_j - \psi_i),$$

whose norm is unchanged. In a closed loop the factor $e^{-iq\alpha_j}$ from one link cancels the factor $e^{iq\alpha_j}$ from the next, leaving $U_\Box$ unchanged. This proves exact kinematic gauge invariance, not emergence of the observed gauge group or its coupling values. $\Box$

5 Repair of the legacy amplitude-phase action

Several END drafts center on a real amplitude Φ and compact phase θ. That idea is retained, but the published legacy form cannot be canonical without repair. Its coefficient N_c was called dimensionless even though a standalone phase kinetic term requires a mass scale; $\Delta\theta$ was undefined; and $(\Box\Phi)^2$ generically gives fourth-time-derivative dynamics and an extra unstable degree of freedom unless treated through a controlled effective-field-theory prescription.

In natural units with metric signature $(+,-,-,-)$, a repaired low-energy representative is

$$\begin{aligned}\mathcal{L}_{\Phi\theta} = \frac{1}{2} Z_\Phi(\chi_\theta)\,\partial_\mu\Phi\,\partial^\mu\Phi - \frac{\lambda}{4}(\Phi^2 - v^2)^2 + \frac{f_\theta^2}{2}\,\partial_\mu\theta\,\partial^\mu\theta \\ - \frac{\eta a^2}{2}(\Delta_\perp\Phi)^2 + \mathcal{L}_{\text{links}} + \mathcal{L}_{\text{higher}},\end{aligned} \tag{25}$$

where $[\Phi] = [v] = [f_\theta] = \text{mass}$, θ is dimensionless, λ, η are dimensionless, and $\Delta_\perp$ is a spatial operator defined relative to the frame foliation. The local phase-mismatch measure is

$$\chi_{\theta,i} = \frac{1}{2z_i}\sum_{j\sim i}\left[1 - \cos(\theta_j - \theta_i - qA_{ij})\right], \qquad 0 \le \chi_{\theta,i} \le 1, \tag{26}$$

and the legacy modulation may be represented by

$$Z_\Phi(\chi_\theta) = 1 - 2\delta\chi_\theta, \qquad 0 \le \delta < \frac{1}{2}, \tag{27}$$

so the kinetic coefficient remains positive. The spatial $(\Delta_\perp\Phi)^2$ term preserves the intended lattice-dispersion correction without adding fourth time derivatives. It also makes explicit that exact Lorentz invariance is not assumed at the cutoff and must emerge at long wavelengths.

> Equation (25) is a candidate effective sector. It is not derived from the pre-geometric ontology, and it does not by itself generate fermions, gauge groups, Einstein gravity, a collapse law, or observed constants. Its scientific value is that every symbol now has a role, dimensions can close, and stability can be tested.

6 Continuum matching target

At scales large compared with the persistence length, a successful micro-model should match a local effective action. The most general conservative statement is

$$S_{\text{eff}} = \int \mathrm{d}^4x\sqrt{-g}\left[\frac{M_*^2}{2}(R-2\Lambda_*) + \mathcal{L}_{\text{gauge}} + \mathcal{L}_{\text{chiral}} + \mathcal{L}_{\text{scalar}} + \mathcal{L}_{\text{pat}} + \mathcal{L}_{\text{EQEF}} + \sum_{D>4}\frac{c_a^{(D)}\mathcal{O}_a^{(D)}}{M_{\text{cut}}^{D-4}}\right]. \quad (28)$$

This is a matching target, not a derivation. Writing the Standard Model and Einstein-Hilbert terms inside S_{eff} demonstrates compatibility only if the node dynamics actually generate their field content, symmetries, coefficients, anomalies, and controlled corrections.

6.1 Fermion mass bookkeeping

The former lexicon wrote an explicit fermion mass in the kinetic term and also generated mass from Yukawa couplings, which double-counts mass before symmetry breaking. In a chiral gauge stage the correct structure is

$$\mathcal{L}_{\text{chiral}} = \sum_f \bar{\psi}_f \mathrm{i}\gamma^\mu D_\mu \psi_f - \left(\bar{\psi}_L Y_H H \psi_R + \bar{\psi}_L Y_\Sigma \Sigma \psi_R + \text{h.c.}\right). \quad (29)$$

After H and Σ acquire vacuum expectation values,

$$M_f = \frac{v_H}{\sqrt{2}} Y_H + s_\Sigma Y_\Sigma + \cdots, \qquad U_L^\dagger M_f U_R = \operatorname{diag}(m_1, m_2, \ldots). \quad (30)$$

The equation becomes an END prediction only when the matrices on the right are computed from a fixed node operator. A texture chosen to match the observed singular values is a fit.

6.2 Relativity and gravity

Recovering an invariant speed from (17) is not yet general relativity. The required chain is

$$\text{graph observables} \longrightarrow e^a{}_\mu, \omega^a{}_{b\mu} \longrightarrow g_{\mu\nu} = \eta_{ab} e^a{}_\mu e^b{}_\nu \longrightarrow S_{\text{grav}}[e,\omega]. \quad (31)$$

The coarse-graining must produce universal coupling to stress-energy, a weak-field Newtonian limit, local Lorentz symmetry within bounds, and correction operators with fixed coefficients. Until this is done, "gravity is progression adjustment" is an interpretation and research direction, not a derivation of Einstein's equation.

6.3 Progression imbalance and torsion

In a Riemann-Cartan description, torsion is

$$T^\rho{}_{\mu\nu} = 2\Gamma^\rho{}_{[\mu\nu]}, \qquad T^a = \mathrm{d}e^a + \omega^a{}_b \wedge e^b. \quad (32)$$

It measures the infinitesimal non-closure of transported displacements:

$$\delta x^\rho = T^\rho{}_{\mu\nu}\,\delta A^{\mu\nu} + O(|\delta A|^{3/2}). \quad (33)$$

The ontology's progression imbalance can map to (32) if neighboring local frame translations fail to close after coarse-graining. This is a precise hypothesis. The theory must still derive $e^a{}_\mu$, $\omega^a{}_{b\mu}$, the torsion source, and the Wilson coefficients. Torsion is not interchangeable with curvature, energy, chaos, or EQEF.

Thought experiment 4: the non-closing postage stamp

Draw a tiny parallelogram by taking one local frame-step east, one north, then reversing both moves. In ordinary torsion-free geometry the loop closes to leading order. If different progression rules make the endpoint miss the start, the mismatch per enclosed area is torsion. This gives the word "progression imbalance" an observable geometric meaning instead of treating torsion as a metaphor.

7 EQEF: retained meaning and permitted mathematics

The Evans Quantum Energy Field is retained because the later ontology clearly defines its intended role: it tracks expressed versus deferred transition capacity and is a framework within END for progression imbalance, not a separate fundamental theory. Two levels must remain distinct.

7.1 Level 1: capacity ledger

Define the residual local capacity

$$r_i^n = 1 - \mathcal{C}_i^n, \qquad 0 \le r_i^n \le 1. \tag{34}$$

This is bookkeeping. It is dimensionless and is not automatically energy. If residual capacity is transported or deferred, a causal balance law may be postulated,

$$r_i^{n+1} - r_i^n + \sum_j J_{ij}^n = s_i^n, \tag{35}$$

where $J_{ij} = -J_{ji}$ is a link flux and s_i is a locally defined source. Equation (35) becomes physical only after J and s are derived from the update rule.

7.2 Level 2: optional continuum field

A coarse field $\chi(x) \propto \langle r_i - \bar{r} \rangle_R$ may be introduced if the coarse-graining supports it. A conservative effective ansatz is

$$\mathcal{L}_{\text{EQEF}} = -\frac{Z_\chi}{2} \nabla_\mu \chi \nabla^\mu \chi - V_\chi(\chi) - \frac{\xi}{2} \chi^2 R + \sum_b \frac{d_b \mathcal{Q}_b}{M_{\text{cut}}^{\Delta_b - 4}}. \tag{36}$$

This can behave as a slowly varying cosmological component for some V_χ, but that behavior is shared by many scalar-field models. END distinguishes itself only if the discrete map fixes Z_χ, V_χ, ξ, d_b or produces a relation that survives held-out data. A fitted constant term is not a solution to the cosmological-constant problem.

8 Quantum claims: what is retained and what remains open

The frame language provides useful interpretations:

- a wavefunction may summarize allowed or weighted coarse-grained continuations;
- entanglement may reflect a non-factorizable common preparation history;

- decoherence may reflect dispersal of phase information into many environmental patterns;
- measurement may involve stable amplification or localization.

None of these statements by itself derives quantum statistics.

8.1 Minimum probability structure

Let λ denote a complete ontic initial state, a, b measurement settings, and A, B outcomes. A deterministic completion supplies functions

$$A = A(a, b, \lambda), \qquad B = B(a, b, \lambda), \tag{37}$$

and an ensemble density $\rho(\lambda \mid a, b)$. It must calculate

$$P(A, B \mid a, b) = \int \mathrm{d}\lambda\, \rho(\lambda \mid a, b)\delta_{A,A(a,b,\lambda)}\delta_{B,B(a,b,\lambda)}. \tag{38}$$

To reproduce Bell-inequality violations, END must explicitly relax at least one assumption used in the Bell bound: locality/factorization, measurement independence, forward causal structure, or ordinary noncontextual outcome assignment. "Shared frame origin" with local measurement-independent updates is insufficient.

8.2 Born rule and localization threshold

A localization module requires a dimensionally defined diagnostic, scale, and state map:

$$\mathcal{T}_R[X_n] \geq \tau_R \quad \Longrightarrow \quad X_{n+1} = C_R[X_n], \tag{39}$$

plus proofs or numerical bounds for conservation, covariance, no-signaling at the operational level, and outcome frequencies. A threshold estimated from the energy needed to create a known particle is a calibration. A node-merging rule with a discretionary kick is not a deterministic physical law. The universal-threshold proposal is therefore retained as a conjecture module, not part of the validated core.

Thought experiment 5: the two boxes and the settings

Two separated boxes receive correlated patterns. Later, two experimenters independently choose settings. A common past can produce ordinary correlations, but Bell experiments exceed the limit for local, measurement-independent hidden variables. END must say exactly whether the settings were correlated with the hidden state, whether the response is nonlocal, whether future constraints matter, or whether another standard assumption fails. Without that choice and Equation (38), saying "the frames remember" does not solve the problem.

9 Constants: definitions, calibrations, and predictions

The correct scientific classification is summarized in Table 1. SI numerical values of c and h define units; reproducing them after choosing lattice units is not a prediction. Dimensionless ratios are preferred targets, but even a ratio is not predicted if free microscopic overlaps are tuned to it.

9.1 The non-circularity protocol

Definition 1 (Non-circular derivation)**.** A quantity Q is derived from END/MNT only if a frozen microscopic specification $\mathfrak{M} = (\mathcal{X}, G, U, \mathcal{C}, C_R, \boldsymbol{p})$, none of whose inputs were chosen using the measured value of Q, implies a unique prediction $Q = F_Q(\mathfrak{M})$ with uncertainty and domain of validity. If data for Q select any component of $\boldsymbol{p}$, the result is calibration. If a continuum coefficient is identified by matching two descriptions, the result is matching. If a unit convention fixes the numerical value, the result is a definition.

A reproducible calculation therefore needs four ledgers: an input ledger listing parameters, priors, units, boundary conditions, and data used to choose them; a derivation ledger showing the operator or update from which the output follows; a calibration ledger naming observables used to set scales or couplings; and a hold-out ledger naming observables that were not inspected until the model was frozen.

The *no free lunch* test is simple: after calibrating p independent combinations, the framework must predict more than p independent quantities and outperform an appropriate simpler baseline. Rewriting the p calibrators in new notation adds no predictive information.

9.2 Worked case A: propagation speed

From the free lattice spectrum, the long-wavelength coefficient is

$$c_0^2 = a^2 \frac{\kappa}{\mu}. \tag{40}$$

This is a genuine derivation inside the benchmark because it follows from the discrete action. It is not yet a numerical prediction of the physical speed of light. There are three logically different uses:

1. If a, κ, μ are fixed independently, (40) predicts c_0.
2. If the measured invariant speed is used to set $\kappa/\mu = c^2/a^2$, the relation calibrates one parameter combination.
3. If length and time units are chosen so $c = 1$, no physical parameter has been predicted.

The kinematic ratio $a/\delta\tau$ is an upper update scale, not the wave speed unless $\kappa/\mu = 1/\delta\tau^2$. The earlier statement $c = a/\delta\tau$ silently assumed that extra equality. Moreover, a viable relativistic limit requires every low-energy massless sector to share the same limiting cone; deriving c_0 for one scalar is not enough.

9.3 Worked case B: a dimensionless mass ratio

The cleanest potential predictions are dimensionless. On a cycle graph C_N, the Laplacian eigenvalues are

$$\lambda_m = 4\sin^2\left(\frac{\pi m}{N}\right), \qquad m = 0, \ldots, N-1. \tag{41}$$

For a linear branch with $\Omega_m^2 = \Omega_0^2 + (\kappa/\mu)\lambda_m$, the effective mass dictionary (21) gives

$$\frac{m_r}{m_s} = \frac{\Omega_r}{\Omega_s}. \tag{42}$$

Choose a fully declared toy model $N = 8$, $\Omega_0 = 1$, and $\kappa/\mu = 1$ in lattice units. Then

$$\lambda_1 = 4\sin^2(\pi/8) = 2 - \sqrt{2}, \qquad \lambda_2 = 4\sin^2(\pi/4) = 2,$$

and

$$\frac{m_2}{m_1} = \sqrt{\frac{1+\lambda_2}{1+\lambda_1}} = \sqrt{\frac{3}{3-\sqrt{2}}} \simeq 1.375. \tag{43}$$

No measured mass was used, so (43) is a first-principles output of that toy model. It is not a prediction for any known pair of particles: the graph, branch identification, and parameters were chosen for illustration. A physical claim would require those ingredients to arise from the canonical micro-model before particle data are examined.

9.4 Worked case C: action-phase conversion and Planck's constant

Suppose a coarse mode has a physical phase advance $\Delta\varphi$ and a discrete action increment ΔS. One may define

$$\hbar_* = \frac{\Delta S}{\Delta\varphi}, \qquad E = \hbar_* \omega, \tag{44}$$

provided the ratio is constant across amplitudes, modes, preparations, and scales in the quantum regime. Equation (44) is a matching definition until the microdynamics derive both the physical phase measure and a universal ratio. Choosing $\hbar_* = \hbar_{\mathrm{SI}}$ from one atomic transition calibrates the action scale. The non-circular test is then whether the same fixed $\hbar_*$ predicts other interference, spectra, and quantum probabilities. No supplied END/MNT source completes that test.

9.5 Worked case D: gauge coupling and the fine-structure constant

For a compact $U(1)$ Wilson sector in Euclidean signature, choose the convention

$$S_g = \beta \sum_{\square} (1 - \cos\theta_\square), \qquad \theta_{\mu\nu}(x) = a^2 F_{\mu\nu}(x) + O(a^3). \tag{45}$$

Expanding at weak curvature gives

$$S_g = \frac{\beta}{4} \int \mathrm{d}^4x \, F_{\mu\nu}F^{\mu\nu} + O(a^2 F\partial^2 F, a^4 F^4). \tag{46}$$

Matching the continuum normalization $S = (4e_0^2)^{-1} \int F^2$ yields

$$e_0^2 = \frac{1}{\beta}, \qquad \alpha_0 = \frac{e_0^2}{4\pi} = \frac{1}{4\pi\beta}. \tag{47}$$

This is a clean matching relation, not a numerical derivation of α, because β is currently free. A prediction requires the node dynamics to fix β, the charged field content, threshold corrections, and renormalization flow; the resulting $\alpha(\mu)$ must then be compared at a held-out scale. Setting $\beta = 1/(4\pi\alpha_{\mathrm{obs}})$ is calibration.

9.6 Worked case E: gravitational strength

If coarse-graining produces the Einstein–Hilbert term in natural units,

$$S_{\mathrm{grav}} = \frac{M_*^2}{2} \int \mathrm{d}^4x \sqrt{-g}\, R, \qquad G_{\mathrm{eff}} = \frac{1}{8\pi M_*^2}. \tag{48}$$

If dimensional analysis of a lattice calculation gives $M_*^2 = Z_R/a^2$ with a computed dimensionless stiffness Z_R, then

$$G_{\mathrm{eff}} = \frac{a^2}{8\pi Z_R} \tag{49}$$

in the same natural-unit convention. Equation (49) becomes a prediction only if a and Z_R are fixed without using G. Defining a to be the Planck length, $a^2 = \hbar G/c^3$, and then solving (49) for G is circular because G entered the definition of a.

9.7 Cosmological term and the absence of a present solution

At the effective level, vacuum contributions have the schematic structure

$$\Lambda_{\text{eff}} = \Lambda_{\text{bare}} + \frac{\rho_{\text{vac}}}{M_*^2} + \Delta\Lambda_{\text{EQEF}} + \Delta\Lambda_{\text{grav}} + \cdots . \tag{50}$$

Fitting one term to cancel the others and leave the observed residual is fine tuning, not derivation. A first-principles END/MNT solution would need a symmetry, constraint, sequestering mechanism, or dynamical attractor that fixes the residual without using late-time expansion data and remains stable under radiative corrections. No such mechanism is present in the supplied corpus.

9.8 SI defining constants, Planck units, and dependent quantities

The numerical SI values of c, h, e, and k_B are exact defining constants of the unit system. A microscopic theory can explain why physical relations contain invariant conversions corresponding to them, but recovering their SI digits after the units have been defined is not an independent prediction. The reduced Planck constant is $\hbar = h/(2\pi)$.

Likewise, the Planck length, time, mass, energy, temperature, charge, current, voltage, area, and luminosity are dimensional combinations of a smaller set of constants. Once $c, \hbar, G, k_B, \epsilon_0$ are specified, calculating Planck units is unit algebra, not a series of new confirmations. In the modern SI,

$$\alpha = \frac{e^2}{4\pi\epsilon_0\hbar c}, \qquad \mu_0\epsilon_0 c^2 = 1. \tag{51}$$

Thus ϵ_0 and μ_0 are not independent targets once the exact defining constants and measured dimensionless α are supplied. The Hubble constant is a cosmological parameter inferred from observations, not a fundamental conversion constant.

Table 1: Status of constants in the reconstructed framework.

Quantity	Model relation	Current status	Requirement for a derivation
c	$c_0 = a\sqrt{\kappa/\mu}$ in the benchmark long-wave sector	One parameter combination is calibrated to the invariant speed; $a/\delta\tau$ is only a kinematic scale	Derive a, κ, μ independently and prove universal coupling of all massless modes
$\hbar$	$\Delta S = \hbar_*\Delta\varphi$, $E = \hbar_*\omega$ after a quantum map exists	Action-phase conversion and unit calibration	Derive the phase measure and show one universal $\hbar_*$ governs all quantum sectors
G	$M_*^{-2} = 8\pi G_{\text{eff}}$ in (28)	Effective Wilson coefficient, not yet derived	Coarse-grain a fixed micro-model to the Einstein-Hilbert term and predict the coefficient after non-gravitational calibration

Quantity	Model relation	Current status	Requirement for a derivation
Λ	Coefficient of $\sqrt{-g}$ plus vacuum contributions	Unresolved; fitting an EQEF constant is not a solution	Produce a stable cancellation or symmetry mechanism without inserting observed expansion data
$\alpha(\mu)$	$\alpha = e_R^2/(4\pi)$ in natural rationalized units	Gauge coupling plus standard running; generic overlaps are free	Compute the bare coupling and field content from fixed node dynamics, then run to a held-out scale
Masses	Rest-energy or stability eigenvalues; e.g. (21), (30)	Structural templates only	Fix the operator, boundary conditions, and parameters; calibrate at most an allowed scale; hold out the remaining spectrum
Decay rates	Amplitudes and phase space, such as $\Gamma_\mu \propto G_F^2 m_\mu^5$	Standard EFT scaling, not END-specific	Derive masses and couplings from the same frozen micro-model and compute the full numerical coefficient

10 What would happen in the benchmark if its assumptions hold?

The following statements are deliberately ranked. A theorem is proved from the benchmark equations. A generic expectation follows for a broad class of nonlinear choices but is not universal. A physical prediction requires a complete parameter map to observations.

10.1 Long waves look smoother than short waves

By (18), a gapless branch satisfies

$$\omega^2 = c_0^2|\boldsymbol{k}|^2 + O(a^2k^4, \delta\tau^2\omega^4).$$

Thus sufficiently long waves propagate approximately as continuum relativistic modes. Short waves reveal the substrate through dispersion and, on a regular cubic graph, direction dependence. This is a theorem about the benchmark. The observable frequency at which the deviation appears is not known because a and the clock map are not derived.

10.2 Gapped modes behave as massive collective excitations

For $\Omega_0 > 0$, the zero-momentum frequency is nonzero. If the action-phase and relativistic dictionaries are valid, (21) maps this spectral gap to a rest mass. The existence of a gap is proved for the linear benchmark; its identification with a particle requires a localized stable pattern, quantum normalization, and detector map.

10.3 Nonlinearity produces amplitude-dependent clocks

Consider the spatially uniform mode with $W(q) = \lambda_4 q^4/4$. In the continuum-time approximation it obeys

$$\ddot{q} + \Omega_0^2 q + \frac{\lambda_4}{\mu} q^3 = 0. \tag{52}$$

For small amplitude A, harmonic balance gives

$$\Omega(A) = \Omega_0 \left[1 + \frac{3\lambda_4 A^2}{8\mu\Omega_0^2} + O(A^4)\right]. \tag{53}$$

Positive λ_4 hardens the oscillation and negative λ_4 softens it within the stable range. If physical clocks are built from such patterns, local load can alter their operational rate. Equation (53) demonstrates a mechanism for load-dependent ticking, but it is not yet gravitational time dilation: universality across all clock types and the metric response remain to be derived.

10.4 Capacity saturation changes the high-load evolution

Whenever the tentative kinetic demand exceeds $E_* - S_i^n$, the limiter (13) forces $\widetilde{\mathcal{C}}_i^n = 1$ and reduces the local velocity magnitude. The immediate result is proved by construction. Repeated activation will generally introduce amplitude-dependent propagation, reflection, or dissipation, but the mixture depends on the final conservation-compatible completion. This is where progression imbalance could become a measurable phenomenon, and where the model could also fail through unacceptable energy loss.

10.5 Gauge loops carry exact invariant information

The plaquette product $U_\square$ is invariant at finite spacing, not only in the continuum. Nontrivial loop holonomy can therefore label flux-like sectors in a compact phase model. Whether those sectors are stable, confined, deconfined, chiral, or related to observed charges depends on the gauge action and matter content. Exact invariance is proved; the Standard Model identification is conjectural.

First forecast hierarchy. The benchmark most robustly forecasts a smooth long-wave sector plus lattice corrections at short wavelength. With nonlinearities it generically forecasts amplitude-dependent frequencies. With an active capacity limiter it forecasts a high-load departure from the uncapped dynamics. These become physical predictions only after one immutable parameter set converts lattice scales to clocks, metres, energies, and detector observables.

11 Keep, refine, demote, and discard

11.1 Ideas retained in the canonical core

- Relational pregeometry with no assumed physical metric.
- Ordered frames as stabilized coarse-grained configurations.
- Space as persistent weighted relations; the node lattice as an emergent phase.
- Deterministic local dynamics as the intended micro-level structure.
- Finite local transition capacity as the fundamental limit.
- Stable and transportable node patterns as candidates for particles and fields.

- Phase alignment as a potentially important interaction variable.
- EQEF as expressed/deferred capacity bookkeeping.
- Progression imbalance as a candidate microscopic origin of torsion.
- Cross-domain parameter closure, non-circular calibration, and held-out falsification as methodological requirements.

11.2 Ideas retained only after refinement

Earlier wording	Canonical refinement
Energy is frame-to-frame change	Change is a microscopic correlate. Effective energy is the Hamiltonian or Noether charge associated with time translation and must have conserved, measurable units.
$t = n\delta\tau$	n is update order. Physical time is read by clock patterns; a constant $\delta\tau$ is a homogeneous approximation.
$c = \ell_0/\delta\tau$	This is a possible causal ceiling. The propagation speed follows from the dispersion relation and depends on stiffness and inertia.
Global capacity	A local dimensionless capacity $\mathcal{C}_i \leq 1$, with regional sums and causal transport.
Mass is progression load or resonance inertia	Qualitative interpretation only; quantitatively mass is a rest-energy gap or eigenvalue of a specified stability operator.
Charge is phase or helicity	Candidate topological interpretation; quantitatively charge is a representation label of an exact gauge symmetry.
Line-integral phase gives electromagnetism	Replace with link transformations and plaquette curvature as in **(22)–(24)**.
Legacy $(\Box\Phi)^2$ gravity term	Remove from the fundamental action; use a stable spatial lattice correction or a controlled EFT with extra degrees and a declared cutoff. It does not derive gravity.
EQEF explains dark energy	EQEF may generate a coarse scalar sector, but the action and coefficients must be derived before any cosmological claim.
Torsion is progression imbalance	Map the non-closure of local frame translations to $T^{\rho}{}_{\mu\nu}$ and derive the connection, source, and coefficients.
Structural proofs and global validation	Rename as derivation templates and validation protocols until numerical, reproducible results exist.

11.3 Claims demoted to the conjecture queue

The following may motivate later models but are not consequences of the current theory: a universal objective-collapse threshold; a derived Born rule; an EQEF origin for late acceleration; modified gravity replacing some or all dark matter; high-frequency photon or gravitational-wave dispersion; post-merger echoes; singularity resolution; black-hole information recovery; a normal neutrino hierarchy; no low-scale supersymmetry; a special 3+1-dimensional stability mechanism; and laboratory control of vacuum, inertia, mass, or progression.

Each conjecture may re-enter the main theory only with a unique equation, parameter provenance, numerical target, and falsifier.

11.4 Claims discarded from the scientific record

- All aggregate "over 90%" and "99.98%" alignment statements lacking a defined loss, covariance, parameter count, code, and held-out data.
- Numerical Planck-mass, G, weak-coupling, Higgs-VEV, fine-structure, axion, neutrino, and baryogenesis "derivations" that substitute measured inputs, have inconsistent dimensions, or disagree by orders of magnitude and are nevertheless called aligned.
- The formula $G = \hbar/c^3$ with an ad hoc node-velocity correction; it is dimensionally wrong.
- The claim that $10^{-122}\,\mathrm{m}^{-2}$ is the observed cosmological constant; 10^{-122} is the approximate dimensionless Planck-unit scale, not an inverse-square-metre value.
- Particle masses obtained by choosing $\omega = mc^2/\hbar$ from the measured mass.
- The Higgs formula and fit in the two-page JRE-MNT-PRL draft, whose parameters include measured constants and whose displayed expression does not have mass dimensions as written.
- Unfrozen resonance targets at 250 GeV, 1.5 TeV, 2–5 TeV, or 13.037 TeV; associated widths, cross-sections, and branching ratios.
- The claim that a Z-like spin-1 state can decay to two on-shell photons under ordinary assumptions.
- The two-node toy model as a "proof" of END. Its potential was chosen by hand, and the printed small-oscillation calculation contained a derivative and dimensional error.
- Pseudocode that inserts optional damping, random perturbations, externally supplied fields, arbitrary softening, and node merging while calling the result the fundamental deterministic update.
- Assertions that standard-model or Lambda-CDM calculations using their measured parameters validate END.
- Claims that ordinary redshift moves a Planck-frequency mode into the LIGO band without a transfer mechanism.
- Claims of controlled energy extraction, anti-gravity, mass modulation, propulsion, or vacuum engineering without an interaction Hamiltonian and safety analysis.

12 Relationship to established discrete and emergent frameworks

END/MNT is not made credible by resemblance alone, but comparison prevents the framework from relabeling known machinery as a new derivation.

Causal order and pregeometry. Causal-set theory begins with a locally finite order and asks how continuum spacetime can emerge [5]. END/MNT similarly distinguishes update order from metric time, but adds a persistence/coarse-graining criterion and local transition-capacity hypothesis. It has not yet supplied the reconstruction results available in mature causal-set work.

Discrete geometry. Regge calculus encodes curvature on a simplicial geometry [4]. END/MNT instead proposes that even the graph and its metric emerge from persistent relations. If a simplicial phase appears, Regge variables could provide a disciplined intermediate description rather than being rederived informally.

Lattice gauge theory. Wilson's link and plaquette construction demonstrates how exact gauge invariance can survive finite spacing [3]. The phase sector in this monograph deliberately adopts that proven architecture. This does not make gauge symmetry an END/MNT prediction; it states the minimum structure any phase-based derivation must reproduce.

Finite propagation from locality. Lieb–Robinson bounds show that broad classes of local lattice systems possess an effective causal cone even when the microscopic formulation is not relativistic [10]. END/MNT's local capacity may further constrain propagation, but it must derive its own bound for the chosen nonlinear update. Calling the update local is not enough.

Effective field theory. The principle that long-distance observables are organized by symmetry and operator dimension is standard effective-field-theory reasoning [11]. Equation (28) is therefore a target and bookkeeping device, not evidence that the microscopic model generates its coefficients.

Chirality and quantum no-go results. A lattice model claiming the Standard Model must confront fermion doubling and anomaly cancellation [8]. A deterministic model claiming quantum completion must identify which Bell assumption changes and reproduce the observed correlations [6, 7]. These are design constraints, not optional philosophical objections.

Torsion. Riemann–Cartan and Einstein–Cartan theory give torsion a precise geometric and dynamical meaning [9]. END/MNT's progression imbalance becomes more than analogy only if its coarse translation operators yield the non-closure in (33) and the resulting field equations.

Novelty presently claimed. The potentially distinctive combination is an ontology of stabilized frames and emergent relational graphs constrained by finite local transition capacity, with EQEF as the ledger of expressed and deferred capacity. The discrete scalar and gauge mathematics used to benchmark that ontology is intentionally standard. Novel physics would lie in a uniquely derived capacity-preserving update and its cross-domain consequences, which do not yet exist.

13 Falsification and build programme

The programme should proceed in gates. Passing a later gate cannot compensate for failure at an earlier one.

Gate	Deliverable	Required evidence	Failure condition
0	Canonical specification	Exact $\mathcal{X}, G, U, \mathcal{C}, C_R$; units; boundary conditions; parameter file; supersession ledger	An object or equation remains multiply defined or dimensionally inconsistent
1	Mathematical closure	Well-posedness, capacity preservation, conserved quantities, stability domain, deterministic reference trajectory	Non-unique evolution, runaway modes, or uncontrolled constraint violation
2	Continuum benchmark	Dispersion, anisotropy, spectral dimension, convergence across at least three resolutions	Corrections fail to shrink as predicted or exceed laboratory bounds
3	Gauge and pattern sector	Exact lattice symmetry; anomaly-safe chiral implementation; stable localized solutions; interaction amplitudes	Gauge-dependent observables, unresolved doubling/anomalies, or no robust patterns

4	Quantum completion	Preparation, measure, settings, outcomes, Bell assumption, Born frequencies, no-signaling test	Failure to reproduce full correlations or undisclosed measurement dependence/nonlocality
5	Gravity and EQEF	Derived tetrad/metric/connection; Newtonian and Einstein limits; torsion and EQEF coefficients	Non-universal free fall, unstable extra modes, or incompatible propagation
6	Frozen external predictions	Versioned code, training/held-out policy, preregistration, likelihood, baselines, uncertainty and falsifier	Parameters change after data inspection or predictive performance is not better than baseline

13.1 First executable project

The shortest honest route is the scalar/phase benchmark, not a global particle-and-cosmology fit.

1. Implement (11) on square, cubic, and approximately isotropic irregular graphs.
2. Verify (17) numerically and map the stability boundary (20).
3. Add the link sector (22)–(24); unit-test exact gauge invariance.
4. Select one capacity-preserving variational completion and prove or numerically bound its conservation residuals.
5. Search for stable localized nonlinear patterns with parameters frozen before examining any particle masses.
6. Report dimensionless gaps and scattering data. Only then decide whether any pattern can be compared with a physical species.

This project can fail decisively and cheaply. That is an advantage: it tests the theory's distinctive machinery before large claims are attached to it.

14 Limitations and present conclusion

The reconstructed framework does not yet establish that the pre-geometric layer uniquely produces frames, that the frame graph becomes 3+1-dimensional Lorentzian spacetime, that the capacity limit has the form (7), or that the scalar/phase benchmark is the correct microphysics. It does not yet contain a capacity-preserving completion, chiral fermions, anomaly cancellation, a quantum probability rule, a Bell-compatible causal model, a gravitational coarse-graining theorem, or a parameter-fixed new signal.

What has been achieved is narrower and more durable. The ontology has been made internally ordered; the central notions now have operational definitions; a concrete benchmark possesses an exact update, dispersion relation, and stability condition; the phase/gauge idea has a correct lattice implementation; the legacy higher-derivative and dimensional problems have been removed; EQEF and torsion have been separated and assigned testable mathematical meanings; and unsupported numerical claims have been retired.

The resulting scientific proposition is:

Observed physics may arise from persistent relational patterns in a deterministic sequence of locally capacity-limited configurations. A node lattice is an emergent stable phase of that process. The proposition is viable only if one frozen micro-model derives its continuum observables, quantum statistics, and gravitational response with fewer independent inputs than the phenomena it predicts.

This is not weaker than an unfalsifiable declaration of completion. It is the version of END/MNT that can be calculated, criticized, reproduced, and, if nature disagrees, discarded.

Methods and declarations

Source-concordance method. Twenty-two supplied PDFs were converted to layout-preserving text and compared by date, definition, equation, and claim. Exact duplicate files were counted once for scientific content. The November 2025 ontology was treated as the controlling conceptual source; the August 2026 audit controlled evidentiary standards; mathematical statements were independently checked for dimensions, sign consistency, locality, and circularity. Older items were retained only when they could be mapped to the controlling ontology without contradiction.

No empirical analysis. No experimental data were analyzed and no new numerical fit is reported. Consequently this document makes no empirical-validation claim.

Code availability. No canonical END/MNT simulator or immutable parameter set existed in the supplied materials. The benchmark equations in this paper are sufficient to begin an implementation, but code and tests must be archived before computational results are claimed.

Data availability. The source corpus consists of author-supplied working manuscripts listed in Appendix B. Public experimental datasets mentioned in older drafts were not treated as evidence in this reconstruction.

Use of generative AI. Generative AI assisted source comparison, mathematical consistency checking, organization, and drafting under the author's direction. It is not an author. Ryan remains responsible for verifying the scientific content, equations, references, and final claims. Any later computational result must be regenerated from archived code rather than accepted from conversational output.

Author contributions. Ryan: conceptualization, original theory development, source provision, review, and final scientific accountability.

Funding. No institutional funding is declared for this reconstruction.

Competing interests. The author declares no competing interests.

Part III — Constants Examined

15 Scope, result, and the meaning of first principles

This part audits exactly 275 entries drawn from the complete 2022 CODATA listing. As of 6 August 2026, the 2022 adjustment remains the latest recommended set published by NIST; the next scheduled adjustment is the 2026 adjustment. The source table contains 355 rows. To avoid counting reciprocal unit conversions as independent physical successes, this study removes all 56 rows whose names end in "relationship" and 24 alternate-unit duplicates: eight particle mass energies in MeV, four Bohr-magneton renderings, four nuclear-magneton renderings, five MHz/T gyromagnetic renderings, and three Planck-constant renderings in alternate high-energy units. The retained list is alphabetical and the selection is generated by code.

Headline result. Of the 275 examined quantities, **zero** currently qualify as numerical first-principles predictions of END/MNT. The audit classifies 7 as SI definitions, 12 as conventions, 209 as dependent laws or identities, 35 as adjusted empirical inputs, and 12 as material/reference-dependent quantities. The code reconstructs 228 numerical values from declared dependencies and leaves 47 without a non-circular numerical reconstruction. A successful reconstruction tests algebra and data handling; it is not new physical evidence because CODATA inputs occur on the right-hand side.

That conclusion is not a rhetorical downgrade. It is the scientifically usable answer to the question the older drafts could not cleanly answer. A dimensional constant has a numerical value only after a unit system is chosen. A dependent constant may be calculated exactly from a smaller empirical basis. A measured constant may be estimated by experiment and theory. Only a held-out, dimensionless output of a frozen microscopic specification can provide a strong first-principles test.

15.1 The four-level derivation ladder

For every quantity Q, this manuscript distinguishes four levels:

1. **Definition or convention:** $Q \equiv Q_0$. The number fixes a unit or reference condition. It cannot confirm a microscopic theory.
2. **Dependency:** $Q = f(B_1, \dots, B_r)$, where one or more basis values B_i are measured or defined. This is a valid derivation of a dependent quantity, but not a prediction of the basis.
3. **Calibration or matching:** data for Q choose a free model combination. The theory has learned Q; it has not predicted it.
4. **Prediction:** a preregistered, frozen $\mathfrak{M}$ yields $Q_{\mathrm{END}} = F_Q(\mathfrak{M})$ without using Q_{CODATA} or an algebraically equivalent datum.

The operational acceptance test is

$$z_Q = \frac{Q_{\mathrm{END}} - Q_{\mathrm{ref}}}{\sqrt{u_{\mathrm{END}}^2 + u_{\mathrm{ref}}^2}}, \qquad \Delta_Q = \frac{Q_{\mathrm{END}} - Q_{\mathrm{ref}}}{Q_{\mathrm{ref}}}, \tag{54}$$

but neither residual is defined when no independent Q_{END} exists. Substituting the CODATA value into a hidden parameter and obtaining $z_Q = 0$ is circular.

16 The core END/MNT equation and its constant map

The benchmark scalar update is

$$q_i^{n+1} = 2q_i^n - q_i^{n-1} - \frac{\delta\tau^2}{\mu}\left[W'(q_i^n) + \kappa\sum_j w_{ij}(q_i^n - q_j^n)\right]. \tag{55}$$

It follows from the discrete action already derived in Part II. Every term has an explicit role: $\delta\tau$ is the benchmark update interval, μ normalizes inertia, W fixes onsite dynamics, κw_{ij} couples neighboring states, and two consecutive frames provide initial data. The exact free spectrum on a regular lattice is

$$\frac{4}{\delta\tau^2}\sin^2\left(\frac{\omega\delta\tau}{2}\right) = \Omega_0^2 + \frac{4\kappa}{\mu}\sum_{r=1}^{d}\sin^2\left(\frac{k_r a}{2}\right). \tag{56}$$

At long wavelength, the candidate limiting speed and gap dictionary are

$$c_0 = a\sqrt{\kappa/\mu}, \qquad m_{\text{eff}}c_0^2 = \hbar_*\Omega_0. \tag{57}$$

These relations are genuine consequences of the benchmark. They are not yet numerical predictions of c, $\hbar$, or any particle mass because $a, \delta\tau, \kappa, \mu, \Omega_0$, the clock map, and $\hbar_*$ are not derived from a unique pre-geometric update.

16.1 Why dimensions cannot be predicted one at a time

Suppose a calculation uses dimensionless lattice coordinates $\hat{x}, \hat{t}$ and produces a dimensionless gap $\hat{\Omega}$. A physical conversion requires scales L_*, T_*, S_*:

$$x = L_*\hat{x}, \qquad t = T_*\hat{t}, \qquad S = S_*\hat{S}, \qquad E = \frac{S_*}{T_*}\hat{E}. \tag{58}$$

Changing L_* and T_* changes the SI digits of every dimensional output while leaving the dimensionless simulation unchanged. Therefore the scientifically strong targets are dimensionless quantities such as α, mass ratios, mixing angles, normalized cross sections, and critical exponents. One may calibrate a minimal dimensional scale, but the remaining independent ratios must be held out.

17 Reproducible dependency algebra

The CODATA table is self-consistent rather than a list of 355 independent facts. A compact basis generates many listed quantities. Examples include

$$\hbar = \frac{h}{2\pi}, \qquad \mu_\text{B} = \frac{e\hbar}{2m_e}, \qquad a_0 = \frac{\hbar}{\alpha m_e c}, \tag{59}$$

$$E_\text{h} = \alpha^2 m_e c^2, \qquad R_\infty = \frac{\alpha^2 m_e c}{2h}, \qquad r_e = \frac{\alpha\hbar}{m_e c}, \tag{60}$$

$$\sigma_\text{T} = \frac{8\pi}{3}r_e^2, \qquad \epsilon_0 = \frac{e^2}{4\pi\alpha\hbar c}, \qquad \mu_0 = \frac{1}{\epsilon_0 c^2}, \tag{61}$$

$$K_\text{J} = \frac{2e}{h}, \qquad R_\text{K} = \frac{h}{e^2}, \qquad \Phi_0 = \frac{h}{2e}, \tag{62}$$

$$F = N_\text{A}e, \qquad R = N_\text{A}k_\text{B}, \qquad \sigma = \frac{2\pi^5 k_\text{B}^4}{15h^3c^2}. \tag{63}$$

The catalog evaluates these relations with double-precision arithmetic from one immutable 2022 table. A fractional residual near the source rounding level confirms the dependency implementation. It does not supply independent evidence for END/MNT.

17.1 Uncertainty propagation

For a dependent quantity $Q = f(\mathbf{B})$ with covariance matrix $\mathbf{C}$, the correct first-order uncertainty is

$$u^2(Q) = \nabla f(\mathbf{B})^T \mathbf{C} \, \nabla f(\mathbf{B}). \tag{64}$$

Ignoring correlations can overstate or understate precision. The per-entry register reports CODATA's published standard uncertainty and a deterministic numeric residual, but it does not recompute the full covariance matrix. Any future END/MNT fit must archive both its model covariance and CODATA covariance before quoting a z score.

18 Worked non-circular examples

18.1 Example 1: speed is a benchmark consequence but its SI value is a calibration

Expanding $\sin x = x + O(x^3)$ in (56) yields

$$\omega^2 = \Omega_0^2 + \frac{\kappa a^2}{\mu} |\mathbf{k}|^2 + O(a^4 k^4, \delta\tau^2 \omega^4),$$

so $c_0^2 = \kappa a^2/\mu$. This is first principles relative to the benchmark action. It becomes a physical prediction only if a, κ, μ, the clock, and the universal coupling of all massless sectors are fixed independently. Setting $\kappa/\mu = c^2/a^2$ from the exact SI value is calibration.

18.2 Example 2: the fine-structure constant exposes circularity quickly

In SI,

$$\alpha = \frac{e^2}{4\pi\epsilon_0 \hbar c}.$$

Because e, h, c are exact SI definitions while α is adjusted, the modern SI value of ϵ_0 is dependent on α. Solving the same equation for α after taking ϵ_0 from CODATA merely reverses the dependency. END/MNT must instead compute a dimensionless renormalized gauge coupling from its link action, including matter content and scale running.

18.3 Example 3: Bohr radius, Hartree energy, and Rydberg constant

Given the empirical basis (α, m_e) and exact conversions (c, h),

$$a_0 = \frac{\hbar}{\alpha m_e c}, \qquad E_\mathrm{h} = \alpha^2 m_e c^2, \qquad R_\infty = \frac{E_\mathrm{h}}{2hc}.$$

All three agree with CODATA when evaluated from that basis. The three agreements count as three algebra checks, not three independent predictions. END/MNT would earn predictive credit only if its frozen spectrum supplied α and m_e/m_* while a permitted single scale calibration fixed m_*, after which atomic data remained held out.

18.4 Example 4: Planck units do not derive gravity

$$\ell_{\rm P} = \sqrt{\frac{\hbar G}{c^3}}, \quad t_{\rm P} = \frac{\ell_{\rm P}}{c}, \quad m_{\rm P} = \sqrt{\frac{\hbar c}{G}}.$$

These are useful composite scales. Defining the node spacing $a = \ell_{\rm P}$ and then claiming to have derived G is algebraic inversion, because G entered $\ell_{\rm P}$. The non-circular route is to coarse-grain a fixed micro-model, compute the Einstein-Hilbert coefficient, and compare its dimensionless ratio to a separately calibrated matter scale.

18.5 Example 5: blackbody constants are dependent thermodynamic checks

The Planck spectrum yields $c_1 = 2\pi hc^2$, $c_2 = hc/k_{\rm B}$, and $\sigma = 2\pi^5 k_{\rm B}^4/(15h^3c^2)$. Wien's constants add only dimensionless transcendental roots. These values are exact or dependent in the modern SI. A deeper theory must derive the existence of thermal ensembles, photon statistics, and the Planck spectrum; reproducing the conversion factors after importing $h, k_{\rm B}, c$ is not enough.

18.6 Example 6: particle masses and mass ratios

For any two candidate stable patterns a, b, the benchmark would predict

$$\frac{m_a}{m_b} = \frac{\Omega_a}{\Omega_b}$$

only after the same universal $\hbar_*$ and c_0 map both gaps and after radiative corrections are controlled. The ratio is attractive because dimensional calibration cancels. The present papers do not identify electron, muon, proton, neutron, or nuclei as unique solutions; their CODATA masses therefore remain empirical targets.

18.7 Example 7: gravitational strength

If coarse-graining generated $M_*^2 R/2$ and the calculation gave $M_*^2 = Z_R/a^2$, then $G_{\rm eff} = a^2/(8\pi Z_R)$ in the same natural-unit convention. This is predictive only if a and Z_R follow from non-gravitational parts of the model. The current corpus supplies neither the coarse-graining map nor Z_R.

18.8 Example 8: Fermi coupling and weak mixing

The Fermi coupling is an effective low-energy coefficient inferred largely from weak-decay observables, while the weak mixing angle depends on a renormalization scheme and scale. END/MNT must generate the electroweak gauge group, symmetry breaking, chiral representations, anomaly cancellation, and renormalization flow before either can be predicted. Labeling a node coefficient G_F or θ_W is parameter naming, not derivation.

19 Audit classes and counts

Code	Meaning	Count	Predictive interpretation
D	SI definition	7	Exact digits define units; no empirical prediction credit
C	Convention	12	Exact only under a named reference convention
L	Dependent law/identity	209	Valid algebra from a basis that may contain measurements
A	Adjusted empirical input	35	Independent target until a frozen micro-model predicts it
R	Material/reference dependent	12	Requires composition, environment, or apparatus model
	Total	275	Numerical END/MNT predictions at present: 0

Claim discipline. The phrase “worked out” in this book means that every quantity has an explicit provenance path: definition, dependency equation, experimental adjustment, or unresolved derivation gate. It does not mean the present END/MNT equations secretly predict all 275 CODATA values. Any future edition may promote an entry to prediction only with versioned code, a frozen parameter file, a predeclared calibration set, and a held-out comparison.

20 The 275-quantity register

Entries are alphabetical. Values and standard uncertainties are the 2022 CODATA recommendations. “Dependency reconstruction” evaluates the displayed relation from the same CODATA basis and therefore checks arithmetic and provenance only. A missing numeric audit is deliberate: it prevents a measured value from being echoed as a prediction.

21 Nineteen derivation plates

Plate 1 — Dimensional invariance

Let base units transform as $L \mapsto \lambda_L L$, $T \mapsto \lambda_T T$, $M \mapsto \lambda_M M$, and $I \mapsto \lambda_I I$. A quantity with dimensions $L^a T^b M^c I^d$ changes numerically with inverse powers of these scale factors. Buckingham's Π theorem says that n quantities spanning a rank-r dimension matrix contain only $n - r$ independent dimensionless combinations. END/MNT may calibrate minimal dimensional scales; scientific credit must then come from held-out mass ratios, couplings, normalized moments, mixing angles, critical exponents, or dimensionless spectra.

Gate. Publish the dimension matrix and rank before counting successes. SI digits alone are not first-principles predictions.

Plate 2 — Identifiability and predictive surplus

For parameters $\mathbf{p} \in \mathbb{R}^p$ and observables $\mathbf{Q}(\mathbf{p}) \in \mathbb{R}^n$, let $J_{ai} = \partial Q_a / \partial p_i$. The rank of J counts locally identifiable parameter combinations. Calibrating that many observables determines combinations; it does not predict them. Use a declared likelihood,

$$-2 \log L = (\mathbf{y} - \mathbf{Q})^T \mathbf{V}^{-1} (\mathbf{y} - \mathbf{Q}).$$

Calibration and hold-out sets must be frozen before optimization.

Gate. Release one parameter file, sensitivity rank, all calibrators, and more independent held-out outputs than fitted combinations.

Plate 3 — CODATA covariance

CODATA combines observational equations, experiments, theory corrections, and correlations. For $\mathbf{y} = \mathbf{f}(\mathbf{a}) + \boldsymbol{\epsilon}$,

$$\chi^2 = (\mathbf{y} - \mathbf{f})^T \mathbf{V}^{-1} (\mathbf{y} - \mathbf{f}).$$

Dependent rows are evaluated after adjustment. Highly correlated table rows cannot be counted as independent confirmations. The companion CSV checks one-row algebra but does not reproduce the full least-squares adjustment.

Gate. Collapse deterministic dependencies and use the official covariance or underlying likelihoods for joint END/MNT tests.

Plate 4 — Masses as spectra

Linear modes satisfy $K\mathbf{u}_s = \mu \Omega_s^2 \mathbf{u}_s$. The dictionary

$$m_s c_0^2 = \hbar_* \Omega_s$$

maps a gap to mass only after a universal clock, action scale, and relativistic sector exist. Interacting masses are poles or correlation lengths with finite-volume and renormalization errors. Ratios can cancel dimensional scales, $m_a/m_b = \Omega_a/\Omega_b$, only after both states are independently identified.

Gate. Find stable sectors before reading the target spectrum and hold out a complete multiplet.

Plate 5 — Nuclear binding

Nuclear mass contains binding and corrections:

$$M(Z,N)c^2 = Zm_pc^2 + Nm_nc^2 - B(Z,N) - E_{\text{electronic}} + E_{\text{recoil}} + \cdots .$$

The neutron-proton difference has strong-isospin and electromagnetic pieces. Converting one difference into several units creates dependencies, not tests. END/MNT requires confinement or an empirical equivalent, residual forces, and many-body solutions.

Gate. Compute a dimensionless binding ratio after constituent sectors are frozen and before nuclear data are used.

Plate 6 — Magnetic moments

For spin I, $\boldsymbol{\mu} = g(q/2m)\mathbf{S}$, with

$$\mu_{\text{B}} = \frac{e\hbar}{2m_e}, \quad \mu_{\text{N}} = \frac{e\hbar}{2m_p}, \quad |\gamma| = \frac{|\mu|}{I\hbar}.$$

Lepton anomalies are quantum corrections; nuclear moments encode composite structure. Gauge links alone do not provide spinors, chirality, loop effects, or hadronic form factors.

Gate. Derive a charged spin-1/2 sector, current, and form factors, then calculate g with controlled errors.

Plate 7 — Atomic units

From

$$a_0 = \frac{\hbar}{\alpha m_e c}, \qquad E_{\text{h}} = \alpha^2 m_e c^2,$$

follow atomic time, velocity, momentum, fields, and response units. Matching many such rows after importing α, m_e, e, h, c is one dependency check, not many predictions.

Gate. Predict a dimensionless coupling and electron mass ratio, derive a bound-state Hamiltonian, and hold out transition ratios.

Plate 8 — Electromagnetic running

The fine-structure constant runs with scale:

$$\mu\frac{d\alpha}{d\mu} = \beta_\alpha(\alpha, \{m_i/\mu\}).$$

A link-action coefficient is a bare parameter. Matter content, charge normalization, regulator, scheme, and flow are needed. Reversing $\alpha = e^2/(4\pi\epsilon_0\hbar c)$ after importing dependent ϵ_0 is circular.

Gate. Freeze ultraviolet node dynamics and predict α at a held-out scale.

Plate 9 — Quantum electrical standards

The dependencies

$$K_\mathrm{J} = \frac{2e}{h}, \quad R_\mathrm{K} = \frac{h}{e^2}, \quad G_0 = \frac{2e^2}{h}, \quad \Phi_0 = \frac{h}{2e}$$

are exact in revised SI because e and h are exact. A deeper theory must explain charge quantization, coherent pairing, phase-voltage conversion, and topological transport.

Gate. Derive compact phase, charge representations, many-body coherence, and the transport invariant.

Plate 10 — Blackbody constants

Planck's spectrum yields

$$c_1 = 2\pi h c^2, \quad c_2 = \frac{hc}{k_\mathrm{B}}, \quad \sigma = \frac{2\pi^5 k_\mathrm{B}^4}{15 h^3 c^2}.$$

Wien constants add transcendental roots; ideal-gas references add stipulated temperature and pressure. The hard problem is deriving ensembles, entropy, occupation statistics, and temperature from deterministic updates.

Gate. Define an invariant ensemble and derive the Planck distribution without importing quantum probabilities.

Plate 11 — Planck scales

$$\ell_\mathrm{P} = \sqrt{\frac{\hbar G}{c^3}}, \quad t_\mathrm{P} = \frac{\ell_\mathrm{P}}{c}, \quad m_\mathrm{P} = \sqrt{\frac{\hbar c}{G}}.$$

These composites do not establish a lattice spacing. A useful invariant is $\alpha_G(m) = Gm^2/(\hbar c)$. The scalar benchmark derives neither a metric sector nor the Einstein-Hilbert coefficient.

Gate. Never set $a = \ell_\mathrm{P}$ to derive G. Compute a gravitational Wilson coefficient and held-out α_G.

Plate 12 — Charge radii

An rms electric radius is a form-factor slope,

$$r_E^2 = -6 \left. \frac{dG_E(Q^2)}{dQ^2} \right|_{Q^2=0},$$

with conventions and radiative corrections. It is a response scale, not a hard edge. END/MNT has no canonical particle solution, conserved current, or detector map yet.

Gate. Derive the current and elastic matrix element, control $Q^2 \to 0$, and keep radius data out of calibration.

Plate 13 — Material references

Silicon spacings, molar volume, X-ray units, and shielding shifts depend on composition, temperature, pressure, crystal quality, bound-state structure, and measurement convention. They become calculable only after particle physics, chemistry, and condensed matter have emerged.

Gate. State sample conditions, derive the many-body Hamiltonian, and separate universal parameters from material boundary data.

Plate 14 — Electroweak quantities

Tree-level relations

$$\frac{m_W}{m_Z} = \cos\theta_W, \qquad G_F = \frac{1}{\sqrt{2}\,v^2}$$

receive scheme- and scale-dependent corrections. END/MNT must generate chiral gauge structure, anomaly cancellation, symmetry breaking, masses, and renormalization flow.

Gate. Produce chiral representations and a renormalized electroweak action, declare the scheme, and hold out precision observables.

Plate 15 — Domains of proof

A theorem follows from assumptions. Numerical verification checks code against a theorem. Empirical evidence compares a frozen model with nature. Benchmark dispersion and gauge invariance are mathematical results; simulating them validates code, not the claim that spacetime is a node graph. Each constant claim needs assumptions, dimensions, dependencies, parameter provenance, code, convergence, uncertainty, data partition, covariance, and a baseline.

Gate. Qualify every proof claim by its domain.

Plate 16 — Frozen simulations

A reproducible run hashes the update rule, graph generator, boundaries, parameters, initial states, seeds, runtime, observables, calibration data, and stopping criteria. Resolution studies vary spacing, volume, time step, and graph irregularity. Archive trajectories or sufficient statistics, estimator code, autocorrelations, extrapolation, and all uncertainty components.

Gate. Verify analytic dispersion and stability, then search for localized states with no particle target in optimization.

Plate 17 — Rounding and residuals

Printed CODATA rows are rounded. Reconstructing one rounded, correlated row from others can leave a residual above machine epsilon even when the unrounded adjustment is consistent. CSV residuals are implementation diagnostics, not new-physics significances.

Gate. Before interpreting a final-digit discrepancy, use official precision, covariance, suitable arithmetic, and the published observational equations.

Plate 18 — Falsification matrix

END/MNT can fail if the update violates admissibility; numerical dispersion misses the theorem; continuum errors do not shrink; localized sectors do not exist; gauge or chiral construction fails; parameter rank removes predictive surplus; held-out ratios disagree; or quantum and gravitational tests fail. Passing an early gate does not imply a later one.

Gate. Promotion to prediction requires one dimensionless held-out number with full provenance and a predeclared rejection threshold.

Plate 19 — Beyond CODATA

A unification programme must also address quark masses and CKM parameters, neutrino masses and PMNS phases, QCD running, Higgs parameters, possible dark sectors, baryon asymmetry, cosmological expansion and perturbations, and vacuum energy. Many are scheme-, scale-, or model-dependent.

Gate. Complete particle, quantum, gravity, and cosmology bridges before expanding numerical claims. Seek the smallest independent basis yielding the broadest held-out structure.

C001 alpha particle-electron mass ratio

CODATA 2022. 7294.29954171 `dimensionless`, $u = 1.7 \times 10^{-7}$, $u_r = 2.331 \times 10^{-11}$.

Class. L — dependent law/identity; Dimensionless mass ratio.

Dependency equation. $R_{ab} = m_a/m_b$. *Inputs:* alpha particle mass; electron mass.

Numerical audit. dependency reconstruction 7294.29954176 `dimensionless`; fractional residual 6.602×10^{-12}.

First-principles verdict. Algebraically reproducible, but not a first-principles physical prediction: the CODATA basis values enter the right-hand side.

END/MNT completion gate. Derive the independent dimensionless basis from one frozen node operator, then propagate its covariance without using this target.

C002 alpha particle mass

CODATA 2022. $6.644657345 \times 10^{-27}$ `kg`, $u = 2.1 \times 10^{-36}$, $u_r = 3.16 \times 10^{-10}$.

Class. A — adjusted empirical input; Measured particle/nuclear scale.

Dependency equation. $mc^2 = E_{\text{pole}} \quad \text{or} \quad m = E_0/c^2$. *Inputs:* spectroscopy, kinematics, or mass-frequency ratios.

Numerical audit. no independent numerical END/MNT output; residual and z score are undefined.

First-principles verdict. The value is empirical. END/MNT currently has a mass-gap dictionary but no particle-identifying eigenproblem that predicts this number.

END/MNT completion gate. Derive a stable localized state, its renormalized pole energy, quantum numbers, and uncertainty without tuning to the listed mass.

C003 alpha particle mass energy equivalent

CODATA 2022. $5.9719201997 \times 10^{-10}$ J, $u = 1.9 \times 10^{-19}$, $u_r = 3.182 \times 10^{-10}$.

Class. L — dependent law/identity; Relativistic mass-energy identity.

Dependency equation. $E_m = mc^2$. *Inputs:* alpha particle mass; c.

Numerical audit. dependency reconstruction $5.97192019975 \times 10^{-10}$ J; fractional residual 8.437×10^{-12}.

First-principles verdict. Algebraically reproducible, but not a first-principles physical prediction: the CODATA basis values enter the right-hand side.

END/MNT completion gate. Derive the independent dimensionless basis from one frozen node operator, then propagate its covariance without using this target.

C004 alpha particle mass in u

CODATA 2022. $4.00150617913\,\mathrm{u}$, $u = 6.2 \times 10^{-11}$, $u_r = 1.549 \times 10^{-11}$.

Class. L — dependent law/identity; Relative-mass conversion.

Dependency equation. $m/\mathrm{u} = m/m_\mathrm{u}$. *Inputs:* alpha particle mass; atomic mass constant.

Numerical audit. dependency reconstruction $4.00150617915\,\mathrm{u}$; fractional residual 4.741×10^{-12}.

First-principles verdict. Algebraically reproducible, but not a first-principles physical prediction: the CODATA basis values enter the right-hand side.

END/MNT completion gate. Derive the independent dimensionless basis from one frozen node operator, then propagate its covariance without using this target.

C005 alpha particle molar mass

CODATA 2022. 0.0040015061833 `kg mol^-1`, $u = 1.2 \times 10^{-12}$, $u_r = 2.999 \times 10^{-10}$.

Class. L — dependent law/identity; Molar mass from single-particle mass.

Dependency equation. $M(X) = N_{\mathrm{A}} m_X$. *Inputs:* Avogadro constant; alpha particle mass.

Numerical audit. dependency reconstruction 0.00400150618336 `kg mol^-1`; fractional residual 1.394×10^{-11}.

First-principles verdict. Algebraically reproducible, but not a first-principles physical prediction: the CODATA basis values enter the right-hand side.

END/MNT completion gate. Derive the independent dimensionless basis from one frozen node operator, then propagate its covariance without using this target.

C006 alpha particle-proton mass ratio

CODATA 2022. 3.97259969025 `dimensionless`, $u = 7 \times 10^{-11}$, $u_r = 1.762 \times 10^{-11}$.

Class. L — dependent law/identity; Dimensionless mass ratio.

Dependency equation. $R_{ab} = m_a/m_b$. *Inputs:* alpha particle mass; proton mass.

Numerical audit. dependency reconstruction 3.97259969029 `dimensionless`; fractional residual 9.38×10^{-12}.

First-principles verdict. Algebraically reproducible, but not a first-principles physical prediction: the CODATA basis values enter the right-hand side.

END/MNT completion gate. Derive the independent dimensionless basis from one frozen node operator, then propagate its covariance without using this target.

C007 alpha particle relative atomic mass

CODATA 2022. 4.00150617913 `dimensionless`, $u = 6.2 \times 10^{-11}$, $u_r = 1.549 \times 10^{-11}$.

Class. L — dependent law/identity; Relative atomic mass.

Dependency equation. $A_{\mathrm{r}}(X) = m_X/m_{\mathrm{u}}$. *Inputs:* alpha particle mass; atomic mass constant.

Numerical audit. dependency reconstruction 4.00150617915 `dimensionless`; fractional residual 4.741×10^{-12}.

First-principles verdict. Algebraically reproducible, but not a first-principles physical prediction: the CODATA basis values enter the right-hand side.

END/MNT completion gate. Derive the independent dimensionless basis from one frozen node operator, then propagate its covariance without using this target.

C008 alpha particle rms charge radius

CODATA 2022. 1.6785×10^{-15} `m`, $u = 2.1 \times 10^{-18}$, $u_r = 0.001251$.

Class. A — adjusted empirical input; Adjusted empirical or theory-assisted input.

Dependency equation. $Q = \arg\min_{Q} (\mathbf{y} - \mathbf{f}(Q))^T \mathbf{V}^{-1} (\mathbf{y} - \mathbf{f}(Q))$. *Inputs:* CODATA observational equations and covariance.

Numerical audit. no independent numerical END/MNT output; residual and z score are undefined.

First-principles verdict. No END/MNT first-principles value exists in the current papers; CODATA supplies the comparison target, not an allowed model input for a prediction.

END/MNT completion gate. Generate the relevant spectrum, form factor, or decay amplitude from the frozen micro-model and compare only after preregistration.

C009 Angstrom star

CODATA 2022. $1.00001495 \times 10^{-10}\,\mathtt{m}$, $u = 9 \times 10^{-17}$, $u_r = 9 \times 10^{-7}$.

Class. R — material/reference dependent; Material or environment-dependent reference.

Dependency equation. $Q = Q(T, p, \text{composition, preparation})$. *Inputs:* experimental reference conditions.

Numerical audit. no independent numerical END/MNT output; residual and z score are undefined.

First-principles verdict. Not a universal constant of a microscopic theory; it must be measured or calculated from a detailed material model.

END/MNT completion gate. Derive the relevant bound-state/material Hamiltonian and the stated experimental conditions before comparison.

C010 atomic mass constant

CODATA 2022. $1.66053906892 \times 10^{-27}\,\mathtt{kg}$, $u = 5.2 \times 10^{-37}$, $u_r = 3.132 \times 10^{-10}$.

Class. A — adjusted empirical input; Adjusted empirical or theory-assisted input.

Dependency equation. $Q = \arg\min_Q (\mathbf{y} - \mathbf{f}(Q))^T \mathbf{V}^{-1} (\mathbf{y} - \mathbf{f}(Q))$. *Inputs:* CODATA observational equations and covariance.

Numerical audit. no independent numerical END/MNT output; residual and z score are undefined.

First-principles verdict. No END/MNT first-principles value exists in the current papers; CODATA supplies the comparison target, not an allowed model input for a prediction.

END/MNT completion gate. Generate the relevant spectrum, form factor, or decay amplitude from the frozen micro-model and compare only after preregistration.

C011 atomic mass constant energy equivalent

CODATA 2022. $1.49241808768 \times 10^{-10}$ J, $u = 4.6 \times 10^{-20}$, $u_r = 3.082 \times 10^{-10}$.

Class. L — dependent law/identity; Atomic mass energy.

Dependency equation. $m_\mathrm{u}c^2$. *Inputs:* atomic mass constant; c.

Numerical audit. dependency reconstruction $1.49241808769 \times 10^{-10}$ J; fractional residual 4.465×10^{-12}.

First-principles verdict. Algebraically reproducible, but not a first-principles physical prediction: the CODATA basis values enter the right-hand side.

END/MNT completion gate. Derive the independent dimensionless basis from one frozen node operator, then propagate its covariance without using this target.

C012 atomic mass constant energy equivalent in MeV

CODATA 2022. 931.49410372 MeV, $u = 2.9 \times 10^{-7}$, $u_r = 3.113 \times 10^{-10}$.

Class. L — dependent law/identity; Atomic mass energy in MeV.

Dependency equation. $m_\mathrm{u}c^2/(10^6 e)$. *Inputs:* atomic mass constant; c; e.

Numerical audit. dependency reconstruction 931.494103719 MeV; fractional residual -1.536×10^{-12}.

First-principles verdict. Algebraically reproducible, but not a first-principles physical prediction: the CODATA basis values enter the right-hand side.

END/MNT completion gate. Derive the independent dimensionless basis from one frozen node operator, then propagate its covariance without using this target.

C013 atomic unit of 1st hyperpolarizability

CODATA 2022. $3.2063612996 \times 10^{-53}$ `C^3 m^3 J^-2`, $u = 1.5 \times 10^{-62}$, $u_r = 4.678 \times 10^{-10}$.

Class. L — dependent law/identity; Atomic-unit dependency.

Dependency equation. $Q_{\mathrm{au}} = e^3 a_0^3 / E_{\mathrm{h}}^2$. *Inputs:* e; Bohr radius; Hartree energy.

Numerical audit. dependency reconstruction $3.20636129957 \times 10^{-53}$ `C^3 m^3 J^-2`; fractional residual -7.97×10^{-12}.

First-principles verdict. Algebraically reproducible, but not a first-principles physical prediction: the CODATA basis values enter the right-hand side.

END/MNT completion gate. Derive the independent dimensionless basis from one frozen node operator, then propagate its covariance without using this target.

C014 atomic unit of 2nd hyperpolarizability

CODATA 2022. $6.2353799735 \times 10^{-65}$ `C^4 m^4 J^-3`, $u = 3.9 \times 10^{-74}$, $u_r = 6.255 \times 10^{-10}$.

Class. L — dependent law/identity; Atomic-unit dependency.

Dependency equation. $Q_{\mathrm{au}} = e^4 a_0^4 / E_{\mathrm{h}}^3$. *Inputs:* e; Bohr radius; Hartree energy.

Numerical audit. dependency reconstruction $6.23537997354 \times 10^{-65}$ `C^4 m^4 J^-3`; fractional residual 6.717×10^{-12}.

First-principles verdict. Algebraically reproducible, but not a first-principles physical prediction: the CODATA basis values enter the right-hand side.

END/MNT completion gate. Derive the independent dimensionless basis from one frozen node operator, then propagate its covariance without using this target.

C015 atomic unit of action

CODATA 2022. $1.05457181765 \times 10^{-34}$ `J s` (exact in the stated system).

Class. L — dependent law/identity; Atomic-unit dependency.

Dependency equation. $Q_{\mathrm{au}} = \hbar$. *Inputs:* reduced Planck constant.

Numerical audit. dependency reconstruction $1.05457181765 \times 10^{-34}$ `J s`; fractional residual 0.

First-principles verdict. Algebraically reproducible, but not a first-principles physical prediction: the CODATA basis values enter the right-hand side.

END/MNT completion gate. Derive the independent dimensionless basis from one frozen node operator, then propagate its covariance without using this target.

C016 atomic unit of charge

CODATA 2022. $1.602176634 \times 10^{-19}$ `C` (exact in the stated system).

Class. L — dependent law/identity; Atomic-unit dependency.

Dependency equation. $Q_{\mathrm{au}} = e$. *Inputs:* elementary charge.

Numerical audit. dependency reconstruction $1.602176634 \times 10^{-19}$ `C`; fractional residual 0.

First-principles verdict. Algebraically reproducible, but not a first-principles physical prediction: the CODATA basis values enter the right-hand side.

END/MNT completion gate. Derive the independent dimensionless basis from one frozen node operator, then propagate its covariance without using this target.

C017 atomic unit of charge density

CODATA 2022. $1.08120238677 \times 10^{12}$ `C m^-3`, $u = 510$, $u_r = 4.717 \times 10^{-10}$.

Class. L — dependent law/identity; Atomic-unit dependency.

Dependency equation. $Q_{\mathrm{au}} = e/a_0^3$. *Inputs:* e; Bohr radius.

Numerical audit. dependency reconstruction $1.08120238677 \times 10^{12}$ `C m^-3`; fractional residual -2.781×10^{-12}.

First-principles verdict. Algebraically reproducible, but not a first-principles physical prediction: the CODATA basis values enter the right-hand side.

END/MNT completion gate. Derive the independent dimensionless basis from one frozen node operator, then propagate its covariance without using this target.

C018 atomic unit of current

CODATA 2022. 0.00662361823751 `A`, $u = 7.2 \times 10^{-15}$, $u_r = 1.087 \times 10^{-12}$.

Class. L — dependent law/identity; Atomic-unit dependency.

Dependency equation. $Q_{\mathrm{au}} = eE_{\mathrm{h}}/\hbar$. *Inputs:* e; Hartree energy; reduced Planck constant.

Numerical audit. dependency reconstruction 0.00662361823751 `A`; fractional residual 2.75×10^{-15}.

First-principles verdict. Algebraically reproducible, but not a first-principles physical prediction: the CODATA basis values enter the right-hand side.

END/MNT completion gate. Derive the independent dimensionless basis from one frozen node operator, then propagate its covariance without using this target.

C019 atomic unit of electric dipole mom.

CODATA 2022. $8.4783536198 \times 10^{-30}$ `C m`, $u = 1.3 \times 10^{-39}$, $u_r = 1.533 \times 10^{-10}$.

Class. L — dependent law/identity; Atomic-unit dependency.

Dependency equation. $Q_{\mathrm{au}} = ea_0$. *Inputs:* e; Bohr radius.

Numerical audit. dependency reconstruction $8.47835361979 \times 10^{-30}$ `C m`; fractional residual -1.303×10^{-12}.

First-principles verdict. Algebraically reproducible, but not a first-principles physical prediction: the CODATA basis values enter the right-hand side.

END/MNT completion gate. Derive the independent dimensionless basis from one frozen node operator, then propagate its covariance without using this target.

C020 atomic unit of electric field

CODATA 2022. $5.14220675112 \times 10^{11}$ `V m^-1`, $u = 80$, $u_r = 1.556 \times 10^{-10}$.

Class. L — dependent law/identity; Atomic-unit dependency.

Dependency equation. $Q_{\mathrm{au}} = E_{\mathrm{h}}/(ea_0)$. *Inputs:* Hartree energy; e; Bohr radius.

Numerical audit. dependency reconstruction $5.14220675112 \times 10^{11}$ `V m^-1`; fractional residual -3.3×10^{-14}.

First-principles verdict. Algebraically reproducible, but not a first-principles physical prediction: the CODATA basis values enter the right-hand side.

END/MNT completion gate. Derive the independent dimensionless basis from one frozen node operator, then propagate its covariance without using this target.

C021 atomic unit of electric field gradient

CODATA 2022. $9.7173624424 \times 10^{21}$ `V m^-2`, $u = 3 \times 10^{12}$, $u_r = 3.087 \times 10^{-10}$.

Class. L — dependent law/identity; Atomic-unit dependency.

Dependency equation. $Q_{\rm au} = E_{\rm h}/(ea_0^2)$. *Inputs:* Hartree energy; e; Bohr radius.

Numerical audit. dependency reconstruction $9.71736244241 \times 10^{21}$ `V m^-2`; fractional residual 1.083×10^{-12}.

First-principles verdict. Algebraically reproducible, but not a first-principles physical prediction: the CODATA basis values enter the right-hand side.

END/MNT completion gate. Derive the independent dimensionless basis from one frozen node operator, then propagate its covariance without using this target.

C022 atomic unit of electric polarizability

CODATA 2022. $1.64877727212 \times 10^{-41}$ `C^2 m^2 J^-1`, $u = 5.1 \times 10^{-51}$, $u_r = 3.093 \times 10^{-10}$.

Class. L — dependent law/identity; Atomic-unit dependency.

Dependency equation. $Q_{\rm au} = e^2a_0^2/E_{\rm h}$. *Inputs:* e; Bohr radius; Hartree energy.

Numerical audit. dependency reconstruction $1.64877727212 \times 10^{-41}$ `C^2 m^2 J^-1`; fractional residual 6.462×10^{-14}.

First-principles verdict. Algebraically reproducible, but not a first-principles physical prediction: the CODATA basis values enter the right-hand side.

END/MNT completion gate. Derive the independent dimensionless basis from one frozen node operator, then propagate its covariance without using this target.

C023 atomic unit of electric potential

CODATA 2022. 27.211386246 `V`, $u = 3 \times 10^{-11}$, $u_r = 1.102 \times 10^{-12}$.

Class. L — dependent law/identity; Atomic-unit dependency.

Dependency equation. $Q_{\mathrm{au}} = E_{\mathrm{h}}/e$. *Inputs:* Hartree energy; e.

Numerical audit. dependency reconstruction 27.211386246 `V`; fractional residual 6.136×10^{-15}.

First-principles verdict. Algebraically reproducible, but not a first-principles physical prediction: the CODATA basis values enter the right-hand side.

END/MNT completion gate. Derive the independent dimensionless basis from one frozen node operator, then propagate its covariance without using this target.

C024 atomic unit of electric quadrupole mom.

CODATA 2022. $4.4865515185 \times 10^{-40}$ `C m^2`, $u = 1.4 \times 10^{-49}$, $u_r = 3.12 \times 10^{-10}$.

Class. L — dependent law/identity; Atomic-unit dependency.

Dependency equation. $Q_{\mathrm{au}} = ea_0^2$. *Inputs:* e; Bohr radius.

Numerical audit. dependency reconstruction $4.48655151853 \times 10^{-40}$ `C m^2`; fractional residual 5.693×10^{-12}.

First-principles verdict. Algebraically reproducible, but not a first-principles physical prediction: the CODATA basis values enter the right-hand side.

END/MNT completion gate. Derive the independent dimensionless basis from one frozen node operator, then propagate its covariance without using this target.

C025 atomic unit of energy

CODATA 2022. $4.35974472221 \times 10^{-18}$ J, $u = 4.8 \times 10^{-30}$, $u_r = 1.101 \times 10^{-12}$.

Class. L — dependent law/identity; Atomic-unit dependency.

Dependency equation. $Q_{\mathrm{au}} = E_{\mathrm{h}} = \alpha^2 m_e c^2$. *Inputs:* alpha; electron mass; c.

Numerical audit. dependency reconstruction $4.35974472216 \times 10^{-18}$ J; fractional residual -1.08×10^{-11}.

First-principles verdict. Algebraically reproducible, but not a first-principles physical prediction: the CODATA basis values enter the right-hand side.

END/MNT completion gate. Derive the independent dimensionless basis from one frozen node operator, then propagate its covariance without using this target.

C026 atomic unit of force

CODATA 2022. $8.2387235038 \times 10^{-8}$ N, $u = 1.3 \times 10^{-17}$, $u_r = 1.578 \times 10^{-10}$.

Class. L — dependent law/identity; Atomic-unit dependency.

Dependency equation. $Q_{\mathrm{au}} = E_{\mathrm{h}}/a_0$. *Inputs:* Hartree energy; Bohr radius.

Numerical audit. dependency reconstruction $8.23872350384 \times 10^{-8}$ N; fractional residual 5.006×10^{-12}.

First-principles verdict. Algebraically reproducible, but not a first-principles physical prediction: the CODATA basis values enter the right-hand side.

END/MNT completion gate. Derive the independent dimensionless basis from one frozen node operator, then propagate its covariance without using this target.

C027 atomic unit of length

CODATA 2022. $5.29177210544 \times 10^{-11}$ `m`, $u = 8.2 \times 10^{-21}$, $u_r = 1.55 \times 10^{-10}$.

Class. L — dependent law/identity; Atomic-unit dependency.

Dependency equation. $Q_{\text{au}} = a_0$. *Inputs:* Bohr radius.

Numerical audit. dependency reconstruction $5.29177210544 \times 10^{-11}$ `m`; fractional residual 0.

First-principles verdict. Algebraically reproducible, but not a first-principles physical prediction: the CODATA basis values enter the right-hand side.

END/MNT completion gate. Derive the independent dimensionless basis from one frozen node operator, then propagate its covariance without using this target.

C028 atomic unit of mag. dipole mom.

CODATA 2022. $1.85480201315 \times 10^{-23}$ `J T^-1`, $u = 5.8 \times 10^{-33}$, $u_r = 3.127 \times 10^{-10}$.

Class. L — dependent law/identity; Atomic-unit dependency.

Dependency equation. $Q_{\text{au}} = 2\mu_{\text{B}}$. *Inputs:* Bohr magneton.

Numerical audit. dependency reconstruction $1.85480201314 \times 10^{-23}$ `J T^-1`; fractional residual -5.391×10^{-12}.

First-principles verdict. Algebraically reproducible, but not a first-principles physical prediction: the CODATA basis values enter the right-hand side.

END/MNT completion gate. Derive the independent dimensionless basis from one frozen node operator, then propagate its covariance without using this target.

C029 atomic unit of mag. flux density

CODATA 2022. $2.35051757077 \times 10^5$ `T`, $u = 7.3 \times 10^{-5}$, $u_r = 3.106 \times 10^{-10}$.

Class. L — dependent law/identity; Atomic-unit dependency.

Dependency equation. $Q_{\mathrm{au}} = \hbar/(ea_0^2)$. *Inputs:* hbar; e; Bohr radius.

Numerical audit. dependency reconstruction $2.35051757077 \times 10^5$ `T`; fractional residual 2.325×10^{-13}.

First-principles verdict. Algebraically reproducible, but not a first-principles physical prediction: the CODATA basis values enter the right-hand side.

END/MNT completion gate. Derive the independent dimensionless basis from one frozen node operator, then propagate its covariance without using this target.

C030 atomic unit of magnetizability

CODATA 2022. $7.8910365794 \times 10^{-29}$ `J T^-2`, $u = 4.9 \times 10^{-38}$, $u_r = 6.21 \times 10^{-10}$.

Class. A — adjusted empirical input; Adjusted or reference quantity.

Dependency equation. $Q = Q_{\mathrm{CODATA}} \pm u(Q)$. *Inputs:* CODATA adjustment or stated reference procedure.

Numerical audit. no independent numerical END/MNT output; residual and z score are undefined.

First-principles verdict. No independent END/MNT numerical prediction is present; numerical agreement cannot be assessed without inventing an input.

END/MNT completion gate. Specify the observable map and derive the value and uncertainty from a frozen micro-model before inspecting this target.

C031 atomic unit of mass

CODATA 2022. $9.1093837139 \times 10^{-31}$ `kg`, $u = 2.8 \times 10^{-40}$, $u_r = 3.074 \times 10^{-10}$.

Class. L — dependent law/identity; Atomic-unit dependency.

Dependency equation. $Q_{\mathrm{au}} = m_e$. *Inputs:* electron mass.

Numerical audit. dependency reconstruction $9.1093837139 \times 10^{-31}$ `kg`; fractional residual 0.

First-principles verdict. Algebraically reproducible, but not a first-principles physical prediction: the CODATA basis values enter the right-hand side.

END/MNT completion gate. Derive the independent dimensionless basis from one frozen node operator, then propagate its covariance without using this target.

C032 atomic unit of momentum

CODATA 2022. $1.99285191545 \times 10^{-24}$ `kg m s^-1`, $u = 3.1 \times 10^{-34}$, $u_r = 1.556 \times 10^{-10}$.

Class. L — dependent law/identity; Atomic-unit dependency.

Dependency equation. $Q_{\mathrm{au}} = \hbar/a_0$. *Inputs:* hbar; Bohr radius.

Numerical audit. dependency reconstruction $1.99285191545 \times 10^{-24}$ `kg m s^-1`; fractional residual 1.003×10^{-12}.

First-principles verdict. Algebraically reproducible, but not a first-principles physical prediction: the CODATA basis values enter the right-hand side.

END/MNT completion gate. Derive the independent dimensionless basis from one frozen node operator, then propagate its covariance without using this target.

C033 atomic unit of permittivity

CODATA 2022. $1.1126500562 \times 10^{-10}$ `F m^-1`, $u = 1.7 \times 10^{-20}$, $u_r = 1.528 \times 10^{-10}$.

Class. L — dependent law/identity; Atomic-unit dependency.

Dependency equation. $Q_{\mathrm{au}} = e^2/(a_0 E_{\mathrm{h}}) = 4\pi\epsilon_0$. *Inputs:* e; Bohr radius; Hartree energy.

Numerical audit. dependency reconstruction $1.1126500562 \times 10^{-10}$ `F m^-1`; fractional residual 5.633×10^{-13}.

First-principles verdict. Algebraically reproducible, but not a first-principles physical prediction: the CODATA basis values enter the right-hand side.

END/MNT completion gate. Derive the independent dimensionless basis from one frozen node operator, then propagate its covariance without using this target.

C034 atomic unit of time

CODATA 2022. $2.418884326 59 \times 10^{-17}$ `s`, $u = 2.6 \times 10^{-29}$, $u_r = 1.075 \times 10^{-12}$.

Class. L — dependent law/identity; Atomic-unit dependency.

Dependency equation. $Q_{\mathrm{au}} = \hbar/E_{\mathrm{h}}$. *Inputs:* hbar; Hartree energy.

Numerical audit. dependency reconstruction $2.41888432659 \times 10^{-17}$ `s`; fractional residual -2.905×10^{-14}.

First-principles verdict. Algebraically reproducible, but not a first-principles physical prediction: the CODATA basis values enter the right-hand side.

END/MNT completion gate. Derive the independent dimensionless basis from one frozen node operator, then propagate its covariance without using this target.

C035 atomic unit of velocity

CODATA 2022. $2.18769126216 \times 10^{6}$ `m s^-1`, $u = 3.4 \times 10^{-4}$, $u_r = 1.554 \times 10^{-10}$.

Class. L — dependent law/identity; Atomic-unit dependency.

Dependency equation. $Q_{\mathrm{au}} = \alpha c$. *Inputs:* alpha; c.

Numerical audit. dependency reconstruction $2.18769126214 \times 10^{6}$ `m s^-1`; fractional residual -7.268×10^{-12}.

First-principles verdict. Algebraically reproducible, but not a first-principles physical prediction: the CODATA basis values enter the right-hand side.

END/MNT completion gate. Derive the independent dimensionless basis from one frozen node operator, then propagate its covariance without using this target.

C036 Avogadro constant

CODATA 2022. $6.02214076 \times 10^{23}$ `mol^-1` (exact in the stated system).

Class. D — SI definition; SI defining constant.

Dependency equation. $Q \equiv Q_{\mathrm{SI}} \quad$ (exact by definition). *Inputs:* SI definition.

Numerical audit. identity check $6.02214076 \times 10^{23}$ `mol^-1`; fractional residual 0.

First-principles verdict. Exact numerical identity in SI; this fixes a unit conversion and is not a prediction of nature's dimensionless structure.

END/MNT completion gate. Explain the invariant physical role and derive held-out dimensionless ratios; reproducing the stipulated SI digits is not evidence.

C037 Bohr magneton

CODATA 2022. $9.2740100657 \times 10^{-24}$ `J T^-1`, $u = 2.9 \times 10^{-33}$, $u_r = 3.127 \times 10^{-10}$.

Class. L — dependent law/identity; Electron magneton.

Dependency equation. $\mu_{\mathrm{B}} = e\hbar/(2m_e)$. *Inputs:* e; hbar; electron mass.

Numerical audit. dependency reconstruction $9.27401006574 \times 10^{-24}$ `J T^-1`; fractional residual 4.105×10^{-12}.

First-principles verdict. Algebraically reproducible, but not a first-principles physical prediction: the CODATA basis values enter the right-hand side.

END/MNT completion gate. Derive the independent dimensionless basis from one frozen node operator, then propagate its covariance without using this target.

C038 Bohr radius

CODATA 2022. $5.29177210544 \times 10^{-11}$ `m`, $u = 8.2 \times 10^{-21}$, $u_r = 1.55 \times 10^{-10}$.

Class. L — dependent law/identity; Hydrogenic length.

Dependency equation. $a_0 = \hbar/(\alpha m_e c)$. *Inputs:* hbar; alpha; electron mass; c.

Numerical audit. dependency reconstruction $5.29177210547 \times 10^{-11}$ `m`; fractional residual 5.178×10^{-12}.

First-principles verdict. Algebraically reproducible, but not a first-principles physical prediction: the CODATA basis values enter the right-hand side.

END/MNT completion gate. Derive the independent dimensionless basis from one frozen node operator, then propagate its covariance without using this target.

C039 Boltzmann constant

CODATA 2022. 1.380649×10^{-23} `J K^-1` (exact in the stated system).

Class. D — SI definition; SI defining constant.

Dependency equation. $Q \equiv Q_{\mathrm{SI}}$ (exact by definition). *Inputs:* SI definition.

Numerical audit. identity check 1.380649×10^{-23} `J K^-1`; fractional residual 0.

First-principles verdict. Exact numerical identity in SI; this fixes a unit conversion and is not a prediction of nature's dimensionless structure.

END/MNT completion gate. Explain the invariant physical role and derive held-out dimensionless ratios; reproducing the stipulated SI digits is not evidence.

C040 Boltzmann constant in eV/K

CODATA 2022. $8.61733326215 \times 10^{-5}$ `eV K^-1` (exact in the stated system).

Class. A — adjusted empirical input; Adjusted or reference quantity.

Dependency equation. $Q = Q_{\mathrm{CODATA}} \pm u(Q)$. *Inputs:* CODATA adjustment or stated reference procedure.

Numerical audit. no independent numerical END/MNT output; residual and z score are undefined.

First-principles verdict. No independent END/MNT numerical prediction is present; numerical agreement cannot be assessed without inventing an input.

END/MNT completion gate. Specify the observable map and derive the value and uncertainty from a frozen micro-model before inspecting this target.

C041 Boltzmann constant in Hz/K

CODATA 2022. $2.08366191233 \times 10^{10}$ `Hz K^-1` (exact in the stated system).

Class. A — adjusted empirical input; Adjusted or reference quantity.

Dependency equation. $Q = Q_{\text{CODATA}} \pm u(Q)$. *Inputs:* CODATA adjustment or stated reference procedure.

Numerical audit. no independent numerical END/MNT output; residual and z score are undefined.

First-principles verdict. No independent END/MNT numerical prediction is present; numerical agreement cannot be assessed without inventing an input.

END/MNT completion gate. Specify the observable map and derive the value and uncertainty from a frozen micro-model before inspecting this target.

C042 Boltzmann constant in inverse meter per kelvin

CODATA 2022. 69.5034800486 `m^-1 K^-1` (exact in the stated system).

Class. A — adjusted empirical input; Adjusted or reference quantity.

Dependency equation. $Q = Q_{\text{CODATA}} \pm u(Q)$. *Inputs:* CODATA adjustment or stated reference procedure.

Numerical audit. no independent numerical END/MNT output; residual and z score are undefined.

First-principles verdict. No independent END/MNT numerical prediction is present; numerical agreement cannot be assessed without inventing an input.

END/MNT completion gate. Specify the observable map and derive the value and uncertainty from a frozen micro-model before inspecting this target.

C043 characteristic impedance of vacuum

CODATA 2022. 376.730313412 `ohm`, $u = 5.9 \times 10^{-8}$, $u_r = 1.566 \times 10^{-10}$.

Class. L — dependent law/identity; Vacuum impedance.

Dependency equation. $Z_0 = \mu_0 c$. *Inputs:* mu0; c.

Numerical audit. dependency reconstruction 376.730313412 `ohm`; fractional residual 7.952×10^{-14}.

First-principles verdict. Algebraically reproducible, but not a first-principles physical prediction: the CODATA basis values enter the right-hand side.

END/MNT completion gate. Derive the independent dimensionless basis from one frozen node operator, then propagate its covariance without using this target.

C044 classical electron radius

CODATA 2022. $2.8179403205 \times 10^{-15}$ `m`, $u = 1.3 \times 10^{-24}$, $u_r = 4.613 \times 10^{-10}$.

Class. L — dependent law/identity; Classical electron scale.

Dependency equation. $r_e = \alpha\hbar/(m_e c)$. *Inputs:* alpha; hbar; electron mass; c.

Numerical audit. dependency reconstruction $2.81794032045 \times 10^{-15}$ `m`; fractional residual -1.89×10^{-11}.

First-principles verdict. Algebraically reproducible, but not a first-principles physical prediction: the CODATA basis values enter the right-hand side.

END/MNT completion gate. Derive the independent dimensionless basis from one frozen node operator, then propagate its covariance without using this target.

C045 Compton wavelength

CODATA 2022. $2.42631023538 \times 10^{-12}\,\mathtt{m}$, $u = 7.6 \times 10^{-22}$, $u_r = 3.132 \times 10^{-10}$.

Class. L — dependent law/identity; Compton wavelength.

Dependency equation. $\lambda_C = h/(mc)$. *Inputs:* Planck constant; particle mass; c.

Numerical audit. dependency reconstruction $2.42631023538 \times 10^{-12}\,\mathtt{m}$; fractional residual 1.307×10^{-13}.

First-principles verdict. Algebraically reproducible, but not a first-principles physical prediction: the CODATA basis values enter the right-hand side.

END/MNT completion gate. Derive the independent dimensionless basis from one frozen node operator, then propagate its covariance without using this target.

C046 conductance quantum

CODATA 2022. $7.74809172986 \times 10^{-5}\,\mathtt{S}$ (exact in the stated system).

Class. L — dependent law/identity; Quantum electrical conductance.

Dependency equation. $G_0 = 2e^2/h$. *Inputs:* e; h.

Numerical audit. dependency reconstruction $7.74809172986 \times 10^{-5}\,\mathtt{S}$; fractional residual 0.

First-principles verdict. Algebraically reproducible, but not a first-principles physical prediction: the CODATA basis values enter the right-hand side.

END/MNT completion gate. Derive the independent dimensionless basis from one frozen node operator, then propagate its covariance without using this target.

C047 conventional value of ampere-90

CODATA 2022. 1.00000008887 A (exact in the stated system).

Class. C — convention; Conventional reference quantity.

Dependency equation. $Q \equiv Q_{\mathrm{conv}}$ (stipulated reference). *Inputs:* named convention.

Numerical audit. dependency reconstruction 1.00000008887 A; fractional residual 0.

First-principles verdict. Exact only inside the stated metrological convention; not a universal-law prediction.

END/MNT completion gate. No END/MNT derivation is required unless the theory predicts the physical realization used by the convention.

C048 conventional value of coulomb-90

CODATA 2022. 1.00000008887 C (exact in the stated system).

Class. C — convention; Conventional reference quantity.

Dependency equation. $Q \equiv Q_{\mathrm{conv}}$ (stipulated reference). *Inputs:* named convention.

Numerical audit. dependency reconstruction 1.00000008887 C; fractional residual 0.

First-principles verdict. Exact only inside the stated metrological convention; not a universal-law prediction.

END/MNT completion gate. No END/MNT derivation is required unless the theory predicts the physical realization used by the convention.

C049 conventional value of farad-90

CODATA 2022. 0.999999982206 `F` (exact in the stated system).

Class. C — convention; Conventional reference quantity.

Dependency equation. $Q \equiv Q_{\mathrm{conv}} \quad \text{(stipulated reference)}$. *Inputs:* named convention.

Numerical audit. dependency reconstruction 0.999999982206 `F`; fractional residual 0.

First-principles verdict. Exact only inside the stated metrological convention; not a universal-law prediction.

END/MNT completion gate. No END/MNT derivation is required unless the theory predicts the physical realization used by the convention.

C050 conventional value of henry-90

CODATA 2022. 1.00000001779 `H` (exact in the stated system).

Class. C — convention; Conventional reference quantity.

Dependency equation. $Q \equiv Q_{\mathrm{conv}} \quad \text{(stipulated reference)}$. *Inputs:* named convention.

Numerical audit. dependency reconstruction 1.00000001779 `H`; fractional residual 0.

First-principles verdict. Exact only inside the stated metrological convention; not a universal-law prediction.

END/MNT completion gate. No END/MNT derivation is required unless the theory predicts the physical realization used by the convention.

C051 conventional value of Josephson constant

CODATA 2022. 4.835979×10^{14} `Hz V^-1` (exact in the stated system).

Class. C — convention; Conventional reference quantity.

Dependency equation. $Q \equiv Q_{\mathrm{conv}}$ (stipulated reference). *Inputs:* named convention.

Numerical audit. dependency reconstruction 4.835979×10^{14} `Hz V^-1`; fractional residual 0.

First-principles verdict. Exact only inside the stated metrological convention; not a universal-law prediction.

END/MNT completion gate. No END/MNT derivation is required unless the theory predicts the physical realization used by the convention.

C052 conventional value of ohm-90

CODATA 2022. 1.00000001779 `ohm` (exact in the stated system).

Class. C — convention; Conventional reference quantity.

Dependency equation. $Q \equiv Q_{\mathrm{conv}}$ (stipulated reference). *Inputs:* named convention.

Numerical audit. dependency reconstruction 1.00000001779 `ohm`; fractional residual 0.

First-principles verdict. Exact only inside the stated metrological convention; not a universal-law prediction.

END/MNT completion gate. No END/MNT derivation is required unless the theory predicts the physical realization used by the convention.

C053 conventional value of volt-90

CODATA 2022. 1.00000010667 `V` (exact in the stated system).

Class. C — convention; Conventional reference quantity.

Dependency equation. $Q \equiv Q_{\mathrm{conv}} \quad$ (stipulated reference). *Inputs:* named convention.

Numerical audit. dependency reconstruction 1.00000010667 `V`; fractional residual 0.

First-principles verdict. Exact only inside the stated metrological convention; not a universal-law prediction.

END/MNT completion gate. No END/MNT derivation is required unless the theory predicts the physical realization used by the convention.

C054 conventional value of von Klitzing constant

CODATA 2022. 25812.807 `ohm` (exact in the stated system).

Class. C — convention; Conventional reference quantity.

Dependency equation. $Q \equiv Q_{\mathrm{conv}} \quad$ (stipulated reference). *Inputs:* named convention.

Numerical audit. dependency reconstruction 25812.807 `ohm`; fractional residual 0.

First-principles verdict. Exact only inside the stated metrological convention; not a universal-law prediction.

END/MNT completion gate. No END/MNT derivation is required unless the theory predicts the physical realization used by the convention.

C055 conventional value of watt-90

CODATA 2022. 1.00000019554 $\mathtt{W}$ (exact in the stated system).

Class. C — convention; Conventional reference quantity.

Dependency equation. $Q \equiv Q_{\mathrm{conv}}$ (stipulated reference). *Inputs:* named convention.

Numerical audit. dependency reconstruction 1.00000019554 $\mathtt{W}$; fractional residual 0.

First-principles verdict. Exact only inside the stated metrological convention; not a universal-law prediction.

END/MNT completion gate. No END/MNT derivation is required unless the theory predicts the physical realization used by the convention.

C056 Copper x unit

CODATA 2022. $1.00207697 \times 10^{-13}\,\mathtt{m}$, $u = 2.8 \times 10^{-20}$, $u_r = 2.794 \times 10^{-7}$.

Class. R — material/reference dependent; Material or environment-dependent reference.

Dependency equation. $Q = Q(T, p, \text{composition, preparation})$. *Inputs:* experimental reference conditions.

Numerical audit. no independent numerical END/MNT output; residual and z score are undefined.

First-principles verdict. Not a universal constant of a microscopic theory; it must be measured or calculated from a detailed material model.

END/MNT completion gate. Derive the relevant bound-state/material Hamiltonian and the stated experimental conditions before comparison.

C057 deuteron-electron mag. mom. ratio

CODATA 2022. $-4.66434555 \times 10^{-4}$ `dimensionless`, $u = 1.2 \times 10^{-12}$, $u_r = 2.573 \times 10^{-9}$.

Class. L — dependent law/identity; Magnetic-moment ratio.

Dependency equation. $R_{\mu,ab} = \mu_a/\mu_b$. *Inputs:* deuteron and electron magnetic moments.

Numerical audit. dependency reconstruction $-4.66434554973 \times 10^{-4}$ `dimensionless`; fractional residual -5.837×10^{-11}.

First-principles verdict. Algebraically reproducible, but not a first-principles physical prediction: the CODATA basis values enter the right-hand side.

END/MNT completion gate. Derive the independent dimensionless basis from one frozen node operator, then propagate its covariance without using this target.

C058 deuteron-electron mass ratio

CODATA 2022. 3670.48296765 `dimensionless`, $u = 6.3 \times 10^{-8}$, $u_r = 1.716 \times 10^{-11}$.

Class. L — dependent law/identity; Dimensionless mass ratio.

Dependency equation. $R_{ab} = m_a/m_b$. *Inputs:* deuteron mass; electron mass.

Numerical audit. dependency reconstruction 3670.48296769 `dimensionless`; fractional residual 8.859×10^{-12}.

First-principles verdict. Algebraically reproducible, but not a first-principles physical prediction: the CODATA basis values enter the right-hand side.

END/MNT completion gate. Derive the independent dimensionless basis from one frozen node operator, then propagate its covariance without using this target.

C059 deuteron g factor

CODATA 2022. 0.8574382335 `dimensionless`, $u = 2.2 \times 10^{-9}$, $u_r = 2.566 \times 10^{-9}$.

Class. L — dependent law/identity; Magnetic g factor.

Dependency equation. $g_X = \mu_X/(I_X \mu_{\text{ref}})$. *Inputs:* deuteron magnetic moment; spin; reference magneton.

Numerical audit. dependency reconstruction 0.857438233457 `dimensionless`; fractional residual -4.986×10^{-11}.

First-principles verdict. Algebraically reproducible, but not a first-principles physical prediction: the CODATA basis values enter the right-hand side.

END/MNT completion gate. Derive the independent dimensionless basis from one frozen node operator, then propagate its covariance without using this target.

C060 deuteron mag. mom.

CODATA 2022. $4.330735087 \times 10^{-27}$ `J T^-1`, $u = 1.1 \times 10^{-35}$, $u_r = 2.54 \times 10^{-9}$.

Class. A — adjusted empirical input; Adjusted or reference quantity.

Dependency equation. $Q = Q_{\text{CODATA}} \pm u(Q)$. *Inputs:* CODATA adjustment or stated reference procedure.

Numerical audit. no independent numerical END/MNT output; residual and z score are undefined.

First-principles verdict. No independent END/MNT numerical prediction is present; numerical agreement cannot be assessed without inventing an input.

END/MNT completion gate. Specify the observable map and derive the value and uncertainty from a frozen micro-model before inspecting this target.

C061 deuteron mag. mom. to Bohr magneton ratio

CODATA 2022. $4.669754568 \times 10^{-4}$ `dimensionless`, $u = 1.2 \times 10^{-12}$, $u_r = 2.57 \times 10^{-9}$.

Class. L — dependent law/identity; Magnetic moment in Bohr magnetons.

Dependency equation. μ_X/μ_B. *Inputs:* deuteron magnetic moment; Bohr magneton.

Numerical audit. dependency reconstruction $4.66975456822 \times 10^{-4}$ `dimensionless`; fractional residual 4.663×10^{-11}.

First-principles verdict. Algebraically reproducible, but not a first-principles physical prediction: the CODATA basis values enter the right-hand side.

END/MNT completion gate. Derive the independent dimensionless basis from one frozen node operator, then propagate its covariance without using this target.

C062 deuteron mag. mom. to nuclear magneton ratio

CODATA 2022. 0.8574382335 `dimensionless`, $u = 2.2 \times 10^{-9}$, $u_r = 2.566 \times 10^{-9}$.

Class. L — dependent law/identity; Magnetic moment in nuclear magnetons.

Dependency equation. μ_X/μ_N. *Inputs:* deuteron magnetic moment; nuclear magneton.

Numerical audit. dependency reconstruction 0.857438233457 `dimensionless`; fractional residual -4.986×10^{-11}.

First-principles verdict. Algebraically reproducible, but not a first-principles physical prediction: the CODATA basis values enter the right-hand side.

END/MNT completion gate. Derive the independent dimensionless basis from one frozen node operator, then propagate its covariance without using this target.

C063 deuteron mass

CODATA 2022. $3.3435837768 \times 10^{-27}$ `kg`, $u = 1 \times 10^{-36}$, $u_r = 2.991 \times 10^{-10}$.

Class. A — adjusted empirical input; Measured particle/nuclear scale.

Dependency equation. $mc^2 = E_{\text{pole}} \quad \text{or} \quad m = E_0/c^2$. *Inputs:* spectroscopy, kinematics, or mass-frequency ratios.

Numerical audit. no independent numerical END/MNT output; residual and z score are undefined.

First-principles verdict. The value is empirical. END/MNT currently has a mass-gap dictionary but no particle-identifying eigenproblem that predicts this number.

END/MNT completion gate. Derive a stable localized state, its renormalized pole energy, quantum numbers, and uncertainty without tuning to the listed mass.

C064 deuteron mass energy equivalent

CODATA 2022. $3.00506323491 \times 10^{-10}$ `J`, $u = 9.4 \times 10^{-20}$, $u_r = 3.128 \times 10^{-10}$.

Class. L — dependent law/identity; Relativistic mass-energy identity.

Dependency equation. $E_m = mc^2$. *Inputs:* deuteron mass; c.

Numerical audit. dependency reconstruction $3.00506323494 \times 10^{-10}$ `J`; fractional residual 9.786×10^{-12}.

First-principles verdict. Algebraically reproducible, but not a first-principles physical prediction: the CODATA basis values enter the right-hand side.

END/MNT completion gate. Derive the independent dimensionless basis from one frozen node operator, then propagate its covariance without using this target.

C065 deuteron mass in u

CODATA 2022. 2.01355321254 `u`, $u = 1.5 \times 10^{-11}$, $u_r = 7.45 \times 10^{-12}$.

Class. L — dependent law/identity; Relative-mass conversion.

Dependency equation. $m/\mathrm{u} = m/m_\mathrm{u}$. *Inputs:* deuteron mass; atomic mass constant.

Numerical audit. dependency reconstruction 2.01355321256 `u`; fractional residual 6.374×10^{-12}.

First-principles verdict. Algebraically reproducible, but not a first-principles physical prediction: the CODATA basis values enter the right-hand side.

END/MNT completion gate. Derive the independent dimensionless basis from one frozen node operator, then propagate its covariance without using this target.

C066 deuteron molar mass

CODATA 2022. 0.00201355321466 `kg mol^-1`, $u = 6.3 \times 10^{-13}$, $u_r = 3.129 \times 10^{-10}$.

Class. L — dependent law/identity; Molar mass from single-particle mass.

Dependency equation. $M(X) = N_\mathrm{A} m_X$. *Inputs:* Avogadro constant; deuteron mass.

Numerical audit. dependency reconstruction 0.00201355321467 `kg mol^-1`; fractional residual 7.054×10^{-12}.

First-principles verdict. Algebraically reproducible, but not a first-principles physical prediction: the CODATA basis values enter the right-hand side.

END/MNT completion gate. Derive the independent dimensionless basis from one frozen node operator, then propagate its covariance without using this target.

C067 deuteron-neutron mag. mom. ratio

CODATA 2022. $-0.44820652\,\texttt{dimensionless}$, $u = 1.1 \times 10^{-7}$, $u_r = 2.454 \times 10^{-7}$.

Class. L — dependent law/identity; Magnetic-moment ratio.

Dependency equation. $R_{\mu,ab} = \mu_a/\mu_b$. *Inputs:* deuteron and neutron magnetic moments.

Numerical audit. dependency reconstruction $-0.448206515955\,\texttt{dimensionless}$; fractional residual -9.024×10^{-9}.

First-principles verdict. Algebraically reproducible, but not a first-principles physical prediction: the CODATA basis values enter the right-hand side.

END/MNT completion gate. Derive the independent dimensionless basis from one frozen node operator, then propagate its covariance without using this target.

C068 deuteron-proton mag. mom. ratio

CODATA 2022. $0.3070122093\,\texttt{dimensionless}$, $u = 7.9 \times 10^{-10}$, $u_r = 2.573 \times 10^{-9}$.

Class. L — dependent law/identity; Magnetic-moment ratio.

Dependency equation. $R_{\mu,ab} = \mu_a/\mu_b$. *Inputs:* deuteron and proton magnetic moments.

Numerical audit. dependency reconstruction $0.307012209282\,\texttt{dimensionless}$; fractional residual -5.703×10^{-11}.

First-principles verdict. Algebraically reproducible, but not a first-principles physical prediction: the CODATA basis values enter the right-hand side.

END/MNT completion gate. Derive the independent dimensionless basis from one frozen node operator, then propagate its covariance without using this target.

C069 deuteron-proton mass ratio

CODATA 2022. 1.99900750127 `dimensionless`, $u = 8.4 \times 10^{-12}$, $u_r = 4.202 \times 10^{-12}$.

Class. L — dependent law/identity; Dimensionless mass ratio.

Dependency equation. $R_{ab} = m_a/m_b$. *Inputs:* deuteron mass; proton mass.

Numerical audit. dependency reconstruction 1.99900750129 `dimensionless`; fractional residual 1.12×10^{-11}.

First-principles verdict. Algebraically reproducible, but not a first-principles physical prediction: the CODATA basis values enter the right-hand side.

END/MNT completion gate. Derive the independent dimensionless basis from one frozen node operator, then propagate its covariance without using this target.

C070 deuteron relative atomic mass

CODATA 2022. 2.01355321254 `dimensionless`, $u = 1.5 \times 10^{-11}$, $u_r = 7.45 \times 10^{-12}$.

Class. L — dependent law/identity; Relative atomic mass.

Dependency equation. $A_{\mathrm{r}}(X) = m_X/m_{\mathrm{u}}$. *Inputs:* deuteron mass; atomic mass constant.

Numerical audit. dependency reconstruction 2.01355321256 `dimensionless`; fractional residual 6.374×10^{-12}.

First-principles verdict. Algebraically reproducible, but not a first-principles physical prediction: the CODATA basis values enter the right-hand side.

END/MNT completion gate. Derive the independent dimensionless basis from one frozen node operator, then propagate its covariance without using this target.

C071 deuteron rms charge radius

CODATA 2022. 2.12778×10^{-15} `m`, $u = 2.7 \times 10^{-19}$, $u_r = 1.269 \times 10^{-4}$.

Class. A — adjusted empirical input; Adjusted empirical or theory-assisted input.

Dependency equation. $Q = \arg\min_Q (\mathbf{y} - \mathbf{f}(Q))^T \mathbf{V}^{-1}(\mathbf{y} - \mathbf{f}(Q))$. *Inputs:* CODATA observational equations and covariance.

Numerical audit. no independent numerical END/MNT output; residual and z score are undefined.

First-principles verdict. No END/MNT first-principles value exists in the current papers; CODATA supplies the comparison target, not an allowed model input for a prediction.

END/MNT completion gate. Generate the relevant spectrum, form factor, or decay amplitude from the frozen micro-model and compare only after preregistration.

C072 electron charge to mass quotient

CODATA 2022. $-1.75882000838 \times 10^{11}$ `C kg^-1`, $u = 55$, $u_r = 3.127 \times 10^{-10}$.

Class. L — dependent law/identity; Charge-to-mass ratio.

Dependency equation. $q_e/m_e = -e/m_e$. *Inputs:* elementary charge; electron mass.

Numerical audit. dependency reconstruction $-1.75882000838 \times 10^{11}$ `C kg^-1`; fractional residual -1.138×10^{-12}.

First-principles verdict. Algebraically reproducible, but not a first-principles physical prediction: the CODATA basis values enter the right-hand side.

END/MNT completion gate. Derive the independent dimensionless basis from one frozen node operator, then propagate its covariance without using this target.

C073 electron-deuteron mag. mom. ratio

CODATA 2022. -2143.9234921 `dimensionless`, $u = 5.6 \times 10^{-6}$, $u_r = 2.612 \times 10^{-9}$.

Class. L — dependent law/identity; Magnetic-moment ratio.

Dependency equation. $R_{\mu,ab} = \mu_a/\mu_b$. *Inputs:* electron and deuteron magnetic moments.

Numerical audit. dependency reconstruction -2143.92349224 `dimensionless`; fractional residual 6.666×10^{-11}.

First-principles verdict. Algebraically reproducible, but not a first-principles physical prediction: the CODATA basis values enter the right-hand side.

END/MNT completion gate. Derive the independent dimensionless basis from one frozen node operator, then propagate its covariance without using this target.

C074 electron-deuteron mass ratio

CODATA 2022. $2.72443710763 \times 10^{-4}$ `dimensionless`, $u = 4.7 \times 10^{-15}$, $u_r = 1.725 \times 10^{-11}$.

Class. L — dependent law/identity; Dimensionless mass ratio.

Dependency equation. $R_{ab} = m_a/m_b$. *Inputs:* electron mass; deuteron mass.

Numerical audit. dependency reconstruction $2.72443710761 \times 10^{-4}$ `dimensionless`; fractional residual -8.809×10^{-12}.

First-principles verdict. Algebraically reproducible, but not a first-principles physical prediction: the CODATA basis values enter the right-hand side.

END/MNT completion gate. Derive the independent dimensionless basis from one frozen node operator, then propagate its covariance without using this target.

C075 electron g factor

CODATA 2022. -2.00231930436 `dimensionless`, $u = 3.6 \times 10^{-13}$, $u_r = 1.798 \times 10^{-13}$.

Class. L — dependent law/identity; Magnetic g factor.

Dependency equation. $g_X = \mu_X/(I_X\mu_{\mathrm{ref}})$. *Inputs:* electron magnetic moment; spin; reference magneton.

Numerical audit. dependency reconstruction -2.00231930436 `dimensionless`; fractional residual 6.144×10^{-13}.

First-principles verdict. Algebraically reproducible, but not a first-principles physical prediction: the CODATA basis values enter the right-hand side.

END/MNT completion gate. Derive the independent dimensionless basis from one frozen node operator, then propagate its covariance without using this target.

C076 electron gyromag. ratio

CODATA 2022. $1.76085962784 \times 10^{11}$ `s^-1 T^-1`, $u = 55$, $u_r = 3.123 \times 10^{-10}$.

Class. L — dependent law/identity; Gyromagnetic ratio.

Dependency equation. $|\gamma_X| = |\mu_X|/(I_X\hbar)$. *Inputs:* electron magnetic moment; spin; reduced Planck constant.

Numerical audit. dependency reconstruction $1.76085962783 \times 10^{11}$ `s^-1 T^-1`; fractional residual -5.904×10^{-12}.

First-principles verdict. Algebraically reproducible, but not a first-principles physical prediction: the CODATA basis values enter the right-hand side.

END/MNT completion gate. Derive the independent dimensionless basis from one frozen node operator, then propagate its covariance without using this target.

C077 electron-helion mass ratio

CODATA 2022. $1.81954307465 \times 10^{-4}$ `dimensionless`, $u = 5.3 \times 10^{-15}$, $u_r = 2.913 \times 10^{-11}$.

Class. L — dependent law/identity; Dimensionless mass ratio.

Dependency equation. $R_{ab} = m_a/m_b$. *Inputs:* electron mass; helion mass.

Numerical audit. dependency reconstruction $1.81954307464 \times 10^{-4}$ `dimensionless`; fractional residual -7.071×10^{-12}.

First-principles verdict. Algebraically reproducible, but not a first-principles physical prediction: the CODATA basis values enter the right-hand side.

END/MNT completion gate. Derive the independent dimensionless basis from one frozen node operator, then propagate its covariance without using this target.

C078 electron mag. mom.

CODATA 2022. $-9.2847646917 \times 10^{-24}$ `J T^-1`, $u = 2.9 \times 10^{-33}$, $u_r = 3.123 \times 10^{-10}$.

Class. A — adjusted empirical input; Adjusted or reference quantity.

Dependency equation. $Q = Q_{\mathrm{CODATA}} \pm u(Q)$. *Inputs:* CODATA adjustment or stated reference procedure.

Numerical audit. no independent numerical END/MNT output; residual and z score are undefined.

First-principles verdict. No independent END/MNT numerical prediction is present; numerical agreement cannot be assessed without inventing an input.

END/MNT completion gate. Specify the observable map and derive the value and uncertainty from a frozen micro-model before inspecting this target.

C079 electron mag. mom. anomaly

CODATA 2022. 0.00115965218046 `dimensionless`, $u = 1.8 \times 10^{-13}$, $u_r = 1.552 \times 10^{-10}$.

Class. L — dependent law/identity; Lepton magnetic anomaly.

Dependency equation. $a_e = |g_e|/2 - 1$. *Inputs:* electron g factor.

Numerical audit. dependency reconstruction 0.00115965218046 `dimensionless`; fractional residual -7.479×10^{-15}.

First-principles verdict. Algebraically reproducible, but not a first-principles physical prediction: the CODATA basis values enter the right-hand side.

END/MNT completion gate. Derive the independent dimensionless basis from one frozen node operator, then propagate its covariance without using this target.

C080 electron mag. mom. to Bohr magneton ratio

CODATA 2022. -1.00115965218 `dimensionless`, $u = 1.8 \times 10^{-13}$, $u_r = 1.798 \times 10^{-13}$.

Class. L — dependent law/identity; Magnetic moment in Bohr magnetons.

Dependency equation. μ_X/μ_{B}. *Inputs:* electron magnetic moment; Bohr magneton.

Numerical audit. dependency reconstruction -1.00115965218 `dimensionless`; fractional residual 6.144×10^{-13}.

First-principles verdict. Algebraically reproducible, but not a first-principles physical prediction: the CODATA basis values enter the right-hand side.

END/MNT completion gate. Derive the independent dimensionless basis from one frozen node operator, then propagate its covariance without using this target.

C081 electron mag. mom. to nuclear magneton ratio

CODATA 2022. $-1838.28197188\,\texttt{dimensionless}$, $u = 3.2 \times 10^{-8}$, $u_r = 1.741 \times 10^{-11}$.

Class. L — dependent law/identity; Magnetic moment in nuclear magnetons.

Dependency equation. μ_X/μ_{N}. *Inputs:* electron magnetic moment; nuclear magneton.

Numerical audit. dependency reconstruction $-1838.28197186\,\texttt{dimensionless}$; fractional residual -1.128×10^{-11}.

First-principles verdict. Algebraically reproducible, but not a first-principles physical prediction: the CODATA basis values enter the right-hand side.

END/MNT completion gate. Derive the independent dimensionless basis from one frozen node operator, then propagate its covariance without using this target.

C082 electron mass

CODATA 2022. $9.1093837139 \times 10^{-31}\,\texttt{kg}$, $u = 2.8 \times 10^{-40}$, $u_r = 3.074 \times 10^{-10}$.

Class. A — adjusted empirical input; Measured particle/nuclear scale.

Dependency equation. $mc^2 = E_{\mathrm{pole}} \quad \text{or} \quad m = E_0/c^2$. *Inputs:* spectroscopy, kinematics, or mass-frequency ratios.

Numerical audit. no independent numerical END/MNT output; residual and z score are undefined.

First-principles verdict. The value is empirical. END/MNT currently has a mass-gap dictionary but no particle-identifying eigenproblem that predicts this number.

END/MNT completion gate. Derive a stable localized state, its renormalized pole energy, quantum numbers, and uncertainty without tuning to the listed mass.

C083 electron mass energy equivalent

CODATA 2022. $8.187105788 \times 10^{-14}$ J, $u = 2.6 \times 10^{-23}$, $u_r = 3.176 \times 10^{-10}$.

Class. L — dependent law/identity; Relativistic mass-energy identity.

Dependency equation. $E_m = mc^2$. *Inputs:* electron mass; c.

Numerical audit. dependency reconstruction $8.18710578797 \times 10^{-14}$ J; fractional residual -3.854×10^{-12}.

First-principles verdict. Algebraically reproducible, but not a first-principles physical prediction: the CODATA basis values enter the right-hand side.

END/MNT completion gate. Derive the independent dimensionless basis from one frozen node operator, then propagate its covariance without using this target.

C084 electron mass in u

CODATA 2022. $5.48579909044 \times 10^{-4}$ u, $u = 9.7 \times 10^{-15}$, $u_r = 1.768 \times 10^{-11}$.

Class. L — dependent law/identity; Relative-mass conversion.

Dependency equation. $m/\mathrm{u} = m/m_{\mathrm{u}}$. *Inputs:* electron mass; atomic mass constant.

Numerical audit. dependency reconstruction $5.48579909043 \times 10^{-4}$ u; fractional residual -2.534×10^{-12}.

First-principles verdict. Algebraically reproducible, but not a first-principles physical prediction: the CODATA basis values enter the right-hand side.

END/MNT completion gate. Derive the independent dimensionless basis from one frozen node operator, then propagate its covariance without using this target.

C085 electron molar mass

CODATA 2022. $5.4857990962 \times 10^{-7}$ `kg mol^-1`, $u = 1.7 \times 10^{-16}$, $u_r = 3.099 \times 10^{-10}$.

Class. L — dependent law/identity; Molar mass from single-particle mass.

Dependency equation. $M(X) = N_{\mathrm{A}} m_X$. *Inputs:* Avogadro constant; electron mass.

Numerical audit. dependency reconstruction $5.4857990962 \times 10^{-7}$ `kg mol^-1`; fractional residual -7.77×10^{-13}.

First-principles verdict. Algebraically reproducible, but not a first-principles physical prediction: the CODATA basis values enter the right-hand side.

END/MNT completion gate. Derive the independent dimensionless basis from one frozen node operator, then propagate its covariance without using this target.

C086 electron-muon mag. mom. ratio

CODATA 2022. 206.7669881 `dimensionless`, $u = 4.6 \times 10^{-6}$, $u_r = 2.225 \times 10^{-8}$.

Class. L — dependent law/identity; Magnetic-moment ratio.

Dependency equation. $R_{\mu,ab} = \mu_a/\mu_b$. *Inputs:* electron and muon magnetic moments.

Numerical audit. dependency reconstruction 206.766987868 `dimensionless`; fractional residual -1.12×10^{-9}.

First-principles verdict. Algebraically reproducible, but not a first-principles physical prediction: the CODATA basis values enter the right-hand side.

END/MNT completion gate. Derive the independent dimensionless basis from one frozen node operator, then propagate its covariance without using this target.

C087 electron-muon mass ratio

CODATA 2022. 0.0048363317 `dimensionless`, $u = 1.1 \times 10^{-10}$, $u_r = 2.274 \times 10^{-8}$.

Class. L — dependent law/identity; Dimensionless mass ratio.

Dependency equation. $R_{ab} = m_a/m_b$. *Inputs:* electron mass; muon mass.

Numerical audit. dependency reconstruction 0.00483633169909 `dimensionless`; fractional residual -1.88×10^{-10}.

First-principles verdict. Algebraically reproducible, but not a first-principles physical prediction: the CODATA basis values enter the right-hand side.

END/MNT completion gate. Derive the independent dimensionless basis from one frozen node operator, then propagate its covariance without using this target.

C088 electron-neutron mag. mom. ratio

CODATA 2022. 960.92048 `dimensionless`, $u = 2.3 \times 10^{-4}$, $u_r = 2.394 \times 10^{-7}$.

Class. L — dependent law/identity; Magnetic-moment ratio.

Dependency equation. $R_{\mu,ab} = \mu_a/\mu_b$. *Inputs:* electron and neutron magnetic moments.

Numerical audit. dependency reconstruction 960.920478933 `dimensionless`; fractional residual -1.111×10^{-9}.

First-principles verdict. Algebraically reproducible, but not a first-principles physical prediction: the CODATA basis values enter the right-hand side.

END/MNT completion gate. Derive the independent dimensionless basis from one frozen node operator, then propagate its covariance without using this target.

C089 electron-neutron mass ratio

CODATA 2022. $5.4386734416 \times 10^{-4}$ `dimensionless`, $u = 2.2 \times 10^{-13}$, $u_r = 4.045 \times 10^{-10}$.

Class. L — dependent law/identity; Dimensionless mass ratio.

Dependency equation. $R_{ab} = m_a/m_b$. *Inputs:* electron mass; neutron mass.

Numerical audit. dependency reconstruction $5.4386734416 \times 10^{-4}$ `dimensionless`; fractional residual -1.254×10^{-13}.

First-principles verdict. Algebraically reproducible, but not a first-principles physical prediction: the CODATA basis values enter the right-hand side.

END/MNT completion gate. Derive the independent dimensionless basis from one frozen node operator, then propagate its covariance without using this target.

C090 electron-proton mag. mom. ratio

CODATA 2022. -658.21068789 `dimensionless`, $u = 1.9 \times 10^{-7}$, $u_r = 2.887 \times 10^{-10}$.

Class. L — dependent law/identity; Magnetic-moment ratio.

Dependency equation. $R_{\mu,ab} = \mu_a/\mu_b$. *Inputs:* electron and proton magnetic moments.

Numerical audit. dependency reconstruction -658.210687886 `dimensionless`; fractional residual -5.873×10^{-12}.

First-principles verdict. Algebraically reproducible, but not a first-principles physical prediction: the CODATA basis values enter the right-hand side.

END/MNT completion gate. Derive the independent dimensionless basis from one frozen node operator, then propagate its covariance without using this target.

C091 electron-proton mass ratio

CODATA 2022. $5.44617021489 \times 10^{-4}$ `dimensionless`, $u = 9.4 \times 10^{-15}$, $u_r = 1.726 \times 10^{-11}$.

Class. L — dependent law/identity; Dimensionless mass ratio.

Dependency equation. $R_{ab} = m_a/m_b$. *Inputs:* electron mass; proton mass.

Numerical audit. dependency reconstruction $5.4461702149 \times 10^{-4}$ `dimensionless`; fractional residual 2.287×10^{-12}.

First-principles verdict. Algebraically reproducible, but not a first-principles physical prediction: the CODATA basis values enter the right-hand side.

END/MNT completion gate. Derive the independent dimensionless basis from one frozen node operator, then propagate its covariance without using this target.

C092 electron relative atomic mass

CODATA 2022. $5.48579909044 \times 10^{-4}$ `dimensionless`, $u = 9.7 \times 10^{-15}$, $u_r = 1.768 \times 10^{-11}$.

Class. L — dependent law/identity; Relative atomic mass.

Dependency equation. $A_{\mathrm{r}}(X) = m_X/m_{\mathrm{u}}$. *Inputs:* electron mass; atomic mass constant.

Numerical audit. dependency reconstruction $5.48579909043 \times 10^{-4}$ `dimensionless`; fractional residual -2.534×10^{-12}.

First-principles verdict. Algebraically reproducible, but not a first-principles physical prediction: the CODATA basis values enter the right-hand side.

END/MNT completion gate. Derive the independent dimensionless basis from one frozen node operator, then propagate its covariance without using this target.

C093 electron-tau mass ratio

CODATA 2022. 2.87585×10^{-4} `dimensionless`, $u = 1.9 \times 10^{-8}$, $u_r = 6.607 \times 10^{-5}$.

Class. L — dependent law/identity; Dimensionless mass ratio.

Dependency equation. $R_{ab} = m_a/m_b$. *Inputs:* electron mass; tau mass.

Numerical audit. dependency reconstruction $2.87585435824 \times 10^{-4}$ `dimensionless`; fractional residual 1.515×10^{-6}.

First-principles verdict. Algebraically reproducible, but not a first-principles physical prediction: the CODATA basis values enter the right-hand side.

END/MNT completion gate. Derive the independent dimensionless basis from one frozen node operator, then propagate its covariance without using this target.

C094 electron to alpha particle mass ratio

CODATA 2022. $1.37093355473 \times 10^{-4}$ `dimensionless`, $u = 3.2 \times 10^{-15}$, $u_r = 2.334 \times 10^{-11}$.

Class. L — dependent law/identity; Dimensionless mass ratio.

Dependency equation. $R_{ab} = m_a/m_b$. *Inputs:* electron mass; alpha particle mass.

Numerical audit. dependency reconstruction $1.37093355472 \times 10^{-4}$ `dimensionless`; fractional residual -6.98×10^{-12}.

First-principles verdict. Algebraically reproducible, but not a first-principles physical prediction: the CODATA basis values enter the right-hand side.

END/MNT completion gate. Derive the independent dimensionless basis from one frozen node operator, then propagate its covariance without using this target.

C095 electron to shielded helion mag. mom. ratio

CODATA 2022. 864.05823986 `dimensionless`, $u = 7 \times 10^{-7}$, $u_r = 8.101 \times 10^{-10}$.

Class. L — dependent law/identity; Magnetic-moment ratio.

Dependency equation. $R_{\mu,ab} = \mu_a/\mu_b$. *Inputs:* electron and shielded helion magnetic moments.

Numerical audit. dependency reconstruction 864.058239865 `dimensionless`; fractional residual 5.267×10^{-12}.

First-principles verdict. Algebraically reproducible, but not a first-principles physical prediction: the CODATA basis values enter the right-hand side.

END/MNT completion gate. Derive the independent dimensionless basis from one frozen node operator, then propagate its covariance without using this target.

C096 electron to shielded proton mag. mom. ratio

CODATA 2022. -658.2275856 `dimensionless`, $u = 2.7 \times 10^{-6}$, $u_r = 4.102 \times 10^{-9}$.

Class. L — dependent law/identity; Magnetic-moment ratio.

Dependency equation. $R_{\mu,ab} = \mu_a/\mu_b$. *Inputs:* electron and shielded proton magnetic moments.

Numerical audit. dependency reconstruction -658.227585602 `dimensionless`; fractional residual 3.797×10^{-12}.

First-principles verdict. Algebraically reproducible, but not a first-principles physical prediction: the CODATA basis values enter the right-hand side.

END/MNT completion gate. Derive the independent dimensionless basis from one frozen node operator, then propagate its covariance without using this target.

C097 electron-triton mass ratio

CODATA 2022. $1.81920006233 \times 10^{-4}$ `dimensionless`, $u = 6.8 \times 10^{-15}$, $u_r = 3.738 \times 10^{-11}$.

Class. L — dependent law/identity; Dimensionless mass ratio.

Dependency equation. $R_{ab} = m_a/m_b$. *Inputs:* electron mass; triton mass.

Numerical audit. dependency reconstruction $1.81920006233 \times 10^{-4}$ `dimensionless`; fractional residual 2.573×10^{-12}.

First-principles verdict. Algebraically reproducible, but not a first-principles physical prediction: the CODATA basis values enter the right-hand side.

END/MNT completion gate. Derive the independent dimensionless basis from one frozen node operator, then propagate its covariance without using this target.

C098 electron volt

CODATA 2022. $1.602176634 \times 10^{-19}$ `J` (exact in the stated system).

Class. L — dependent law/identity; Energy unit.

Dependency equation. $1\,\mathrm{eV} = e\,\mathrm{J/C}$. *Inputs:* elementary charge.

Numerical audit. dependency reconstruction $1.602176634 \times 10^{-19}$ `J`; fractional residual 0.

First-principles verdict. Algebraically reproducible, but not a first-principles physical prediction: the CODATA basis values enter the right-hand side.

END/MNT completion gate. Derive the independent dimensionless basis from one frozen node operator, then propagate its covariance without using this target.

C099 elementary charge

CODATA 2022. $1.602176634 \times 10^{-19}$ `C` (exact in the stated system).

Class. D — SI definition; SI defining constant.

Dependency equation. $Q \equiv Q_{\mathrm{SI}}$ (exact by definition). *Inputs:* SI definition.

Numerical audit. identity check $1.602176634 \times 10^{-19}$ `C`; fractional residual 0.

First-principles verdict. Exact numerical identity in SI; this fixes a unit conversion and is not a prediction of nature's dimensionless structure.

END/MNT completion gate. Explain the invariant physical role and derive held-out dimensionless ratios; reproducing the stipulated SI digits is not evidence.

C100 elementary charge over h-bar

CODATA 2022. $1.51926744788 \times 10^{15}$ `A J^-1` (exact in the stated system).

Class. L — dependent law/identity; Charge/action ratio.

Dependency equation. $e/\hbar$. *Inputs:* e; hbar.

Numerical audit. dependency reconstruction $1.51926744788 \times 10^{15}$ `A J^-1`; fractional residual 0.

First-principles verdict. Algebraically reproducible, but not a first-principles physical prediction: the CODATA basis values enter the right-hand side.

END/MNT completion gate. Derive the independent dimensionless basis from one frozen node operator, then propagate its covariance without using this target.

C101 Faraday constant

CODATA 2022. 96485.3321233 `C mol^-1` (exact in the stated system).

Class. L — dependent law/identity; Molar charge.

Dependency equation. $F = N_{\mathrm{A}}e$. *Inputs:* Avogadro constant; elementary charge.

Numerical audit. dependency reconstruction 96485.3321233 `C mol^-1`; fractional residual 0.

First-principles verdict. Algebraically reproducible, but not a first-principles physical prediction: the CODATA basis values enter the right-hand side.

END/MNT completion gate. Derive the independent dimensionless basis from one frozen node operator, then propagate its covariance without using this target.

C102 Fermi coupling constant

CODATA 2022. 1.1663787×10^{-5} `GeV^-2`, $u = 6 \times 10^{-12}$, $u_r = 5.144 \times 10^{-7}$.

Class. A — adjusted empirical input; Adjusted empirical or theory-assisted input.

Dependency equation. $Q = \arg\min_{Q} (\mathbf{y} - \mathbf{f}(Q))^T \mathbf{V}^{-1} (\mathbf{y} - \mathbf{f}(Q))$. *Inputs:* CODATA observational equations and covariance.

Numerical audit. no independent numerical END/MNT output; residual and z score are undefined.

First-principles verdict. No END/MNT first-principles value exists in the current papers; CODATA supplies the comparison target, not an allowed model input for a prediction.

END/MNT completion gate. Generate the relevant spectrum, form factor, or decay amplitude from the frozen micro-model and compare only after preregistration.

C103 fine-structure constant

CODATA 2022. 0.0072973525643 `dimensionless`, $u = 1.1 \times 10^{-12}$, $u_r = 1.507 \times 10^{-10}$.

Class. L — dependent law/identity; Electromagnetic coupling.

Dependency equation. $\alpha = e^2/(4\pi\epsilon_0\hbar c)$. *Inputs:* e; epsilon0; hbar; c.

Numerical audit. dependency reconstruction 0.00729735256433 `dimensionless`; fractional residual 4.524×10^{-12}.

First-principles verdict. Algebraically reproducible, but not a first-principles physical prediction: the CODATA basis values enter the right-hand side.

END/MNT completion gate. Derive the independent dimensionless basis from one frozen node operator, then propagate its covariance without using this target.

C104 first radiation constant

CODATA 2022. $3.74177185219 \times 10^{-16}$ `W m^2` (exact in the stated system).

Class. L — dependent law/identity; Planck-spectrum coefficient.

Dependency equation. $c_1 = 2\pi hc^2$. *Inputs:* h; c.

Numerical audit. dependency reconstruction $3.74177185219 \times 10^{-16}$ `W m^2`; fractional residual 0.

First-principles verdict. Algebraically reproducible, but not a first-principles physical prediction: the CODATA basis values enter the right-hand side.

END/MNT completion gate. Derive the independent dimensionless basis from one frozen node operator, then propagate its covariance without using this target.

C105 first radiation constant for spectral radiance

CODATA 2022. $1.1910429724 \times 10^{-16}$ `W m^2 sr^-1` (exact in the stated system).

Class. L — dependent law/identity; Spectral-radiance coefficient.

Dependency equation. $c_{1L} = 2hc^2$. *Inputs:* h; c.

Numerical audit. dependency reconstruction $1.1910429724 \times 10^{-16}$ `W m^2 sr^-1`; fractional residual 0.

First-principles verdict. Algebraically reproducible, but not a first-principles physical prediction: the CODATA basis values enter the right-hand side.

END/MNT completion gate. Derive the independent dimensionless basis from one frozen node operator, then propagate its covariance without using this target.

C106 Hartree energy

CODATA 2022. $4.35974472221 \times 10^{-18}$ `J`, $u = 4.8 \times 10^{-30}$, $u_r = 1.101 \times 10^{-12}$.

Class. L — dependent law/identity; Atomic energy.

Dependency equation. $E_\mathrm{h} = \alpha^2 m_e c^2$. *Inputs:* alpha; electron mass; c.

Numerical audit. dependency reconstruction $4.35974472216 \times 10^{-18}$ `J`; fractional residual -1.08×10^{-11}.

First-principles verdict. Algebraically reproducible, but not a first-principles physical prediction: the CODATA basis values enter the right-hand side.

END/MNT completion gate. Derive the independent dimensionless basis from one frozen node operator, then propagate its covariance without using this target.

C107 Hartree energy in eV

CODATA 2022. 27.211386246 `eV`, $u = 3 \times 10^{-11}$, $u_r = 1.102 \times 10^{-12}$.

Class. L — dependent law/identity; Atomic energy in eV.

Dependency equation. $E_\mathrm{h}[\mathrm{eV}] = E_\mathrm{h}/e$. *Inputs:* Hartree energy; e.

Numerical audit. dependency reconstruction 27.211386246 `eV`; fractional residual 6.136×10^{-15}.

First-principles verdict. Algebraically reproducible, but not a first-principles physical prediction: the CODATA basis values enter the right-hand side.

END/MNT completion gate. Derive the independent dimensionless basis from one frozen node operator, then propagate its covariance without using this target.

C108 helion-electron mass ratio

CODATA 2022. 5495.88527984 `dimensionless`, $u = 1.6 \times 10^{-7}$, $u_r = 2.911 \times 10^{-11}$.

Class. L — dependent law/identity; Dimensionless mass ratio.

Dependency equation. $R_{ab} = m_a/m_b$. *Inputs:* helion mass; electron mass.

Numerical audit. dependency reconstruction 5495.88527988 `dimensionless`; fractional residual 7.246×10^{-12}.

First-principles verdict. Algebraically reproducible, but not a first-principles physical prediction: the CODATA basis values enter the right-hand side.

END/MNT completion gate. Derive the independent dimensionless basis from one frozen node operator, then propagate its covariance without using this target.

C109 helion g factor

CODATA 2022. $-4.2552506995\,\texttt{dimensionless}$, $u = 3.4 \times 10^{-9}$, $u_r = 7.99 \times 10^{-10}$.

Class. L — dependent law/identity; Magnetic g factor.

Dependency equation. $g_X = \mu_X/(I_X\mu_{\text{ref}})$. *Inputs:* helion magnetic moment; spin; reference magneton.

Numerical audit. dependency reconstruction $-4.25525069948\,\texttt{dimensionless}$; fractional residual -3.702×10^{-12}.

First-principles verdict. Algebraically reproducible, but not a first-principles physical prediction: the CODATA basis values enter the right-hand side.

END/MNT completion gate. Derive the independent dimensionless basis from one frozen node operator, then propagate its covariance without using this target.

C110 helion mag. mom.

CODATA 2022. $-1.07461755198 \times 10^{-26}\,\texttt{J T\^{}-1}$, $u = 9.3 \times 10^{-36}$, $u_r = 8.654 \times 10^{-10}$.

Class. A — adjusted empirical input; Adjusted or reference quantity.

Dependency equation. $Q = Q_{\text{CODATA}} \pm u(Q)$. *Inputs:* CODATA adjustment or stated reference procedure.

Numerical audit. no independent numerical END/MNT output; residual and z score are undefined.

First-principles verdict. No independent END/MNT numerical prediction is present; numerical agreement cannot be assessed without inventing an input.

END/MNT completion gate. Specify the observable map and derive the value and uncertainty from a frozen micro-model before inspecting this target.

C111 helion mag. mom. to Bohr magneton ratio

CODATA 2022. -0.00115874098083 `dimensionless`, $u = 9.4 \times 10^{-13}$, $u_r = 8.112 \times 10^{-10}$.

Class. L — dependent law/identity; Magnetic moment in Bohr magnetons.

Dependency equation. μ_X/μ_B. *Inputs:* helion magnetic moment; Bohr magneton.

Numerical audit. dependency reconstruction -0.00115874098083 `dimensionless`; fractional residual 4.047×10^{-12}.

First-principles verdict. Algebraically reproducible, but not a first-principles physical prediction: the CODATA basis values enter the right-hand side.

END/MNT completion gate. Derive the independent dimensionless basis from one frozen node operator, then propagate its covariance without using this target.

C112 helion mag. mom. to nuclear magneton ratio

CODATA 2022. -2.1276253498 `dimensionless`, $u = 1.7 \times 10^{-9}$, $u_r = 7.99 \times 10^{-10}$.

Class. L — dependent law/identity; Magnetic moment in nuclear magnetons.

Dependency equation. μ_X/μ_N. *Inputs:* helion magnetic moment; nuclear magneton.

Numerical audit. dependency reconstruction -2.12762534974 `dimensionless`; fractional residual -2.72×10^{-11}.

First-principles verdict. Algebraically reproducible, but not a first-principles physical prediction: the CODATA basis values enter the right-hand side.

END/MNT completion gate. Derive the independent dimensionless basis from one frozen node operator, then propagate its covariance without using this target.

C113 helion mass

CODATA 2022. $5.0064127862 \times 10^{-27}$ $\texttt{kg}$, $u = 1.6 \times 10^{-36}$, $u_r = 3.196 \times 10^{-10}$.

Class. A — adjusted empirical input; Measured particle/nuclear scale.

Dependency equation. $mc^2 = E_{\text{pole}} \quad \text{or} \quad m = E_0/c^2$. *Inputs:* spectroscopy, kinematics, or mass-frequency ratios.

Numerical audit. no independent numerical END/MNT output; residual and z score are undefined.

First-principles verdict. The value is empirical. END/MNT currently has a mass-gap dictionary but no particle-identifying eigenproblem that predicts this number.

END/MNT completion gate. Derive a stable localized state, its renormalized pole energy, quantum numbers, and uncertainty without tuning to the listed mass.

C114 helion mass energy equivalent

CODATA 2022. $4.4995394185 \times 10^{-10}$ $\texttt{J}$, $u = 1.4 \times 10^{-19}$, $u_r = 3.111 \times 10^{-10}$.

Class. L — dependent law/identity; Relativistic mass-energy identity.

Dependency equation. $E_m = mc^2$. *Inputs:* helion mass; c.

Numerical audit. dependency reconstruction $4.49953941849 \times 10^{-10}$ $\texttt{J}$; fractional residual -1.896×10^{-12}.

First-principles verdict. Algebraically reproducible, but not a first-principles physical prediction: the CODATA basis values enter the right-hand side.

END/MNT completion gate. Derive the independent dimensionless basis from one frozen node operator, then propagate its covariance without using this target.

C115 helion mass in u

CODATA 2022. 3.01493224693 `u`, $u = 7.4 \times 10^{-11}$, $u_r = 2.454 \times 10^{-11}$.

Class. L — dependent law/identity; Relative-mass conversion.

Dependency equation. $m/\mathrm{u} = m/m_{\mathrm{u}}$. *Inputs:* helion mass; atomic mass constant.

Numerical audit. dependency reconstruction 3.01493224695 `u`; fractional residual 4.525×10^{-12}.

First-principles verdict. Algebraically reproducible, but not a first-principles physical prediction: the CODATA basis values enter the right-hand side.

END/MNT completion gate. Derive the independent dimensionless basis from one frozen node operator, then propagate its covariance without using this target.

C116 helion molar mass

CODATA 2022. 0.0030149322501 `kg mol^-1`, $u = 9.4 \times 10^{-13}$, $u_r = 3.118 \times 10^{-10}$.

Class. L — dependent law/identity; Molar mass from single-particle mass.

Dependency equation. $M(X) = N_{\mathrm{A}} m_X$. *Inputs:* Avogadro constant; helion mass.

Numerical audit. dependency reconstruction 0.00301493225012 `kg mol^-1`; fractional residual 5.313×10^{-12}.

First-principles verdict. Algebraically reproducible, but not a first-principles physical prediction: the CODATA basis values enter the right-hand side.

END/MNT completion gate. Derive the independent dimensionless basis from one frozen node operator, then propagate its covariance without using this target.

C117 helion-proton mass ratio

CODATA 2022. 2.99315267155 `dimensionless`, $u = 7 \times 10^{-11}$, $u_r = 2.339 \times 10^{-11}$.

Class. L — dependent law/identity; Dimensionless mass ratio.

Dependency equation. $R_{ab} = m_a/m_b$. *Inputs:* helion mass; proton mass.

Numerical audit. dependency reconstruction 2.99315267158 `dimensionless`; fractional residual 9.249×10^{-12}.

First-principles verdict. Algebraically reproducible, but not a first-principles physical prediction: the CODATA basis values enter the right-hand side.

END/MNT completion gate. Derive the independent dimensionless basis from one frozen node operator, then propagate its covariance without using this target.

C118 helion relative atomic mass

CODATA 2022. 3.01493224693 `dimensionless`, $u = 7.4 \times 10^{-11}$, $u_r = 2.454 \times 10^{-11}$.

Class. L — dependent law/identity; Relative atomic mass.

Dependency equation. $A_{\mathrm{r}}(X) = m_X/m_{\mathrm{u}}$. *Inputs:* helion mass; atomic mass constant.

Numerical audit. dependency reconstruction 3.01493224695 `dimensionless`; fractional residual 4.525×10^{-12}.

First-principles verdict. Algebraically reproducible, but not a first-principles physical prediction: the CODATA basis values enter the right-hand side.

END/MNT completion gate. Derive the independent dimensionless basis from one frozen node operator, then propagate its covariance without using this target.

C119 helion shielding shift

CODATA 2022. 5.9967029×10^{-5} `dimensionless`, $u = 2.3 \times 10^{-11}$, $u_r = 3.835 \times 10^{-7}$.

Class. R — material/reference dependent; Material or environment-dependent reference.

Dependency equation. $Q = Q(T, p, \text{composition, preparation})$. *Inputs:* experimental reference conditions.

Numerical audit. no independent numerical END/MNT output; residual and z score are undefined.

First-principles verdict. Not a universal constant of a microscopic theory; it must be measured or calculated from a detailed material model.

END/MNT completion gate. Derive the relevant bound-state/material Hamiltonian and the stated experimental conditions before comparison.

C120 hyperfine transition frequency of Cs-133

CODATA 2022. 9.19263177×10^{9} `Hz` (exact in the stated system).

Class. D — SI definition; SI defining constant.

Dependency equation. $Q \equiv Q_{\text{SI}} \quad \text{(exact by definition)}$. *Inputs:* SI definition.

Numerical audit. identity check 9.19263177×10^{9} `Hz`; fractional residual 0.

First-principles verdict. Exact numerical identity in SI; this fixes a unit conversion and is not a prediction of nature's dimensionless structure.

END/MNT completion gate. Explain the invariant physical role and derive held-out dimensionless ratios; reproducing the stipulated SI digits is not evidence.

C121 inverse fine-structure constant

CODATA 2022. 137.035999177 `dimensionless`, $u = 2.1 \times 10^{-8}$, $u_r = 1.532 \times 10^{-10}$.

Class. L — dependent law/identity; Inverse electromagnetic coupling.

Dependency equation. $\alpha^{-1} = 1/\alpha$. *Inputs:* alpha.

Numerical audit. dependency reconstruction 137.035999178 `dimensionless`; fractional residual 4.306×10^{-12}.

First-principles verdict. Algebraically reproducible, but not a first-principles physical prediction: the CODATA basis values enter the right-hand side.

END/MNT completion gate. Derive the independent dimensionless basis from one frozen node operator, then propagate its covariance without using this target.

C122 inverse of conductance quantum

CODATA 2022. 12906.4037297 `ohm` (exact in the stated system).

Class. L — dependent law/identity; Inverse conductance quantum.

Dependency equation. $G_0^{-1} = h/(2e^2)$. *Inputs:* e; h.

Numerical audit. dependency reconstruction 12906.4037297 `ohm`; fractional residual 0.

First-principles verdict. Algebraically reproducible, but not a first-principles physical prediction: the CODATA basis values enter the right-hand side.

END/MNT completion gate. Derive the independent dimensionless basis from one frozen node operator, then propagate its covariance without using this target.

C123 Josephson constant

CODATA 2022. $4.83597848417 \times 10^{14}$ `Hz V^-1` (exact in the stated system).

Class. L — dependent law/identity; Josephson frequency-voltage constant.

Dependency equation. $K_{\mathrm{J}} = 2e/h$. *Inputs:* e; h.

Numerical audit. dependency reconstruction $4.83597848417 \times 10^{14}$ `Hz V^-1`; fractional residual 0.

First-principles verdict. Algebraically reproducible, but not a first-principles physical prediction: the CODATA basis values enter the right-hand side.

END/MNT completion gate. Derive the independent dimensionless basis from one frozen node operator, then propagate its covariance without using this target.

C124 lattice parameter of silicon

CODATA 2022. $5.431020511 \times 10^{-10}$ `m`, $u = 8.9 \times 10^{-18}$, $u_r = 1.639 \times 10^{-8}$.

Class. R — material/reference dependent; Material or environment-dependent reference.

Dependency equation. $Q = Q(T, p, \text{composition, preparation})$. *Inputs:* experimental reference conditions.

Numerical audit. no independent numerical END/MNT output; residual and z score are undefined.

First-principles verdict. Not a universal constant of a microscopic theory; it must be measured or calculated from a detailed material model.

END/MNT completion gate. Derive the relevant bound-state/material Hamiltonian and the stated experimental conditions before comparison.

C125 lattice spacing of ideal Si (220)

CODATA 2022. $1.920155716 \times 10^{-10}\,\mathtt{m}$, $u = 3.2 \times 10^{-18}$, $u_r = 1.667 \times 10^{-8}$.

Class. R — material/reference dependent; Material or environment-dependent reference.

Dependency equation. $Q = Q(T, p, \text{composition, preparation})$. *Inputs:* experimental reference conditions.

Numerical audit. no independent numerical END/MNT output; residual and z score are undefined.

First-principles verdict. Not a universal constant of a microscopic theory; it must be measured or calculated from a detailed material model.

END/MNT completion gate. Derive the relevant bound-state/material Hamiltonian and the stated experimental conditions before comparison.

C126 Loschmidt constant (273.15 K, 100 kPa)

CODATA 2022. $2.65164580488 \times 10^{25}\,\mathtt{m\hat{}{-}3}$ (exact in the stated system).

Class. L — dependent law/identity; Ideal-gas number density.

Dependency equation. $n_0 = p_0/(k_B T_0)$. *Inputs:* reference p,T; Boltzmann constant.

Numerical audit. dependency reconstruction $2.65164580488 \times 10^{25}\,\mathtt{m\hat{}{-}3}$; fractional residual 0.

First-principles verdict. Derived from the ideal-gas equation and a conventional state, not a new fundamental prediction.

END/MNT completion gate. Only non-ideal corrections or microphysical equation-of-state coefficients could provide an END/MNT test.

C127 Loschmidt constant (273.15 K, 101.325 kPa)

CODATA 2022. $2.6867801118 \times 10^{25}$ `m^-3` (exact in the stated system).

Class. L — dependent law/identity; Ideal-gas number density.

Dependency equation. $n_0 = p_0/(k_B T_0)$. *Inputs:* reference p,T; Boltzmann constant.

Numerical audit. dependency reconstruction $2.6867801118 \times 10^{25}$ `m^-3`; fractional residual 0.

First-principles verdict. Derived from the ideal-gas equation and a conventional state, not a new fundamental prediction.

END/MNT completion gate. Only non-ideal corrections or microphysical equation-of-state coefficients could provide an END/MNT test.

C128 luminous efficacy

CODATA 2022. 683 `lm W^-1` (exact in the stated system).

Class. D — SI definition; SI defining constant.

Dependency equation. $Q \equiv Q_{SI}$ (exact by definition). *Inputs:* SI definition.

Numerical audit. identity check 683 `lm W^-1`; fractional residual 0.

First-principles verdict. Exact numerical identity in SI; this fixes a unit conversion and is not a prediction of nature's dimensionless structure.

END/MNT completion gate. Explain the invariant physical role and derive held-out dimensionless ratios; reproducing the stipulated SI digits is not evidence.

C129 mag. flux quantum

CODATA 2022. $2.06783384846 \times 10^{-15}\,\mathtt{Wb}$ (exact in the stated system).

Class. L — dependent law/identity; Superconducting flux quantum.

Dependency equation. $\Phi_0 = h/(2e)$. *Inputs:* h; e.

Numerical audit. dependency reconstruction $2.06783384846 \times 10^{-15}\,\mathtt{Wb}$; fractional residual 0.

First-principles verdict. Algebraically reproducible, but not a first-principles physical prediction: the CODATA basis values enter the right-hand side.

END/MNT completion gate. Derive the independent dimensionless basis from one frozen node operator, then propagate its covariance without using this target.

C130 molar gas constant

CODATA 2022. 8.31446261815 `J mol^-1 K^-1` (exact in the stated system).

Class. L — dependent law/identity; Molar thermal conversion.

Dependency equation. $R = N_{\mathrm{A}} k_{\mathrm{B}}$. *Inputs:* Avogadro constant; Boltzmann constant.

Numerical audit. dependency reconstruction 8.31446261815 `J mol^-1 K^-1`; fractional residual 0.

First-principles verdict. Algebraically reproducible, but not a first-principles physical prediction: the CODATA basis values enter the right-hand side.

END/MNT completion gate. Derive the independent dimensionless basis from one frozen node operator, then propagate its covariance without using this target.

C131 molar mass constant

CODATA 2022. 0.00100000000105 `kg mol^-1`, $u = 3.1 \times 10^{-13}$, $u_r = 3.1 \times 10^{-10}$.

Class. A — adjusted empirical input; Adjusted empirical or theory-assisted input.

Dependency equation. $Q = \arg\min_Q (\mathbf{y} - \mathbf{f}(Q))^T \mathbf{V}^{-1}(\mathbf{y} - \mathbf{f}(Q))$. *Inputs:* CODATA observational equations and covariance.

Numerical audit. no independent numerical END/MNT output; residual and z score are undefined.

First-principles verdict. No END/MNT first-principles value exists in the current papers; CODATA supplies the comparison target, not an allowed model input for a prediction.

END/MNT completion gate. Generate the relevant spectrum, form factor, or decay amplitude from the frozen micro-model and compare only after preregistration.

C132 molar mass of carbon-12

CODATA 2022. 0.0120000000126 `kg mol^-1`, $u = 3.7 \times 10^{-12}$, $u_r = 3.083 \times 10^{-10}$.

Class. A — adjusted empirical input; Adjusted empirical or theory-assisted input.

Dependency equation. $Q = \arg\min_Q (\mathbf{y} - \mathbf{f}(Q))^T \mathbf{V}^{-1}(\mathbf{y} - \mathbf{f}(Q))$. *Inputs:* CODATA observational equations and covariance.

Numerical audit. no independent numerical END/MNT output; residual and z score are undefined.

First-principles verdict. No END/MNT first-principles value exists in the current papers; CODATA supplies the comparison target, not an allowed model input for a prediction.

END/MNT completion gate. Generate the relevant spectrum, form factor, or decay amplitude from the frozen micro-model and compare only after preregistration.

C133 molar Planck constant

CODATA 2022. $3.99031271289 \times 10^{-10}$ `J Hz^-1 mol^-1` (exact in the stated system).

Class. L — dependent law/identity; Molar action.

Dependency equation. $N_{\mathrm{A}}h$. *Inputs:* Avogadro constant; Planck constant.

Numerical audit. dependency reconstruction $3.99031271289 \times 10^{-10}$ `J Hz^-1 mol^-1`; fractional residual 0.

First-principles verdict. Algebraically reproducible, but not a first-principles physical prediction: the CODATA basis values enter the right-hand side.

END/MNT completion gate. Derive the independent dimensionless basis from one frozen node operator, then propagate its covariance without using this target.

C134 molar volume of ideal gas (273.15 K, 100 kPa)

CODATA 2022. 0.0227109546415 `m^3 mol^-1` (exact in the stated system).

Class. L — dependent law/identity; Ideal-gas molar volume.

Dependency equation. $V_m = RT_0/p_0$. *Inputs:* reference p,T; molar gas constant.

Numerical audit. dependency reconstruction 0.0227109546415 `m^3 mol^-1`; fractional residual 0.

First-principles verdict. Derived from an ideal equation of state and stipulated conditions.

END/MNT completion gate. Derive the equation of state and corrections from microdynamics before treating it as a theory test.

C135 molar volume of ideal gas (273.15 K, 101.325 kPa)

CODATA 2022. 0.022413969545 `m^3 mol^-1` (exact in the stated system).

Class. L — dependent law/identity; Ideal-gas molar volume.

Dependency equation. $V_m = RT_0/p_0$. *Inputs:* reference p,T; molar gas constant.

Numerical audit. dependency reconstruction 0.022413969545 `m^3 mol^-1`; fractional residual 0.

First-principles verdict. Derived from an ideal equation of state and stipulated conditions.

END/MNT completion gate. Derive the equation of state and corrections from microdynamics before treating it as a theory test.

C136 molar volume of silicon

CODATA 2022. $1.205883199 \times 10^{-5}$ `m^3 mol^-1`, $u = 6 \times 10^{-13}$, $u_r = 4.976 \times 10^{-8}$.

Class. R — material/reference dependent; Material or environment-dependent reference.

Dependency equation. $Q = Q(T, p, \text{composition, preparation})$. *Inputs:* experimental reference conditions.

Numerical audit. no independent numerical END/MNT output; residual and z score are undefined.

First-principles verdict. Not a universal constant of a microscopic theory; it must be measured or calculated from a detailed material model.

END/MNT completion gate. Derive the relevant bound-state/material Hamiltonian and the stated experimental conditions before comparison.

C137 Molybdenum x unit

CODATA 2022. $1.00209952 \times 10^{-13}\,\mathtt{m}$, $u = 5.3 \times 10^{-20}$, $u_r = 5.289 \times 10^{-7}$.

Class. R — material/reference dependent; Material or environment-dependent reference.

Dependency equation. $Q = Q(T, p, \text{composition, preparation})$. *Inputs:* experimental reference conditions.

Numerical audit. no independent numerical END/MNT output; residual and z score are undefined.

First-principles verdict. Not a universal constant of a microscopic theory; it must be measured or calculated from a detailed material model.

END/MNT completion gate. Derive the relevant bound-state/material Hamiltonian and the stated experimental conditions before comparison.

C138 muon Compton wavelength

CODATA 2022. $1.17344411 \times 10^{-14}\,\mathtt{m}$, $u = 2.6 \times 10^{-22}$, $u_r = 2.216 \times 10^{-8}$.

Class. L — dependent law/identity; Compton wavelength.

Dependency equation. $\lambda_C = h/(mc)$. *Inputs:* Planck constant; particle mass; c.

Numerical audit. dependency reconstruction $1.17344411032 \times 10^{-14}\,\mathtt{m}$; fractional residual 2.725×10^{-10}.

First-principles verdict. Algebraically reproducible, but not a first-principles physical prediction: the CODATA basis values enter the right-hand side.

END/MNT completion gate. Derive the independent dimensionless basis from one frozen node operator, then propagate its covariance without using this target.

C139 muon-electron mass ratio

CODATA 2022. 206.7682827 `dimensionless`, $u = 4.6 \times 10^{-6}$, $u_r = 2.225 \times 10^{-8}$.

Class. L — dependent law/identity; Dimensionless mass ratio.

Dependency equation. $R_{ab} = m_a/m_b$. *Inputs:* muon mass; electron mass.

Numerical audit. dependency reconstruction 206.768282702 `dimensionless`; fractional residual 1.144×10^{-11}.

First-principles verdict. Algebraically reproducible, but not a first-principles physical prediction: the CODATA basis values enter the right-hand side.

END/MNT completion gate. Derive the independent dimensionless basis from one frozen node operator, then propagate its covariance without using this target.

C140 muon g factor

CODATA 2022. -2.00233184123 `dimensionless`, $u = 8.2 \times 10^{-10}$, $u_r = 4.095 \times 10^{-10}$.

Class. L — dependent law/identity; Magnetic g factor.

Dependency equation. $g_X = \mu_X/(I_X \mu_{\text{ref}})$. *Inputs:* muon magnetic moment; spin; reference magneton.

Numerical audit. dependency reconstruction -2.00233184345 `dimensionless`; fractional residual 1.108×10^{-9}.

First-principles verdict. Algebraically reproducible, but not a first-principles physical prediction: the CODATA basis values enter the right-hand side.

END/MNT completion gate. Derive the independent dimensionless basis from one frozen node operator, then propagate its covariance without using this target.

C141 muon mag. mom.

CODATA 2022. $-4.4904483 \times 10^{-26}$ `J T^-1`, $u = 1 \times 10^{-33}$, $u_r = 2.227 \times 10^{-8}$.

Class. A — adjusted empirical input; Adjusted or reference quantity.

Dependency equation. $Q = Q_{\text{CODATA}} \pm u(Q)$. *Inputs:* CODATA adjustment or stated reference procedure.

Numerical audit. no independent numerical END/MNT output; residual and z score are undefined.

First-principles verdict. No independent END/MNT numerical prediction is present; numerical agreement cannot be assessed without inventing an input.

END/MNT completion gate. Specify the observable map and derive the value and uncertainty from a frozen micro-model before inspecting this target.

C142 muon mag. mom. anomaly

CODATA 2022. 0.00116592062 `dimensionless`, $u = 4.1 \times 10^{-10}$, $u_r = 3.517 \times 10^{-7}$.

Class. L — dependent law/identity; Lepton magnetic anomaly.

Dependency equation. $a_\mu = |g_\mu|/2 - 1$. *Inputs:* muon g factor.

Numerical audit. dependency reconstruction 0.001165920615 `dimensionless`; fractional residual -4.288×10^{-9}.

First-principles verdict. Algebraically reproducible, but not a first-principles physical prediction: the CODATA basis values enter the right-hand side.

END/MNT completion gate. Derive the independent dimensionless basis from one frozen node operator, then propagate its covariance without using this target.

C143 muon mag. mom. to Bohr magneton ratio

CODATA 2022. -0.00484197048 `dimensionless`, $u = 1.1 \times 10^{-10}$, $u_r = 2.272 \times 10^{-8}$.

Class. L — dependent law/identity; Magnetic moment in Bohr magnetons.

Dependency equation. μ_X/μ_B. *Inputs:* muon magnetic moment; Bohr magneton.

Numerical audit. dependency reconstruction -0.00484197048331 `dimensionless`; fractional residual 6.827×10^{-10}.

First-principles verdict. Algebraically reproducible, but not a first-principles physical prediction: the CODATA basis values enter the right-hand side.

END/MNT completion gate. Derive the independent dimensionless basis from one frozen node operator, then propagate its covariance without using this target.

C144 muon mag. mom. to nuclear magneton ratio

CODATA 2022. -8.89059704 `dimensionless`, $u = 2 \times 10^{-7}$, $u_r = 2.25 \times 10^{-8}$.

Class. L — dependent law/identity; Magnetic moment in nuclear magnetons.

Dependency equation. μ_X/μ_N. *Inputs:* muon magnetic moment; nuclear magneton.

Numerical audit. dependency reconstruction -8.89059704746 `dimensionless`; fractional residual 8.395×10^{-10}.

First-principles verdict. Algebraically reproducible, but not a first-principles physical prediction: the CODATA basis values enter the right-hand side.

END/MNT completion gate. Derive the independent dimensionless basis from one frozen node operator, then propagate its covariance without using this target.

C145 muon mass

CODATA 2022. $1.883531627 \times 10^{-28}\,\mathtt{kg}$, $u = 4.2 \times 10^{-36}$, $u_r = 2.23 \times 10^{-8}$.

Class. A — adjusted empirical input; Measured particle/nuclear scale.

Dependency equation. $mc^2 = E_{\text{pole}} \quad \text{or} \quad m = E_0/c^2$. *Inputs:* spectroscopy, kinematics, or mass-frequency ratios.

Numerical audit. no independent numerical END/MNT output; residual and z score are undefined.

First-principles verdict. The value is empirical. END/MNT currently has a mass-gap dictionary but no particle-identifying eigenproblem that predicts this number.

END/MNT completion gate. Derive a stable localized state, its renormalized pole energy, quantum numbers, and uncertainty without tuning to the listed mass.

C146 muon mass energy equivalent

CODATA 2022. $1.692833804 \times 10^{-11}\,\mathtt{J}$, $u = 3.8 \times 10^{-19}$, $u_r = 2.245 \times 10^{-8}$.

Class. L — dependent law/identity; Relativistic mass-energy identity.

Dependency equation. $E_m = mc^2$. *Inputs:* muon mass; c.

Numerical audit. dependency reconstruction $1.69283380408 \times 10^{-11}\,\mathtt{J}$; fractional residual 4.775×10^{-11}.

First-principles verdict. Algebraically reproducible, but not a first-principles physical prediction: the CODATA basis values enter the right-hand side.

END/MNT completion gate. Derive the independent dimensionless basis from one frozen node operator, then propagate its covariance without using this target.

C147 muon mass in u

CODATA 2022. $0.1134289257\,\mathtt{u}$, $u = 2.5 \times 10^{-9}$, $u_r = 2.204 \times 10^{-8}$.

Class. L — dependent law/identity; Relative-mass conversion.

Dependency equation. $m/\mathrm{u} = m/m_{\mathrm{u}}$. *Inputs:* muon mass; atomic mass constant.

Numerical audit. dependency reconstruction $0.113428925718\,\mathtt{u}$; fractional residual 1.568×10^{-10}.

First-principles verdict. Algebraically reproducible, but not a first-principles physical prediction: the CODATA basis values enter the right-hand side.

END/MNT completion gate. Derive the independent dimensionless basis from one frozen node operator, then propagate its covariance without using this target.

C148 muon molar mass

CODATA 2022. $1.134289258 \times 10^{-4}$ `kg mol^-1`, $u = 2.5 \times 10^{-12}$, $u_r = 2.204 \times 10^{-8}$.

Class. L — dependent law/identity; Molar mass from single-particle mass.

Dependency equation. $M(X) = N_{\mathrm{A}} m_X$. *Inputs:* Avogadro constant; muon mass.

Numerical audit. dependency reconstruction $1.13428925837 \times 10^{-4}$ `kg mol^-1`; fractional residual 3.267×10^{-10}.

First-principles verdict. Algebraically reproducible, but not a first-principles physical prediction: the CODATA basis values enter the right-hand side.

END/MNT completion gate. Derive the independent dimensionless basis from one frozen node operator, then propagate its covariance without using this target.

C149 muon-neutron mass ratio

CODATA 2022. 0.1124545168 `dimensionless`, $u = 2.5 \times 10^{-9}$, $u_r = 2.223 \times 10^{-8}$.

Class. L — dependent law/identity; Dimensionless mass ratio.

Dependency equation. $R_{ab} = m_a/m_b$. *Inputs:* muon mass; neutron mass.

Numerical audit. dependency reconstruction 0.11245451677 `dimensionless`; fractional residual -2.681×10^{-10}.

First-principles verdict. Algebraically reproducible, but not a first-principles physical prediction: the CODATA basis values enter the right-hand side.

END/MNT completion gate. Derive the independent dimensionless basis from one frozen node operator, then propagate its covariance without using this target.

C150 muon-proton mag. mom. ratio

CODATA 2022. -3.183345146 `dimensionless`, $u = 7.1 \times 10^{-8}$, $u_r = 2.23 \times 10^{-8}$.

Class. L — dependent law/identity; Magnetic-moment ratio.

Dependency equation. $R_{\mu,ab} = \mu_a/\mu_b$. *Inputs:* muon and proton magnetic moments.

Numerical audit. dependency reconstruction -3.1833451494 `dimensionless`; fractional residual 1.067×10^{-9}.

First-principles verdict. Algebraically reproducible, but not a first-principles physical prediction: the CODATA basis values enter the right-hand side.

END/MNT completion gate. Derive the independent dimensionless basis from one frozen node operator, then propagate its covariance without using this target.

C151 muon-proton mass ratio

CODATA 2022. 0.1126095262 `dimensionless`, $u = 2.5 \times 10^{-9}$, $u_r = 2.22 \times 10^{-8}$.

Class. L — dependent law/identity; Dimensionless mass ratio.

Dependency equation. $R_{ab} = m_a/m_b$. *Inputs:* muon mass; proton mass.

Numerical audit. dependency reconstruction 0.112609526264 `dimensionless`; fractional residual 5.683×10^{-10}.

First-principles verdict. Algebraically reproducible, but not a first-principles physical prediction: the CODATA basis values enter the right-hand side.

END/MNT completion gate. Derive the independent dimensionless basis from one frozen node operator, then propagate its covariance without using this target.

C152 muon-tau mass ratio

CODATA 2022. 0.0594635 `dimensionless`, $u = 4 \times 10^{-6}$, $u_r = 6.727 \times 10^{-5}$.

Class. L — dependent law/identity; Dimensionless mass ratio.

Dependency equation. $R_{ab} = m_a/m_b$. *Inputs:* muon mass; tau mass.

Numerical audit. dependency reconstruction 0.0594635466955 `dimensionless`; fractional residual 7.853×10^{-7}.

First-principles verdict. Algebraically reproducible, but not a first-principles physical prediction: the CODATA basis values enter the right-hand side.

END/MNT completion gate. Derive the independent dimensionless basis from one frozen node operator, then propagate its covariance without using this target.

C153 natural unit of action

CODATA 2022. $1.05457181765 \times 10^{-34}$ `J s` (exact in the stated system).

Class. L — dependent law/identity; Electron natural-unit dependency.

Dependency equation. $Q_{\mathrm{nat}} = \hbar$. *Inputs:* hbar.

Numerical audit. dependency reconstruction $1.05457181765 \times 10^{-34}$ `J s`; fractional residual 0.

First-principles verdict. Algebraically reproducible, but not a first-principles physical prediction: the CODATA basis values enter the right-hand side.

END/MNT completion gate. Derive the independent dimensionless basis from one frozen node operator, then propagate its covariance without using this target.

C154 natural unit of action in eV s

CODATA 2022. $6.58211956951 \times 10^{-16}$ `eV s` (exact in the stated system).

Class. L — dependent law/identity; Electron natural-unit dependency.

Dependency equation. $Q_{\mathrm{nat}} = \hbar/e$. *Inputs:* hbar; eV definition.

Numerical audit. dependency reconstruction $6.58211956951 \times 10^{-16}$ `eV s`; fractional residual 0.

First-principles verdict. Algebraically reproducible, but not a first-principles physical prediction: the CODATA basis values enter the right-hand side.

END/MNT completion gate. Derive the independent dimensionless basis from one frozen node operator, then propagate its covariance without using this target.

C155 natural unit of energy

CODATA 2022. $8.187105788 \times 10^{-14}$ `J`, $u = 2.6 \times 10^{-23}$, $u_r = 3.176 \times 10^{-10}$.

Class. L — dependent law/identity; Electron natural-unit dependency.

Dependency equation. $Q_{\rm nat} = m_e c^2$. *Inputs:* electron mass; c.

Numerical audit. dependency reconstruction $8.18710578797 \times 10^{-14}$ `J`; fractional residual -3.854×10^{-12}.

First-principles verdict. Algebraically reproducible, but not a first-principles physical prediction: the CODATA basis values enter the right-hand side.

END/MNT completion gate. Derive the independent dimensionless basis from one frozen node operator, then propagate its covariance without using this target.

C156 natural unit of energy in MeV

CODATA 2022. 0.51099895069 `MeV`, $u = 1.6 \times 10^{-10}$, $u_r = 3.131 \times 10^{-10}$.

Class. L — dependent law/identity; Electron natural-unit dependency.

Dependency equation. $Q_{\rm nat} = m_e c^2/(10^6 e)$. *Inputs:* electron mass; c; e.

Numerical audit. dependency reconstruction 0.510998950692 `MeV`; fractional residual 3.431×10^{-12}.

First-principles verdict. Algebraically reproducible, but not a first-principles physical prediction: the CODATA basis values enter the right-hand side.

END/MNT completion gate. Derive the independent dimensionless basis from one frozen node operator, then propagate its covariance without using this target.

C157 natural unit of length

CODATA 2022. $3.8615926744 \times 10^{-13}\,\texttt{m}$, $u = 1.2 \times 10^{-22}$, $u_r = 3.108 \times 10^{-10}$.

Class. L — dependent law/identity; Electron natural-unit dependency.

Dependency equation. $Q_{\text{nat}} = \hbar/(m_e c)$. *Inputs:* hbar; electron mass; c.

Numerical audit. dependency reconstruction $3.86159267435 \times 10^{-13}\,\texttt{m}$; fractional residual -1.233×10^{-11}.

First-principles verdict. Algebraically reproducible, but not a first-principles physical prediction: the CODATA basis values enter the right-hand side.

END/MNT completion gate. Derive the independent dimensionless basis from one frozen node operator, then propagate its covariance without using this target.

C158 natural unit of mass

CODATA 2022. $9.1093837139 \times 10^{-31}\,\texttt{kg}$, $u = 2.8 \times 10^{-40}$, $u_r = 3.074 \times 10^{-10}$.

Class. L — dependent law/identity; Electron natural-unit dependency.

Dependency equation. $Q_{\text{nat}} = m_e$. *Inputs:* electron mass.

Numerical audit. dependency reconstruction $9.1093837139 \times 10^{-31}\,\texttt{kg}$; fractional residual 0.

First-principles verdict. Algebraically reproducible, but not a first-principles physical prediction: the CODATA basis values enter the right-hand side.

END/MNT completion gate. Derive the independent dimensionless basis from one frozen node operator, then propagate its covariance without using this target.

C159 natural unit of momentum

CODATA 2022. $2.73092453446 \times 10^{-22}$ `kg m s^-1`, $u = 8.5 \times 10^{-32}$, $u_r = 3.112 \times 10^{-10}$.

Class. L — dependent law/identity; Electron natural-unit dependency.

Dependency equation. $Q_{\mathrm{nat}} = m_e c$. *Inputs:* electron mass; c.

Numerical audit. dependency reconstruction $2.73092453446 \times 10^{-22}$ `kg m s^-1`; fractional residual -1.739×10^{-12}.

First-principles verdict. Algebraically reproducible, but not a first-principles physical prediction: the CODATA basis values enter the right-hand side.

END/MNT completion gate. Derive the independent dimensionless basis from one frozen node operator, then propagate its covariance without using this target.

C160 natural unit of momentum in MeV/c

CODATA 2022. 0.51099895069 `MeV/c`, $u = 1.6 \times 10^{-10}$, $u_r = 3.131 \times 10^{-10}$.

Class. L — dependent law/identity; Electron natural-unit dependency.

Dependency equation. $Q_{\mathrm{nat}} = m_e c^2/(10^6 e)$. *Inputs:* electron mass; c; e.

Numerical audit. dependency reconstruction 0.510998950692 `MeV/c`; fractional residual 3.431×10^{-12}.

First-principles verdict. Algebraically reproducible, but not a first-principles physical prediction: the CODATA basis values enter the right-hand side.

END/MNT completion gate. Derive the independent dimensionless basis from one frozen node operator, then propagate its covariance without using this target.

C161 natural unit of time

CODATA 2022. $1.28808866644 \times 10^{-21}$ `s`, $u = 4 \times 10^{-31}$, $u_r = 3.105 \times 10^{-10}$.

Class. L — dependent law/identity; Electron natural-unit dependency.

Dependency equation. $Q_{\text{nat}} = \hbar/(m_e c^2)$. *Inputs:* hbar; electron mass; c.

Numerical audit. dependency reconstruction $1.28808866644 \times 10^{-21}$ `s`; fractional residual 3.232×10^{-12}.

First-principles verdict. Algebraically reproducible, but not a first-principles physical prediction: the CODATA basis values enter the right-hand side.

END/MNT completion gate. Derive the independent dimensionless basis from one frozen node operator, then propagate its covariance without using this target.

C162 natural unit of velocity

CODATA 2022. 2.99792458×10^{8} `m s^-1` (exact in the stated system).

Class. L — dependent law/identity; Electron natural-unit dependency.

Dependency equation. $Q_{\text{nat}} = c$. *Inputs:* speed of light.

Numerical audit. dependency reconstruction 2.99792458×10^{8} `m s^-1`; fractional residual 0.

First-principles verdict. Algebraically reproducible, but not a first-principles physical prediction: the CODATA basis values enter the right-hand side.

END/MNT completion gate. Derive the independent dimensionless basis from one frozen node operator, then propagate its covariance without using this target.

C163 neutron Compton wavelength

CODATA 2022. $1.31959090382 \times 10^{-15}\,\mathtt{m}$, $u = 6.7 \times 10^{-25}$, $u_r = 5.077 \times 10^{-10}$.

Class. L — dependent law/identity; Compton wavelength.

Dependency equation. $\lambda_C = h/(mc)$. *Inputs:* Planck constant; particle mass; c.

Numerical audit. dependency reconstruction $1.31959090382 \times 10^{-15}\,\mathtt{m}$; fractional residual 3.298×10^{-12}.

First-principles verdict. Algebraically reproducible, but not a first-principles physical prediction: the CODATA basis values enter the right-hand side.

END/MNT completion gate. Derive the independent dimensionless basis from one frozen node operator, then propagate its covariance without using this target.

C164 neutron-electron mag. mom. ratio

CODATA 2022. $0.00104066884\,\mathtt{dimensionless}$, $u = 2.4 \times 10^{-10}$, $u_r = 2.306 \times 10^{-7}$.

Class. L — dependent law/identity; Magnetic-moment ratio.

Dependency equation. $R_{\mu,ab} = \mu_a/\mu_b$. *Inputs:* neutron and electron magnetic moments.

Numerical audit. dependency reconstruction $0.00104066883985\,\mathtt{dimensionless}$; fractional residual -1.433×10^{-10}.

First-principles verdict. Algebraically reproducible, but not a first-principles physical prediction: the CODATA basis values enter the right-hand side.

END/MNT completion gate. Derive the independent dimensionless basis from one frozen node operator, then propagate its covariance without using this target.

C165 neutron-electron mass ratio

CODATA 2022. 1838.683662 `dimensionless`, $u = 7.4 \times 10^{-7}$, $u_r = 4.025 \times 10^{-10}$.

Class. L — dependent law/identity; Dimensionless mass ratio.

Dependency equation. $R_{ab} = m_a/m_b$. *Inputs:* neutron mass; electron mass.

Numerical audit. dependency reconstruction 1838.683662 `dimensionless`; fractional residual -2.198×10^{-12}.

First-principles verdict. Algebraically reproducible, but not a first-principles physical prediction: the CODATA basis values enter the right-hand side.

END/MNT completion gate. Derive the independent dimensionless basis from one frozen node operator, then propagate its covariance without using this target.

C166 neutron g factor

CODATA 2022. -3.82608552 `dimensionless`, $u = 9 \times 10^{-7}$, $u_r = 2.352 \times 10^{-7}$.

Class. L — dependent law/identity; Magnetic g factor.

Dependency equation. $g_X = \mu_X/(I_X \mu_{\mathrm{ref}})$. *Inputs:* neutron magnetic moment; spin; reference magneton.

Numerical audit. dependency reconstruction -3.82608553394 `dimensionless`; fractional residual 3.644×10^{-9}.

First-principles verdict. Algebraically reproducible, but not a first-principles physical prediction: the CODATA basis values enter the right-hand side.

END/MNT completion gate. Derive the independent dimensionless basis from one frozen node operator, then propagate its covariance without using this target.

C167 neutron gyromag. ratio

CODATA 2022. 1.83247174×10^8 `s^-1 T^-1`, $u = 43$, $u_r = 2.347 \times 10^{-7}$.

Class. L — dependent law/identity; Gyromagnetic ratio.

Dependency equation. $|\gamma_X| = |\mu_X|/(I_X \hbar)$. *Inputs:* neutron magnetic moment; spin; reduced Planck constant.

Numerical audit. dependency reconstruction $1.83247174603 \times 10^8$ `s^-1 T^-1`; fractional residual 3.293×10^{-9}.

First-principles verdict. Algebraically reproducible, but not a first-principles physical prediction: the CODATA basis values enter the right-hand side.

END/MNT completion gate. Derive the independent dimensionless basis from one frozen node operator, then propagate its covariance without using this target.

C168 neutron mag. mom.

CODATA 2022. $-9.6623653 \times 10^{-27}$ `J T^-1`, $u = 2.3 \times 10^{-33}$, $u_r = 2.38 \times 10^{-7}$.

Class. A — adjusted empirical input; Adjusted or reference quantity.

Dependency equation. $Q = Q_{\mathrm{CODATA}} \pm u(Q)$. *Inputs:* CODATA adjustment or stated reference procedure.

Numerical audit. no independent numerical END/MNT output; residual and z score are undefined.

First-principles verdict. No independent END/MNT numerical prediction is present; numerical agreement cannot be assessed without inventing an input.

END/MNT completion gate. Specify the observable map and derive the value and uncertainty from a frozen micro-model before inspecting this target.

C169 neutron mag. mom. to Bohr magneton ratio

CODATA 2022. $-0.00104187565\,\texttt{dimensionless}$, $u = 2.5 \times 10^{-10}$, $u_r = 2.4 \times 10^{-7}$.

Class. L — dependent law/identity; Magnetic moment in Bohr magnetons.

Dependency equation. $\mu_X/\mu_{\rm B}$. *Inputs:* neutron magnetic moment; Bohr magneton.

Numerical audit. dependency reconstruction $-0.00104187565374\,\texttt{dimensionless}$; fractional residual 3.59×10^{-9}.

First-principles verdict. Algebraically reproducible, but not a first-principles physical prediction: the CODATA basis values enter the right-hand side.

END/MNT completion gate. Derive the independent dimensionless basis from one frozen node operator, then propagate its covariance without using this target.

C170 neutron mag. mom. to nuclear magneton ratio

CODATA 2022. $-1.91304276\,\texttt{dimensionless}$, $u = 4.5 \times 10^{-7}$, $u_r = 2.352 \times 10^{-7}$.

Class. L — dependent law/identity; Magnetic moment in nuclear magnetons.

Dependency equation. $\mu_X/\mu_{\rm N}$. *Inputs:* neutron magnetic moment; nuclear magneton.

Numerical audit. dependency reconstruction $-1.91304276697\,\texttt{dimensionless}$; fractional residual 3.644×10^{-9}.

First-principles verdict. Algebraically reproducible, but not a first-principles physical prediction: the CODATA basis values enter the right-hand side.

END/MNT completion gate. Derive the independent dimensionless basis from one frozen node operator, then propagate its covariance without using this target.

C171 neutron mass

CODATA 2022. $1.67492750056 \times 10^{-27}\,\texttt{kg}$, $u = 8.5 \times 10^{-37}$, $u_r = 5.075 \times 10^{-10}$.

Class. A — adjusted empirical input; Measured particle/nuclear scale.

Dependency equation. $mc^2 = E_{\text{pole}} \quad \text{or} \quad m = E_0/c^2$. *Inputs:* spectroscopy, kinematics, or mass-frequency ratios.

Numerical audit. no independent numerical END/MNT output; residual and z score are undefined.

First-principles verdict. The value is empirical. END/MNT currently has a mass-gap dictionary but no particle-identifying eigenproblem that predicts this number.

END/MNT completion gate. Derive a stable localized state, its renormalized pole energy, quantum numbers, and uncertainty without tuning to the listed mass.

C172 neutron mass energy equivalent

CODATA 2022. $1.50534976514 \times 10^{-10}\,\texttt{J}$, $u = 7.6 \times 10^{-20}$, $u_r = 5.049 \times 10^{-10}$.

Class. L — dependent law/identity; Relativistic mass-energy identity.

Dependency equation. $E_m = mc^2$. *Inputs:* neutron mass; c.

Numerical audit. dependency reconstruction $1.50534976514 \times 10^{-10}\,\texttt{J}$; fractional residual -1.984×10^{-12}.

First-principles verdict. Algebraically reproducible, but not a first-principles physical prediction: the CODATA basis values enter the right-hand side.

END/MNT completion gate. Derive the independent dimensionless basis from one frozen node operator, then propagate its covariance without using this target.

C173 neutron mass in u

CODATA 2022. 1.00866491606 `u`, $u = 4 \times 10^{-10}$, $u_r = 3.966 \times 10^{-10}$.

Class. L — dependent law/identity; Relative-mass conversion.

Dependency equation. $m/\mathrm{u} = m/m_\mathrm{u}$. *Inputs:* neutron mass; atomic mass constant.

Numerical audit. dependency reconstruction 1.00866491606 `u`; fractional residual -3.906×10^{-12}.

First-principles verdict. Algebraically reproducible, but not a first-principles physical prediction: the CODATA basis values enter the right-hand side.

END/MNT completion gate. Derive the independent dimensionless basis from one frozen node operator, then propagate its covariance without using this target.

C174 neutron molar mass

CODATA 2022. 0.00100866491712 `kg mol^-1`, $u = 5.1 \times 10^{-13}$, $u_r = 5.056 \times 10^{-10}$.

Class. L — dependent law/identity; Molar mass from single-particle mass.

Dependency equation. $M(X) = N_\mathrm{A} m_X$. *Inputs:* Avogadro constant; neutron mass.

Numerical audit. dependency reconstruction 0.00100866491712 `kg mol^-1`; fractional residual -3.242×10^{-12}.

First-principles verdict. Algebraically reproducible, but not a first-principles physical prediction: the CODATA basis values enter the right-hand side.

END/MNT completion gate. Derive the independent dimensionless basis from one frozen node operator, then propagate its covariance without using this target.

C175 neutron-muon mass ratio

CODATA 2022. 8.89248408 `dimensionless`, $u = 2 \times 10^{-7}$, $u_r = 2.249 \times 10^{-8}$.

Class. L — dependent law/identity; Dimensionless mass ratio.

Dependency equation. $R_{ab} = m_a/m_b$. *Inputs:* neutron mass; muon mass.

Numerical audit. dependency reconstruction 8.89248407911 `dimensionless`; fractional residual -9.994×10^{-11}.

First-principles verdict. Algebraically reproducible, but not a first-principles physical prediction: the CODATA basis values enter the right-hand side.

END/MNT completion gate. Derive the independent dimensionless basis from one frozen node operator, then propagate its covariance without using this target.

C176 neutron-proton mag. mom. ratio

CODATA 2022. -0.68497935 `dimensionless`, $u = 1.6 \times 10^{-7}$, $u_r = 2.336 \times 10^{-7}$.

Class. L — dependent law/identity; Magnetic-moment ratio.

Dependency equation. $R_{\mu,ab} = \mu_a/\mu_b$. *Inputs:* neutron and proton magnetic moments.

Numerical audit. dependency reconstruction -0.68497935294 `dimensionless`; fractional residual 4.292×10^{-9}.

First-principles verdict. Algebraically reproducible, but not a first-principles physical prediction: the CODATA basis values enter the right-hand side.

END/MNT completion gate. Derive the independent dimensionless basis from one frozen node operator, then propagate its covariance without using this target.

C177 neutron-proton mass difference

CODATA 2022. $2.30557461 \times 10^{-30}$ `kg`, $u = 6.7 \times 10^{-37}$, $u_r = 2.906 \times 10^{-7}$.

Class. L — dependent law/identity; Mass difference.

Dependency equation. $\Delta m_{np} = m_n - m_p$. *Inputs:* neutron mass; proton mass.

Numerical audit. dependency reconstruction $2.30557461 \times 10^{-30}$ `kg`; fractional residual 8.524×10^{-14}.

First-principles verdict. Algebraically reproducible, but not a first-principles physical prediction: the CODATA basis values enter the right-hand side.

END/MNT completion gate. Derive the independent dimensionless basis from one frozen node operator, then propagate its covariance without using this target.

C178 neutron-proton mass difference energy equivalent

CODATA 2022. $2.07214712 \times 10^{-13}$ `J`, $u = 6 \times 10^{-20}$, $u_r = 2.896 \times 10^{-7}$.

Class. L — dependent law/identity; Mass-difference energy.

Dependency equation. $\Delta E_{np} = (m_n - m_p)c^2$. *Inputs:* neutron mass; proton mass; c.

Numerical audit. dependency reconstruction $2.0721471207 \times 10^{-13}$ `J`; fractional residual 3.387×10^{-10}.

First-principles verdict. Algebraically reproducible, but not a first-principles physical prediction: the CODATA basis values enter the right-hand side.

END/MNT completion gate. Derive the independent dimensionless basis from one frozen node operator, then propagate its covariance without using this target.

C179 neutron-proton mass difference energy equivalent in MeV

CODATA 2022. 1.29333251 `MeV`, $u = 3.8 \times 10^{-7}$, $u_r = 2.938 \times 10^{-7}$.

Class. A — adjusted empirical input; Adjusted or reference quantity.

Dependency equation. $Q = Q_{\mathrm{CODATA}} \pm u(Q)$. *Inputs:* CODATA adjustment or stated reference procedure.

Numerical audit. no independent numerical END/MNT output; residual and z score are undefined.

First-principles verdict. No independent END/MNT numerical prediction is present; numerical agreement cannot be assessed without inventing an input.

END/MNT completion gate. Specify the observable map and derive the value and uncertainty from a frozen micro-model before inspecting this target.

C180 neutron-proton mass difference in u

CODATA 2022. 0.00138844948 `u`, $u = 4 \times 10^{-10}$, $u_r = 2.881 \times 10^{-7}$.

Class. L — dependent law/identity; Relative mass difference.

Dependency equation. $\Delta m_{np}/\mathrm{u} = (m_n - m_p)/m_{\mathrm{u}}$. *Inputs:* neutron mass; proton mass; atomic mass constant.

Numerical audit. dependency reconstruction 0.00138844948195 `u`; fractional residual 1.405×10^{-9}.

First-principles verdict. Algebraically reproducible, but not a first-principles physical prediction: the CODATA basis values enter the right-hand side.

END/MNT completion gate. Derive the independent dimensionless basis from one frozen node operator, then propagate its covariance without using this target.

C181 neutron-proton mass ratio

CODATA 2022. 1.00137841946 `dimensionless`, $u = 4 \times 10^{-10}$, $u_r = 3.994 \times 10^{-10}$.

Class. L — dependent law/identity; Dimensionless mass ratio.

Dependency equation. $R_{ab} = m_a/m_b$. *Inputs:* neutron mass; proton mass.

Numerical audit. dependency reconstruction 1.00137841946 `dimensionless`; fractional residual -1.165×10^{-12}.

First-principles verdict. Algebraically reproducible, but not a first-principles physical prediction: the CODATA basis values enter the right-hand side.

END/MNT completion gate. Derive the independent dimensionless basis from one frozen node operator, then propagate its covariance without using this target.

C182 neutron relative atomic mass

CODATA 2022. 1.00866491606 `dimensionless`, $u = 4 \times 10^{-10}$, $u_r = 3.966 \times 10^{-10}$.

Class. L — dependent law/identity; Relative atomic mass.

Dependency equation. $A_{\mathrm{r}}(X) = m_X/m_{\mathrm{u}}$. *Inputs:* neutron mass; atomic mass constant.

Numerical audit. dependency reconstruction 1.00866491606 `dimensionless`; fractional residual -3.906×10^{-12}.

First-principles verdict. Algebraically reproducible, but not a first-principles physical prediction: the CODATA basis values enter the right-hand side.

END/MNT completion gate. Derive the independent dimensionless basis from one frozen node operator, then propagate its covariance without using this target.

C183 neutron-tau mass ratio

CODATA 2022. 0.528779 `dimensionless`, $u = 3.6 \times 10^{-5}$, $u_r = 6.808 \times 10^{-5}$.

Class. L — dependent law/identity; Dimensionless mass ratio.

Dependency equation. $R_{ab} = m_a/m_b$. *Inputs:* neutron mass; tau mass.

Numerical audit. dependency reconstruction 0.528778642278 `dimensionless`; fractional residual -6.765×10^{-7}.

First-principles verdict. Algebraically reproducible, but not a first-principles physical prediction: the CODATA basis values enter the right-hand side.

END/MNT completion gate. Derive the independent dimensionless basis from one frozen node operator, then propagate its covariance without using this target.

C184 neutron to shielded proton mag. mom. ratio

CODATA 2022. -0.68499694 `dimensionless`, $u = 1.6 \times 10^{-7}$, $u_r = 2.336 \times 10^{-7}$.

Class. L — dependent law/identity; Magnetic-moment ratio.

Dependency equation. $R_{\mu,ab} = \mu_a/\mu_b$. *Inputs:* neutron and shielded proton magnetic moments.

Numerical audit. dependency reconstruction -0.684996937867 `dimensionless`; fractional residual -3.114×10^{-9}.

First-principles verdict. Algebraically reproducible, but not a first-principles physical prediction: the CODATA basis values enter the right-hand side.

END/MNT completion gate. Derive the independent dimensionless basis from one frozen node operator, then propagate its covariance without using this target.

C185 Newtonian constant of gravitation

CODATA 2022. 6.6743×10^{-11} `m^3 kg^-1 s^-2`, $u = 1.5 \times 10^{-15}$, $u_r = 2.247 \times 10^{-5}$.

Class. A — adjusted empirical input; Adjusted empirical or theory-assisted input.

Dependency equation. $Q = \arg\min_{Q} (\mathbf{y} - \mathbf{f}(Q))^T \mathbf{V}^{-1} (\mathbf{y} - \mathbf{f}(Q))$. *Inputs:* CODATA observational equations and covariance.

Numerical audit. no independent numerical END/MNT output; residual and z score are undefined.

First-principles verdict. No END/MNT first-principles value exists in the current papers; CODATA supplies the comparison target, not an allowed model input for a prediction.

END/MNT completion gate. Generate the relevant spectrum, form factor, or decay amplitude from the frozen micro-model and compare only after preregistration.

C186 Newtonian constant of gravitation over h-bar c

CODATA 2022. 6.70883×10^{-39} `(GeV/c^2)^-2`, $u = 1.5 \times 10^{-43}$, $u_r = 2.236 \times 10^{-5}$.

Class. A — adjusted empirical input; Adjusted or reference quantity.

Dependency equation. $Q = Q_{\mathrm{CODATA}} \pm u(Q)$. *Inputs:* CODATA adjustment or stated reference procedure.

Numerical audit. no independent numerical END/MNT output; residual and z score are undefined.

First-principles verdict. No independent END/MNT numerical prediction is present; numerical agreement cannot be assessed without inventing an input.

END/MNT completion gate. Specify the observable map and derive the value and uncertainty from a frozen micro-model before inspecting this target.

C187 nuclear magneton

CODATA 2022. $5.0507837393 \times 10^{-27}$ `J T^-1`, $u = 1.6 \times 10^{-36}$, $u_r = 3.168 \times 10^{-10}$.

Class. L — dependent law/identity; Proton magneton.

Dependency equation. $\mu_{\mathrm{N}} = e\hbar/(2m_p)$. *Inputs:* e; hbar; proton mass.

Numerical audit. dependency reconstruction $5.05078373927 \times 10^{-27}$ `J T^-1`; fractional residual -5.564×10^{-12}.

First-principles verdict. Algebraically reproducible, but not a first-principles physical prediction: the CODATA basis values enter the right-hand side.

END/MNT completion gate. Derive the independent dimensionless basis from one frozen node operator, then propagate its covariance without using this target.

C188 Planck constant

CODATA 2022. $6.62607015 \times 10^{-34}$ `J Hz^-1` (exact in the stated system).

Class. D — SI definition; SI definition and END phase-action bridge.

Dependency equation. $\Delta S = \hbar_* \Delta\varphi$. *Inputs:* SI definition of h; proposed END phase map.

Numerical audit. identity check $6.62607015 \times 10^{-34}$ `J Hz^-1`; fractional residual 0.

First-principles verdict. The SI value is exact by definition. END/MNT has a matching coefficient hbar*, not a microscopic derivation of quantum action.

END/MNT completion gate. Derive the phase measure, Born statistics, and one universal hbar* across held-out atomic and interference observables.

C189 Planck length

CODATA 2022. $1.616255 \times 10^{-35}\,\mathtt{m}$, $u = 1.8 \times 10^{-40}$, $u_r = 1.114 \times 10^{-5}$.

Class. L — dependent law/identity; Planck-unit dependency.

Dependency equation. $\ell_\mathrm{P} = \sqrt{\hbar G/c^3}$. *Inputs:* hbar; c; G; and kB where needed.

Numerical audit. dependency reconstruction $1.61625502442 \times 10^{-35}\,\mathtt{m}$; fractional residual 1.511×10^{-8}.

First-principles verdict. Unit algebra once G and the SI defining constants are supplied; not an independent quantum-gravity prediction.

END/MNT completion gate. Derive a dimensionless gravitational coupling or G from the frozen micro-model without defining the node spacing as a Planck unit.

C190 Planck mass

CODATA 2022. $2.176434 \times 10^{-8}\,\mathtt{kg}$, $u = 2.4 \times 10^{-13}$, $u_r = 1.103 \times 10^{-5}$.

Class. L — dependent law/identity; Planck-unit dependency.

Dependency equation. $m_\mathrm{P} = \sqrt{\hbar c/G}$. *Inputs:* hbar; c; G; and kB where needed.

Numerical audit. dependency reconstruction $2.17643434272 \times 10^{-8}\,\mathtt{kg}$; fractional residual 1.575×10^{-7}.

First-principles verdict. Unit algebra once G and the SI defining constants are supplied; not an independent quantum-gravity prediction.

END/MNT completion gate. Derive a dimensionless gravitational coupling or G from the frozen micro-model without defining the node spacing as a Planck unit.

C191 Planck mass energy equivalent in GeV

CODATA 2022. 1.22089×10^{19} `GeV`, $u = 1.4 \times 10^{14}$, $u_r = 1.147 \times 10^{-5}$.

Class. L — dependent law/identity; Planck-unit dependency.

Dependency equation. $m_{\mathrm{P}}c^2/(10^9 e)$. *Inputs:* hbar; c; G; and kB where needed.

Numerical audit. dependency reconstruction $1.22089012858 \times 10^{19}$ `GeV`; fractional residual 1.053×10^{-7}.

First-principles verdict. Unit algebra once G and the SI defining constants are supplied; not an independent quantum-gravity prediction.

END/MNT completion gate. Derive a dimensionless gravitational coupling or G from the frozen micro-model without defining the node spacing as a Planck unit.

C192 Planck temperature

CODATA 2022. 1.416784×10^{32} `K`, $u = 1.6 \times 10^{27}$, $u_r = 1.129 \times 10^{-5}$.

Class. L — dependent law/identity; Planck-unit dependency.

Dependency equation. $T_{\mathrm{P}} = m_{\mathrm{P}}c^2/k_{\mathrm{B}}$. *Inputs:* hbar; c; G; and kB where needed.

Numerical audit. dependency reconstruction $1.41678416216 \times 10^{32}$ `K`; fractional residual 1.145×10^{-7}.

First-principles verdict. Unit algebra once G and the SI defining constants are supplied; not an independent quantum-gravity prediction.

END/MNT completion gate. Derive a dimensionless gravitational coupling or G from the frozen micro-model without defining the node spacing as a Planck unit.

C193 Planck time

CODATA 2022. 5.391247×10^{-44} `s`, $u = 6 \times 10^{-49}$, $u_r = 1.113 \times 10^{-5}$.

Class. L — dependent law/identity; Planck-unit dependency.

Dependency equation. $t_{\mathrm{P}} = \sqrt{\hbar G/c^5}$. *Inputs:* hbar; c; G; and kB where needed.

Numerical audit. dependency reconstruction $5.39124644831 \times 10^{-44}$ `s`; fractional residual -1.023×10^{-7}.

First-principles verdict. Unit algebra once G and the SI defining constants are supplied; not an independent quantum-gravity prediction.

END/MNT completion gate. Derive a dimensionless gravitational coupling or G from the frozen micro-model without defining the node spacing as a Planck unit.

C194 proton charge to mass quotient

CODATA 2022. $9.578833143 \times 10^{7}$ `C kg^-1`, $u = 0.03$, $u_r = 3.132 \times 10^{-10}$.

Class. L — dependent law/identity; Charge-to-mass ratio.

Dependency equation. $q_p/m_p = e/m_p$. *Inputs:* elementary charge; proton mass.

Numerical audit. dependency reconstruction $9.578833143 \times 10^{7}$ `C kg^-1`; fractional residual 1.028×10^{-13}.

First-principles verdict. Algebraically reproducible, but not a first-principles physical prediction: the CODATA basis values enter the right-hand side.

END/MNT completion gate. Derive the independent dimensionless basis from one frozen node operator, then propagate its covariance without using this target.

C195 proton Compton wavelength

CODATA 2022. $1.3214098536 \times 10^{-15}\,\texttt{m}$, $u = 4.1 \times 10^{-25}$, $u_r = 3.103 \times 10^{-10}$.

Class. L — dependent law/identity; Compton wavelength.

Dependency equation. $\lambda_C = h/(mc)$. *Inputs:* Planck constant; particle mass; c.

Numerical audit. dependency reconstruction $1.3214098536 \times 10^{-15}\,\texttt{m}$; fractional residual 2.938×10^{-12}.

First-principles verdict. Algebraically reproducible, but not a first-principles physical prediction: the CODATA basis values enter the right-hand side.

END/MNT completion gate. Derive the independent dimensionless basis from one frozen node operator, then propagate its covariance without using this target.

C196 proton-electron mass ratio

CODATA 2022. $1836.15267343\,\texttt{dimensionless}$, $u = 3.2 \times 10^{-8}$, $u_r = 1.743 \times 10^{-11}$.

Class. L — dependent law/identity; Dimensionless mass ratio.

Dependency equation. $R_{ab} = m_a/m_b$. *Inputs:* proton mass; electron mass.

Numerical audit. dependency reconstruction $1836.15267342\,\texttt{dimensionless}$; fractional residual -2.436×10^{-12}.

First-principles verdict. Algebraically reproducible, but not a first-principles physical prediction: the CODATA basis values enter the right-hand side.

END/MNT completion gate. Derive the independent dimensionless basis from one frozen node operator, then propagate its covariance without using this target.

C197 proton g factor

CODATA 2022. 5.5856946893 `dimensionless`, $u = 1.6 \times 10^{-9}$, $u_r = 2.864 \times 10^{-10}$.

Class. L — dependent law/identity; Magnetic g factor.

Dependency equation. $g_X = \mu_X/(I_X\mu_{\rm ref})$. *Inputs:* proton magnetic moment; spin; reference magneton.

Numerical audit. dependency reconstruction 5.58569468922 `dimensionless`; fractional residual -1.456×10^{-11}.

First-principles verdict. Algebraically reproducible, but not a first-principles physical prediction: the CODATA basis values enter the right-hand side.

END/MNT completion gate. Derive the independent dimensionless basis from one frozen node operator, then propagate its covariance without using this target.

C198 proton gyromag. ratio

CODATA 2022. $2.6752218708 \times 10^{8}$ `s^-1 T^-1`, $u = 0.11$, $u_r = 4.112 \times 10^{-10}$.

Class. L — dependent law/identity; Gyromagnetic ratio.

Dependency equation. $|\gamma_X| = |\mu_X|/(I_X\hbar)$. *Inputs:* proton magnetic moment; spin; reduced Planck constant.

Numerical audit. dependency reconstruction $2.6752218708 \times 10^{8}$ `s^-1 T^-1`; fractional residual 1.309×10^{-12}.

First-principles verdict. Algebraically reproducible, but not a first-principles physical prediction: the CODATA basis values enter the right-hand side.

END/MNT completion gate. Derive the independent dimensionless basis from one frozen node operator, then propagate its covariance without using this target.

C199 proton mag. mom.

CODATA 2022. $1.41060679545 \times 10^{-26}$ `J T^-1`, $u = 6 \times 10^{-36}$, $u_r = 4.253 \times 10^{-10}$.

Class. A — adjusted empirical input; Adjusted or reference quantity.

Dependency equation. $Q = Q_{\text{CODATA}} \pm u(Q)$. *Inputs:* CODATA adjustment or stated reference procedure.

Numerical audit. no independent numerical END/MNT output; residual and z score are undefined.

First-principles verdict. No independent END/MNT numerical prediction is present; numerical agreement cannot be assessed without inventing an input.

END/MNT completion gate. Specify the observable map and derive the value and uncertainty from a frozen micro-model before inspecting this target.

C200 proton mag. mom. to Bohr magneton ratio

CODATA 2022. 0.0015210322023 `dimensionless`, $u = 4.5 \times 10^{-13}$, $u_r = 2.959 \times 10^{-10}$.

Class. L — dependent law/identity; Magnetic moment in Bohr magnetons.

Dependency equation. μ_X/μ_{B}. *Inputs:* proton magnetic moment; Bohr magneton.

Numerical audit. dependency reconstruction 0.00152103220231 `dimensionless`; fractional residual 8.221×10^{-12}.

First-principles verdict. Algebraically reproducible, but not a first-principles physical prediction: the CODATA basis values enter the right-hand side.

END/MNT completion gate. Derive the independent dimensionless basis from one frozen node operator, then propagate its covariance without using this target.

C201 proton mag. mom. to nuclear magneton ratio

CODATA 2022. 2.79284734463 `dimensionless`, $u = 8.2 \times 10^{-10}$, $u_r = 2.936 \times 10^{-10}$.

Class. L — dependent law/identity; Magnetic moment in nuclear magnetons.

Dependency equation. μ_X/μ_N. *Inputs:* proton magnetic moment; nuclear magneton.

Numerical audit. dependency reconstruction 2.79284734461 `dimensionless`; fractional residual -7.4×10^{-12}.

First-principles verdict. Algebraically reproducible, but not a first-principles physical prediction: the CODATA basis values enter the right-hand side.

END/MNT completion gate. Derive the independent dimensionless basis from one frozen node operator, then propagate its covariance without using this target.

C202 proton mag. shielding correction

CODATA 2022. 2.56715×10^{-5} `dimensionless`, $u = 4.1 \times 10^{-9}$, $u_r = 1.597 \times 10^{-4}$.

Class. R — material/reference dependent; Material or environment-dependent reference.

Dependency equation. $Q = Q(T, p, \text{composition, preparation})$. *Inputs:* experimental reference conditions.

Numerical audit. no independent numerical END/MNT output; residual and z score are undefined.

First-principles verdict. Not a universal constant of a microscopic theory; it must be measured or calculated from a detailed material model.

END/MNT completion gate. Derive the relevant bound-state/material Hamiltonian and the stated experimental conditions before comparison.

C203 proton mass

CODATA 2022. $1.67262192595 \times 10^{-27}\,\mathtt{kg}$, $u = 5.2 \times 10^{-37}$, $u_r = 3.109 \times 10^{-10}$.

Class. A — adjusted empirical input; Measured particle/nuclear scale.

Dependency equation. $mc^2 = E_{\text{pole}} \quad \text{or} \quad m = E_0/c^2$. *Inputs:* spectroscopy, kinematics, or mass-frequency ratios.

Numerical audit. no independent numerical END/MNT output; residual and z score are undefined.

First-principles verdict. The value is empirical. END/MNT currently has a mass-gap dictionary but no particle-identifying eigenproblem that predicts this number.

END/MNT completion gate. Derive a stable localized state, its renormalized pole energy, quantum numbers, and uncertainty without tuning to the listed mass.

C204 proton mass energy equivalent

CODATA 2022. $1.50327761802 \times 10^{-10}\,\mathtt{J}$, $u = 4.7 \times 10^{-20}$, $u_r = 3.127 \times 10^{-10}$.

Class. L — dependent law/identity; Relativistic mass-energy identity.

Dependency equation. $E_m = mc^2$. *Inputs:* proton mass; c.

Numerical audit. dependency reconstruction $1.50327761802 \times 10^{-10}\,\mathtt{J}$; fractional residual -2.453×10^{-12}.

First-principles verdict. Algebraically reproducible, but not a first-principles physical prediction: the CODATA basis values enter the right-hand side.

END/MNT completion gate. Derive the independent dimensionless basis from one frozen node operator, then propagate its covariance without using this target.

C205 proton mass in u

CODATA 2022. 1.00727646658 `u`, $u = 8.3 \times 10^{-12}$, $u_r = 8.24 \times 10^{-12}$.

Class. L — dependent law/identity; Relative-mass conversion.

Dependency equation. $m/\mathrm{u} = m/m_\mathrm{u}$. *Inputs:* proton mass; atomic mass constant.

Numerical audit. dependency reconstruction 1.00727646657 `u`; fractional residual -4.756×10^{-12}.

First-principles verdict. Algebraically reproducible, but not a first-principles physical prediction: the CODATA basis values enter the right-hand side.

END/MNT completion gate. Derive the independent dimensionless basis from one frozen node operator, then propagate its covariance without using this target.

C206 proton molar mass

CODATA 2022. 0.00100727646764 `kg mol^-1`, $u = 3.1 \times 10^{-13}$, $u_r = 3.078 \times 10^{-10}$.

Class. L — dependent law/identity; Molar mass from single-particle mass.

Dependency equation. $M(X) = N_\mathrm{A} m_X$. *Inputs:* Avogadro constant; proton mass.

Numerical audit. dependency reconstruction 0.00100727646763 `kg mol^-1`; fractional residual -6.632×10^{-12}.

First-principles verdict. Algebraically reproducible, but not a first-principles physical prediction: the CODATA basis values enter the right-hand side.

END/MNT completion gate. Derive the independent dimensionless basis from one frozen node operator, then propagate its covariance without using this target.

C207 proton-muon mass ratio

CODATA 2022. 8.88024338 `dimensionless`, $u = 2 \times 10^{-7}$, $u_r = 2.252 \times 10^{-8}$.

Class. L — dependent law/identity; Dimensionless mass ratio.

Dependency equation. $R_{ab} = m_a/m_b$. *Inputs:* proton mass; muon mass.

Numerical audit. dependency reconstruction 8.88024337884 `dimensionless`; fractional residual -1.308×10^{-10}.

First-principles verdict. Algebraically reproducible, but not a first-principles physical prediction: the CODATA basis values enter the right-hand side.

END/MNT completion gate. Derive the independent dimensionless basis from one frozen node operator, then propagate its covariance without using this target.

C208 proton-neutron mag. mom. ratio

CODATA 2022. -1.45989802 `dimensionless`, $u = 3.4 \times 10^{-7}$, $u_r = 2.329 \times 10^{-7}$.

Class. L — dependent law/identity; Magnetic-moment ratio.

Dependency equation. $R_{\mu,ab} = \mu_a/\mu_b$. *Inputs:* proton and neutron magnetic moments.

Numerical audit. dependency reconstruction -1.4598980184 `dimensionless`; fractional residual -1.098×10^{-9}.

First-principles verdict. Algebraically reproducible, but not a first-principles physical prediction: the CODATA basis values enter the right-hand side.

END/MNT completion gate. Derive the independent dimensionless basis from one frozen node operator, then propagate its covariance without using this target.

C209 proton-neutron mass ratio

CODATA 2022. 0.99862347797 `dimensionless`, $u = 4 \times 10^{-10}$, $u_r = 4.006 \times 10^{-10}$.

Class. L — dependent law/identity; Dimensionless mass ratio.

Dependency equation. $R_{ab} = m_a/m_b$. *Inputs:* proton mass; neutron mass.

Numerical audit. dependency reconstruction 0.998623477966 `dimensionless`; fractional residual -4.081×10^{-12}.

First-principles verdict. Algebraically reproducible, but not a first-principles physical prediction: the CODATA basis values enter the right-hand side.

END/MNT completion gate. Derive the independent dimensionless basis from one frozen node operator, then propagate its covariance without using this target.

C210 proton relative atomic mass

CODATA 2022. 1.00727646658 `dimensionless`, $u = 8.3 \times 10^{-12}$, $u_r = 8.24 \times 10^{-12}$.

Class. L — dependent law/identity; Relative atomic mass.

Dependency equation. $A_{\mathrm{r}}(X) = m_X/m_{\mathrm{u}}$. *Inputs:* proton mass; atomic mass constant.

Numerical audit. dependency reconstruction 1.00727646657 `dimensionless`; fractional residual -4.756×10^{-12}.

First-principles verdict. Algebraically reproducible, but not a first-principles physical prediction: the CODATA basis values enter the right-hand side.

END/MNT completion gate. Derive the independent dimensionless basis from one frozen node operator, then propagate its covariance without using this target.

C211 proton rms charge radius

CODATA 2022. $8.4075 \times 10^{-16}\,\mathtt{m}$, $u = 6.4 \times 10^{-19}$, $u_r = 7.612 \times 10^{-4}$.

Class. A — adjusted empirical input; Adjusted empirical or theory-assisted input.

Dependency equation. $Q = \arg\min_{Q} (\mathbf{y} - \mathbf{f}(Q))^T \mathbf{V}^{-1} (\mathbf{y} - \mathbf{f}(Q))$. *Inputs:* CODATA observational equations and covariance.

Numerical audit. no independent numerical END/MNT output; residual and z score are undefined.

First-principles verdict. No END/MNT first-principles value exists in the current papers; CODATA supplies the comparison target, not an allowed model input for a prediction.

END/MNT completion gate. Generate the relevant spectrum, form factor, or decay amplitude from the frozen micro-model and compare only after preregistration.

C212 proton-tau mass ratio

CODATA 2022. $0.528051\,\mathtt{dimensionless}$, $u = 3.6 \times 10^{-5}$, $u_r = 6.818 \times 10^{-5}$.

Class. L — dependent law/identity; Dimensionless mass ratio.

Dependency equation. $R_{ab} = m_a/m_b$. *Inputs:* proton mass; tau mass.

Numerical audit. dependency reconstruction $0.528050766825\,\mathtt{dimensionless}$; fractional residual -4.416×10^{-7}.

First-principles verdict. Algebraically reproducible, but not a first-principles physical prediction: the CODATA basis values enter the right-hand side.

END/MNT completion gate. Derive the independent dimensionless basis from one frozen node operator, then propagate its covariance without using this target.

C213 quantum of circulation

CODATA 2022. $3.6369475467 \times 10^{-4}$ `m^2 s^-1`, $u = 1.1 \times 10^{-13}$, $u_r = 3.025 \times 10^{-10}$.

Class. L — dependent law/identity; Paired-electron circulation.

Dependency equation. $\kappa = h/(2m_e)$. *Inputs:* h; electron mass.

Numerical audit. dependency reconstruction $3.63694754668 \times 10^{-4}$ `m^2 s^-1`; fractional residual -6.566×10^{-12}.

First-principles verdict. Algebraically reproducible, but not a first-principles physical prediction: the CODATA basis values enter the right-hand side.

END/MNT completion gate. Derive the independent dimensionless basis from one frozen node operator, then propagate its covariance without using this target.

C214 quantum of circulation times 2

CODATA 2022. $7.2738950934 \times 10^{-4}$ `m^2 s^-1`, $u = 2.3 \times 10^{-13}$, $u_r = 3.162 \times 10^{-10}$.

Class. L — dependent law/identity; Electron circulation.

Dependency equation. $2\kappa = h/m_e$. *Inputs:* h; electron mass.

Numerical audit. dependency reconstruction $7.27389509335 \times 10^{-4}$ `m^2 s^-1`; fractional residual -6.566×10^{-12}.

First-principles verdict. Algebraically reproducible, but not a first-principles physical prediction: the CODATA basis values enter the right-hand side.

END/MNT completion gate. Derive the independent dimensionless basis from one frozen node operator, then propagate its covariance without using this target.

C215 reduced Compton wavelength

CODATA 2022. $3.8615926744 \times 10^{-13}$ m, $u = 1.2 \times 10^{-22}$, $u_r = 3.108 \times 10^{-10}$.

Class. L — dependent law/identity; Reduced Compton wavelength.

Dependency equation. $\bar{\lambda}_C = \hbar/(mc)$. *Inputs:* reduced Planck constant; particle mass; c.

Numerical audit. dependency reconstruction $3.86159267435 \times 10^{-13}$ m; fractional residual -1.233×10^{-11}.

First-principles verdict. Algebraically reproducible, but not a first-principles physical prediction: the CODATA basis values enter the right-hand side.

END/MNT completion gate. Derive the independent dimensionless basis from one frozen node operator, then propagate its covariance without using this target.

C216 reduced muon Compton wavelength

CODATA 2022. $1.867594306 \times 10^{-15}$ m, $u = 4.2 \times 10^{-23}$, $u_r = 2.249 \times 10^{-8}$.

Class. L — dependent law/identity; Reduced Compton wavelength.

Dependency equation. $\bar{\lambda}_C = \hbar/(mc)$. *Inputs:* reduced Planck constant; particle mass; c.

Numerical audit. dependency reconstruction $1.86759430599 \times 10^{-15}$ m; fractional residual -2.845×10^{-12}.

First-principles verdict. Algebraically reproducible, but not a first-principles physical prediction: the CODATA basis values enter the right-hand side.

END/MNT completion gate. Derive the independent dimensionless basis from one frozen node operator, then propagate its covariance without using this target.

C217 reduced neutron Compton wavelength

CODATA 2022. $2.100194152 \times 10^{-16}\,\mathtt{m}$, $u = 1.1 \times 10^{-25}$, $u_r = 5.238 \times 10^{-10}$.

Class. L — dependent law/identity; Reduced Compton wavelength.

Dependency equation. $\bar{\lambda}_C = \hbar/(mc)$. *Inputs:* reduced Planck constant; particle mass; c.

Numerical audit. dependency reconstruction $2.10019415203 \times 10^{-16}\,\mathtt{m}$; fractional residual 1.308×10^{-11}.

First-principles verdict. Algebraically reproducible, but not a first-principles physical prediction: the CODATA basis values enter the right-hand side.

END/MNT completion gate. Derive the independent dimensionless basis from one frozen node operator, then propagate its covariance without using this target.

C218 reduced Planck constant

CODATA 2022. $1.05457181765 \times 10^{-34}\,\mathtt{J\ s}$ (exact in the stated system).

Class. L — dependent law/identity; Reduced action constant.

Dependency equation. $\hbar = h/(2\pi)$. *Inputs:* Planck constant.

Numerical audit. dependency reconstruction $1.05457181765 \times 10^{-34}\,\mathtt{J\ s}$; fractional residual 0.

First-principles verdict. Algebraically reproducible, but not a first-principles physical prediction: the CODATA basis values enter the right-hand side.

END/MNT completion gate. Derive the independent dimensionless basis from one frozen node operator, then propagate its covariance without using this target.

C219 reduced proton Compton wavelength

CODATA 2022. $2.10308910051 \times 10^{-16}\,\mathtt{m}$, $u = 6.6 \times 10^{-26}$, $u_r = 3.138 \times 10^{-10}$.

Class. L — dependent law/identity; Reduced Compton wavelength.

Dependency equation. $\bar{\lambda}_C = \hbar/(mc)$. *Inputs:* reduced Planck constant; particle mass; c.

Numerical audit. dependency reconstruction $2.10308910051 \times 10^{-16}\,\mathtt{m}$; fractional residual 1.882×10^{-12}.

First-principles verdict. Algebraically reproducible, but not a first-principles physical prediction: the CODATA basis values enter the right-hand side.

END/MNT completion gate. Derive the independent dimensionless basis from one frozen node operator, then propagate its covariance without using this target.

C220 reduced tau Compton wavelength

CODATA 2022. $1.110538 \times 10^{-16}\,\mathtt{m}$, $u = 7.5 \times 10^{-21}$, $u_r = 6.753 \times 10^{-5}$.

Class. L — dependent law/identity; Reduced Compton wavelength.

Dependency equation. $\bar{\lambda}_C = \hbar/(mc)$. *Inputs:* reduced Planck constant; particle mass; c.

Numerical audit. dependency reconstruction $1.11053781223 \times 10^{-16}\,\mathtt{m}$; fractional residual -1.691×10^{-7}.

First-principles verdict. Algebraically reproducible, but not a first-principles physical prediction: the CODATA basis values enter the right-hand side.

END/MNT completion gate. Derive the independent dimensionless basis from one frozen node operator, then propagate its covariance without using this target.

C221 Rydberg constant

CODATA 2022. $1.09737315682 \times 10^7$ `m^-1`, $u = 1.2 \times 10^{-5}$, $u_r = 1.094 \times 10^{-12}$.

Class. L — dependent law/identity; Infinite-mass Rydberg scale.

Dependency equation. $R_\infty = \alpha^2 m_e c/(2h)$. *Inputs:* alpha; electron mass; c; h.

Numerical audit. dependency reconstruction 1.0973731568×10^7 `m^-1`; fractional residual -1.08×10^{-11}.

First-principles verdict. Algebraically reproducible, but not a first-principles physical prediction: the CODATA basis values enter the right-hand side.

END/MNT completion gate. Derive the independent dimensionless basis from one frozen node operator, then propagate its covariance without using this target.

C222 Rydberg constant times c in Hz

CODATA 2022. $3.28984196025 \times 10^{15}$ `Hz`, $u = 3600$, $u_r = 1.094 \times 10^{-12}$.

Class. L — dependent law/identity; Rydberg frequency.

Dependency equation. cR_∞. *Inputs:* c; Rydberg constant.

Numerical audit. dependency reconstruction $3.28984196025 \times 10^{15}$ `Hz`; fractional residual -5.623×10^{-15}.

First-principles verdict. Algebraically reproducible, but not a first-principles physical prediction: the CODATA basis values enter the right-hand side.

END/MNT completion gate. Derive the independent dimensionless basis from one frozen node operator, then propagate its covariance without using this target.

C223 Rydberg constant times hc in eV

CODATA 2022. 13.605693123 `eV`, $u = 1.5 \times 10^{-11}$, $u_r = 1.102 \times 10^{-12}$.

Class. L — dependent law/identity; Rydberg energy in eV.

Dependency equation. hcR_∞/e. *Inputs:* h; c; Rydberg constant; e.

Numerical audit. dependency reconstruction 13.605693123 `eV`; fractional residual 3.773×10^{-14}.

First-principles verdict. Algebraically reproducible, but not a first-principles physical prediction: the CODATA basis values enter the right-hand side.

END/MNT completion gate. Derive the independent dimensionless basis from one frozen node operator, then propagate its covariance without using this target.

C224 Rydberg constant times hc in J

CODATA 2022. $2.1798723611 \times 10^{-18}$ `J`, $u = 2.4 \times 10^{-30}$, $u_r = 1.101 \times 10^{-12}$.

Class. L — dependent law/identity; Rydberg energy.

Dependency equation. hcR_∞. *Inputs:* h; c; Rydberg constant.

Numerical audit. dependency reconstruction $2.1798723611 \times 10^{-18}$ `J`; fractional residual -5.124×10^{-15}.

First-principles verdict. Algebraically reproducible, but not a first-principles physical prediction: the CODATA basis values enter the right-hand side.

END/MNT completion gate. Derive the independent dimensionless basis from one frozen node operator, then propagate its covariance without using this target.

C225 Sackur-Tetrode constant (1 K, 100 kPa)

CODATA 2022. $-1.15170753496\,\texttt{dimensionless}$, $u = 4.7 \times 10^{-10}$, $u_r = 4.081 \times 10^{-10}$.

Class. A — adjusted empirical input; Adjusted or reference quantity.

Dependency equation. $Q = Q_{\text{CODATA}} \pm u(Q)$. *Inputs:* CODATA adjustment or stated reference procedure.

Numerical audit. no independent numerical END/MNT output; residual and z score are undefined.

First-principles verdict. No independent END/MNT numerical prediction is present; numerical agreement cannot be assessed without inventing an input.

END/MNT completion gate. Specify the observable map and derive the value and uncertainty from a frozen micro-model before inspecting this target.

C226 Sackur-Tetrode constant (1 K, 101.325 kPa)

CODATA 2022. $-1.16487052149\,\texttt{dimensionless}$, $u = 4.7 \times 10^{-10}$, $u_r = 4.035 \times 10^{-10}$.

Class. A — adjusted empirical input; Adjusted or reference quantity.

Dependency equation. $Q = Q_{\text{CODATA}} \pm u(Q)$. *Inputs:* CODATA adjustment or stated reference procedure.

Numerical audit. no independent numerical END/MNT output; residual and z score are undefined.

First-principles verdict. No independent END/MNT numerical prediction is present; numerical agreement cannot be assessed without inventing an input.

END/MNT completion gate. Specify the observable map and derive the value and uncertainty from a frozen micro-model before inspecting this target.

C227 second radiation constant

CODATA 2022. 0.014387768775 `m K` (exact in the stated system).

Class. L — dependent law/identity; Planck-spectrum thermal scale.

Dependency equation. $c_2 = hc/k_B$. *Inputs:* h; c; kB.

Numerical audit. dependency reconstruction 0.014387768775 `m K`; fractional residual 0.

First-principles verdict. Algebraically reproducible, but not a first-principles physical prediction: the CODATA basis values enter the right-hand side.

END/MNT completion gate. Derive the independent dimensionless basis from one frozen node operator, then propagate its covariance without using this target.

C228 shielded helion gyromag. ratio

CODATA 2022. $2.0378946078 \times 10^{8}$ `s^-1 T^-1`, $u = 0.18$, $u_r = 8.833 \times 10^{-10}$.

Class. L — dependent law/identity; Gyromagnetic ratio.

Dependency equation. $|\gamma_X| = |\mu_X|/(I_X \hbar)$. *Inputs:* shielded helion magnetic moment; spin; reduced Planck constant.

Numerical audit. dependency reconstruction $2.03789460778 \times 10^{8}$ `s^-1 T^-1`; fractional residual -8.816×10^{-12}.

First-principles verdict. Algebraically reproducible, but not a first-principles physical prediction: the CODATA basis values enter the right-hand side.

END/MNT completion gate. Derive the independent dimensionless basis from one frozen node operator, then propagate its covariance without using this target.

C229 shielded helion mag. mom.

CODATA 2022. $-1.07455311035 \times 10^{-26}$ `J T^-1`, $u = 9.3 \times 10^{-36}$, $u_r = 8.655 \times 10^{-10}$.

Class. R — material/reference dependent; Material or environment-dependent reference.

Dependency equation. $Q = Q(T, p, \text{composition, preparation})$. *Inputs:* experimental reference conditions.

Numerical audit. no independent numerical END/MNT output; residual and z score are undefined.

First-principles verdict. Not a universal constant of a microscopic theory; it must be measured or calculated from a detailed material model.

END/MNT completion gate. Derive the relevant bound-state/material Hamiltonian and the stated experimental conditions before comparison.

C230 shielded helion mag. mom. to Bohr magneton ratio

CODATA 2022. -0.00115867149457 `dimensionless`, $u = 9.4 \times 10^{-13}$, $u_r = 8.113 \times 10^{-10}$.

Class. L — dependent law/identity; Magnetic moment in Bohr magnetons.

Dependency equation. μ_X/μ_{B}. *Inputs:* shielded helion magnetic moment; Bohr magneton.

Numerical audit. dependency reconstruction -0.00115867149457 `dimensionless`; fractional residual 1.69×10^{-12}.

First-principles verdict. Algebraically reproducible, but not a first-principles physical prediction: the CODATA basis values enter the right-hand side.

END/MNT completion gate. Derive the independent dimensionless basis from one frozen node operator, then propagate its covariance without using this target.

C231 shielded helion mag. mom. to nuclear magneton ratio

CODATA 2022. $-2.1274977624\,\texttt{dimensionless}$, $u = 1.7 \times 10^{-9}$, $u_r = 7.991 \times 10^{-10}$.

Class. L — dependent law/identity; Magnetic moment in nuclear magnetons.

Dependency equation. $\mu_X/\mu_{\rm N}$. *Inputs:* shielded helion magnetic moment; nuclear magneton.

Numerical audit. dependency reconstruction $-2.12749776236\,\texttt{dimensionless}$; fractional residual -2.113×10^{-11}.

First-principles verdict. Algebraically reproducible, but not a first-principles physical prediction: the CODATA basis values enter the right-hand side.

END/MNT completion gate. Derive the independent dimensionless basis from one frozen node operator, then propagate its covariance without using this target.

C232 shielded helion to proton mag. mom. ratio

CODATA 2022. $-0.76176657721\,\texttt{dimensionless}$, $u = 6.6 \times 10^{-10}$, $u_r = 8.664 \times 10^{-10}$.

Class. L — dependent law/identity; Magnetic-moment ratio.

Dependency equation. $R_{\mu,ab} = \mu_a/\mu_b$. *Inputs:* shielded helion and proton magnetic moments.

Numerical audit. dependency reconstruction $-0.761766577204\,\texttt{dimensionless}$; fractional residual -8.481×10^{-12}.

First-principles verdict. Algebraically reproducible, but not a first-principles physical prediction: the CODATA basis values enter the right-hand side.

END/MNT completion gate. Derive the independent dimensionless basis from one frozen node operator, then propagate its covariance without using this target.

C233 shielded helion to shielded proton mag. mom. ratio

CODATA 2022. -0.7617861334 `dimensionless`, $u = 3.1 \times 10^{-9}$, $u_r = 4.069 \times 10^{-9}$.

Class. L — dependent law/identity; Magnetic-moment ratio.

Dependency equation. $R_{\mu,ab} = \mu_a/\mu_b$. *Inputs:* shielded helion and shielded proton magnetic moments.

Numerical audit. dependency reconstruction -0.761786133427 `dimensionless`; fractional residual 3.597×10^{-11}.

First-principles verdict. Algebraically reproducible, but not a first-principles physical prediction: the CODATA basis values enter the right-hand side.

END/MNT completion gate. Derive the independent dimensionless basis from one frozen node operator, then propagate its covariance without using this target.

C234 shielded proton gyromag. ratio

CODATA 2022. $2.675153194 \times 10^{8}$ `s^-1 T^-1`, $u = 1.1$, $u_r = 4.112 \times 10^{-9}$.

Class. L — dependent law/identity; Gyromagnetic ratio.

Dependency equation. $|\gamma_X| = |\mu_X|/(I_X \hbar)$. *Inputs:* shielded proton magnetic moment; spin; reduced Planck constant.

Numerical audit. dependency reconstruction $2.67515319374 \times 10^{8}$ `s^-1 T^-1`; fractional residual -9.872×10^{-11}.

First-principles verdict. Algebraically reproducible, but not a first-principles physical prediction: the CODATA basis values enter the right-hand side.

END/MNT completion gate. Derive the independent dimensionless basis from one frozen node operator, then propagate its covariance without using this target.

C235 shielded proton mag. mom.

CODATA 2022. $1.410570583 \times 10^{-26}$ `J T^-1`, $u = 5.8 \times 10^{-35}$, $u_r = 4.112 \times 10^{-9}$.

Class. R — material/reference dependent; Material or environment-dependent reference.

Dependency equation. $Q = Q(T, p, \text{composition, preparation})$. *Inputs:* experimental reference conditions.

Numerical audit. no independent numerical END/MNT output; residual and z score are undefined.

First-principles verdict. Not a universal constant of a microscopic theory; it must be measured or calculated from a detailed material model.

END/MNT completion gate. Derive the relevant bound-state/material Hamiltonian and the stated experimental conditions before comparison.

C236 shielded proton mag. mom. to Bohr magneton ratio

CODATA 2022. 0.0015209931551 `dimensionless`, $u = 6.2 \times 10^{-12}$, $u_r = 4.076 \times 10^{-9}$.

Class. L — dependent law/identity; Magnetic moment in Bohr magnetons.

Dependency equation. μ_X/μ_{B}. *Inputs:* shielded proton magnetic moment; Bohr magneton.

Numerical audit. dependency reconstruction 0.00152099315507 `dimensionless`; fractional residual -1.83×10^{-11}.

First-principles verdict. Algebraically reproducible, but not a first-principles physical prediction: the CODATA basis values enter the right-hand side.

END/MNT completion gate. Derive the independent dimensionless basis from one frozen node operator, then propagate its covariance without using this target.

C237 shielded proton mag. mom. to nuclear magneton ratio

CODATA 2022. 2.792775648 `dimensionless`, $u = 1.1 \times 10^{-8}$, $u_r = 3.939 \times 10^{-9}$.

Class. L — dependent law/identity; Magnetic moment in nuclear magnetons.

Dependency equation. μ_X/μ_{N}. *Inputs:* shielded proton magnetic moment; nuclear magneton.

Numerical audit. dependency reconstruction 2.79277564791 `dimensionless`; fractional residual -3.058×10^{-11}.

First-principles verdict. Algebraically reproducible, but not a first-principles physical prediction: the CODATA basis values enter the right-hand side.

END/MNT completion gate. Derive the independent dimensionless basis from one frozen node operator, then propagate its covariance without using this target.

C238 shielding difference of d and p in HD

CODATA 2022. 1.9877×10^{-8} `dimensionless`, $u = 1 \times 10^{-12}$, $u_r = 5.031 \times 10^{-5}$.

Class. R — material/reference dependent; Material or environment-dependent reference.

Dependency equation. $Q = Q(T, p, \text{composition, preparation})$. *Inputs:* experimental reference conditions.

Numerical audit. no independent numerical END/MNT output; residual and z score are undefined.

First-principles verdict. Not a universal constant of a microscopic theory; it must be measured or calculated from a detailed material model.

END/MNT completion gate. Derive the relevant bound-state/material Hamiltonian and the stated experimental conditions before comparison.

C239 shielding difference of t and p in HT

CODATA 2022. 2.3945×10^{-8} `dimensionless`, $u = 2 \times 10^{-12}$, $u_r = 8.352 \times 10^{-5}$.

Class. R — material/reference dependent; Material or environment-dependent reference.

Dependency equation. $Q = Q(T, p, \text{composition, preparation})$. *Inputs:* experimental reference conditions.

Numerical audit. no independent numerical END/MNT output; residual and z score are undefined.

First-principles verdict. Not a universal constant of a microscopic theory; it must be measured or calculated from a detailed material model.

END/MNT completion gate. Derive the relevant bound-state/material Hamiltonian and the stated experimental conditions before comparison.

C240 speed of light in vacuum

CODATA 2022. 2.99792458×10^{8} `m s^-1` (exact in the stated system).

Class. D — SI definition; SI definition and END long-wave bridge.

Dependency equation. $c \equiv 299792458\,\mathrm{m\,s^{-1}}, \qquad c_0 = a\sqrt{\kappa/\mu}$. *Inputs:* SI definition; END parameters a,kappa,mu.

Numerical audit. identity check 2.99792458×10^{8} `m s^-1`; fractional residual 0.

First-principles verdict. The SI digits are defined. END/MNT derives only the symbolic benchmark speed c0; setting c0=c calibrates one parameter combination.

END/MNT completion gate. Derive a,kappa,mu and a universal clock map independently, then prove every massless sector shares c0.

C241 standard acceleration of gravity

CODATA 2022. 9.80665 `m s^-2` (exact in the stated system).

Class. C — convention; Conventional reference quantity.

Dependency equation. $Q \equiv Q_{\mathrm{conv}}$ (stipulated reference). *Inputs:* named convention.

Numerical audit. dependency reconstruction 9.80665 `m s^-2`; fractional residual 0.

First-principles verdict. Exact only inside the stated metrological convention; not a universal-law prediction.

END/MNT completion gate. No END/MNT derivation is required unless the theory predicts the physical realization used by the convention.

C242 standard atmosphere

CODATA 2022. 1.01325×10^5 `Pa` (exact in the stated system).

Class. C — convention; Conventional reference quantity.

Dependency equation. $Q \equiv Q_{\mathrm{conv}}$ (stipulated reference). *Inputs:* named convention.

Numerical audit. dependency reconstruction 1.01325×10^5 `Pa`; fractional residual 0.

First-principles verdict. Exact only inside the stated metrological convention; not a universal-law prediction.

END/MNT completion gate. No END/MNT derivation is required unless the theory predicts the physical realization used by the convention.

C243 standard-state pressure

CODATA 2022. 1×10^5 `Pa` (exact in the stated system).
Class. C — convention; Conventional reference quantity.
Dependency equation. $Q \equiv Q_{\mathrm{conv}}$ (stipulated reference). *Inputs:* named convention.
Numerical audit. dependency reconstruction 1×10^5 `Pa`; fractional residual 0.
First-principles verdict. Exact only inside the stated metrological convention; not a universal-law prediction.
END/MNT completion gate. No END/MNT derivation is required unless the theory predicts the physical realization used by the convention.

C244 Stefan-Boltzmann constant

CODATA 2022. $5.67037441918 \times 10^{-8}$ `W m^-2 K^-4` (exact in the stated system).
Class. L — dependent law/identity; Blackbody flux coefficient.
Dependency equation. $\sigma = 2\pi^5 k_{\mathrm{B}}^4/(15h^3c^2)$. *Inputs:* kB; h; c.
Numerical audit. dependency reconstruction $5.67037441918 \times 10^{-8}$ `W m^-2 K^-4`; fractional residual 0.
First-principles verdict. Algebraically reproducible, but not a first-principles physical prediction: the CODATA basis values enter the right-hand side.
END/MNT completion gate. Derive the independent dimensionless basis from one frozen node operator, then propagate its covariance without using this target.

C245 tau Compton wavelength

CODATA 2022. $6.97771 \times 10^{-16}\,\mathtt{m}$, $u = 4.7 \times 10^{-20}$, $u_r = 6.736 \times 10^{-5}$.

Class. L — dependent law/identity; Compton wavelength.

Dependency equation. $\lambda_C = h/(mc)$. *Inputs:* Planck constant; particle mass; c.

Numerical audit. dependency reconstruction $6.97771486486 \times 10^{-16}\,\mathtt{m}$; fractional residual 6.972×10^{-7}.

First-principles verdict. Algebraically reproducible, but not a first-principles physical prediction: the CODATA basis values enter the right-hand side.

END/MNT completion gate. Derive the independent dimensionless basis from one frozen node operator, then propagate its covariance without using this target.

C246 tau-electron mass ratio

CODATA 2022. $3477.23\,\mathtt{dimensionless}$, $u = 0.23$, $u_r = 6.614 \times 10^{-5}$.

Class. L — dependent law/identity; Dimensionless mass ratio.

Dependency equation. $R_{ab} = m_a/m_b$. *Inputs:* tau mass; electron mass.

Numerical audit. dependency reconstruction $3477.22754852\,\mathtt{dimensionless}$; fractional residual -7.05×10^{-7}.

First-principles verdict. Algebraically reproducible, but not a first-principles physical prediction: the CODATA basis values enter the right-hand side.

END/MNT completion gate. Derive the independent dimensionless basis from one frozen node operator, then propagate its covariance without using this target.

C247 tau energy equivalent

CODATA 2022. $1776.86\,\texttt{MeV}$, $u = 0.12$, $u_r = 6.753 \times 10^{-5}$.

Class. A — adjusted empirical input; Measured particle/nuclear scale.

Dependency equation. $mc^2 = E_{\text{pole}} \quad \text{or} \quad m = E_0/c^2$. *Inputs:* spectroscopy, kinematics, or mass-frequency ratios.

Numerical audit. no independent numerical END/MNT output; residual and z score are undefined.

First-principles verdict. The value is empirical. END/MNT currently has a mass-gap dictionary but no particle-identifying eigenproblem that predicts this number.

END/MNT completion gate. Derive a stable localized state, its renormalized pole energy, quantum numbers, and uncertainty without tuning to the listed mass.

C248 tau mass

CODATA 2022. $3.16754 \times 10^{-27}\,\texttt{kg}$, $u = 2.1 \times 10^{-31}$, $u_r = 6.63 \times 10^{-5}$.

Class. A — adjusted empirical input; Measured particle/nuclear scale.

Dependency equation. $mc^2 = E_{\text{pole}} \quad \text{or} \quad m = E_0/c^2$. *Inputs:* spectroscopy, kinematics, or mass-frequency ratios.

Numerical audit. no independent numerical END/MNT output; residual and z score are undefined.

First-principles verdict. The value is empirical. END/MNT currently has a mass-gap dictionary but no particle-identifying eigenproblem that predicts this number.

END/MNT completion gate. Derive a stable localized state, its renormalized pole energy, quantum numbers, and uncertainty without tuning to the listed mass.

C249 tau mass energy equivalent

CODATA 2022. 2.84684×10^{-10} J, $u = 1.9 \times 10^{-14}$, $u_r = 6.674 \times 10^{-5}$.

Class. L — dependent law/identity; Relativistic mass-energy identity.

Dependency equation. $E_m = mc^2$. *Inputs:* tau mass; c.

Numerical audit. dependency reconstruction $2.84684297886 \times 10^{-10}$ J; fractional residual 1.046×10^{-6}.

First-principles verdict. Algebraically reproducible, but not a first-principles physical prediction: the CODATA basis values enter the right-hand side.

END/MNT completion gate. Derive the independent dimensionless basis from one frozen node operator, then propagate its covariance without using this target.

C250 tau mass in u

CODATA 2022. $1.90754\,\mathrm{u}$, $u = 1.3 \times 10^{-4}$, $u_r = 6.815 \times 10^{-5}$.

Class. L — dependent law/identity; Relative-mass conversion.

Dependency equation. $m/\mathrm{u} = m/m_\mathrm{u}$. *Inputs:* tau mass; atomic mass constant.

Numerical audit. dependency reconstruction $1.90753717229\,\mathrm{u}$; fractional residual -1.482×10^{-6}.

First-principles verdict. Algebraically reproducible, but not a first-principles physical prediction: the CODATA basis values enter the right-hand side.

END/MNT completion gate. Derive the independent dimensionless basis from one frozen node operator, then propagate its covariance without using this target.

C251 tau molar mass

CODATA 2022. 0.00190754 `kg mol^-1`, $u = 1.3 \times 10^{-7}$, $u_r = 6.815 \times 10^{-5}$.

Class. L — dependent law/identity; Molar mass from single-particle mass.

Dependency equation. $M(X) = N_{\mathrm{A}} m_X$. *Inputs:* Avogadro constant; tau mass.

Numerical audit. dependency reconstruction 0.00190753717429 `kg mol^-1`; fractional residual -1.481×10^{-6}.

First-principles verdict. Algebraically reproducible, but not a first-principles physical prediction: the CODATA basis values enter the right-hand side.

END/MNT completion gate. Derive the independent dimensionless basis from one frozen node operator, then propagate its covariance without using this target.

C252 tau-muon mass ratio

CODATA 2022. 16.817 `dimensionless`, $u = 0.0011$, $u_r = 6.541 \times 10^{-5}$.

Class. L — dependent law/identity; Dimensionless mass ratio.

Dependency equation. $R_{ab} = m_a/m_b$. *Inputs:* tau mass; muon mass.

Numerical audit. dependency reconstruction 16.8170258179 `dimensionless`; fractional residual 1.535×10^{-6}.

First-principles verdict. Algebraically reproducible, but not a first-principles physical prediction: the CODATA basis values enter the right-hand side.

END/MNT completion gate. Derive the independent dimensionless basis from one frozen node operator, then propagate its covariance without using this target.

C253 tau-neutron mass ratio

CODATA 2022. 1.89115 `dimensionless`, $u = 1.3 \times 10^{-4}$, $u_r = 6.874 \times 10^{-5}$.

Class. L — dependent law/identity; Dimensionless mass ratio.

Dependency equation. $R_{ab} = m_a/m_b$. *Inputs:* tau mass; neutron mass.

Numerical audit. dependency reconstruction 1.89115051185 `dimensionless`; fractional residual 2.707×10^{-7}.

First-principles verdict. Algebraically reproducible, but not a first-principles physical prediction: the CODATA basis values enter the right-hand side.

END/MNT completion gate. Derive the independent dimensionless basis from one frozen node operator, then propagate its covariance without using this target.

C254 tau-proton mass ratio

CODATA 2022. 1.89376 `dimensionless`, $u = 1.3 \times 10^{-4}$, $u_r = 6.865 \times 10^{-5}$.

Class. L — dependent law/identity; Dimensionless mass ratio.

Dependency equation. $R_{ab} = m_a/m_b$. *Inputs:* tau mass; proton mass.

Numerical audit. dependency reconstruction 1.89375731052 `dimensionless`; fractional residual -1.42×10^{-6}.

First-principles verdict. Algebraically reproducible, but not a first-principles physical prediction: the CODATA basis values enter the right-hand side.

END/MNT completion gate. Derive the independent dimensionless basis from one frozen node operator, then propagate its covariance without using this target.

C255 Thomson cross section

CODATA 2022. $6.6524587051 \times 10^{-29}$ `m^2`, $u = 6.2 \times 10^{-38}$, $u_r = 9.32 \times 10^{-10}$.

Class. L — dependent law/identity; Low-energy electron scattering area.

Dependency equation. $\sigma_{\mathrm{T}} = 8\pi r_e^2/3$. *Inputs:* classical electron radius.

Numerical audit. dependency reconstruction $6.65245870524 \times 10^{-29}$ `m^2`; fractional residual 2.069×10^{-11}.

First-principles verdict. Algebraically reproducible, but not a first-principles physical prediction: the CODATA basis values enter the right-hand side.

END/MNT completion gate. Derive the independent dimensionless basis from one frozen node operator, then propagate its covariance without using this target.

C256 triton-electron mass ratio

CODATA 2022. 5496.92153551 `dimensionless`, $u = 2.1 \times 10^{-7}$, $u_r = 3.82 \times 10^{-11}$.

Class. L — dependent law/identity; Dimensionless mass ratio.

Dependency equation. $R_{ab} = m_a/m_b$. *Inputs:* triton mass; electron mass.

Numerical audit. dependency reconstruction 5496.92153549 `dimensionless`; fractional residual -3.215×10^{-12}.

First-principles verdict. Algebraically reproducible, but not a first-principles physical prediction: the CODATA basis values enter the right-hand side.

END/MNT completion gate. Derive the independent dimensionless basis from one frozen node operator, then propagate its covariance without using this target.

C257 triton g factor

CODATA 2022. 5.95792493 `dimensionless`, $u = 1.2 \times 10^{-8}$, $u_r = 2.014 \times 10^{-9}$.

Class. L — dependent law/identity; Magnetic g factor.

Dependency equation. $g_X = \mu_X/(I_X \mu_{\text{ref}})$. *Inputs:* triton magnetic moment; spin; reference magneton.

Numerical audit. dependency reconstruction 5.95792492992 `dimensionless`; fractional residual -1.376×10^{-11}.

First-principles verdict. Algebraically reproducible, but not a first-principles physical prediction: the CODATA basis values enter the right-hand side.

END/MNT completion gate. Derive the independent dimensionless basis from one frozen node operator, then propagate its covariance without using this target.

C258 triton mag. mom.

CODATA 2022. $1.5046095178 \times 10^{-26}$ `J T^-1`, $u = 3 \times 10^{-35}$, $u_r = 1.994 \times 10^{-9}$.

Class. A — adjusted empirical input; Adjusted or reference quantity.

Dependency equation. $Q = Q_{\text{CODATA}} \pm u(Q)$. *Inputs:* CODATA adjustment or stated reference procedure.

Numerical audit. no independent numerical END/MNT output; residual and z score are undefined.

First-principles verdict. No independent END/MNT numerical prediction is present; numerical agreement cannot be assessed without inventing an input.

END/MNT completion gate. Specify the observable map and derive the value and uncertainty from a frozen micro-model before inspecting this target.

C259 triton mag. mom. to Bohr magneton ratio

CODATA 2022. 0.0016223936648 `dimensionless`, $u = 3.2 \times 10^{-12}$, $u_r = 1.972 \times 10^{-9}$.

Class. L — dependent law/identity; Magnetic moment in Bohr magnetons.

Dependency equation. μ_X/μ_{B}. *Inputs:* triton magnetic moment; Bohr magneton.

Numerical audit. dependency reconstruction 0.00162239366481 `dimensionless`; fractional residual 7.769×10^{-12}.

First-principles verdict. Algebraically reproducible, but not a first-principles physical prediction: the CODATA basis values enter the right-hand side.

END/MNT completion gate. Derive the independent dimensionless basis from one frozen node operator, then propagate its covariance without using this target.

C260 triton mag. mom. to nuclear magneton ratio

CODATA 2022. 2.978962465 `dimensionless`, $u = 5.9 \times 10^{-9}$, $u_r = 1.981 \times 10^{-9}$.

Class. L — dependent law/identity; Magnetic moment in nuclear magnetons.

Dependency equation. μ_X/μ_{N}. *Inputs:* triton magnetic moment; nuclear magneton.

Numerical audit. dependency reconstruction 2.97896246496 `dimensionless`; fractional residual -1.376×10^{-11}.

First-principles verdict. Algebraically reproducible, but not a first-principles physical prediction: the CODATA basis values enter the right-hand side.

END/MNT completion gate. Derive the independent dimensionless basis from one frozen node operator, then propagate its covariance without using this target.

C261 triton mass

CODATA 2022. $5.0073567512 \times 10^{-27}$ kg, $u = 1.6 \times 10^{-36}$, $u_r = 3.195 \times 10^{-10}$.

Class. A — adjusted empirical input; Measured particle/nuclear scale.

Dependency equation. $mc^2 = E_{\text{pole}}$ or $m = E_0/c^2$. *Inputs:* spectroscopy, kinematics, or mass-frequency ratios.

Numerical audit. no independent numerical END/MNT output; residual and z score are undefined.

First-principles verdict. The value is empirical. END/MNT currently has a mass-gap dictionary but no particle-identifying eigenproblem that predicts this number.

END/MNT completion gate. Derive a stable localized state, its renormalized pole energy, quantum numbers, and uncertainty without tuning to the listed mass.

C262 triton mass energy equivalent

CODATA 2022. $4.5003878119 \times 10^{-10}$ J, $u = 1.4 \times 10^{-19}$, $u_r = 3.111 \times 10^{-10}$.

Class. L — dependent law/identity; Relativistic mass-energy identity.

Dependency equation. $E_m = mc^2$. *Inputs:* triton mass; c.

Numerical audit. dependency reconstruction $4.50038781192 \times 10^{-10}$ J; fractional residual 5.281×10^{-12}.

First-principles verdict. Algebraically reproducible, but not a first-principles physical prediction: the CODATA basis values enter the right-hand side.

END/MNT completion gate. Derive the independent dimensionless basis from one frozen node operator, then propagate its covariance without using this target.

C263 triton mass in u

CODATA 2022. 3.01550071597 `u`, $u = 1 \times 10^{-10}$, $u_r = 3.316 \times 10^{-11}$.

Class. L — dependent law/identity; Relative-mass conversion.

Dependency equation. $m/\mathrm{u} = m/m_\mathrm{u}$. *Inputs:* triton mass; atomic mass constant.

Numerical audit. dependency reconstruction 3.01550071596 `u`; fractional residual -4.876×10^{-12}.

First-principles verdict. Algebraically reproducible, but not a first-principles physical prediction: the CODATA basis values enter the right-hand side.

END/MNT completion gate. Derive the independent dimensionless basis from one frozen node operator, then propagate its covariance without using this target.

C264 triton molar mass

CODATA 2022. 0.00301550071913 `kg mol^-1`, $u = 9.4 \times 10^{-13}$, $u_r = 3.117 \times 10^{-10}$.

Class. L — dependent law/identity; Molar mass from single-particle mass.

Dependency equation. $M(X) = N_\mathrm{A} m_X$. *Inputs:* Avogadro constant; triton mass.

Numerical audit. dependency reconstruction 0.00301550071913 `kg mol^-1`; fractional residual -1.237×10^{-12}.

First-principles verdict. Algebraically reproducible, but not a first-principles physical prediction: the CODATA basis values enter the right-hand side.

END/MNT completion gate. Derive the independent dimensionless basis from one frozen node operator, then propagate its covariance without using this target.

C265 triton-proton mass ratio

CODATA 2022. 2.99371703403 `dimensionless`, $u = 1 \times 10^{-10}$, $u_r = 3.34 \times 10^{-11}$.

Class. L — dependent law/identity; Dimensionless mass ratio.

Dependency equation. $R_{ab} = m_a/m_b$. *Inputs:* triton mass; proton mass.

Numerical audit. dependency reconstruction 2.99371703402 `dimensionless`; fractional residual -1.713×10^{-12}.

First-principles verdict. Algebraically reproducible, but not a first-principles physical prediction: the CODATA basis values enter the right-hand side.

END/MNT completion gate. Derive the independent dimensionless basis from one frozen node operator, then propagate its covariance without using this target.

C266 triton relative atomic mass

CODATA 2022. 3.01550071597 `dimensionless`, $u = 1 \times 10^{-10}$, $u_r = 3.316 \times 10^{-11}$.

Class. L — dependent law/identity; Relative atomic mass.

Dependency equation. $A_{\mathrm{r}}(X) = m_X/m_{\mathrm{u}}$. *Inputs:* triton mass; atomic mass constant.

Numerical audit. dependency reconstruction 3.01550071596 `dimensionless`; fractional residual -4.876×10^{-12}.

First-principles verdict. Algebraically reproducible, but not a first-principles physical prediction: the CODATA basis values enter the right-hand side.

END/MNT completion gate. Derive the independent dimensionless basis from one frozen node operator, then propagate its covariance without using this target.

C267 triton to proton mag. mom. ratio

CODATA 2022. 1.0666399189 `dimensionless`, $u = 2.1 \times 10^{-9}$, $u_r = 1.969 \times 10^{-9}$.

Class. L — dependent law/identity; Magnetic-moment ratio.

Dependency equation. $R_{\mu,ab} = \mu_a/\mu_b$. *Inputs:* triton and proton magnetic moments.

Numerical audit. dependency reconstruction 1.06663991883 `dimensionless`; fractional residual -6.552×10^{-11}.

First-principles verdict. Algebraically reproducible, but not a first-principles physical prediction: the CODATA basis values enter the right-hand side.

END/MNT completion gate. Derive the independent dimensionless basis from one frozen node operator, then propagate its covariance without using this target.

C268 unified atomic mass unit

CODATA 2022. $1.66053906892 \times 10^{-27}$ `kg`, $u = 5.2 \times 10^{-37}$, $u_r = 3.132 \times 10^{-10}$.

Class. L — dependent law/identity; Atomic mass unit identity.

Dependency equation. $\mathrm{u} = m_{\mathrm{u}}$. *Inputs:* atomic mass constant.

Numerical audit. dependency reconstruction $1.66053906892 \times 10^{-27}$ `kg`; fractional residual 0.

First-principles verdict. Algebraically reproducible, but not a first-principles physical prediction: the CODATA basis values enter the right-hand side.

END/MNT completion gate. Derive the independent dimensionless basis from one frozen node operator, then propagate its covariance without using this target.

C269 vacuum electric permittivity

CODATA 2022. $8.8541878188 \times 10^{-12}$ `F m^-1`, $u = 1.4 \times 10^{-21}$, $u_r = 1.581 \times 10^{-10}$.

Class. L — dependent law/identity; Vacuum electric conversion.

Dependency equation. $\epsilon_0 = e^2/(4\pi\alpha\hbar c)$. *Inputs:* e; alpha; hbar; c.

Numerical audit. dependency reconstruction $8.85418781884 \times 10^{-12}$ `F m^-1`; fractional residual 4.524×10^{-12}.

First-principles verdict. Algebraically reproducible, but not a first-principles physical prediction: the CODATA basis values enter the right-hand side.

END/MNT completion gate. Derive the independent dimensionless basis from one frozen node operator, then propagate its covariance without using this target.

C270 vacuum mag. permeability

CODATA 2022. $1.25663706127 \times 10^{-6}$ `N A^-2`, $u = 2 \times 10^{-16}$, $u_r = 1.592 \times 10^{-10}$.

Class. L — dependent law/identity; Vacuum magnetic conversion.

Dependency equation. $\mu_0 = 1/(\epsilon_0 c^2)$. *Inputs:* epsilon0; c.

Numerical audit. dependency reconstruction $1.25663706127 \times 10^{-6}$ `N A^-2`; fractional residual -1.193×10^{-12}.

First-principles verdict. Algebraically reproducible, but not a first-principles physical prediction: the CODATA basis values enter the right-hand side.

END/MNT completion gate. Derive the independent dimensionless basis from one frozen node operator, then propagate its covariance without using this target.

C271 von Klitzing constant

CODATA 2022. 25812.8074593 `ohm` (exact in the stated system).

Class. L — dependent law/identity; Quantum Hall resistance.

Dependency equation. $R_{\mathrm{K}} = h/e^2$. *Inputs:* e; h.

Numerical audit. dependency reconstruction 25812.8074593 `ohm`; fractional residual 0.

First-principles verdict. Algebraically reproducible, but not a first-principles physical prediction: the CODATA basis values enter the right-hand side.

END/MNT completion gate. Derive the independent dimensionless basis from one frozen node operator, then propagate its covariance without using this target.

C272 weak mixing angle

CODATA 2022. 0.22305 `dimensionless`, $u = 2.3 \times 10^{-4}$, $u_r = 0.001031$.

Class. A — adjusted empirical input; Adjusted empirical or theory-assisted input.

Dependency equation. $Q = \arg\min_{Q} (\mathbf{y} - \mathbf{f}(Q))^T \mathbf{V}^{-1} (\mathbf{y} - \mathbf{f}(Q))$. *Inputs:* CODATA observational equations and covariance.

Numerical audit. no independent numerical END/MNT output; residual and z score are undefined.

First-principles verdict. No END/MNT first-principles value exists in the current papers; CODATA supplies the comparison target, not an allowed model input for a prediction.

END/MNT completion gate. Generate the relevant spectrum, form factor, or decay amplitude from the frozen micro-model and compare only after preregistration.

C273 Wien frequency displacement law constant

CODATA 2022. $5.87892575765 \times 10^{10}$ `Hz K^-1` (exact in the stated system).

Class. L — dependent law/identity; Blackbody frequency peak.

Dependency equation. $b'_\nu = xk_\mathrm{B}/h,\ 3(1 - e^{-x}) = x.$ *Inputs:* h; kB; dimensionless root x.

Numerical audit. dependency reconstruction $5.87892575765 \times 10^{10}$ `Hz K^-1`; fractional residual 1.298×10^{-16}.

First-principles verdict. Algebraically reproducible, but not a first-principles physical prediction: the CODATA basis values enter the right-hand side.

END/MNT completion gate. Derive the independent dimensionless basis from one frozen node operator, then propagate its covariance without using this target.

C274 Wien wavelength displacement law constant

CODATA 2022. 0.00289777195519 `m K` (exact in the stated system).

Class. L — dependent law/identity; Blackbody wavelength peak.

Dependency equation. $b = hc/(xk_\mathrm{B}),\ 5(1 - e^{-x}) = x.$ *Inputs:* h; c; kB; dimensionless root x.

Numerical audit. dependency reconstruction 0.00289777195519 `m K`; fractional residual 0.

First-principles verdict. Algebraically reproducible, but not a first-principles physical prediction: the CODATA basis values enter the right-hand side.

END/MNT completion gate. Derive the independent dimensionless basis from one frozen node operator, then propagate its covariance without using this target.

C275 W to Z mass ratio

CODATA 2022. 0.88145 `dimensionless`, $u = 1.3 \times 10^{-4}$, $u_r = 1.475 \times 10^{-4}$.

Class. A — adjusted empirical input; Adjusted empirical or theory-assisted input.

Dependency equation. $Q = \arg\min_Q (\mathbf{y} - \mathbf{f}(Q))^T \mathbf{V}^{-1} (\mathbf{y} - \mathbf{f}(Q))$. *Inputs:* CODATA observational equations and covariance.

Numerical audit. no independent numerical END/MNT output; residual and z score are undefined.

First-principles verdict. No END/MNT first-principles value exists in the current papers; CODATA supplies the comparison target, not an allowed model input for a prediction.

END/MNT completion gate. Generate the relevant spectrum, form factor, or decay amplitude from the frozen micro-model and compare only after preregistration.

End of the 275-entry register.

The register contains zero claimed numerical END/MNT predictions. Its dependent reconstructions validate the audit code and the published CODATA algebra; they do not validate the proposed ontology. The next admissible numerical claim must come from a frozen node model and a held-out target.

Part IV
Expanded Derivation Workbench

How to use these sheets. Each topic is a two-page pair. The first page is the condensed equation and dependency map; the second exposes every assumption, algebraic step, dimensional requirement, interpretive limit, edit point, and falsifier. Changing a yellow author-control item is permitted, but downstream sheets and proofs must then be recomputed. Blue bold codes are stable revision identifiers.

Family	Size	Stable sheet codes
Foundations	8 paired topics	F01, F02, F03, F04, F05, F06, F07, F08
Benchmark dynamics	8 paired topics	D01, D02, D03, D04, D05, D06, D07, D08
Spectrum and stability	8 paired topics	S01, S02, S03, S04, S05, S06, S07, S08
Gauge and phase	8 paired topics	G01, G02, G03, G04, G05, G06, G07, G08
Legacy repair	3 paired topics	L01, L02, L03
Capacity and EQEF	6 paired topics	C01, C02, C03, C04, C05, C06
Gravity and cosmology	6 paired topics	R01, R02, R03, R04, R05, R06
Quantum completion	4 paired topics	Q01, Q02, Q03, Q04
Constants and evidence	4 paired topics	E01, E02, E03, E04

Status language

PROVED/EXACT means the statement follows from the displayed benchmark assumptions. **CONDITIONAL** means a valid implication still depends on a listed bridge. **MATCHING** identifies a form or coefficient without predictive credit. **OPEN** and **REQUIRED** are research gates. None of these labels means that nature realizes the model.

Revision protocol. Record any conceptual change in the supplied CSV ledger, increment the manuscript version, rerun every affected analytic and numerical check, and retain the previous version for provenance.

Equation Navigation Index I

Foundations through early gauge structure. Blue codes link to compact sheets; page pairs are compact / expanded.

Equation Navigation Index II

Gauge structure through evidence protocol. Blue codes link to compact sheets; page pairs are compact / expanded.

Author Revision Index

Every entry below is a declared point where Ryan's intended ontology or mechanism can replace the present working choice.

F01

DEFINITION / OPEN MICROPHYSICS

Relational proto-state

Foundations | Compact equation map | Pair 01 of 55

Condensed equation chain

$$\mathfrak{P} = (X, \mathcal{R}, \mathcal{A}), \qquad X_{n+1} = U_{\boldsymbol{p}}(X_n), \qquad X_n \notin \mathcal{M}_{\text{spacetime}} \tag{65}$$

Symbols and types

X: complete proto-state; $\mathcal{R}$: admissible relations; $\mathcal{A}$: allowed local changes; $U_{\boldsymbol{p}}$: update map.

Dependency and scientific reading

The ontology begins before distance and duration. A graph, lattice spacing, metric, field, and clock must therefore be outputs of a persistence/coarse-graining map, not silent inputs.

Author-control point. Decide whether the proto-state is a graph, hypergraph, causal order, tensor network, or another object. This choice controls every later derivation.

NEXT: The facing work-through states the assumptions, expands the algebra, checks dimensions, and names a failure condition.

Expanded sheet

F01-X

EXPANDED WORK-THROUGH

Relational proto-state

Foundations | Assumptions, derivation, dimensions, interpretation, falsifier

Assumptions used

A state space exists; admissibility is local; the parameter vector $\boldsymbol{p}$ is fixed; no background metric is used to define $U_{\boldsymbol{p}}$.

Expansion

Choose a finite alphabet Σ and a relational hypergraph H_n. A prototype state is $X_n = (H_n, s_n)$ with $s_n : V(H_n) \to \Sigma$. Locality means $[U(X)]_i$ depends only on a bounded neighbourhood $N_R(i)$. The history is then $\Gamma(X_0) = \{X_0, U(X_0), U^2(X_0), \ldots\}$. Geometry is absent until an observable on histories supplies an effective distance.

Dimensional and normalization check

All quantities on this sheet are dimensionless structural objects. Metres and seconds cannot appear until a metric and a clock map are defined.

Thought experiment

Imagine a game whose legal moves are known but whose board has not yet been drawn. Repeatedly compatible moves may eventually define which positions behave as neighbours; the board is inferred from play.

Failure condition. The foundation fails if the update requires a pre-existing metric that the theory later claims to derive, or if two inequivalent proto-state choices remain observationally unconstrained.

Back to compact sheet

F02

DEFINITION / CONDITIONAL

Ordered updates before time

Foundations | Compact equation map | Pair 02 of 55

Condensed equation chain

$$n \in \mathbb{Z}, \qquad X_{n+1} = U(X_n), \qquad t_K(n) = \sum_{m<n} \Delta t_K(X_m) \tag{66}$$

Symbols and types

n: ordering index; t_K: time read by clock pattern K; Δt_K: state-dependent tick duration.

Dependency and scientific reading

Update order is primitive; physical duration is operational. Relativistic time requires different clocks to agree in a common regime and to acquire the correct universal dilation when loaded or moving.

Author-control point. Specify the clock observable and whether capacity load changes its phase rate, rather than treating one update as one universal physical instant.

NEXT: The facing work-through states the assumptions, expands the algebra, checks dimensions, and names a failure condition.

Expanded sheet

F02-X

EXPANDED WORK-THROUGH

Ordered updates before time

Foundations | Assumptions, derivation, dimensions, interpretation, falsifier

Assumptions used

The update is deterministic; a persistent subsystem K has a repeatable cycle; cycle counting is insensitive to microscopic relabeling.

Expansion

Let $P_K(X_n) \in [0, 2\pi)$ be the phase of a clock pattern. Define a tick whenever the unwrapped phase increases by 2π. If $\Omega_K(X_n) = P_K(X_{n+1}) - P_K(X_n)$, then $\Delta t_K = \Omega_{K,0}^{-1}\Omega_K\,\delta t_0$ after choosing one reference. A universal time coordinate exists only if distinct clocks satisfy $t_K/t_L \to$ constant in the same low-load regime.

Dimensional and normalization check

n and phase are dimensionless. δt_0 is a calibration unless a dimensionful scale is independently generated.

Thought experiment

A flipbook has page order without seconds. A clock inside the flipbook counts a repeating motion; its reading can slow even while page numbers advance uniformly.

Failure condition. The proposal fails if different low-energy clocks do not converge to one operational time or if the predicted dilation depends on clock construction.

Back to compact sheet

F03

CONDITIONAL DERIVATION

Operational clock map

Foundations | Compact equation map | Pair 03 of 55

Condensed equation chain

$$\Theta_K(n) = \arg Z_K(X_n), \qquad N_K(n) = \frac{\operatorname{unwrap}\Theta_K(n)}{2\pi}, \qquad t_K = T_K N_K \tag{67}$$

Symbols and types

Z_K: complex clock observable; N_K: counted cycles; T_K: calibrated period.

Dependency and scientific reading

A usable clock is a stable limit cycle or quasiperiodic mode. The map separates microscopic ordering from the duration inferred by an internal observer.

Author-control point. Choose a concrete clock solution and tolerance. State how two separated clocks are synchronized without assuming the geometry being derived.

NEXT: The facing work-through states the assumptions, expands the algebra, checks dimensions, and names a failure condition.

Expanded sheet

F03-X

EXPANDED WORK-THROUGH

Operational clock map

Foundations | Assumptions, derivation, dimensions, interpretation, falsifier

Assumptions used

$Z_K \neq 0$ along the orbit; its phase is continuous after unwrapping; perturbations transverse to the clock orbit decay.

Expansion

For a periodic orbit $X_{n+N_0} = X_n$, define $Z_K(X_n) = A_K e^{i\Theta_K(n)}$. The monodromy matrix $M_K = \prod_{r=0}^{N_0-1} DU(X_{n+r})$ must have one neutral phase eigenvalue and all other relevant eigenvalues inside the unit circle. The counted time is robust when small perturbations change N_K only by a bounded phase error.

Dimensional and normalization check

N_K is dimensionless; T_K has units of time and remains a metrological bridge unless related to another predicted scale.

Thought experiment

A pendulum is not time; it is a stable process used to label duration. The same distinction applies to a repeating node pattern.

Failure condition. Failure occurs if no robust recurrent patterns exist, if their rates depend uncontrollably on microscopic details, or if synchronization requires superluminal coordination.

Back to compact sheet PAIR 03/55

F04

DEFINITION / TESTABLE

Persistence and identity across frames

Foundations | Compact equation map | Pair 04 of 55

Condensed equation chain

$$d_R(C_R X_{n+T},\, g\, C_R X_n) < \varepsilon, \qquad g \in \mathcal{G}_R, \qquad T \geq T_{\min} \tag{68}$$

Symbols and types

C_R: coarse-graining at resolution R; d_R: comparison metric; $\mathcal{G}_R$: allowed relabelings/motions; ε: identity tolerance.

Dependency and scientific reading

A node or particle candidate is a persistent equivalence class, not a primitive bead. The definition becomes physical only after $C_R, d_R, \mathcal{G}_R$ are fixed before searching the data.

Author-control point. Ryan can change the allowed equivalence group: translation only, translation plus phase, or topology-preserving deformation. Each choice changes the particle catalogue.

NEXT: The facing work-through states the assumptions, expands the algebra, checks dimensions, and names a failure condition.

Expanded sheet

F04-X

EXPANDED WORK-THROUGH

Persistence and identity across frames

Foundations | Assumptions, derivation, dimensions, interpretation, falsifier

Assumptions used

Coarse-graining is deterministic; equivalence transformations preserve declared observables; the persistence threshold is preregistered.

Expansion

Define $[X]_{R,\varepsilon} = \{Y : \inf_{g\in\mathcal{G}_R} d_R(C_R Y, gC_R X) < \varepsilon\}$. A pattern persists for T updates when its trajectory remains in this tube. A lifetime estimator is $\tau_R = \inf\{T : d_R(C_R X_{n+T}, \mathcal{G}_R C_R X_n) \geq \varepsilon\}$. Stable identities correspond to τ_R much larger than their internal period.

Dimensional and normalization check

d_R should be dimensionless or normalized by an explicit scale; T counts updates until a clock conversion is applied.

Thought experiment

A whirlpool keeps its identity although its water changes. END/MNT needs the mathematical equivalent of recognizing the whirlpool without deciding in advance where it must be.

Failure condition. The claim fails if persistence appears only after tuning the comparison metric to known particles or disappears under small changes of resolution.

Back to compact sheet

F05

CONDITIONAL CONSTRUCTION

Emergent weighted graph

Foundations | Compact equation map | Pair 05 of 55

Condensed equation chain

$$V_R = \{[X]_a\}, \qquad w_{ab} = \frac{1}{T}\sum_{n=1}^{T} I_{ab}(n), \qquad G_R = (V_R, E_R, w) \tag{69}$$

Symbols and types

I_{ab}: measured direct influence between persistent classes; w_{ab}: time-averaged link weight; E_R: links above a fixed threshold.

Dependency and scientific reading

The graph is inferred from stable influence, not drawn first. A fixed lattice remains a useful benchmark phase but cannot substitute for this emergence step.

Author-control point. Choose whether links encode causal influence, mutual information, transfer capacity, or action coupling. Mixing them would make the derived geometry ambiguous.

NEXT: The facing work-through states the assumptions, expands the algebra, checks dimensions, and names a failure condition.

Expanded sheet

F05-X

EXPANDED WORK-THROUGH

Emergent weighted graph

Foundations | Assumptions, derivation, dimensions, interpretation, falsifier

Assumptions used

Persistent classes have been identified; influence can be intervened on or computed causally; thresholds are fixed independently of desired dimension.

Expansion

For two persistent subsystems a, b, perturb a within the admissible set and measure $I_{ab}(n) = \|C_R X_n^{(a+\delta)} - C_R X_n\|_b / \|\delta\|$. Set $w_{ab} = \langle I_{ab} \rangle$ and retain (a, b) if $w_{ab} > w_{\min}$. Symmetry is not assumed: a directed graph is permitted until reciprocal low-energy propagation is demonstrated.

Dimensional and normalization check

Influence ratios are dimensionless. A physical link length requires a separate conversion function $\ell(w)$.

Thought experiment

Instead of placing dots on graph paper, tap one stable pattern and watch which others respond. The response network draws the effective neighbourhood.

Failure condition. Failure occurs if the inferred graph changes wildly with the probe, has no stable scale range, or produces influence links inconsistent with causal propagation.

Back to compact sheet

F06

CONDITIONAL DERIVATION

Graph distance and dimension

Foundations | Compact equation map | Pair 06 of 55

Condensed equation chain

$$\ell_{ab} = \ell_0 f(w_{ab}), \qquad d_G(a,b) = \min_{\gamma : a \to b} \sum_{e \in \gamma} \ell_e, \qquad d_s = -2 \frac{d \ln P(\sigma)}{d \ln \sigma} \tag{70}$$

Symbols and types

ℓ_{ab}: effective edge length; d_G: shortest-path distance; $P(\sigma)$: diffusion return probability; d_s: spectral dimension.

Dependency and scientific reading

A graph becomes spatial only if several independent dimension estimators stabilize and long-wave propagation is approximately isotropic.

Author-control point. The choice of $f(w)$ is a major vision point. It must be tied to dynamics or tested for universality across alternatives.

NEXT: The facing work-through states the assumptions, expands the algebra, checks dimensions, and names a failure condition.

Expanded sheet

F06-X

EXPANDED WORK-THROUGH

Graph distance and dimension

Foundations | Assumptions, derivation, dimensions, interpretation, falsifier

Assumptions used

$f(w) > 0$ is monotone and preregistered; the persistent graph has a scale window; diffusion is defined by its Laplacian.

Expansion

Choose $f(w) = w^{-1/2}$ as one declared hypothesis. The graph Laplacian $L = D - W$ generates diffusion $K(\sigma) = e^{-\sigma L}$. The average return probability is $P(\sigma) = |V|^{-1} \operatorname{Tr} K(\sigma)$. A plateau $d_s \approx 3$ over many scales is evidence for three spatial dimensions; it is not obtained by declaring the graph cubic.

Dimensional and normalization check

ℓ_0 carries length; f, P, and d_s are dimensionless. Without an independently fixed ℓ_0, only ratios of distances are predicted.

Thought experiment

A traveller knows geometry from the cheapest routes and the way random walks spread, not from labels printed on the vertices.

Failure condition. The spatial claim fails if dimension does not plateau, if different probes see different incompatible metrics, or if anisotropy exceeds observational bounds.

Back to compact sheet

F07

AXIOM / OPEN UPDATE LAW

Finite local transition capacity

Foundations | Compact equation map | Pair 07 of 55

Condensed equation chain

$$\mathcal{C}_i[X_n, X_{n+1}] = \frac{D_i}{D_{*,i}} \leq 1, \qquad D_i = \alpha|\Delta q_i|^2 + \beta \sum_j w_{ij}|\Delta q_i - \Delta q_j|^2 \tag{71}$$

Symbols and types

D_i: local transition demand; $D_{*,i}$: local capacity; $\alpha, \beta \geq 0$: declared weights.

Dependency and scientific reading

This local bound replaces older global sums that could require instantaneous accounting across the universe. The functional is illustrative until derived from the micro-state.

Author-control point. Decide whether capacity limits amplitude change, phase change, link rewiring, information transfer, action, or a weighted combination.

NEXT: The facing work-through states the assumptions, expands the algebra, checks dimensions, and names a failure condition.

Expanded sheet

F07-X

EXPANDED WORK-THROUGH

Finite local transition capacity

Foundations | Assumptions, derivation, dimensions, interpretation, falsifier

Assumptions used

Demand is nonnegative, neighbourhood-local, and computed from the same update variables; capacities are finite and not retuned per phenomenon.

Expansion

The admissible set is $\mathfrak{A} = \{(X_n, X_{n+1}) : \mathcal{C}_i \leq 1\ \forall i\}$. If the unconstrained proposal is $Y = F(X_n, X_{n-1})$, a limiter must map Y into $\mathfrak{A}$ using only local information. A componentwise rescaling is easy to write but may violate conservation; a successful rule must prove both invariance of $\mathfrak{A}$ and the intended conserved charges.

Dimensional and normalization check

$D_i/D_{*,i}$ is dimensionless. If D_i is energy, every term must share energy units and D_* cannot be silently set from a target constant.

Thought experiment

Each intersection can process only finite traffic per tick. Congestion changes nearby motion without consulting a universal traffic accountant.

Failure condition. The axiom fails physically if no local rule preserves it, if it breaks established conservation laws, or if saturation effects are already excluded experimentally.

Back to compact sheet

F08

REQUIRED COMPLETION GATE

Admissible deterministic update

Foundations | Compact equation map | Pair 08 of 55

Condensed equation chain

$$(X_{n+1}, X_n) = \mathbb{U}_{\boldsymbol{p}}(X_n, X_{n-1}), \qquad \mathbb{U}(\mathfrak{A}) \subseteq \mathfrak{A}, \qquad Q[X_{n+1}, X_n] = Q[X_n, X_{n-1}] \tag{72}$$

Symbols and types

$\mathbb{U}$: second-order state update; $\mathfrak{A}$: capacity-admissible set; Q: conserved charge or controlled Lyapunov function.

Dependency and scientific reading

A final END/MNT model needs one immutable map satisfying locality, determinism, capacity preservation, stability, and declared conservation.

Author-control point. This is the main author decision. Replace the illustrative limiter with the unique rule that best matches Ryan's intended progression mechanism.

NEXT: The facing work-through states the assumptions, expands the algebra, checks dimensions, and names a failure condition.

Expanded sheet

F08-X

EXPANDED WORK-THROUGH

Admissible deterministic update

Foundations | Assumptions, derivation, dimensions, interpretation, falsifier

Assumptions used

Initial data lie in $\mathfrak{A}$; boundary conditions are specified; every branch and tie-break is deterministic.

Expansion

Prove closure by assuming $(X_n, X_{n-1}) \in \mathfrak{A}$, evaluating the local proposal, and showing each output demand remains bounded. Prove determinism by showing the right-hand side is single-valued. Prove conservation directly, $Q_{n+1} - Q_n = 0$, or controlled dissipation, $Q_{n+1} \leq Q_n$. These are separate obligations; none follows from the word deterministic.

Dimensional and normalization check

$\mathbb{U}$ maps like-dimensioned states. Every parameter in $\boldsymbol{p}$ requires a declared unit or dimensionless normalization.

Thought experiment

A rulebook is not complete if it tells players what is forbidden but not which legal move happens next.

Failure condition. END/MNT remains an ontology rather than complete microphysics until this map is supplied and its closure and stability are proved.

Back to compact sheet

D01

PROVED WITHIN BENCHMARK

Discrete graph action

Benchmark dynamics | Compact equation map | Pair 09 of 55

Condensed equation chain

$$S_d = \sum_n \delta\tau \left[\frac{\mu}{2} \sum_i \left(\frac{q_i^{n+1} - q_i^n}{\delta\tau} \right)^2 - \frac{\kappa}{2} \sum_{(ij)} w_{ij} (q_i^n - q_j^n)^2 - \sum_i V(q_i^n) \right] \tag{73}$$

Symbols and types

q_i^n: scalar node coordinate; μ: inertia; κ: link stiffness; V: onsite potential.

Dependency and scientific reading

This is the calculable benchmark underlying the exact spectrum and stability proofs. It is not claimed to be the unique microscopic action.

Author-control point. Ryan can replace the scalar coordinate, potential, or fixed graph, but doing so changes the spectrum and requires new proofs.

NEXT: The facing work-through states the assumptions, expands the algebra, checks dimensions, and names a failure condition.

Expanded sheet

D01-X

EXPANDED WORK-THROUGH

Discrete graph action

Benchmark dynamics | Assumptions, derivation, dimensions, interpretation, falsifier

Assumptions used

The effective graph is fixed during the phase studied; weights are symmetric and nonnegative; boundary terms are controlled.

Expansion

Write $L_n = T_n - U_n$ with $T_n = \mu \sum_i (\Delta_t q_i^n)^2/2$ and $U_n = \kappa \sum_{(ij)} w_{ij}(q_i - q_j)^2/2 + \sum_i V(q_i)$. Vary q_i^n while holding endpoints fixed. Contributions from T_n and T_{n-1} yield the centered second difference; link variations yield the graph Laplacian.

Dimensional and normalization check

Every term in brackets has energy units; multiplication by $\delta\tau$ gives action. Thus $[\kappa q^2] = [V] = E$ and $[\mu q^2/\delta\tau^2] = E$.

Thought experiment

Think of weighted masses connected by springs, with each mass also feeling a local potential. The analogy makes the benchmark transparent without asserting literal springs in nature.

Failure condition. The benchmark cannot represent nature if its continuum modes, symmetries, or nonlinear solutions disagree with observation after parameters are frozen.

Back to compact sheet

D02

PROVED WITHIN BENCHMARK

Discrete Euler–Lagrange update

Benchmark dynamics | Compact equation map | Pair 10 of 55

Condensed equation chain

$$q_i^{n+1} = 2q_i^n - q_i^{n-1} - \frac{\delta\tau^2}{\mu}\left[V'(q_i^n) + \kappa \sum_j w_{ij}(q_i^n - q_j^n)\right] \tag{74}$$

Symbols and types

V': onsite restoring force; $\sum_j w_{ij}(q_i - q_j) = (L_G q)_i$: graph Laplacian.

Dependency and scientific reading

The update is explicit: two consecutive configurations determine the third wherever V' is defined.

Author-control point. If Ryan's vision uses first-order progression, irreversible selection, or changing topology, this second-order reversible update must be replaced or embedded.

NEXT: The facing work-through states the assumptions, expands the algebra, checks dimensions, and names a failure condition. **Expanded sheet**

D02-X

EXPANDED WORK-THROUGH

Discrete Euler–Lagrange update

Benchmark dynamics | Assumptions, derivation, dimensions, interpretation, falsifier

Assumptions used

$V \in C^1$; $\mu \neq 0$; weights and timestep are fixed; initial slices q^0, q^1 are supplied.

Expansion

The discrete stationarity condition is $\partial L_n/\partial q_i^n + \partial L_{n-1}/\partial q_i^n = 0$. The kinetic terms give $\mu(2q_i^n - q_i^{n+1} - q_i^{n-1})/\delta\tau^2$. The potential gives $-V'(q_i^n)$, and the link term gives $-\kappa(L_G q^n)_i$. Rearrangement produces the displayed recursion.

Dimensional and normalization check

The bracket has force units in generalized coordinates; multiplying by $\delta\tau^2/\mu$ returns the units of q.

Thought experiment

Knowing a pendulum's position on two adjacent frames fixes its next benchmark position. Determinism here is algebraic, not philosophical.

Failure condition. The proposition fails if V' is multivalued, if the limiter introduces ambiguous branches, or if allowed initial data cause finite-step blow-up.

Back to compact sheet

D03

EXACT IDENTITY

Weighted graph Laplacian

Benchmark dynamics | Compact equation map | Pair 11 of 55

Condensed equation chain

$$(L_G q)_i = \sum_j w_{ij}(q_i - q_j), \qquad L_G = D - W, \qquad q^T L_G q = \frac{1}{2}\sum_{ij} w_{ij}(q_i - q_j)^2 \geq 0 \tag{75}$$

Symbols and types

$W = (w_{ij})$: adjacency weights; $D_{ii} = \sum_j w_{ij}$: degree matrix; L_G: Laplacian.

Dependency and scientific reading

Positive semidefiniteness supplies mode stability and orders spatial eigenmodes. The zero modes encode connected components.

Author-control point. Choose combinatorial, normalized, or covariant Laplacians deliberately. Their spectra and continuum measures are not interchangeable.

NEXT: The facing work-through states the assumptions, expands the algebra, checks dimensions, and names a failure condition.

Expanded sheet

D03-X

EXPANDED WORK-THROUGH

Weighted graph Laplacian

Benchmark dynamics | Assumptions, derivation, dimensions, interpretation, falsifier

Assumptions used

Weights are symmetric and nonnegative. Directed or signed interactions require a different operator and proof.

Expansion

Expand $q^T L_G q = \sum_i d_i q_i^2 - \sum_{ij} w_{ij} q_i q_j$. Symmetry permits regrouping into $\frac{1}{2}\sum_{ij} w_{ij}(q_i - q_j)^2$. Every summand is nonnegative. Hence eigenvalues satisfy $\lambda_a \geq 0$; $L_G \mathbf{1} = 0$ on each connected component.

Dimensional and normalization check

If w has stiffness units, $L_G q$ inherits them; in the normalized spectral analysis w is dimensionless and κ carries stiffness.

Thought experiment

A perfectly synchronized network has no link disagreement, so the Laplacian sees it as a zero mode.

Failure condition. A claimed positive spectrum fails if negative or asymmetric weights are introduced without replacing the quadratic-form argument.

Back to compact sheet

D04

PROVED WITHIN BENCHMARK

Deterministic recursion theorem

Benchmark dynamics | Compact equation map | Pair 12 of 55

Condensed equation chain

$$(q^0, q^1) \mapsto q^2 \mapsto \cdots \mapsto q^N, \qquad q^{n+1} = F_{\boldsymbol{p}}(q^n, q^{n-1}) \tag{76}$$

Symbols and types

$F_{\boldsymbol{p}}$: explicit update function determined by graph, timestep, potential, and fixed parameters.

Dependency and scientific reading

Uniqueness is by induction. This proves determinism for the benchmark, not empirical adequacy or quantum statistics.

Author-control point. If stochasticity is part of Ryan's intended ontology, move it into the declared state or transition law rather than hiding it in unspecified tie-breaking.

NEXT: The facing work-through states the assumptions, expands the algebra, checks dimensions, and names a failure condition. **Expanded sheet**

D04-X

EXPANDED WORK-THROUGH

Deterministic recursion theorem

Benchmark dynamics | Assumptions, derivation, dimensions, interpretation, falsifier

Assumptions used

All parameters, boundary conditions, and initial data are fixed; F is single-valued on its domain.

Expansion

Base step: (q^0, q^1) determines $q^2 = F(q^1, q^0)$. Inductive step: if (q^{n-1}, q^n) is unique, then applying the same single-valued F yields a unique q^{n+1}. Therefore the finite history is unique until an output leaves the domain. Existence for all n additionally requires an invariant bounded domain or an a priori estimate.

Dimensional and normalization check

This is a structural statement; dimensions enter only through the well-typed definition of F.

Thought experiment

A deterministic recipe can still cook an unstable meal. Uniqueness and physical acceptability are different tests.

Failure condition. Global determinism fails if the orbit reaches a singularity, if topology updates have unresolved ties, or if a projection has multiple minimizers.

Back to compact sheet

D05

CONDITIONAL / NUMERICALLY TESTABLE

Discrete energy ledger

Benchmark dynamics | Compact equation map | Pair 13 of 55

Condensed equation chain

$$E^n = \frac{\mu}{2}\sum_i \left(\frac{q_i^{n+1} - q_i^n}{\delta\tau}\right)^2 + \frac{\kappa}{2}\sum_{(ij)} w_{ij}(q_i^n - q_j^n)^2 + \sum_i V(q_i^n) \tag{77}$$

Symbols and types

E^n: benchmark energy proxy evaluated on a staggered discrete slice.

Dependency and scientific reading

The continuum action has a conserved energy under time translation. A simple finite-difference update generally conserves a nearby modified energy, not necessarily this expression exactly.

Author-control point. Choose whether exact discrete energy conservation is mandatory. If so, use a variational/symplectic rule and redo the capacity limiter consistently.

NEXT: The facing work-through states the assumptions, expands the algebra, checks dimensions, and names a failure condition. **Expanded sheet**

D05-X

EXPANDED WORK-THROUGH

Discrete energy ledger

Benchmark dynamics | Assumptions, derivation, dimensions, interpretation, falsifier

Assumptions used

Graph and parameters are update-independent; V has no explicit n; boundary flux vanishes.

Expansion

Multiply the update equation by $(q_i^{n+1} - q_i^{n-1})/(2\delta\tau)$ and sum over nodes. The kinetic term telescopes exactly. Quadratic link and onsite terms telescope under a midpoint or variational integrator; for the explicit central scheme, the remainder is $O(\delta\tau^2)$ per smooth cycle. This identifies the correct numerical diagnostic and motivates a symplectic implementation.

Dimensional and normalization check

Every contribution is energy. A capacity ledger becomes physical energy only after its normalization is matched to this conserved generator.

Thought experiment

A nearly frictionless clock keeps trading kinetic and potential energy. Numerical drift indicates the update rule, not new physics.

Failure condition. The benchmark implementation fails if energy drift does not converge away with timestep refinement or if the limiter injects untracked energy.

Back to compact sheet PAIR 13/55

D06

ILLUSTRATIVE / NOT FINAL

Local proposal limiter

Benchmark dynamics | Compact equation map | Pair 14 of 55

Condensed equation chain

$$y_i^{n+1} = F_i(q^n, q^{n-1}), \quad s_i = \min\left(1, \sqrt{\frac{D_{*,i}}{D_i[y]}}\right), \quad q_i^{n+1} = q_i^n + s_i(y_i^{n+1} - q_i^n) \tag{78}$$

Symbols and types

y: unconstrained proposal; s_i: local scale factor; q^{n+1}: limited update.

Dependency and scientific reading

This demonstrates one way to impose bounded change, but independently scaling neighbouring proposals can spoil reciprocity and conservation.

Author-control point. Treat this formula as a placeholder. Replace it if Ryan intends deferred change, redistribution, or queueing rather than simple amplitude scaling.

NEXT: The facing work-through states the assumptions, expands the algebra, checks dimensions, and names a failure condition.

Expanded sheet

D06-X

EXPANDED WORK-THROUGH

Local proposal limiter

Benchmark dynamics | Assumptions, derivation, dimensions, interpretation, falsifier

Assumptions used

D_i is quadratic and local; $D_{*,i} > 0$; all neighbours needed for the scale are available causally.

Expansion

If $D_i[y] \le D_*$, set $s_i = 1$. Otherwise quadratic homogeneity gives $D_i[q + s_i(y - q)] \approx s_i^2 D_i[y] = D_*$. Exact closure fails when D_i also contains neighbour updates with different s_j. A coupled local solve or flux-based limiter is then required.

Dimensional and normalization check

The ratio D_*/D_i is dimensionless, so s_i is dimensionless and the limited increment has the same units as q.

Thought experiment

Slowing one car at an intersection can create a mismatch with traffic entering from the next intersection; a local cap needs compatible flux accounting.

Failure condition. The limiter is rejected if a counterexample violates $\mathcal{C}_i \le 1$, breaks a required charge, or creates nonlocal dependence through iteration.

Back to compact sheet

D07

CANDIDATE CONSTRUCTION

Capacity projection

Benchmark dynamics | Compact equation map | Pair 15 of 55

Condensed equation chain

$$q^{n+1} = \arg\min_{z\in\mathfrak{A}(q^n)} \frac{1}{2}\|z - y^{n+1}\|_M^2, \qquad \mathfrak{A} = \{z : D_i(q^n, z) \leq D_{*,i}\ \forall i\} \tag{79}$$

Symbols and types

M: positive metric on proposals; $\mathfrak{A}$: convex admissible set when each D_i is convex.

Dependency and scientific reading

Projection gives a mathematically clean capacity-preserving update, but a global minimization would conflict with strict microscopic locality.

Author-control point. Choose between exact projection, iterative local projection, or flux redistribution. The choice expresses what 'deferred progression' means operationally.

NEXT: The facing work-through states the assumptions, expands the algebra, checks dimensions, and names a failure condition.

Expanded sheet

D07-X

EXPANDED WORK-THROUGH

Capacity projection

Benchmark dynamics | Assumptions, derivation, dimensions, interpretation, falsifier

Assumptions used

$M \succ 0$; $\mathfrak{A}$ is nonempty, closed, and convex; a local decomposition or finite message radius is supplied.

Expansion

Existence follows from closedness and coercivity; uniqueness follows from strict convexity. Introduce multipliers $\lambda_i \geq 0$ and solve $M(z-y)+\sum_i \lambda_i \nabla D_i = 0$, with complementary slackness $\lambda_i(D_i - D_{*,i}) = 0$. A physically acceptable version must show that this system factorizes locally or is itself generated by causal micro-updates.

Dimensional and normalization check

The norm and constraints compare like-dimensioned increments; multipliers carry the reciprocal units of the constraint functional.

Thought experiment

Finding the nearest legal move is unambiguous, but asking the whole universe to agree on it at once would reintroduce the global accountant.

Failure condition. Reject the construction if uniqueness fails, if convergence requires unbounded communication, or if projected dynamics erase the desired reversible limit.

Back to compact sheet

D08

CONDITIONAL DERIVATION

Continuum scaling

Benchmark dynamics | Compact equation map | Pair 16 of 55

Condensed equation chain

$$x = ia, \quad t = n\delta\tau, \quad \frac{q_i^{n+1} - 2q_i^n + q_i^{n-1}}{\delta\tau^2} \to \partial_t^2\phi, \quad \frac{q_{i+1} - 2q_i + q_{i-1}}{a^2} \to \partial_x^2\phi \tag{80}$$

Symbols and types

a: regular-phase spacing; $\delta\tau$: update interval; $\phi(x,t)$: smooth interpolation.

Dependency and scientific reading

The limit is a theorem only after a family of refinements and convergence norm are declared. Taylor expansion supplies the formal target.

Author-control point. Ryan must decide whether $a \to 0$ is a mathematical refinement, a physical lattice spacing, or both. These interpretations are not equivalent.

NEXT: The facing work-through states the assumptions, expands the algebra, checks dimensions, and names a failure condition.

Expanded sheet

D08-X

EXPANDED WORK-THROUGH

Continuum scaling

Benchmark dynamics | Assumptions, derivation, dimensions, interpretation, falsifier

Assumptions used

The field is smooth on scales $a, \delta\tau$; ratios are scaled so $c_*^2 = \kappa a^2/\mu$ remains finite.

Expansion

Taylor expand $\phi(x, t \pm \delta\tau) = \phi \pm \delta\tau\phi_t + \delta\tau^2\phi_{tt}/2 + O(\delta\tau^3)$ and similarly in space. Substitution yields $\phi_{tt} - c_*^2\nabla^2\phi + \mu^{-1}V'(\phi) = O(a^2 + \delta\tau^2)$. Convergence additionally needs stability and consistent initial/boundary data.

Dimensional and normalization check

$c_*^2 = \kappa a^2/\mu$ has units length^2/time^2; the remainder has the same field-acceleration units as the leading equation.

Thought experiment

Pixels become a smooth picture only when you step back and when the update does not amplify pixel-scale errors.

Failure condition. The continuum claim fails if refinement changes observables without convergence, if anisotropic terms persist, or if additional modes remain at low energy.

Back to compact sheet PAIR 16/55

S01

EXACT ON REGULAR LATTICE

Plane-wave eigenmodes

Spectrum and stability | Compact equation map | Pair 17 of 55

Condensed equation chain

$$q_{\boldsymbol{r}}^{n} = Ae^{i(\boldsymbol{k}\cdot\boldsymbol{r}-\omega n\delta\tau)}, \qquad L_G q = \lambda(\boldsymbol{k})q, \qquad \lambda(\boldsymbol{k}) = 4\sum_{a=1}^{d}\sin^2\frac{k_a a}{2} \tag{81}$$

Symbols and types

$\boldsymbol{k}$: lattice wave vector; ω: angular frequency; λ: Laplacian eigenvalue.

Dependency and scientific reading

Translation invariance diagonalizes the free update in Fourier modes. Irregular graphs use Laplacian eigenvectors instead of plane waves.

Author-control point. If Ryan's fundamental graph is irregular or evolving, plane waves are benchmark diagnostics, not universal microstates.

NEXT: The facing work-through states the assumptions, expands the algebra, checks dimensions, and names a failure condition.

Expanded sheet

S01-X

EXPANDED WORK-THROUGH

Plane-wave eigenmodes

Spectrum and stability | Assumptions, derivation, dimensions, interpretation, falsifier

Assumptions used

Regular periodic lattice; quadratic onsite potential; amplitudes small enough to neglect nonlinear mode coupling.

Expansion

Apply a one-step shift: $q_{\boldsymbol{r}\pm a\hat{e}_j} = q_{\boldsymbol{r}} e^{\pm ik_j a}$. The nearest-neighbour difference gives $2 - e^{ik_j a} - e^{-ik_j a} = 4\sin^2(k_j a/2)$. Summing directions yields $\lambda(\boldsymbol{k})$. Time shifts similarly yield $-4\sin^2(\omega\delta\tau/2)/\delta\tau^2$.

Dimensional and normalization check

ka and $\omega\delta\tau$ are dimensionless; λ is dimensionless when weights are.

Thought experiment

A repeating wallpaper pattern is unchanged by translation except for a phase. That makes it a natural vibration mode of a regular lattice.

Failure condition. The plane-wave result does not apply when disorder, topology change, or strong nonlinearity couples modes faster than they propagate.

Back to compact sheet

S02

PROVED WITHIN BENCHMARK

Exact lattice dispersion

Spectrum and stability | Compact equation map | Pair 18 of 55

Condensed equation chain

$$\frac{4\mu}{\delta\tau^2}\sin^2\frac{\omega\delta\tau}{2} = m_0^2 + 4\kappa\sum_{a=1}^{d}\sin^2\frac{k_a a}{2} \tag{82}$$

Symbols and types

$m_0^2 = V''(0)$: onsite curvature; remaining symbols as in the benchmark.

Dependency and scientific reading

This exact relation is one of the strongest internal results. It predicts benchmark frequencies once microscopic parameters are fixed.

Author-control point. This dispersion belongs to the scalar benchmark. Do not attach photons, Higgs modes, or gravitons to branches without deriving their symmetries and couplings.

NEXT: The facing work-through states the assumptions, expands the algebra, checks dimensions, and names a failure condition. **Expanded sheet**

S02-X

EXPANDED WORK-THROUGH

Exact lattice dispersion

Spectrum and stability | Assumptions, derivation, dimensions, interpretation, falsifier

Assumptions used

Linearization about $q = 0$; regular lattice; stable real-frequency branch.

Expansion

Insert the plane wave into $\mu\Delta_t^2 q + m_0^2 q + \kappa L_G q = 0$. Divide by the nonzero amplitude. Use the spatial and temporal shift identities from S01. The resulting equality is exact at finite a and $\delta\tau$; no continuum approximation has been taken.

Dimensional and normalization check

Both sides have energy per q^2, equivalently generalized inertia per time squared. The sine arguments are dimensionless.

Thought experiment

A discrete guitar string has a real, testable pitch curve; high notes reveal the spacing because they bend away from the continuum relation.

Failure condition. The chosen parameter set fails if any resolved benchmark simulation disagrees with this curve beyond numerical error.

Back to compact sheet PAIR 18/55

S03

PROVED ASYMPTOTICALLY

Long-wavelength expansion

Spectrum and stability | Compact equation map | Pair 19 of 55

Condensed equation chain

$$\omega^2 = \omega_0^2 + c_*^2 k^2 - \frac{c_*^2 a^2}{12} \sum_a k_a^4 + \frac{\delta\tau^2}{12}(\omega_0^2 + c_*^2 k^2)^2 + \cdots \tag{83}$$

Symbols and types

$\omega_0^2 = m_0^2/\mu$; $c_*^2 = \kappa a^2/\mu$.

Dependency and scientific reading

The leading terms resemble a massive relativistic scalar. The quartic corrections expose preferred lattice structure and become experimental targets only after the physical map is fixed.

Author-control point. Ryan can use this correction as a falsifiable signature only after fixing whether the lattice is fundamental and determining the physical a.

NEXT: The facing work-through states the assumptions, expands the algebra, checks dimensions, and names a failure condition.

Expanded sheet

S03-X

EXPANDED WORK-THROUGH

Long-wavelength expansion

Spectrum and stability | Assumptions, derivation, dimensions, interpretation, falsifier

Assumptions used

$|k_a a| \ll 1$, $|\omega\delta\tau| \ll 1$; the branch is analytic near the origin.

Expansion

Use $4\sin^2(x/2) = x^2 - x^4/12 + O(x^6)$ on both sides of S02. First solve the quadratic order, $\omega^2 = \omega_0^2 + c_*^2 k^2$. Reinsert it into the temporal quartic term to obtain the displayed correction. Spatial anisotropy appears through $\sum k_a^4$, not merely k^4.

Dimensional and normalization check

Every term has units time^{-2}. The correction coefficients include the explicit powers of a or $\delta\tau$ required by dimensions.

Thought experiment

Long ocean waves ignore individual water molecules; short ripples reveal microscopic structure. A lattice likewise hides at long wavelength and reappears at high momentum.

Failure condition. A fundamental regular lattice is excluded if the induced anisotropy or energy-dependent propagation exceeds observational bounds at its fixed scale.

Back to compact sheet

S04

CONDITIONAL BENCHMARK RESULT

Group velocity and causal cone

Spectrum and stability | Compact equation map | Pair 20 of 55

Condensed equation chain

$$v_{g,a} = \frac{\partial \omega}{\partial k_a} = \frac{\kappa a \delta\tau \, \sin(k_a a)}{\mu \sin(\omega \delta\tau)}, \qquad |v_g| \to c_* \text{ for } m_0, k \to 0 \tag{84}$$

Symbols and types

v_g: wave-packet group velocity; c_*: scalar low-energy limiting speed.

Dependency and scientific reading

A finite signal cone requires more than group velocity: locality bounds the earliest influence, while dispersion controls packet motion.

Author-control point. Decide whether capacity, nearest-neighbour locality, or both define the ultimate cone. They need not yield the same speed.

NEXT: The facing work-through states the assumptions, expands the algebra, checks dimensions, and names a failure condition.

Expanded sheet

S04-X

EXPANDED WORK-THROUGH

Group velocity and causal cone

Spectrum and stability | Assumptions, derivation, dimensions, interpretation, falsifier

Assumptions used

Differentiate on a real stable branch; packets are narrow in $\boldsymbol{k}$; the update is nearest-neighbour local.

Expansion

Implicitly differentiate S02. The temporal derivative gives $(2\mu/\delta\tau)\sin(\omega\delta\tau)\,\partial\omega/\partial k_a$. The spatial derivative gives $2\kappa a\sin(k_a a)$. Their ratio yields the expression. In the long-wave massless limit, both sines linearize and the ratio approaches $a\sqrt{\kappa/\mu} = c_*$.

Dimensional and normalization check

The result has units length/time. The SI value of c is a calibration unless $a, \delta\tau, \kappa/\mu$ are independently fixed.

Thought experiment

A stadium wave travels much slower than any spectator can react. Pattern speed and microscopic influence speed must be distinguished.

Failure condition. Universal relativity fails if different low-energy species approach different limiting speeds or if information outruns the claimed cone.

Back to compact sheet

S05

PROVED FOR LINEAR BENCHMARK

Courant stability domain

Spectrum and stability | Compact equation map | Pair 21 of 55

Condensed equation chain

$$0 \le \frac{\delta\tau^2}{\mu}\left(m_0^2 + \kappa\lambda_a\right) \le 4 \quad \forall a, \qquad \delta\tau^2 \le \frac{4\mu}{m_0^2 + \kappa\lambda_{\max}} \tag{85}$$

Symbols and types

λ_a: graph-Laplacian eigenvalues; $\lambda_{\max}$: largest eigenvalue.

Dependency and scientific reading

The condition keeps every linear mode on the unit circle. It is necessary for the explicit update and does not prove nonlinear stability.

Author-control point. If one update is fundamental rather than numerical, the inequality becomes a constraint on allowed microscopic parameters.

NEXT: The facing work-through states the assumptions, expands the algebra, checks dimensions, and names a failure condition.

Expanded sheet

S05-X

EXPANDED WORK-THROUGH

Courant stability domain

Spectrum and stability | Assumptions, derivation, dimensions, interpretation, falsifier

Assumptions used

$\mu > 0$, $m_0^2 \geq 0$, $L_G \succeq 0$; modes decouple linearly.

Expansion

For eigenmode amplitude z_n, write $z_{n+1} - 2z_n + z_{n-1} + \Omega_a^2 \delta\tau^2 z_n = 0$. The characteristic roots satisfy $r^2 - (2 - \Omega_a^2 \delta\tau^2)r + 1 = 0$. Both roots have modulus one exactly when $|2 - \Omega_a^2 \delta\tau^2| \leq 2$, giving $0 \leq \Omega_a^2 \delta\tau^2 \leq 4$.

Dimensional and normalization check

$\Omega_a^2 \delta\tau^2$ is dimensionless. The bound is therefore unit invariant.

Thought experiment

Taking time steps too large makes a perfectly stable spring explode in a simulation. That is numerical instability, not exotic physics.

Failure condition. Reject a proposed parameter set if it violates the bound or if nonlinear runs show nonconvergent growth inside the nominal linear domain.

Back to compact sheet

S06

CONDITIONAL PHYSICAL INTERPRETATION

Mass gap

Spectrum and stability | Compact equation map | Pair 22 of 55

Condensed equation chain

$$\Delta E = \hbar_{\text{eff}}\omega(\mathbf{0}), \qquad \omega(\mathbf{0}) = \frac{2}{\delta\tau}\arcsin\left(\frac{m_0\delta\tau}{2\sqrt{\mu}}\right), \qquad m_{\text{eff}} = \frac{\Delta E}{c_*^2} \tag{86}$$

Symbols and types

ΔE: lowest excitation energy; $\hbar_{\text{eff}}$: action–phase conversion; m_{eff}: relativistic interpretation.

Dependency and scientific reading

The benchmark has a spectral gap. Calling it a particle mass additionally requires quantization/statistics, stability, coupling, and a universal relativistic sector.

Author-control point. Use 'mass gap' for the proven spectral property and reserve particle names until representation labels and scattering behavior are derived.

NEXT: The facing work-through states the assumptions, expands the algebra, checks dimensions, and names a failure condition. **Expanded sheet**

S06-X

EXPANDED WORK-THROUGH

Mass gap

Spectrum and stability | Assumptions, derivation, dimensions, interpretation, falsifier

Assumptions used

The stable branch exists; an effective energy quantum is justified; c_* is the universal low-energy speed.

Expansion

Set $\boldsymbol{k} = 0$ in S02 and solve for ω. If a normalized excitation carries energy $\hbar_{\text{eff}}\omega$, the rest-energy relation defines an effective mass. None of the three dimensional bridges $\hbar_{\text{eff}}, \delta\tau, c_*$ is predicted numerically by the current ontology.

Dimensional and normalization check

$\hbar\omega$ is energy; division by speed squared gives mass. Omitting $\hbar$ or inserting a measured frequency would be circular.

Thought experiment

A bell can have a lowest pitch, but that alone does not make the pitch an electron. Identity comes from the full pattern and its interactions.

Failure condition. The particle interpretation fails if the excitation decays immediately, lacks the required spin/charge, or depends on calibration to the target mass.

Back to compact sheet

S07

PERTURBATIVE BENCHMARK RESULT

Nonlinear frequency shift

Spectrum and stability | Compact equation map | Pair 23 of 55

Condensed equation chain

$$V(q) = \frac{1}{2}m_0^2 q^2 + \frac{\lambda}{4}q^4, \qquad \omega(A) = \omega_0\left[1 + \frac{3\lambda A^2}{8m_0^2} + O(A^4)\right] \tag{87}$$

Symbols and types

A: oscillation amplitude; λ: quartic coupling; $\omega_0 = m_0/\sqrt{\mu}$ in the continuum-time limit.

Dependency and scientific reading

Nonlinearity produces amplitude-dependent clocks and resonances. It does not by itself predict a particle spectrum.

Author-control point. Ryan can interpret load-dependent ticking through this mechanism, but must show universality and the correct relativistic/gravitational form.

NEXT: The facing work-through states the assumptions, expands the algebra, checks dimensions, and names a failure condition. **Expanded sheet**

S07-X

EXPANDED WORK-THROUGH

Nonlinear frequency shift

Spectrum and stability | Assumptions, derivation, dimensions, interpretation, falsifier

Assumptions used

Single weakly excited mode; $|\lambda A^2/m_0^2| \ll 1$; mode coupling and lattice-time corrections are negligible.

Expansion

Insert $q = A\cos\omega t + B\cos 3\omega t + \cdots$ into $\mu\ddot{q} + m_0^2 q + \lambda q^3 = 0$. Use $\cos^3 x = (3\cos x + \cos 3x)/4$. Cancel the resonant $\cos\omega t$ coefficient to obtain $\mu\omega^2 = m_0^2 + 3\lambda A^2/4$, then expand the square root.

Dimensional and normalization check

$\lambda A^2/m_0^2$ is dimensionless. Each term in the equation has generalized force units.

Thought experiment

A stiffening guitar string plays slightly sharp when plucked harder. That observable shift reveals nonlinearity without inventing a new constant.

Failure condition. Reject the approximation outside its small-amplitude regime or if observed clock shifts depend on composition contrary to the equivalence principle.

Back to compact sheet

S08

OPEN EXISTENCE PROBLEM

Localized nonlinear modes

Spectrum and stability | Compact equation map | Pair 24 of 55

Condensed equation chain

$$q_i^n = Q_i \cos(\Omega n \delta\tau) + \cdots, \qquad -\mu\Omega^2 Q + \kappa L_G Q + m_0^2 Q + \lambda Q^{\circ 3} = 0, \qquad \sum_i |Q_i|^2 < \infty \tag{88}$$

Symbols and types

Q: localized profile; $Q^{\circ 3}$: componentwise cube; Ω: internal frequency.

Dependency and scientific reading

Stable localized solutions are the shortest mathematical bridge from node dynamics to particle-like persistence.

Author-control point. Choose whether particle candidates are breathers, solitons, topological defects, knots, or invariant subspaces. This is a major vision branch.

NEXT: The facing work-through states the assumptions, expands the algebra, checks dimensions, and names a failure condition. **Expanded sheet**

S08-X

EXPANDED WORK-THROUGH

Localized nonlinear modes

Spectrum and stability | Assumptions, derivation, dimensions, interpretation, falsifier

Assumptions used

A nonlinear potential supports self-focusing or topological trapping; the frequency lies outside the linear radiation band; boundary effects are controlled.

Expansion

Insert the harmonic ansatz into the nonlinear update and retain the fundamental harmonic, producing the displayed nonlinear eigenproblem. Continue solutions from an anti-continuum limit $\kappa = 0$ or solve by Newton iteration. Linearize the full update around the periodic orbit and compute Floquet multipliers; spectral stability requires all non-symmetry multipliers to remain on or within the unit circle under the chosen convention.

Dimensional and normalization check

Every term in the eigenproblem has generalized force units; localization length is measured in graph units until a is fixed.

Thought experiment

A localized stadium pattern must keep recreating itself without radiating away. Existence is not enough; it must also survive small kicks and collisions.

Failure condition. The route fails if no stable localized sector exists over an open parameter region or if all candidates require target-specific tuning.

Back to compact sheet

G01

DEFINITION / BENCHMARK EXTENSION

Complex node field

Gauge and phase | Compact equation map | Pair 25 of 55

Condensed equation chain

$$\psi_i = \rho_i e^{i\theta_i}, \qquad \rho_i \geq 0, \quad \theta_i \sim \theta_i + 2\pi, \qquad |\psi_i|^2 = \rho_i^2 \tag{89}$$

Symbols and types

ρ_i: amplitude; θ_i: compact phase; ψ_i: complex node coordinate.

Dependency and scientific reading

Amplitude and phase separate persistence strength from relational phase information. Probability is not implied until an ensemble/measurement map is derived.

Author-control point. Clarify whether phase is fundamental, emerges from a two-component real state, or labels cyclic progression. Each ontology leads to different constraints.

NEXT: The facing work-through states the assumptions, expands the algebra, checks dimensions, and names a failure condition.

Expanded sheet

G01-X

EXPANDED WORK-THROUGH

Complex node field

Gauge and phase | Assumptions, derivation, dimensions, interpretation, falsifier

Assumptions used

The state supports a compact $U(1)$-like phase; observables are invariant under allowed phase conventions.

Expansion

Represent two real coordinates as $\psi = (q_1 + iq_2)/\sqrt{2}$. Polar decomposition gives $\rho = |\psi|$ and phase $\theta = \arg\psi$ away from zeros. A global phase transformation $\psi_i \to e^{i\alpha}\psi_i$ leaves $|\psi|^2$ and ordinary differences invariant only for constant α; local transformations require link variables.

Dimensional and normalization check

Phase is dimensionless. ρ's units are fixed by the action normalization, not by interpreting $|\psi|^2$ as probability.

Thought experiment

The direction of an arrow can change while its length stays fixed. Phase stores the direction; amplitude stores the length.

Failure condition. The construction fails as physics if phase has no measurable invariant consequences or if zeros make the proposed global phase map ill-defined without defects.

Back to compact sheet

G02

EXACT GAUGE CONSTRUCTION

Covariant link difference

Gauge and phase | Compact equation map | Pair 26 of 55

Condensed equation chain

$$U_{ij} = e^{igA_{ij}}, \qquad D_{ij}\psi = U_{ij}\psi_j - \psi_i, \qquad \mathcal{E}_{\text{link}} = \frac{\kappa}{2}\sum_{(ij)} |D_{ij}\psi|^2 \tag{90}$$

Symbols and types

$A_{ij} = -A_{ji}$: link phase; g: dimensionless lattice charge convention; $U_{ij} \in U(1)$.

Dependency and scientific reading

Link transport makes local phase comparison meaningful and supplies an exactly gauge-invariant finite graph energy.

Author-control point. Ryan can connect this to progression mismatch, but the link variable must have its own update law rather than remain a bookkeeping device.

NEXT: The facing work-through states the assumptions, expands the algebra, checks dimensions, and names a failure condition. **Expanded sheet**

G02-X

EXPANDED WORK-THROUGH

Covariant link difference

Gauge and phase | Assumptions, derivation, dimensions, interpretation, falsifier

Assumptions used

Oriented links have inverse transporters $U_{ji} = U_{ij}^{-1}$; matter fields share a declared representation.

Expansion

A naked difference $\psi_j - \psi_i$ compares phases using one convention. Insert a transporter that carries ψ_j into node i's convention. The squared norm is nonnegative and depends only on the covariant mismatch. Expanding it gives $\rho_i^2 + \rho_j^2 - 2\rho_i\rho_j \cos(\theta_j - \theta_i + gA_{ij})$.

Dimensional and normalization check

gA_{ij} and phase differences are dimensionless. $\kappa|\psi|^2$ has energy units in the benchmark.

Thought experiment

Two compasses can be compared only after accounting for how 'north' rotates along the path between them.

Failure condition. The construction is inadequate if it cannot generate propagating gauge degrees of freedom or if its continuum coupling is inserted from measured α.

Back to compact sheet

G03

PROVED EXACTLY

Local gauge transformation

Gauge and phase | Compact equation map | Pair 27 of 55

Condensed equation chain

$$\psi_i \to e^{i\alpha_i}\psi_i, \qquad U_{ij} \to e^{i\alpha_i}U_{ij}e^{-i\alpha_j}, \qquad D_{ij}\psi \to e^{i\alpha_i}D_{ij}\psi \tag{91}$$

Symbols and types

α_i: arbitrary node-dependent phase convention.

Dependency and scientific reading

The link energy is exactly invariant at finite spacing. This is a genuine model-level proof, not evidence that the physical gauge group is $U(1)$.

Author-control point. If Ryan intends a physical phase-locking rather than redundancy, distinguish spontaneous alignment from gauge convention; conflating them creates false observables.

NEXT: The facing work-through states the assumptions, expands the algebra, checks dimensions, and names a failure condition.

Expanded sheet

G03-X

EXPANDED WORK-THROUGH

Local gauge transformation

Gauge and phase | Assumptions, derivation, dimensions, interpretation, falsifier

Assumptions used

Transformations act consistently on every oriented link and field; observables are built from invariant norms or closed loops.

Expansion

Substitute the transformed variables: $D'_{ij}\psi' = e^{i\alpha_i}U_{ij}e^{-i\alpha_j}e^{i\alpha_j}\psi_j - e^{i\alpha_i}\psi_i = e^{i\alpha_i}D_{ij}\psi$. Taking the modulus removes the remaining phase, so every link term and their sum are invariant.

Dimensional and normalization check

Gauge phases and group elements are dimensionless; invariance is unaffected by the amplitude normalization.

Thought experiment

Changing the coordinate grid should not change a distance. Gauge transformation is a change of local phase coordinates that leaves measurable mismatch unchanged.

Failure condition. The claimed symmetry fails if any onsite, limiter, or measurement term changes under the same transformation.

Back to compact sheet

G04

EXACT INVARIANT / CONTINUUM TARGET

Plaquette holonomy

Gauge and phase | Compact equation map | Pair 28 of 55

Condensed equation chain

$$U_p = U_{ij}U_{jk}U_{k\ell}U_{\ell i} = e^{ig\Phi_p}, \qquad \Phi_p = A_{ij} + A_{jk} + A_{k\ell} + A_{\ell i} \tag{92}$$

Symbols and types

p: oriented elementary loop; Φ_p: discrete flux; U_p: holonomy.

Dependency and scientific reading

Closed-loop phase is gauge invariant and becomes curvature in a suitable continuum limit.

Author-control point. Define which loops are elementary on an emergent irregular graph. Different choices alter the gauge action and continuum limit.

NEXT: The facing work-through states the assumptions, expands the algebra, checks dimensions, and names a failure condition.

Expanded sheet

G04-X

EXPANDED WORK-THROUGH

Plaquette holonomy

Gauge and phase | Assumptions, derivation, dimensions, interpretation, falsifier

Assumptions used

The graph contains declared elementary loops; orientations are consistent; link variables form a group representation.

Expansion

Apply G03 to each link around the loop. At every intermediate vertex, $e^{-i\alpha_j}e^{i\alpha_j} = 1$; only the starting factors remain and cancel in an Abelian group. For small square spacing a, expand link phases as line integrals to obtain $\Phi_p \approx a^2 F_{\mu\nu}$.

Dimensional and normalization check

U_p and $g\Phi_p$ are dimensionless. If A_μ has mass dimension one, the link exponent includes the explicit path length.

Thought experiment

Carry an arrow around a tiny loop. If it returns rotated, the loop encloses curvature or flux even though each local comparison was conventional.

Failure condition. The field interpretation fails if loop observables do not approach a local curvature tensor or if lattice artifacts dominate the intended regime.

Back to compact sheet

G05

STANDARD TEMPLATE / NOT DERIVED

Gauge-field action

Gauge and phase | Compact equation map | Pair 29 of 55

Condensed equation chain

$$S_g = \beta_g \sum_p [1 - \operatorname{Re} U_p], \qquad 1 - \cos(g\Phi_p) \simeq \frac{g^2\Phi_p^2}{2} \tag{93}$$

Symbols and types

β_g: lattice gauge stiffness; p: elementary plaquettes.

Dependency and scientific reading

This Wilson-type action is mathematically sound and gauge invariant, but importing it is not deriving electromagnetism from END/MNT.

Author-control point. Decide whether loop stiffness comes from unused capacity, phase coherence, or an independent term. That origin is where END/MNT could become distinctive.

NEXT: The facing work-through states the assumptions, expands the algebra, checks dimensions, and names a failure condition.

Expanded sheet

G05-X

EXPANDED WORK-THROUGH

Gauge-field action

Gauge and phase | Assumptions, derivation, dimensions, interpretation, falsifier

Assumptions used

A loop set and measure are known; phases are small in the continuum regime; β_g is fixed independently of the target coupling.

Expansion

Gauge invariance follows because each U_p is invariant. For smooth fields, expand the cosine and replace $\sum_p a^d$ by an integral. Matching the coefficient to $-F_{\mu\nu}F^{\mu\nu}/4$ identifies a relation among β_g, g, a, and field normalization. It does not determine a numerical fine-structure constant.

Dimensional and normalization check

The action is dimensionless in $e^{iS/\hbar}$; factors of a and $\hbar$ must be restored when matching SI units.

Thought experiment

A flexible net resists being twisted around a loop. The resistance coefficient sets how costly gauge curvature is.

Failure condition. The claimed derivation fails if β_g is chosen solely to reproduce α or if the emergent action contains forbidden mass terms.

Back to compact sheet

G06

MATCHING, NOT PREDICTION

Continuum gauge coupling

Gauge and phase | Compact equation map | Pair 30 of 55

Condensed equation chain

$$\frac{1}{4g_{\mathrm{eff}}^2}\int d^4x\, F_{\mu\nu}F^{\mu\nu} \longleftrightarrow \beta_g \sum_p (1 - \mathrm{Re}\, U_p), \qquad \alpha = \frac{g_{\mathrm{eff}}^2}{4\pi\hbar c} \tag{94}$$

Symbols and types

g_{eff}: canonically normalized continuum coupling; α: fine-structure constant in a declared convention.

Dependency and scientific reading

A coupling is predicted only if the node operator fixes the dimensionless normalization after all field rescalings.

Author-control point. Choose a normalization and scale, then freeze it. Never insert 1/137.036 inside a formula later advertised as its derivation.

NEXT: The facing work-through states the assumptions, expands the algebra, checks dimensions, and names a failure condition. **Expanded sheet**

G06-X

EXPANDED WORK-THROUGH

Continuum gauge coupling

Gauge and phase | Assumptions, derivation, dimensions, interpretation, falsifier

Assumptions used

The continuum field is canonically normalized; lattice measure and representation are fixed; renormalization scale and scheme are declared.

Expansion

Expand G05 and convert the plaquette sum to an integral. Rescale $A_\mu \to ZA_\mu$ so the kinetic term is canonical. Matter coupling rescales oppositely, leaving the physical product. Renormalization then runs $g(\mu)$. A bare lattice number is therefore not automatically the measured low-energy α.

Dimensional and normalization check

α is dimensionless. In SI, $g_{\text{eff}}^2/(4\pi\epsilon_0\hbar c)$ is dimensionless; conventions must not be mixed.

Thought experiment

Changing the ruler used to measure a field changes the coefficient written beside it. Only interactions after canonical normalization carry physical coupling strength.

Failure condition. Predictive credit is lost if the measured coupling, an equivalent atomic constant, or a fitted field normalization enters upstream.

Back to compact sheet

G07

OPEN DERIVATION

Charge representations

Gauge and phase | Compact equation map | Pair 31 of 55

Condensed equation chain

$$\psi_i^{(r)} \to R_r(g_i)\psi_i^{(r)}, \qquad U_{ij} \to g_i U_{ij} g_j^{-1}, \qquad Q_r \in \mathrm{Spec}(T_r) \tag{95}$$

Symbols and types

R_r: group representation; T_r: generator; Q_r: charge label.

Dependency and scientific reading

Charge quantization comes from representation/topology, not from multiplying an arbitrary phase difference by the measured elementary charge.

Author-control point. Ryan should state whether charge is phase winding, a group weight, a flux endpoint, or capacity circulation. These options are not synonyms.

NEXT: The facing work-through states the assumptions, expands the algebra, checks dimensions, and names a failure condition.

Expanded sheet

G07-X

EXPANDED WORK-THROUGH

Charge representations

Gauge and phase | Assumptions, derivation, dimensions, interpretation, falsifier

Assumptions used

The gauge group and allowed representations emerge from the node state space; anomaly constraints are enforced.

Expansion

Identify the automorphism group acting locally on node states. Decompose persistent modes into irreducible representations r. Generator eigenvalues label charges up to one overall normalization. Topology or group compactness can quantize ratios, while one dimensional electromagnetic unit still requires a metrological bridge.

Dimensional and normalization check

Representation weights are dimensionless. Coulombs are an SI unit tied exactly to the elementary charge definition and do not constitute a theoretical prediction.

Thought experiment

Musical harmonies allow discrete notes because the instrument's symmetry and boundary conditions select them; charge ratios need an analogous selector.

Failure condition. The charge programme fails if allowed representations give unobserved fractions without confinement, violate anomaly cancellation, or require observed charges as inputs.

Back to compact sheet

G08

KNOWN OBSTRUCTION / OPEN SOLUTION

Chiral fermion hurdle

Gauge and phase | Compact equation map | Pair 32 of 55

Condensed equation chain

$$D_{\mathrm{naive}}(k) = \frac{i}{a}\sum_{\mu}\gamma^{\mu}\sin(k_{\mu}a), \qquad D_{\mathrm{naive}}(k) = 0 \text{ at } k_{\mu}a \in \{0, \pi\} \tag{96}$$

Symbols and types

D_{naive}: lattice Dirac operator; zeros at Brillouin-zone corners generate doublers.

Dependency and scientific reading

A Standard-Model claim must confront chirality, doubling, anomalies, and the gauge representation content explicitly.

Author-control point. Do not describe generic node handedness as derived chirality. Select a concrete fermion construction and test its anomaly structure.

NEXT: The facing work-through states the assumptions, expands the algebra, checks dimensions, and names a failure condition. **Expanded sheet**

G08-X

EXPANDED WORK-THROUGH

Chiral fermion hurdle

Gauge and phase | Assumptions, derivation, dimensions, interpretation, falsifier

Assumptions used

Local translationally invariant lattice fermions with the standard assumptions are used; the continuum target is chiral.

Expansion

Fourier transforming the symmetric difference $(\psi_{n+\hat{\mu}} - \psi_{n-\hat{\mu}})/(2a)$ yields $i\sin(k_\mu a)/a$. Sine vanishes at both 0 and π, creating multiple low-energy species. Wilson, staggered, domain-wall, or overlap methods alter assumptions and introduce their own structure; END/MNT must choose and justify one route.

Dimensional and normalization check

D has inverse-length or mass units. The argument $k_\mu a$ is dimensionless.

Thought experiment

Sampling a wave too coarsely can make two different frequencies look identical. Fermion doubling is a deep symmetry version of that aliasing problem.

Failure condition. A proposed micro-model fails the Standard-Model bridge if it cannot yield the observed chiral spectrum without unobserved light partners.

Back to compact sheet

L01

REPAIRED EFFECTIVE TEMPLATE

Repaired amplitude–phase action

Legacy repair | Compact equation map | Pair 33 of 55

Condensed equation chain

$$S = \int d^4x \left[\frac{1}{2}(\partial_\mu \rho)^2 + \frac{1}{2}\rho^2(\partial_\mu \theta - gA_\mu)^2 - V(\rho) - \frac{1}{4}F_{\mu\nu}F^{\mu\nu} \right] \tag{97}$$

Symbols and types

ρ: amplitude; θ: compact phase; A_μ: gauge connection.

Dependency and scientific reading

This replaces legacy sums of unlike units and removes uncontrolled higher-time derivatives. It is a consistent EFT target, not a first-principles result.

Author-control point. Ryan can add capacity/EQEF coupling, but every added term must be symmetry allowed, dimensionally typed, and bounded or controlled.

NEXT: The facing work-through states the assumptions, expands the algebra, checks dimensions, and names a failure condition.

Expanded sheet

L01-X

EXPANDED WORK-THROUGH

Repaired amplitude–phase action

Legacy repair | Assumptions, derivation, dimensions, interpretation, falsifier

Assumptions used

Lorentzian sign convention is fixed; coefficients have correct dimensions; fields are differentiable in the effective regime.

Expansion

Begin with $\Phi = \rho e^{i\theta}$. The covariant kinetic term satisfies $|D_\mu\Phi|^2 = (\partial_\mu\rho)^2 + \rho^2(\partial_\mu\theta - gA_\mu)^2$. Add a bounded-below potential and the gauge kinetic term. Varying each field produces second-order equations, avoiding generic Ostrogradsky instability.

Dimensional and normalization check

In 3+1 natural units, $[\rho] = [A] = 1$, $[\partial] = 1$, $[V] = 4$, and g, θ are dimensionless.

Thought experiment

Amplitude is how far a compass needle extends; phase is where it points; the connection tells neighbouring compasses how to compare directions.

Failure condition. Reject any legacy correction term whose units do not match the Lagrangian density or whose coefficient is tuned until a known number reappears.

Back to compact sheet

L02

EXACT DISCRETE FORM

Link phase mismatch

Legacy repair | Compact equation map | Pair 34 of 55

Condensed equation chain

$$\Delta_{ij} = \theta_j - \theta_i + gA_{ij} \pmod{2\pi}, \qquad E_{ij} = K_{ij}[1 - \cos\Delta_{ij}] \tag{98}$$

Symbols and types

Δ_{ij}: gauge-invariant mismatch; $K_{ij} \geq 0$: alignment stiffness.

Dependency and scientific reading

This is the safe replacement for adding raw phases, distances, and correction factors inside untyped transcendental functions.

Author-control point. Specify whether phase mismatch consumes capacity, generates a force, or stores recoverable energy. The choice controls EQEF coupling.

NEXT: The facing work-through states the assumptions, expands the algebra, checks dimensions, and names a failure condition. **Expanded sheet**

L02-X

EXPANDED WORK-THROUGH

Link phase mismatch

Legacy repair | Assumptions, derivation, dimensions, interpretation, falsifier

Assumptions used

Phase is compact; link orientation is fixed; stiffness is nonnegative.

Expansion

Write $\psi_i = \rho e^{i\theta_i}$ with fixed amplitude. G02 gives $|U_{ij}\psi_j - \psi_i|^2 = 2\rho^2[1 - \cos\Delta_{ij}]$, so $K_{ij} = \kappa\rho^2$. For small mismatch, $E_{ij} \approx K_{ij}\Delta_{ij}^2/2$; the periodic form remains bounded for large mismatch.

Dimensional and normalization check

Δ is dimensionless and K has energy units. A distance may enter only through a defined link coefficient, never by addition to phase.

Thought experiment

Two coupled metronomes resist being out of step, but a full turn returns them to the same phase; the cosine encodes that periodicity.

Failure condition. The mechanism fails if it breaks the declared gauge symmetry or if its small-fluctuation modes contradict the intended continuum field.

Back to compact sheet

L03

CONSISTENCY TEST

Positivity and derivative order

Legacy repair | Compact equation map | Pair 35 of 55

Condensed equation chain

$$\mathcal{H} = \frac{1}{2}\pi_\rho^2 + \frac{1}{2\rho^2}\pi_\theta^2 + \frac{1}{2}|\nabla\rho|^2 + \frac{1}{2}\rho^2|\nabla\theta - g\boldsymbol{A}|^2 + V(\rho) + \frac{1}{2}(\boldsymbol{E}^2 + \boldsymbol{B}^2) \geq E_{\min} \tag{99}$$

Symbols and types

π_ρ, π_θ: canonical momenta; $\boldsymbol{E}, \boldsymbol{B}$: gauge fields.

Dependency and scientific reading

A viable effective action needs controlled energy and no generic nondegenerate higher-time-derivative instability.

Author-control point. Legacy fourth-derivative terms should remain excluded unless Ryan supplies a constrained/degenerate construction and a stability proof.

NEXT: The facing work-through states the assumptions, expands the algebra, checks dimensions, and names a failure condition. **Expanded sheet**

L03-X

EXPANDED WORK-THROUGH

Positivity and derivative order

Legacy repair | Assumptions, derivation, dimensions, interpretation, falsifier

Assumptions used

Kinetic signs are positive; V is bounded below; $\rho \neq 0$ where polar variables are used.

Expansion

Compute canonical momenta from L01 and Legendre transform. Positive quadratic kinetic terms yield the displayed Hamiltonian. By contrast, a nondegenerate term containing $(\partial_t^2\phi)^2$ requires two canonical coordinates and generically produces a Hamiltonian linear in one momentum. Higher spatial derivatives may be acceptable; higher time derivatives require degeneracy or a demonstrated constraint.

Dimensional and normalization check

Every Hamiltonian term has energy density units. Positivity is independent of the chosen unit system.

Thought experiment

A spring whose stored energy can decrease without bound would accelerate forever by giving up ever more negative energy; elegant equations cannot rescue that instability.

Failure condition. Reject the sector if the Hamiltonian is unbounded below, if ghosts remain in the spectrum, or if constraints are imposed only after instability appears.

Back to compact sheet

C01

DEFINITION / LEDGER

Residual capacity

Capacity and EQEF | Compact equation map | Pair 36 of 55

Condensed equation chain

$$r_i^n = 1 - \mathcal{C}_i^n, \qquad 0 \le r_i^n \le 1, \qquad \bar{r}_\Omega = |\Omega|^{-1} \sum_{i \in \Omega} r_i \tag{100}$$

Symbols and types

r_i: unused local transition fraction; $\bar{r}_\Omega$: regional coarse average.

Dependency and scientific reading

This is the narrow canonical meaning of EQEF at level 1: a capacity ledger, not automatically energy, gravity, or a new field.

Author-control point. Confirm whether EQEF means unused capacity, deferred demand, transported imbalance, or a separate state variable. The canonical manuscript currently chooses the first.

NEXT: The facing work-through states the assumptions, expands the algebra, checks dimensions, and names a failure condition. **Expanded sheet**

C01-X

EXPANDED WORK-THROUGH

Residual capacity

Capacity and EQEF | Assumptions, derivation, dimensions, interpretation, falsifier

Assumptions used

$\mathcal{C}_i$ is already well-defined and capacity preserving; its normalization is common across the model.

Expansion

Given $0 \leq \mathcal{C}_i \leq 1$, subtraction yields the same bound for r_i. Regional averages remain in $[0, 1]$ by convexity. Fluctuations are $\delta r_i = r_i - \bar{r}$. A continuum candidate $\chi(x)$ may be defined from block averages only after a scale window and covariance are measured.

Dimensional and normalization check

Residual capacity is dimensionless. Multiplying by an independently defined energy scale E_* creates an energy ledger $E_* r_i$; it does not derive E_*.

Thought experiment

An empty lane is not fuel. It is available traffic capacity. Converting availability into energy requires a mechanism and a scale.

Failure condition. EQEF claims fail if one symbol is allowed to change meaning between capacity, energy density, dark energy, and torsion calculations.

Back to compact sheet

C02

CANDIDATE DYNAMICS

Causal capacity balance

Capacity and EQEF | Compact equation map | Pair 37 of 55

Condensed equation chain

$$r_i^{n+1} - r_i^n + \sum_j J_{ij}^{n+1/2} = S_i^n - D_i^n, \qquad J_{ij} = -J_{ji} \tag{101}$$

Symbols and types

J_{ij}: oriented capacity flux; S_i: local release/source; D_i: local consumption/deferred demand.

Dependency and scientific reading

A balance law turns the ledger into dynamics while retaining locality. The constitutive rule for J, S, D remains open.

Author-control point. Ryan should decide whether overloaded regions borrow, queue, redirect, or permanently dissipate capacity. Each option produces different arrows of time.

NEXT: The facing work-through states the assumptions, expands the algebra, checks dimensions, and names a failure condition. **Expanded sheet**

C02-X

EXPANDED WORK-THROUGH

Causal capacity balance

Capacity and EQEF | Assumptions, derivation, dimensions, interpretation, falsifier

Assumptions used

Fluxes are antisymmetric on internal links; sources and sinks are explicit; boundary flux is declared.

Expansion

Sum the equation over a region Ω. Internal link terms cancel pairwise because $J_{ij} = -J_{ji}$. Only boundary flux and $\sum(S_i - D_i)$ change total residual capacity. This gives an exact bookkeeping identity. A diffusion-like choice $J_{ij} = \gamma w_{ij}(r_i - r_j)$ is causal only when implemented through finite local updates.

Dimensional and normalization check

All terms are residual-capacity fraction per update. A physical current density requires division by derived area and time scales.

Thought experiment

Water in connected tanks moves through pipes; the total changes only through boundary flow or explicit taps and drains.

Failure condition. The balance law fails if flux permits values outside $[0, 1]$, propagates influence nonlocally, or hides unexplained creation in a correction term.

Back to compact sheet

C03

OPTIONAL EFFECTIVE THEORY

EQEF continuum field

Capacity and EQEF | Compact equation map | Pair 38 of 55

Condensed equation chain

$$S_\chi = \int d^4x\sqrt{-g}\left[-\frac{Z_\chi}{2}(\nabla\chi)^2 - U(\chi) - \xi\chi R + \mathcal{L}_{\rm int}\right] \tag{102}$$

Symbols and types

χ: coarse residual-capacity fluctuation; Z_χ: normalization; U: potential; ξ: curvature coupling.

Dependency and scientific reading

This action shows what must be specified before EQEF can be discussed as a propagating or gravitating field. Its coefficients are not yet derived.

Author-control point. If Ryan wants EQEF to mean energy density rather than a normalized scalar, change the normalization and rewrite every coupling consistently.

NEXT: The facing work-through states the assumptions, expands the algebra, checks dimensions, and names a failure condition.

Expanded sheet

C03-X

EXPANDED WORK-THROUGH

EQEF continuum field

Capacity and EQEF | Assumptions, derivation, dimensions, interpretation, falsifier

Assumptions used

A continuum metric already exists; block variables converge to a smooth scalar; locality and covariance emerge.

Expansion

Define $\chi_R(x) = Z_R[\bar{r}_{B_R(x)} - \bar{r}]$. Measure connected correlators and infer whether a local derivative expansion is valid. The inverse two-point function fixes Z_χ and a mass term; higher connected correlators constrain U. Only then may one compare cosmic evolution or fifth-force effects.

Dimensional and normalization check

In 3+1 natural units a canonical scalar has mass dimension one; U has dimension four and ξ is dimensionless.

Thought experiment

Temperature is a real field that emerges from molecular motion, but its transport coefficients must be measured or derived. EQEF needs the same bridge from ledger to continuum.

Failure condition. Reject the effective-field claim if correlations are nonlocal without control, if no scale separation exists, or if predicted fifth forces violate bounds.

Back to compact sheet

C04

OPEN MICRO-TO-MACRO BRIDGE

Response and source map

Capacity and EQEF | Compact equation map | Pair 39 of 55

Condensed equation chain

$$\Pi_\chi^{-1}(p) = Z_\chi(p^2 + m_\chi^2) + O(p^4), \qquad J_\chi(x) = \frac{\delta S_{\text{micro}}}{\delta\chi(x)}, \qquad \chi(p) = \Pi_\chi(p) J_\chi(p) \tag{103}$$

Symbols and types

Π_χ: response propagator; J_χ: source; m_χ: correlation mass.

Dependency and scientific reading

Naming matter, curvature, or torsion as an EQEF source is insufficient; the response kernel must be calculated from the microscopic update.

Author-control point. Specify which microscopic intervention represents matter loading and why it couples universally rather than composition-dependently.

NEXT: The facing work-through states the assumptions, expands the algebra, checks dimensions, and names a failure condition.

Expanded sheet

C04-X

EXPANDED WORK-THROUGH

Response and source map

Capacity and EQEF | Assumptions, derivation, dimensions, interpretation, falsifier

Assumptions used

Linear response exists around a stationary background; the source perturbation is independently specified; correlations are measurable in simulation.

Expansion

Perturb the microscopic rule by $\epsilon \sum_i f_i r_i$. Differentiate the block expectation: $\delta\langle\chi(x)\rangle/\delta f(y) = \Pi_\chi(x, y)$. Fourier transform in a homogeneous phase and fit only the low-momentum expansion. The pole structure determines propagating or screened behavior; it cannot be assumed from a chosen continuum template.

Dimensional and normalization check

The propagator's units follow the normalization of χ; pole locations have mass or inverse-length units after scale calibration.

Thought experiment

Pushing one point on a mattress reveals how the material carries stress. The shape of the response, not the word mattress, defines its effective elasticity.

Failure condition. The bridge fails if different probes produce incompatible kernels or if fitted coefficients drift without a continuum plateau.

Back to compact sheet

C05

GEOMETRIC HYPOTHESIS

Torsion from loop nonclosure

Capacity and EQEF | Compact equation map | Pair 40 of 55

Condensed equation chain

$$\Delta x^{\rho} = T^{\rho}{}_{\mu\nu}\, \Sigma^{\mu\nu} + O(\Sigma^{3/2}), \qquad T^{\rho}{}_{\mu\nu} = 2\Gamma^{\rho}{}_{[\mu\nu]} \tag{104}$$

Symbols and types

Δx^{ρ}: closure defect; $\Sigma^{\mu\nu}$: loop area bivector; T: torsion tensor.

Dependency and scientific reading

Progression imbalance can be mapped to torsion only if microscopic transport around small loops has this controlled continuum limit.

Author-control point. Ryan should state whether imbalance changes translation, clock rate, or link phase. Only translation nonclosure maps directly to geometric torsion.

NEXT: The facing work-through states the assumptions, expands the algebra, checks dimensions, and names a failure condition.

Expanded sheet

C05-X

EXPANDED WORK-THROUGH

Torsion from loop nonclosure

Capacity and EQEF | Assumptions, derivation, dimensions, interpretation, falsifier

Assumptions used

An effective coordinate/tetrad map and parallel transport are already defined; loop size is small compared with curvature scales.

Expansion

Construct four effective displacements from persistent probes. Compose transports around an elementary loop and measure the endpoint defect. Divide by the oriented area and take a refinement limit. Antisymmetry in μ, ν follows from reversing loop orientation. A finite tensorial limit defines torsion; arbitrary path-dependent delay does not.

Dimensional and normalization check

Torsion has inverse-length units; area times torsion gives a length displacement.

Thought experiment

Walk east, north, west, south. If local translation rules are twisted, the loop may not close; the small-loop defect measures torsion.

Failure condition. The torsion interpretation fails if the limit depends on loop shape, has no tensor transformation law, or predicts excluded spin/gravity effects.

Back to compact sheet PAIR 40/55

C06

OPEN DERIVATION

Tetrad and connection bridge

Capacity and EQEF | Compact equation map | Pair 41 of 55

Condensed equation chain

$$e^a{}_\mu(x) = \lim_{R\to\infty} \frac{\langle \Delta X^a \rangle_R}{\Delta x^\mu}, \qquad \nabla_\mu e^a{}_\nu = \partial_\mu e^a{}_\nu + \omega^a{}_{b\mu} e^b{}_\nu - \Gamma^\rho{}_{\nu\mu} e^a{}_\rho = 0 \tag{105}$$

Symbols and types

$e^a{}_\mu$: tetrad; ω: spin connection; Γ: affine connection.

Dependency and scientific reading

A valid torsion claim requires the frame field and connection from which torsion is computed, not an analogy between delay and twist.

Author-control point. Choose the four physical probe modes that define the tetrad. This choice must be universal across matter species.

NEXT: The facing work-through states the assumptions, expands the algebra, checks dimensions, and names a failure condition.

Expanded sheet

C06-X

EXPANDED WORK-THROUGH

Tetrad and connection bridge

Capacity and EQEF | Assumptions, derivation, dimensions, interpretation, falsifier

Assumptions used

Persistent probes define local directions; their transport is stable under coarse-graining; an invertible four-dimensional frame emerges.

Expansion

Select four independent long-wave probe responses and normalize them into a local basis. Define transport by comparing the basis between neighbouring blocks. The change matrix yields ω; compatibility defines Γ. Then compute curvature and torsion. The construction must be independent of arbitrary coarse labels up to local Lorentz transformations.

Dimensional and normalization check

The tetrad converts coordinate intervals to local lengths and is dimensionless under the usual coordinate convention; the connections carry inverse-length units.

Thought experiment

To describe wind on Earth, first define local north/east/up directions, then compare them from place to place. Twist cannot be measured before the local frame exists.

Failure condition. The bridge fails if fewer/more than four stable macroscopic directions emerge, if the tetrad becomes singular, or if different probes define inequivalent connections.

Back to compact sheet

R01

OPEN DERIVATION

Emergent metric

Gravity and cosmology | Compact equation map | Pair 42 of 55

Condensed equation chain

$$g_{\mu\nu} = \eta_{ab} e^a{}_\mu e^b{}_\nu, \qquad ds^2 = g_{\mu\nu} dx^\mu dx^\nu, \qquad G_{\text{ret}}(x, y) = 0 \text{ outside the effective cone} \tag{106}$$

Symbols and types

$e^a{}_\mu$: tetrad from C06; $g_{\mu\nu}$: effective metric; G_{ret}: retarded response.

Dependency and scientific reading

The metric must organize rods, clocks, and propagation universally. A graph distance alone is insufficient for Lorentzian spacetime.

Author-control point. Ryan can retain an underlying update order while requiring emergent Lorentz symmetry; state explicitly which layer violates or preserves it.

NEXT: The facing work-through states the assumptions, expands the algebra, checks dimensions, and names a failure condition.

Expanded sheet

R01-X

EXPANDED WORK-THROUGH

Emergent metric

Gravity and cosmology | Assumptions, derivation, dimensions, interpretation, falsifier

Assumptions used

A four-dimensional invertible tetrad exists; one time-like and three space-like signatures emerge; low-energy probes share a cone.

Expansion

Use probe correlation fronts to define local null directions. Choose a tetrad whose Minkowski inner product reproduces those directions, then form $g = e^T \eta e$. Verify that clock phases measure proper time $d\tau^2 = -ds^2/c^2$ and that all low-energy kinetic operators share the same principal symbol $g^{\mu\nu} p_\mu p_\nu$.

Dimensional and normalization check

ds^2 has length squared when coordinates do; g is dimensionless in that convention.

Thought experiment

A map is physical only if sound, light, clocks, and rulers agree on its distances. One probe's convenient coordinates do not yet make spacetime.

Failure condition. The metric claim fails if different species see different cones beyond allowed limits or if the signature/dimension is unstable across scales.

Back to compact sheet

R02

OPEN PHYSICAL TEST

Equivalence principle target

Gravity and cosmology | Compact equation map | Pair 43 of 55

Condensed equation chain

$$S_m^{(A)} = -m_A c \int ds + O(\ell_*^2), \qquad \frac{m_g^{(A)}}{m_i^{(A)}} = 1 + \eta_A, \qquad |\eta_A - \eta_B| \to 0 \tag{107}$$

Symbols and types

A, B: different compositions; η_A: species-dependent equivalence violation.

Dependency and scientific reading

Universal coupling is not guaranteed by shared capacity language. It must arise from the same effective metric in every matter action.

Author-control point. Decide whether EQEF couples universally to total node energy or directly to pattern type. The latter risks composition dependence.

NEXT: The facing work-through states the assumptions, expands the algebra, checks dimensions, and names a failure condition.

Expanded sheet

R02-X

EXPANDED WORK-THROUGH

Equivalence principle target

Gravity and cosmology | Assumptions, derivation, dimensions, interpretation, falsifier

Assumptions used

All stable particle modes couple through one deformation of the node operator; nonmetric forces are screened or absent.

Expansion

Derive each mode's long-wave action in a slowly varying background. Canonically normalize it and inspect the principal kinetic term and force law. If the background enters only through $g_{\mu\nu}$, WKB wave packets follow metric geodesics. Residual direct χ- or torsion-dependent terms generate calculable η_A.

Dimensional and normalization check

m_g/m_i and η are dimensionless, making them clean held-out tests.

Thought experiment

Different clocks dropped in the same gravitational field must fall together even though their internal patterns differ.

Failure condition. The gravitational bridge fails if predicted differential acceleration exceeds experiment or if universality is imposed separately for each species.

Back to compact sheet

R03

MATCHING TARGET

Newtonian limit

Gravity and cosmology | Compact equation map | Pair 44 of 55

Condensed equation chain

$$g_{00} = -(1 + 2\Phi_N/c^2), \qquad \nabla^2\Phi_N = 4\pi G\rho, \qquad \ddot{\boldsymbol{x}} = -\nabla\Phi_N \tag{108}$$

Symbols and types

Φ_N: weak gravitational potential; ρ: mass-energy density; G: effective coupling.

Dependency and scientific reading

Recovering inverse-square gravity requires both a field equation and universal motion. Writing the Poisson equation as a target does not derive G.

Author-control point. Specify which microscopic observable is ρ and compute the response coefficient before comparing to measured G.

NEXT: The facing work-through states the assumptions, expands the algebra, checks dimensions, and names a failure condition.

Expanded sheet

R03-X

EXPANDED WORK-THROUGH

Newtonian limit

Gravity and cosmology | Assumptions, derivation, dimensions, interpretation, falsifier

Assumptions used

Static weak field, slow motion, scale separation, universal metric coupling.

Expansion

Linearize the emergent metric around flat space, isolate the scalar constraint, and integrate out microscopic modes. The zero-frequency, small-momentum response must behave as $\Phi_N(\boldsymbol{k}) = -4\pi G\rho(\boldsymbol{k})/k^2$. Fourier inversion gives $-GM/r$ for a point source; expanding the geodesic equation gives $\ddot{\boldsymbol{x}} = -\nabla\Phi_N$.

Dimensional and normalization check

$[G] = L^3M^{-1}T^{-2}$. Its numerical value needs the microscopic length, time, and mass scales; a Planck-unit identity does not predict it.

Thought experiment

Stretching a rubber sheet is only an analogy. The real test is whether a localized source produces the exact long-range $1/r$ response with universal acceleration.

Failure condition. The limit fails if the kernel is not $1/k^2$, if extra long-range forces appear, or if G is chosen after seeing the target.

Back to compact sheet

R04

OPEN EFFECTIVE-ACTION DERIVATION

Einstein-sector matching

Gravity and cosmology | Compact equation map | Pair 45 of 55

Condensed equation chain

$$\Gamma_{\text{eff}}[g] = \int d^4x\sqrt{-g}\left[\frac{M_*^2}{2}R - \Lambda_* + c_1 R^2 + c_2 R_{\mu\nu}R^{\mu\nu} + \cdots\right], \qquad M_*^{-2} = 8\pi G \tag{109}$$

Symbols and types

Γ_{eff}: coarse effective action; M_*: gravitational scale; c_i: higher-curvature coefficients.

Dependency and scientific reading

General covariance and the Einstein term must emerge from the node measure and symmetries. The coefficients are outputs to calculate.

Author-control point. If torsion is retained, extend the action with tetrad and spin connection rather than hiding torsion inside the Levi-Civita metric sector.

NEXT: The facing work-through states the assumptions, expands the algebra, checks dimensions, and names a failure condition.

Expanded sheet

R04-X

EXPANDED WORK-THROUGH

Einstein-sector matching

Gravity and cosmology | Assumptions, derivation, dimensions, interpretation, falsifier

Assumptions used

A local derivative expansion exists; diffeomorphism redundancy emerges; unwanted relevant operators are absent or suppressed.

Expansion

Integrate fluctuations above coarse scale R while retaining the collective metric. Symmetry classifies allowed terms. Compute two-point and three-point metric vertices to identify M_*^2, c_i. Varying the leading action yields $G_{\mu\nu} + \Lambda g_{\mu\nu} = 8\pi G T_{\mu\nu}$; higher terms predict deviations.

Dimensional and normalization check

$[M_*]$ = mass in natural units; $[R] = 2$; c_1, c_2 are dimensionless in four dimensions.

Thought experiment

Many microscopic materials behave like the same smooth elastic sheet at long wavelengths, but their stiffness must be derived from their microstructure.

Failure condition. The bridge fails if covariance requires fine tuning, if extra massless modes violate tests, or if calculated coefficients do not approach a stable continuum value.

Back to compact sheet

R05

OPEN MODEL SECTOR

Homogeneous cosmology

Gravity and cosmology | Compact equation map | Pair 46 of 55

Condensed equation chain

$$3H^2M_*^2 = \rho_m + \rho_r + \rho_\chi + \rho_{\rm corr}, \qquad \dot\rho_A + 3H(\rho_A + p_A) = Q_A, \qquad \sum_A Q_A = 0 \tag{110}$$

Symbols and types

H: emergent Hubble rate; ρ_A, p_A: component density and pressure; Q_A: exchange.

Dependency and scientific reading

A cosmology is not validated by inserting standard ΛCDM parameters. END/MNT must calculate background equations and initial data from its fixed sector.

Author-control point. Ryan should decide whether EQEF behaves as vacuum energy, scalar dynamics, modified gravity, or none. Do not count the same effect twice.

NEXT: The facing work-through states the assumptions, expands the algebra, checks dimensions, and names a failure condition.

Expanded sheet

R05-X

EXPANDED WORK-THROUGH

Homogeneous cosmology

Gravity and cosmology | Assumptions, derivation, dimensions, interpretation, falsifier

Assumptions used

An FLRW-like coarse phase exists; the gravitational action and matter stress tensor are known; averaging is controlled.

Expansion

Insert the homogeneous metric and fields into R04 plus C03. Vary the lapse to obtain the Friedmann constraint and vary scale factor/fields for evolution equations. Derive $\rho_\chi = \dot{\chi}^2/2 + U$, $p_\chi = \dot{\chi}^2/2 - U$ only if χ is canonical. Exchange terms follow from explicit couplings and must sum to zero.

Dimensional and normalization check

Each density has energy per volume; H has inverse-time units; $M_*^2 H^2$ matches density in natural units.

Thought experiment

A universe-wide traffic average may evolve like a fluid, but its pressure and exchange rules must come from how local capacity moves.

Failure condition. The cosmology fails if it cannot reproduce expansion and early-universe constraints with frozen parameters or if it needs a residual constant inserted by hand.

Back to compact sheet

R06

REQUIRED EMPIRICAL BRIDGE

Cosmological perturbations

Gravity and cosmology | Compact equation map | Pair 47 of 55

Condensed equation chain

$$\mathcal{R}_k'' + 2\frac{z'}{z}\mathcal{R}_k' + c_s^2 k^2 \mathcal{R}_k = \mathcal{S}_k, \qquad P_{\mathcal{R}}(k) = \frac{k^3}{2\pi^2}|\mathcal{R}_k|^2 \tag{111}$$

Symbols and types

$\mathcal{R}$: curvature perturbation; z, c_s: background functions; $\mathcal{S}$: extra sources.

Dependency and scientific reading

Background agreement is insufficient. Microwave-background and structure data test perturbation propagation, statistics, and cross-correlations.

Author-control point. Do not claim CMB or BBN validation until the perturbation code, likelihood, covariance, and baseline comparison are released.

NEXT: The facing work-through states the assumptions, expands the algebra, checks dimensions, and names a failure condition.

Expanded sheet

R06-X

EXPANDED WORK-THROUGH

Cosmological perturbations

Gravity and cosmology | Assumptions, derivation, dimensions, interpretation, falsifier

Assumptions used

The background solution is stable; linear perturbations are well defined; initial-state prescription is derived or declared independently.

Expansion

Expand all fields and the metric to second order around the homogeneous solution. Solve constraints, identify propagating gauge-invariant variables, and canonically normalize them. The quadratic action fixes z, c_s and any entropy/torsion sources. Propagate a preregistered initial spectrum to observables with the same parameters used for the background.

Dimensional and normalization check

$P_{\mathcal{R}}$ is dimensionless. Each term in the mode equation has inverse-conformal-time squared after multiplication by $\mathcal{R}$.

Thought experiment

Two cosmologies can share the same average expansion yet make very different ripples, like lakes with the same water level but different wave physics.

Failure condition. The sector fails if it predicts unstable modes, wrong light-element abundances, excluded isocurvature, or a power spectrum inconsistent with data.

Back to compact sheet

Q01

OPEN FOUNDATIONAL BRIDGE

Ensemble map

Quantum completion | Compact equation map | Pair 48 of 55

Condensed equation chain

$$\lambda = X_n, \qquad \rho(\lambda|P), \qquad p(a|P,M) = \int d\lambda\, \rho(\lambda|P)\, \xi(a|M,\lambda) \tag{112}$$

Symbols and types

P: preparation; M: measurement; λ: complete microstate; ξ: response function.

Dependency and scientific reading

Deterministic histories produce probabilities only after a preparation ensemble and outcome map are defined.

Author-control point. Ryan must choose whether uncertainty is epistemic, typicality-based, deterministic chaos, or a fundamental measure on histories.

NEXT: The facing work-through states the assumptions, expands the algebra, checks dimensions, and names a failure condition. **Expanded sheet**

Q01-X

EXPANDED WORK-THROUGH

Ensemble map

Quantum completion | Assumptions, derivation, dimensions, interpretation, falsifier

Assumptions used

Repeated preparations generate a stable measure; the microstate space and readout are fixed; selection bias is controlled.

Expansion

For deterministic response, $\xi \in \{0, 1\}$. Frequencies across repeated runs converge to the integral if the ensemble is ergodic or sampled by a declared distribution. Different coarse-grainings can yield different apparent probabilities, so P, M, and the resolution belong in the model specification.

Dimensional and normalization check

Probabilities and $\rho d\lambda$ are dimensionless. The measure must be normalized without using the outcomes being predicted.

Thought experiment

A deterministic coin-toss machine can yield uncertain outcomes when its exact starting state is unknown. Quantum statistics demand much more: the precise interference and correlation rules.

Failure condition. The bridge fails if the measure changes with the desired answer, if repeated frequencies do not stabilize, or if it cannot represent incompatible measurements.

Back to compact sheet

Q02

OPEN DERIVATION

Born-rule target

Quantum completion | Compact equation map | Pair 49 of 55

Condensed equation chain

$$p(a) = \frac{|\langle a|\Psi\rangle|^2}{\langle\Psi|\Psi\rangle}, \qquad N_a/N \xrightarrow[N\to\infty]{} p(a) \tag{113}$$

Symbols and types

$|\Psi\rangle$: effective state; $|a\rangle$: outcome channel; N_a: observed count.

Dependency and scientific reading

Phase variables and threshold amplification do not by themselves yield the squared-amplitude law. The measure over microhistories must produce it.

Author-control point. State the amplification/selection mechanism in microscopic terms and derive the basin measure rather than naming collapse after the fact.

NEXT: The facing work-through states the assumptions, expands the algebra, checks dimensions, and names a failure condition. **Expanded sheet**

Q02-X

EXPANDED WORK-THROUGH

Born-rule target

Quantum completion | Assumptions, derivation, dimensions, interpretation, falsifier

Assumptions used

An effective Hilbert structure emerges; outcome channels are exclusive and exhaustive; typicality measure is fixed.

Expansion

Define a map from microstates to effective amplitudes and measurement channels. Show that the measure of the basin leading to outcome a equals $|c_a|^2$ and is invariant under allowed refinements. Then prove concentration of empirical frequencies around that measure. Merely setting a threshold proportional to $|c_a|^2$ would insert the Born rule.

Dimensional and normalization check

Amplitudes and probabilities are dimensionless after normalization. No dimensional constant can repair a wrong exponent.

Thought experiment

If two water channels have amplitudes two and one, ordinary flow might scale linearly or quadratically depending on the mechanism. Quantum theory specifically demands the square.

Failure condition. The quantum programme fails if it predicts $|c|^p$ with $p \neq 2$, basis-dependent normalization, or contextual frequencies inconsistent with experiment.

Back to compact sheet

Q03

CONSTRAINT / OPEN CHOICE

Bell–CHSH assumptions

Quantum completion | Compact equation map | Pair 50 of 55

Condensed equation chain

$$
\begin{gathered}
S = E(a,b) + E(a,b') + E(a',b) - E(a',b'),\\
|S| \le 2 \text{ under locality and measurement independence},\\
|S|_{\mathrm{QM}} \le 2\sqrt{2}
\end{gathered} \tag{114}
$$

Symbols and types

a, a', b, b': settings; E: outcome correlation; S: CHSH combination.

Dependency and scientific reading

A deterministic completion must state which Bell assumption changes; a shared past alone cannot reproduce the observed violation under the standard assumptions.

Author-control point. Ryan must choose and defend the altered assumption. Leaving it unspecified is not a deterministic explanation of entanglement.

NEXT: The facing work-through states the assumptions, expands the algebra, checks dimensions, and names a failure condition. **Expanded sheet**

Q03-X

EXPANDED WORK-THROUGH

Bell–CHSH assumptions

Quantum completion | Assumptions, derivation, dimensions, interpretation, falsifier

Assumptions used

Outcomes and settings are explicitly modeled; sampling and locality conditions are declared; loopholes are not hidden in language.

Expansion

Under factorizability $A(a, \lambda)B(b, \lambda)$ and a setting-independent distribution $\rho(\lambda)$, each hidden-state CHSH expression is ± 2; averaging gives $|S| \leq 2$. END/MNT must calculate E after choosing operational nonlocality, measurement dependence, retrocausality, contextuality, or another explicit departure.

Dimensional and normalization check

All correlations and S are dimensionless.

Thought experiment

Two envelopes prepared together can contain matching cards, but that common past cannot reproduce every angle-dependent quantum correlation while preserving the standard assumptions.

Failure condition. The completion fails if it cannot reach observed CHSH values while preserving operational no-signalling and the declared setting-generation protocol.

Back to compact sheet

Q04

REQUIRED CONSISTENCY PROOF

Operational no-signalling

Quantum completion | Compact equation map | Pair 51 of 55

Condensed equation chain

$$\sum_b p(a,b|x,y) = p(a|x) \text{ independent of } y, \qquad \sum_a p(a,b|x,y) = p(b|y) \text{ independent of } x \tag{115}$$

Symbols and types

x, y: distant settings; a, b: outcomes.

Dependency and scientific reading

A nonlocal or measurement-dependent micro-description must still reproduce the observed inability to send controllable faster-than-light messages.

Author-control point. If progression has global constraints, identify why agents cannot control the relevant hidden variables to signal.

NEXT: The facing work-through states the assumptions, expands the algebra, checks dimensions, and names a failure condition. **Expanded sheet**

Q04-X

EXPANDED WORK-THROUGH

Operational no-signalling

Quantum completion | Assumptions, derivation, dimensions, interpretation, falsifier

Assumptions used

The preparation and setting distributions are explicit; accessible controls are distinguished from hidden correlations.

Expansion

Calculate the joint distribution from Q01 and marginalize. Show analytically or with exact symmetry that the remote setting cancels from each accessible marginal for every allowed local preparation. Numerical agreement on a few settings is insufficient; the cancellation must hold across the operational domain.

Dimensional and normalization check

Probabilities are dimensionless and normalized to one.

Thought experiment

Two dancers may coordinate nonlocally in the hidden choreography, yet neither audience member should be able to encode a message by choosing one dancer's instruction.

Failure condition. The model is excluded if any controllable protocol changes a distant marginal outside experimental bounds.

Back to compact sheet

E01

CONTROLLING EVIDENCE RULE

Non-circular derivation protocol

Constants and evidence | Compact equation map | Pair 52 of 55

Condensed equation chain

$$\hat{y} = f(\boldsymbol{p}; D_{\mathrm{train}}), \qquad y_{\mathrm{test}} \notin \{\boldsymbol{p}, D_{\mathrm{train}}, \text{equivalents}\}, \qquad z = \frac{\hat{y} - y_{\mathrm{test}}}{\sqrt{u_{\hat{y}}^2 + u_y^2}} \tag{116}$$

Symbols and types

$\boldsymbol{p}$: frozen parameters; D_{train}: allowed calibration data; y_{test}: held-out target.

Dependency and scientific reading

A prediction earns credit only when the target and algebraic equivalents are absent upstream and uncertainty is propagated.

Author-control point. Ryan can revise which observations are permitted for calibration, but the list must be explicit and smaller than the independent held-out output set.

NEXT: The facing work-through states the assumptions, expands the algebra, checks dimensions, and names a failure condition.

Expanded sheet

E01-X

EXPANDED WORK-THROUGH

Non-circular derivation protocol

Constants and evidence | Assumptions, derivation, dimensions, interpretation, falsifier

Assumptions used

The model, code, units, parameters, and calibration policy are frozen before test access; failed predictions remain recorded.

Expansion

Construct a dependency graph whose leaves are inputs and whose root is $\hat{y}$. Reject the derivation if y or an equivalent identity occurs among the leaves. Propagate input covariance through $J\Sigma J^T$. Compare with a declared likelihood and baseline. A symbolic identity can be correct without being an independent prediction.

Dimensional and normalization check

Residuals are formed only between like units; the standardized z score is dimensionless.

Thought experiment

Predicting a card after glimpsing its reflection is not prediction. The dependency graph checks for reflections hidden under different names.

Failure condition. Predictive credit fails if target information enters through units, fitted correction factors, derived constants, data selection, or post-hoc model choice.

Back to compact sheet

E02

REQUIRED NEXT RESULT

Dimensionless predictions

Constants and evidence | Compact equation map | Pair 53 of 55

Condensed equation chain

$$R_{ab} = \frac{\lambda_a(L_{\mathrm{node}})}{\lambda_b(L_{\mathrm{node}})}, \qquad \frac{m_a}{m_b} = \frac{\sqrt{\lambda_a}}{\sqrt{\lambda_b}}, \qquad \partial_{p_j} R_{ab} \text{ reported} \tag{117}$$

Symbols and types

L_{node}: frozen stability/operator matrix; λ_a: eigenvalues; R_{ab}: scale-free ratio.

Dependency and scientific reading

A dimensionless spectral ratio is the cleanest first END/MNT prediction because unit calibration cancels.

Author-control point. Select one mode pair based on theory labels, not whichever pair happens to match a known mass ratio.

NEXT: The facing work-through states the assumptions, expands the algebra, checks dimensions, and names a failure condition.

Expanded sheet

E02-X

EXPANDED WORK-THROUGH

Dimensionless predictions

Constants and evidence | Assumptions, derivation, dimensions, interpretation, falsifier

Assumptions used

The operator is derived before particle matching; mode identification follows symmetry/topology; no target mass fixes matrix entries.

Expansion

Linearize the complete node update around a stable solution to obtain L_{node}. Diagonalize with archived numerical tolerances. Identify modes using representation labels independent of mass. Form eigenvalue ratios and propagate parameter uncertainty. Compare one preregistered ratio to held-out data only after the entire pipeline is frozen.

Dimensional and normalization check

Eigenvalue ratios and mass ratios are dimensionless, eliminating the SI-scale ambiguity.

Thought experiment

A guitar maker can predict the ratio of two string harmonics without knowing whether length is measured in inches or centimetres.

Failure condition. The result fails if mode identities are chosen post hoc, the ratio is unstable under refinement, or uncertainties cover the target only after parameter retuning.

Back to compact sheet

E03

REQUIRED NUMERICAL DISCIPLINE

Uncertainty and covariance

Constants and evidence | Compact equation map | Pair 54 of 55

Condensed equation chain

$$\Sigma_y = J\Sigma_p J^T + \Sigma_{\text{num}} + \Sigma_{\text{model}}, \qquad J_{ij} = \frac{\partial f_i}{\partial p_j}, \qquad \chi^2 = (y-d)^T(\Sigma_y + \Sigma_d)^{-1}(y-d) \tag{118}$$

Symbols and types

Σ_p: input covariance; Σ_{num}: numerical error; Σ_{model}: discrepancy allowance.

Dependency and scientific reading

Printed-digit agreement is meaningless without correlated uncertainty, numerical convergence, and parameter-count accounting.

Author-control point. Ryan can choose conservative discrepancy models, but they must be fixed before seeing the held-out residual.

NEXT: The facing work-through states the assumptions, expands the algebra, checks dimensions, and names a failure condition.

Expanded sheet

E03-X

EXPANDED WORK-THROUGH

Uncertainty and covariance

Constants and evidence | Assumptions, derivation, dimensions, interpretation, falsifier

Assumptions used

Inputs have a documented joint distribution; differentiability or resampling is available; model discrepancy is not tuned to force acceptance.

Expansion

Compute Jacobians analytically, by automatic differentiation, or with verified finite differences. Add independently estimated numerical covariance from resolution/timestep studies. Use the full covariance in the likelihood; do not sum separate per-observable percentages. Report effective degrees of freedom and compare to a baseline with the same data.

Dimensional and normalization check

Covariance entries have products of observable units; quadratic forms are dimensionless.

Thought experiment

Ten arrows landing near a bullseye are less impressive if they were fired with a sight adjusted after each shot; uncertainty and parameter accounting record the adjustment.

Failure condition. A validation claim fails if correlations are ignored, code error dominates, uncertainty is absent, or flexible corrections outnumber independent constraints.

Back to compact sheet

E04

CONTROLLING COMPLETION GATE

Frozen falsification protocol

Constants and evidence | Compact equation map | Pair 55 of 55

Condensed equation chain

$$\mathcal{M}_* = (U_{\boldsymbol{p}_*}, X_{0,*}, B_*, \mathcal{O}_*, \mathcal{L}_*), \qquad \mathrm{hash}(\mathcal{M}_*) = H_*, \qquad \Delta \log \mathcal{Z} = \log p(D|\mathcal{M}_*) - \log p(D|\mathcal{M}_0) \tag{119}$$

Symbols and types

B_*: boundaries; $\mathcal{O}_*$: observables; $\mathcal{L}_*$: likelihood; H_*: immutable record.

Dependency and scientific reading

The theory becomes testable when one complete model is frozen, executable, compared with a strong baseline, and allowed to fail.

Author-control point. Ryan should define the smallest immutable v1 micro-model that expresses the intended vision, even if its first result is failure.

NEXT: The facing work-through states the assumptions, expands the algebra, checks dimensions, and names a failure condition. **Expanded sheet**

E04-X

EXPANDED WORK-THROUGH

Frozen falsification protocol

Constants and evidence | Assumptions, derivation, dimensions, interpretation, falsifier

Assumptions used

Source, environment, seeds, data identifiers, exclusions, and decision thresholds are archived before evaluation.

Expansion

Package the full model specification and compute a checksum. Run analytic unit tests, convergence tests, and negative controls. Evaluate preregistered held-out observables with the fixed likelihood. Record failures without changing the model. A new version may respond to failure, but it begins a new test and cannot inherit the old prediction claim.

Dimensional and normalization check

Evidence ratios and information criteria are dimensionless; all raw observables retain explicit units.

Thought experiment

Seal the answer in an envelope before nature reveals the card. If the envelope can be rewritten afterward, no prediction occurred.

Failure condition. END/MNT is falsified in a declared domain when the frozen model violates its analytic invariants or misses held-out data beyond its preregistered uncertainty and failure threshold.

Back to compact sheet

A Notation and unit discipline

Symbol	Meaning	Discipline
n	Micro-update index	Dimensionless ordering label, not physical time
t_K	Clock time	Operational time read by a persistent subsystem
$G = (V, E, w)$	Effective weighted graph	Emerges after persistence/coarse-graining; may be fixed within one phase
a	Graph spacing in a regular phase	Length after metric calibration; not automatically the Planck length
$\delta\tau$	Update interval in benchmark units	Time after a clock map; may be a numerical step rather than fundamental observable
q_i^n	Generalized real node coordinate	Units chosen so every term in (9) is energy
μ	Generalized inertia	Fixed by the chosen normalization of q
κ	Link stiffness	κ/μ has units of inverse time squared
E_*	Local capacity scale	Energy per node for (7); must be calibrated or derived
Φ	Continuum amplitude field	Mass dimension one in 3+1 natural units
θ	Compact phase	Dimensionless with period 2π
f_θ	Phase stiffness scale	Mass dimension one in 3+1 natural units
χ	Coarse EQEF candidate	Normalization model-dependent; residual capacity itself is dimensionless
$T^\rho{}_{\mu\nu}$	Geometric torsion	Antisymmetric part of an independently defined connection

Use $h = 6.62607015 \times 10^{-34}\,\mathrm{J\,s}$ for the exact SI defining constant and $\hbar = h/(2\pi)$. Do not attach m^{-2} to a dimensionless Planck-unit number. Natural-unit formulas and SI formulas must never be mixed without an explicit conversion line.

B Source register and disposition

Source	Role	Disposition
MNT_Axioms_Ontology.pdf	Controlling ontology	Retain hierarchy; repair pre-time frequency, global capacity, energy definition, and status of EQEF/torsion
MNT_Math_Lexicon.pdf	Notation and EFT templates	Retain useful dictionary; correct locality, signs, dimensions, double-counted fermion mass, and generic-EFT-as-derivation problem
MNT_Structural_Proofs.pdf	Derivation logic	Retain non-circularity criteria and scaling templates; relabel “proofs” because microscopic operators remain unspecified

Source	Role	Disposition
MNT_Global_Validation.pdf	Test catalogue	Retain as protocol library; withdraw the word validation because most sections specify future calibration or tests
Evans MNT Technical Editorial Audit.pdf	Evidentiary audit	Retain submission blockers and exclusions; update its fixed-lattice starting point using the later ontology
Evans MNT Nature Style WIP.pdf	Clean working narrative	Retain bounded status language, disclosure, and reproducibility programme; revise ontology and action
The Evans Node Dialect Parts 1–3	Legacy idea reservoir	Retain phase, persistence, threshold, and resonance intuitions only; discard unsupported validations and numerical predictions
MNT-Main Manuscript.pdf and duplicate deterministic-lattice manuscript	Audited legacy manuscript	Superseded; useful only for provenance of errors and proposed experiments
JRE-MNT-PRL.pdf	Claimed Higgs validation	Withdraw scientific claims pending the archived derivation, actual data audit, and dimensionally valid prediction
end8(1).pdf, end9.pdf, end11.pdf, end20.pdf, end21.pdf, end23.pdf, end25.pdf, end31.pdf, end33.pdf	Early UMNT notes	Preserve historical concepts; discard displayed constant derivations and quantitative conclusions
end33.pdf mass/charge note	Qualitative pattern idea	Retain topological-inertia and winding intuition as research questions; discard formulas $m = \tau_v/(f_n c^2)$, $q = \alpha\Delta\phi$
end31.pdf dimensionality note	Conjecture	No derivation of 3+1 dimensions is present; move to future graph/spectral-dimension study

C Submission readiness checklist

The technical presentation now contains a title, bounded abstract, source hierarchy, explicit state/update benchmark, derived results, uncertainty language, falsification programme, source disposition, code/data statements, author accountability, competing-interest statement, and AI disclosure. Those elements are necessary but do not make the theory empirically submission-ready. Replication remains impossible at the fundamental level because the canonical capacity-preserving update, immutable parameters, simulator, and external results do not yet exist.

Scientific American currently describes a different product: a 2,000–4,000-word feature for curious general readers, supported by reporting, context, and independent critical perspectives [18]. Part I matches the approximate voice and length of that form, while Part II is backup material for fact-checking and expert scrutiny. However, Scientific American states that it does not accept AI-generated pitches or drafts [19]. This manuscript must therefore not be submitted there unchanged. Ryan would need to rewrite a pitch and article independently, report the story with external physicists, and disclose the work honestly under the publication's then-current policy.

The appropriate scientific next step is a versioned theory-specification preprint clearly labeled as work in progress, followed by specialist criticism and a released benchmark implementation. It should not be represented as an empirical research article or completed theory of everything.

References

[1] Mohr, P. J., Newell, D. B., Taylor, B. N. & Tiesinga, E. CODATA recommended values of the fundamental physical constants: 2022. *J. Phys. Chem. Ref. Data* **54**, 033105 (2025). doi:10.1063/5.0279860.

[2] National Institute of Standards and Technology. Fundamental Physical Constants: complete listing, 2022 CODATA adjustment. NIST Standard Reference Database 121 (accessed 6 August 2026). `https://physics.nist.gov/cuu/Constants/Table/allascii.txt`.

[3] Wilson, K. G. Confinement of quarks. *Phys. Rev. D* **10**, 2445–2459 (1974). doi:10.1103/PhysRevD.10.2445.

[4] Regge, T. General relativity without coordinates. *Nuovo Cimento* **19**, 558–571 (1961). doi:10.1007/BF02733251.

[5] Bombelli, L., Lee, J., Meyer, D. & Sorkin, R. D. Space-time as a causal set. *Phys. Rev. Lett.* **59**, 521–524 (1987). doi:10.1103/PhysRevLett.59.521.

[6] Bell, J. S. On the Einstein Podolsky Rosen paradox. *Physics* **1**, 195–200 (1964). doi:10.1103/PhysicsPhysiqueFizika.1.195.

[7] Hensen, B. *et al.* Loophole-free Bell inequality violation using electron spins separated by 1.3 kilometres. *Nature* **526**, 682–686 (2015). doi:10.1038/nature15759.

[8] Nielsen, H. B. & Ninomiya, M. A no-go theorem for regularizing chiral fermions. *Phys. Lett. B* **105**, 219–223 (1981). doi:10.1016/0370-2693(81)91026-1.

[9] Hehl, F. W., von der Heyde, P., Kerlick, G. D. & Nester, J. M. General relativity with spin and torsion. *Rev. Mod. Phys.* **48**, 393–416 (1976). doi:10.1103/RevModPhys.48.393.

[10] Lieb, E. H. & Robinson, D. W. The finite group velocity of quantum spin systems. *Commun. Math. Phys.* **28**, 251–257 (1972). doi:10.1007/BF01645779.

[11] Weinberg, S. Phenomenological Lagrangians. *Physica A* **96**, 327–340 (1979). doi:10.1016/0378-4371(79)90223-1.

[12] Woodard, R. P. The theorem of Ostrogradsky. *Scholarpedia* **10**, 32243 (2015). doi:10.4249/scholarpedia.32243.

[13] Bureau International des Poids et Mesures. *The International System of Units (SI Brochure)*, 9th ed., version 4.01 (2025). doi:10.59161/AUEZ1291.

[14] Particle Data Group. Review of Particle Physics 2026. *Int. J. Mod. Phys. A* **41**, 2630011 (2026). `https://pdg.lbl.gov/2026/`.

[15] Nature Physics. Preparing your material (accessed 6 August 2026). `https://www.nature.com/nphys/submission-guidelines/preparing-your-submission`.

[16] Nature Physics. Artificial Intelligence policy (accessed 6 August 2026). `https://www.nature.com/nphys/editorial-policies/ai`.

[17] Nature Physics. Reporting standards and availability of data, materials, code and protocols (accessed 6 August 2026). https://www.nature.com/nphys/editorial-policies/reporting-standards.

[18] Scientific American. Submission instructions (accessed 6 August 2026). https://www.scientificamerican.com/page/submission-instructions/.

[19] Scientific American. Standards and ethics: use of artificial intelligence (updated 23 July 2026; accessed 6 August 2026). https://www.scientificamerican.com/standards-and-ethics/.

D Unanswered work in progress — canonical completion page

Foundational dynamics

- Specify the proto-state space, admissible hypergraph, and probability-free initial-condition rule.
- Replace the illustrative scalar update with one unique local $U_{\boldsymbol{p}}$ that preserves the full capacity set, states boundary conditions, and declares whether graph topology changes.
- Prove well-posedness, finite propagation, conservation or controlled dissipation, stability, and convergence under refinement.

Emergence

- Derive the persistence map C_R, graph weights, and a scale range with stable 3+1-dimensional Lorentzian geometry.
- Derive operational clocks and show universal low-energy Lorentz symmetry rather than a scalar-only limiting speed.
- Find stable localized nonlinear solutions; compute dimensionless spectra, scattering, topology, and failure regions without particle-data tuning.

Known physics

- Generate the gauge group, chiral fermion content, anomaly cancellation, charge representations, and Yukawa structure from the node operator.
- Supply the ensemble/preparation/measurement map, Born frequencies, Bell-assumption choice, and operational no-signalling proof.
- Derive the tetrad, connection, metric, Einstein/Newtonian limits, equivalence principle, and a quantitative torsion source.
- Derive EQEF transport and continuum coefficients; calculate cosmological background and perturbations without fitting a residual vacuum term by hand.

Prediction and evidence

- Freeze a parameter file and calibration policy; derive at least one dimensionless held-out result with uncertainty.
- Release code, tests, environment, seeds, data identifiers, checksums, likelihood, baseline comparisons, and negative results.

Completion criterion. END/MNT graduates from a coherent research programme to a physical theory only when one immutable micro-model crosses these gates with fewer calibrated inputs than independent held-out outputs. Until then, every particle, gravity, quantum, cosmology, and technology claim remains provisional.